1997

Sonochemical reactions: mass transfer and kinetic studies of a solid-liquid system

Leigh Christine Hagenson
Iowa State University

INFORMATION TO USERS

This manuscript has been reproduced from the microfilm master. UMI films the text directly from the original or copy submitted. Thus, some thesis and dissertation copies are in typewriter face, while others may be from any type of computer printer.

The quality of this reproduction is dependent upon the quality of the copy submitted. Broken or indistinct print, colored or poor quality illustrations and photographs, print bleedthrough, substandard margins, and improper alignment can adversely affect reproduction.

In the unlikely event that the author did not send UMI a complete manuscript and there are missing pages, these will be noted. Also, if unauthorized copyright material had to be removed, a note will indicate the deletion.

Oversize materials (e.g., maps, drawings, charts) are reproduced by sectioning the original, beginning at the upper left-hand corner and continuing from left to right in equal sections with small overlaps. Each original is also photographed in one exposure and is included in reduced form at the back of the book.

Photographs included in the original manuscript have been reproduced xerographically in this copy. Higher quality 6" x 9" black and white photographic prints are available for any photographs or illustrations appearing in this copy for an additional charge. Contact UMI directly to order.

UMI

A Bell & Howell Information Company
300 North Zeeb Road, Ann Arbor MI 48106-1346 USA
313/761-4700 800/521-0600

Sonochemical reactions: Mass transfer and kinetic studies of a solid-liquid system

by

Leigh Christine Hagenson

A dissertation submitted to the graduate faculty

in partial fulfillment of the requirements for the degree of

DOCTOR OF PHILOSOPHY

Major: Chemical Engineering

Major Professor: L. K. Doraiswamy

Iowa State University

Ames, Iowa

1997

Graduate College
Iowa State University

This is to certify that the Doctoral dissertation of

Leigh Christine Hagenson

has met the dissertation requirements of Iowa State University

Signature was redacted for privacy.

Major Professor

Signature was redacted for privacy.

For the Major Program

Signature was redacted for privacy.

For the Graduate College

DEDICATION

I would like to dedicate this thesis to my parents,

Drs. Randy and Mary Jane Hagenson,

who, through their actions and words,

provided me with excellent models to emulate.

TABLE OF CONTENTS

LIST OF FIGURES x

LIST OF TABLES xiv

ACKNOWLEDGEMENTS xv

ABSTRACT xvi

CHAPTER 1. GENERAL INTRODUCTION 1

1.1 Introduction 1

1.2 Dissertation Organization 1

CHAPTER 2. SONOCHEMISTRY: SCIENCE AND ENGINEERING 4

2.1 History 5

2.2 General Introduction 7

2.3 Theory 9

2.3.1 Bubble dynamics 10

2.3.2 Factors affecting cavitation 15

2.3.3 Sonoluminescence 25

2.3.4 Estimation of ultrasonic parameters 26

2.4 Applications in Organic Synthesis 31

2.4.1 Homogeneous systems 42

2.4.2 Heterogeneous systems 43

2.4.3 Effects on chemical bonding 49

2.4.4 Modeling 50

2.5 Other Applications 51

2.5.1 Organometallic chemistry 51

2.5.2 Polymerization 52

2.5.3 Biotechnology 53

2.5.4 Medicinal uses 54

2.6 Ultrasound Used in Conjunction with Other Enhancement Techniques 55

2.6.1 Phase transfer catalysis 55

2.6.2 Biphasing 58

2.6.3 Surfactants 59

2.6.4 Photolysis 59

2.7 Kinetic Analysis 60

2.7.1 Reaction zones 60

2.7.2 Kinetic modeling 63

2.8 Mass Transfer Studies 67

2.8.1 Film transfer 67

2.8.2 Dissolution 71

2.8.3 Permeability 74

2.9 Methods of Producing Cavitation 74

2.9.1 Piezoelectric vs. magnetostrictive transducers 75

2.10 Characterization of the Sound Field 76

2.11 Ultrasonic System Types 77

2.11.1 Ultrasonic bath 77

2.11.2 Probe (horn) systems 79

2.11.3 Planar transducer 81

2.11.4 Comparison of system types 83

2.12 Sonochemical Reactors with Electromechanical Transducers 84

2.12.1 Batch and/or continuous flow reactors 85

2.12.2 Batch reactors with external flow loop 87

2.12.3 Tubular reactors 90

2.13 Reactors Based on Alternative Methods of Generating Cavitation 98

2.13.1 Liquid whistle 98

2.13.2 Hydrodynamic cavitation reactor 99

2.14 Scale-Up Considerations 100

2.15 Conclusions 102

2.16 Nomenclature 103

2.17 References 108

CHAPTER 3. RATE ENHANCEMENTS IN A SOLID-LIQUID REACTION USING PTC, MICROPHASE, ULTRASOUND AND COMBINATIONS THEREOF 131

Abstract 131

3.1 Introduction 132

3.1.1 Objective 135

3.1.2 Previous work on sulfide synthesis 136

3.2 Mechanism of PTC Action 137

3.3 Experimental Apparatus and Procedure 138

3.4 Results and Discussion 140

3.4.1 Reactions with PTC alone 140

3.4.2 Reactions under the influence of microphases 145

3.4.3 Reactions under the influence of ultrasound 150

3.4.4 Summary of individual and combined effects of PTC, microphase and ultrasound 157

3.5 Conclusions 159

3.6 Nomenclature 160

3.7 References 161

CHAPTER 4. COMPARISON OF THE EFFECTS OF ULTRASOUND AND MECHANICAL AGITATION ON A REACTING SOLID-LIQUID SYSTEM 164

Abstract 164

4.1 Introduction 165

4.1.1 General 165

4.1.2 Kinetic modeling approach 169

4.1.3 Objectives 170

4.2 Experimental Apparatus, Procedure and Tools 170

4.3 Results and Discussion 173

4.3 Results and Discussion 173

4.3.1 Power measurement 173

4.3.2 Particle size analysis 177

4.3.3 Kinetic studies 179

4.3.4 Effect on surface area 190

4.3.5 Effect of sodium sulfide purity 191

4.3.6 Morphology of solid surface 187

4.4 Conclusions 195

4.5 Nomenclature 196

4.6 References 198

CHAPTER 5. USE OF ULTRASOUND TO INDUCE SUPERSATURATION IN A SOLID-LIQUID SYSTEM 201

Abstract 201

5.1 Introduction 201

5.2 Theory 202

5.3 Experimental Apparatus, Procedure and Tools 204

5.4 Results 206

5.5 Discussion 209

5.5.1 Formation of supercritical fluid 209

5.5.2 Gibbs-Thompson relationship 211

5.5.3 Supersaturation of an aqueous system 213

5.6 Conclusions 214

5.7 Nomenclature 215

5.8 References 216

CHAPTER 6. GENERAL CONCLUSIONS 217

LIST OF FIGURES

Figure 2.1. Particle degradation of Na_2S in the presence and absence of ultrasound with and without reaction (Hagenson and Doraiswamy, 1997). 45

Figure 2.2. Histogram of average diameter data for samples of Na_2S in the presence of ultrasound (Hagenson and Doraiswamy, 1997). 45

Figure 2.3. The use of PTC, ultrasound, and the combination on the conversion of benzyl chloride for the synthesis of dibenzyl sulfide (Hagenson *et al.*, 1994). 56

Figure 2.4. Use of ultrasound and the combination of PTC and ultrasound on the synthesis of Tos_3TACN (Mason *et al.*, 1994). 56

Figure 2.5. Three reaction zones of sonochemical reactions. 60

Figure 2.6. Symmetric collapse resulting in localized hot spot. 64

Figure 2.7. Ultrasonic horizontal settling column (Woodel and Vibrandt, 1960). 70

Figure 2.8. Effect of ultrasound on the flow pattern within a horizontal settling column (Woodel and Vibrandt, 1960). 70

Figure 2.9. Supersaturation as a result of exposure to ultrasound (Hagenson and Doraiswamy, 1998). 72

Figure 2.10. Ultrasonic enhancement of the rate of dissolution. 73

Figure 2.11. Ultrasonic bath systems with (a) mounted transducers and (b) submersed transducers. 78

Figure 2.12. Planar transducer systems. 81

Figure 2.13. Sonochemical stirred tank reactor (Berger, 1996). 85

Figure 2.14. Hexagonal sonochemical reactor. 86

Figure 2.15. Flow loops used to sonicate external streams of batch and continuous flow reactors. 88

Figure 2.16. Harwell sonochemical reactor. 89

Figure 2.17. Branson sonochemical reactor (tubular configuration). 90

Figure 2.18. Ultrasonic reactor designed to emulsify immiscible liquid streams within the reaction chamber and then send the emulsified mixture through a fixed bed triphase catalyst chamber (Ragaini, 1992). 92

Figure 2.19. Lewis Nearfield Acoustic Processor (NAP). 93

Figure 2.20. Cylindrical pipe reactor. 93

Figure 2.21. Cross sections of two types of tube reactors. 94

Figure 2.22. Martin Walter push-pull system. 95

Figure 2.23. Shell and tube reactor configuration with transducers embedded in shell wall. The reaction mixture is contained on the shell side and the heat transfer fluid in contained in the tube (Ragaini, 1992). 96

Figure 2.24. Sodeva sonotube. 97

Figure 2.25. Liquid whistle. 98

Figure 2.26. Flow through an orifice: hydrodynamically created cavitation. 100

Figure 2.27. Scale-up considerations. 101

Figure 3.1 Visual representation of PTC action. 133

Figure 3.2 Solid-liquid reaction facilitated by microphase action. 133

Figure 3.3 Enhancement of solid-liquid reaction with the combined action of a phase transfer catalyst and microphase. 134

Figure 3.4 Experimental apparatus for sonochemical research. 139

Figure 3.5 Effect of PTC concentration on conversion. 141

Figure 3.6 Effect of ambient reaction temperature on conversion. 141

Figure 3.7 Models used to explain PTC action. 144

Figure 3.8 Effects of the nature of the microphase. 146

Figure 3.9 Effect of combinations of microphase (MP) and PTC action. 147

Figure 3.10 Effect of Na_2S particle size on PTC action. 149

Figure 3.11 Effect of acoustic intensity on the conversion of benzyl chloride. 151

Figure 3.12 Effect of catalyst concentration for reaction with ultrasound. 153

Figure 3.13 Comparison of the individual effect on the base reaction. 153

Figure 3.14 Effect of ambient temperature on reaction with ultrasound. 154

Figure 3.15 Effect of solvent choice on reaction with ultrasound and PTC. 155

Figure 3.16 Combined effect of PTC and microphase in a sonochemical system. 157

Figure 3.17 Individual and combined effects of PTC, microphase and ultrasound. 158

Figure 4.1 Flowchart of modeling approaches when using noncatalytic solid/liquid reaction systems. 169

Figure 4.2 Experimental apparatus used for sonochemical research. 172

Figure 4.3 Determination of power dissipated by the reaction system: power delivered = 166 W. 175

Figure 4.4 The mean particle size of sodium sulfide as a function of time for the different experimental conditions studied. 177

Figure 4.5 Histogram of diameter data for samples under the influence of ultrasound. 178

Figure 4.6 Effect of temperature on the silent reaction: Na_2S lot #14025MF. 185

Figure 4.7 Increase of effective diffusivity with absolute temperature for silent reactions. 186

Figure 4.8 Enhancement of the model reaction with the addition of ultrasound. 187

Figure 4.9 Effect of temperature on the sonochemical reaction. 188

Figure 4.10 Effect of temperature on the intrinsic mass transfer coefficient (k_l) for ultrasound. 189

Figure 4.11 Effect of temperature on the effective diffusivity (D_e) when using ultrasound. 189

Figure 4.12 Effect of mechanical agitation and ultrasound, in the presence and absence of reaction, on the interfacial area. 190

Figure 4.13 Conversion of benzyl chloride to dibenzyl sulfide for different lots of anhydrous sodium sulfide: temperature = 22 °C. 191

Figure 4.14 SEM images of fresh (unaltered) particles of anhydrous sodium sulfide. 193

Figure 4.15 Appearance of solid sodium sulfide particles after exposure to 15 minutes of mechanical agitation (a) or ultrasound (b). 194

Figure 4.16 Appearance of solid sodium sulfide particles in the presence of reaction and mechanical agitation (a) or ultrasound (b). 194

Figure 5.1 Symmetric collapse resulting in localized hot spot. 203

Figure 5.2 Experimental apparatus used for sonochemical research. 205

Figure 5.3 Supersaturation as a result of exposure to ultrasound. 207

Figure 5.4 Crystal formation in filtrate of supersaturated solutions (dissolution temperature = 22 °C). 208

Figure 5.5 Ultrasonic enhancement of dissolution. 209

Figure 5.6 Dissolution of calcium citrate in water. 213

LIST OF TABLES

Table 2.1. Applications of ultrasound. 8

Table 2.2. Estimates of parameters necessary for modeling of ultrasonic systems. 27

Table 2.3. Values given for the constant terms in Equation (12). 28

Table 2.4. Representative list of organic synthetic reactions studied under the influence of ultrasound. 33

Table 2.5. Organometallic Reactions. 51

Table 2.6. Reactions which have investigated using PTC, ultrasound and/or combinations of the two enhancement techniques. 57

Table 2.7. Comparison of piezoelectric and magnetostrictive transducers (Hunicke, 1990). 76

Table 3.1 Rate enhancements attributed to effects of PTC and/or microphases. 150

Table 4.1 Liquid phase reaction model discrimination. 182

Table 4.2 Effect of sodium sulfide lot on the rate parameters k_l and D_e. 192

ACKNOWLEDGEMENTS

I would like to thank my professor, Dr. L. K. Doraiswamy, who taught me to always strive for the highest standards. I would also like to thank my family and friends who provided encouragement and support when times were difficult, and who celebrated with me when times were good.

ABSTRACT

Ultrasound has been shown to have desirable effects on both homogeneous and heterogeneous reactions, such as increasing the conversion, enhancing the selectivity, and improving the yield. Enhancements due to ultrasound may be attributed to chemical effects or mechanical effects, or to both simultaneously. The chemical effects of ultrasound are attributed to the implosion of microbubbles, generating free-radicals with a great propensity for reaction. Mechanical effects are caused by shock waves formed during symmetric cavitation, or by microjets formed when the bubble implodes asymmetrically. Research emphasis in this area attempts to discern the mechanisms behind ultrasound's mechanical effects by selecting a model solid-liquid noncatalytic reacting system in which the chemical effects of ultrasound are negligible. A rigorous kinetic modeling approach is used which allows for reaction in both the liquid and solid phases. After an extensive analysis of the experimental data obtained from the system, it is concluded that the reaction occurs on the solid phase, and that the liquid phase reaction is negligible.

Using several investigative techniques, the expected effects of ultrasound were observed, such as the degradative effects on particle size leading to increased surface area. More importantly, some novel findings of the effects of ultrasound on mass transfer parameters are reported. Results clearly show that ultrasound enhances the intrinsic mass transfer coefficient as well as the effective diffusivity of an organic reactant through the ionic lattice of the product layer. In addition, ultrasound also induces supersaturation of

solid sodium sulfide in the solvent acetonitrile, increasing the solubility by a factor of 1.4 over the equilibrium saturation concentration. This enhanced solubility is attributed to cavitation which creates localized hot spots containing solvent in a supercritical state. The normally sparingly soluble solid is highly soluble in the solvent when it exists as a supercritical fluid. The increased solubility in these localized area has "memory" and is retained, even after the hot-spot dissipates into the bulk liquid. The use of ultrasound to induce supersaturation has significant applications in the areas of chemical kinetics when the reaction occurs in the liquid film or the bulk liquid phase.

CHAPTER 1.
GENERAL INTRODUCTION

1.1 Introduction

The use of ultrasound to facilitate chemical reactions has existed since 1927 when the first chemical (Richards and Loomis, 1927) and biological (Wood and Loomis, 1927) effects were reported. Since then, several scientists and physicists have conducted pioneering work in the field of sonochemistry, and have shown that it is a useful laboratory technique for enhancing reactions by improving yields, increasing conversions, changing reaction pathways and/or initiating reactions. Unfortunately, investigations from an engineering approach are few. More information is necessary concerning the effects of ultrasound on reaction kinetics and mass transfer before these reactions can be scaled up to an industrial scale. This thesis reports the details of a chemical engineering approach developed to explain the ultrasonic enhancement of the chemical and mass transfer processes of a model solid-liquid reaction.

1.2 Dissertation Organization

Chapter 2 is a comprehensive review of what is available in the literature pertaining to the use of ultrasound in organic synthesis. The latter sections of the review contain information concerning scale-up and design of sonochemical reactors.

Chapter 3 contains the initial investigations and experimental data obtained for a model solid-liquid reaction, the synthesis of dibenzyl sulfide from benzyl chloride and sodium sulfide, using a variety of rate enhancement techniques, including microphases, phase transfer catalysis

and ultrasound. The objective of the paper was to investigate the individual and combined effects of these rate enhancement techniques. After this work was completed, the research path bifurcated from the study of phase transfer catalysis and microphases and focused solely on the use of ultrasound.

Chapter 4 is a detailed investigation, including a complete kinetic analysis and mass transfer study, of the model solid-liquid system described in Chapter 3. The objectives of this work were to exhaustively study the reaction from many different angles in order to obtain tangible evidence that could be used to explain the effect of ultrasound on mass transfer and kinetic parameters. Several analytical tools were used to realize this goal, including a scanning electron microscope to track the changes in the morphology of the surface, an image analyzer to determine the effects on the sodium sulfide particle size, an absorption isotherm apparatus using the BET method to determine the effects on the solid surface area, and a gas chromatograph to determine the kinetics of the reaction by measuring the concentrations of reactant and product.

Chapter 5 contains the results of studies on the dissolution of sodium sulfide in acetonitrile (the same solvent used in the kinetic and mass transfer studies in Chapters 3 and 4). Initially, the dissolution studies were performed in an attempt to determine the effect of ultrasound on the intrinsic mass transfer coefficient. However, ultrasound was found to lead to considerable supersaturation of the solid reactant, a finding which had not been previously reported. The objectives of this paper were to report this finding and to speculate the mechanisms which may be causing this phenomenon to occur.

Chapter 6 summarizes the general conclusions of the research contained in this dissertation. It also attempts to convey the importance of these contributions to the field of sonochemistry.

Because each chapter in this thesis is comprised of individual papers which will be submitted for publication (or have been published), they are each self-contained and include their own nomenclature and references. In addition, although the review is very detailed, it has been included in its entirety.

CHAPTER 2.
SONOCHEMISTRY: SCIENCE AND ENGINEERING

A paper submitted to *Industrial Engineering Chemistry Research*

Leigh C. Hagenson and L. K. Doraiswamy

Ultrasound has proven to be a very useful tool in enhancing the reaction rates in a variety of reacting systems. It has successfully increased the conversion, improved the yield, changed the reaction pathway and/or initiated the reaction in biological, chemical and electrochemical systems. This non-classical method of rate enhancement, a field termed *sonochemistry*, is becoming a widely used laboratory technique. Industrially, the process of producing ultrasound is a very inefficient process, burdened with high operating costs. However, the use of ultrasound may reduce or eliminate other process costs by enabling the use of milder operating conditions (e.g. lower temperatures and pressures), eliminating the need for costly solvents, reducing the number of synthesis steps while simultaneously increasing end yields, enabling the use of lower purity reagents and solvents and/or increasing the activity of existing catalysts. The use of ultrasound appears to be a promising alternative for high value chemicals and pharmaceuticals. In addition, advances are constantly being made to make it a feasible option in the continuing effort to intensify large-scale processes. Currently, a pilot plant is being funded by the Electricite de France to sonochemically oxidize cyclohexanol to cyclohexone indirectly (Ondrey *et al.*, 1996). Hoechst and several other companies are working on a project with Germany's Clausthal Technical University (Clausthal-Zellerfeld) which uses a modular sonochemical reactor to produce up to 4 metric tons of Grignard

reagent per year. They found that the use of ultrasound increases the conversion by a factor of five and reduces the induction period from 24 hours to 50 minutes (Ondrey *et al.*, 1996).

With such high enhancements in rates, it is no wonder that the number of publications in the field of sonochemistry has increased significantly in the last twenty years. Much of the pioneering work in the field has been done by chemists and physicists who have found that the chemical, and some mechanical, effects of ultrasound are a result of the implosive collapse of cavitation bubbles. The interest of the chemical engineer in capturing and quantifying the beneficial effects of ultrasound is rising, but publications in such crucial applied areas as mass transfer, reaction kinetics and modeling, and reactor design are sparse. The objective of the present review is to compile and condense information available in the literature, and to organize it in such a fashion as to facilitate and inspire future research in the field of sonochemistry.

2.1 History

The interest in ultrasound and cavitational effects dates back over 100 years. The first report of cavitation was published in 1895 by Thornycroft and Barnaby when they noticed the propeller of their submarine, the H.M.S. Daring, was pitted and eroded. Twenty-two years later, in 1917, Lord Rayleigh published the first mathematical model describing a cavitational event in an incompressible fluid. However, ultrasound was not used to enhance reaction systems until 1927 when Loomis reported the first chemical (Richards and Loomis, 1927) and biological (Woods and Loomis, 1927) effects of ultrasound. Ten years later Brohult (1937)

discovered that ultrasound led to the degradation of a biological polymer. Research in this field of ultrasonics was expanded to the degradation of synthetic polymers by Schmid in 1940.

One of the most basic concepts of sonochemistry is that free radicals are formed as a result of cavitation of microbubbles created during the rarefaction (or negative pressure) period of sound waves. This phenomenon was first reported by Weiss in 1944 when he observed the sonolysis of water ($H_2O \rightarrow H^{\cdot} + OH^{\cdot}$). The same year Harvey *et al.* (1944) introduced the concept of rectified diffusion (the growth of microbubbles due to unequal transfer of mass across the interface during bubble oscillation). The early 1950's brought about several new and exciting developments in the field of sonochemistry. Noltingk and Neppiras (1950) performed the first computer calculations modeling a cavitating bubble. Three years later Schultz and Henglein (1953) reported the sonolysis of an organic liquid. In 1954, Elder *et al.* suggested that bubble induced microstreaming was one of the factors leading to the well-known ultrasonic cleaning effects in heterogeneous systems (see also Elder, 1959).

In the 1960's the majority of sonochemical effects published concerned biological systems. The ultrasonic cleaning bath was starting to be used in many chemical and metallurgical laboratories for cleaning glassware and forming dispersions. Naude and Ellis hypothesized the existence of microjets formed during asymmetric cavitation in 1961. This concept is still alive today and is used to explain the pitting of solid surfaces and overall particle size reduction in heterogeneous systems. In 1953 Weissler published the first observation of a decrease in the rate of a sonochemical reaction with an increase in the ambient reaction temperature, a phenomenon observed in several systems to date. In 1964 Flynn coined the now commonly used terms "transient cavitation" and "stable cavitation".

In the 1970's there was a lull in publications concerning sonochemistry; however, the field regained interest in the 1980's and the number of publications increased dramatically. Neppiras (1980) used the term "sonochemistry" for the first time in a review of acoustic cavitation. Mankio *et al.* (1982) used spin trapping and ESR (electron spin resonance) measurements to validate the findings of Weiss in 1944 on the sonolysis of water. The field of sonochemistry was becoming so popular that in 1986 the first international meeting devoted to it was held by the Royal Society of Chemistry Annual Congress at Warwick University in U.K. Such meetings have since become an annual event. During the year 1987 the Royal Society of Chemistry founded a Sonochemistry Group based at the Harwell laboratory of U.K.'s Atomic Energy Authority with the objective of developing methods to facilitate the use of ultrasound for industry. In the late 1980's and early 1990's several manufacturers started designing and marketing equipment exclusively for sonochemical research. The first issue of a new periodical entitled "Ultrasonics Sonochemistry", dedicated to the applications of ultrasound in chemistry, was released in 1994.

2.2 General Introduction

Ultrasound occurs at a frequency above 16 kHz, higher than the audible frequency of the human ear, and is typically associated with the frequency range of 20 kHz - 500 MHz. The frequency level is inversely proportional to the power output. Low intensity, high frequency ultrasound (in the MHz range) does not alter the state of the medium through which it travels and is commonly used for non-destructive evaluation and medical diagnosis. However, high intensity, low frequency ultrasound does alter the state of the medium and is the type of

ultrasound typically used for sonochemical applications. A current list of the various applications of ultrasound is shown in Table 2.1. Many of these applications are briefly explained in the Kirk-Othmer Encyclopedia of Chemical Technology (1983).

There are several references available which provide a general overview of the field of sonochemistry and the types of chemical reactions which have been studied (see, e.g., Suslick, 1988; Suslick and Doktycz, 1990; Ley and Low, 1991; Mason, 1989 and 1991). Some authors have compared the various effects of ultrasound to other types of chemistry, such as mechanochemisty (Boldyrev, 1995). However, as will be evident from this review, it will take the combined effort of scientists and engineers to thoroughly understand sonochemical reactions and develop rational design procedures for sonochemical reactors.

Table 2.1. Applications of ultrasound.

Chemical and Allied Industries	Other	
Air scrubbing	Abrasion	Medical inhalers
Atomization	Cleaning	Metal-grain refinement
Cell disruption	Coal-oil mixtures	Metal tube drawing
Crystal growth	Cutting	Non destructive testing
Crystallization	Degradation of powders	of metals
Defoaming	Dental descaling	Physiotherapy
Degassing	Drilling	Plastic welding
Depolymerization	Echo-ranging	Powder production
Dispersion of solids	Erosion	Soldering
Dissolution	Fatigue testing	Sterilization
Drying	Flaw detection	Welding
Emulsification	Flow enhancement	
Extraction	Imaging	
Filtration		
Flotation		
Homogenization		
Sonochemistry		
Stimulus for chemical reactions		
Treatment of slurries		

2.3 Theory

The chemical and mechanical effects of ultrasound are caused by cavitation bubbles which are generated during the rarefaction, or negative pressure, period of sound waves. During the negative pressure cycle, the liquid is pulled apart at sites containing some gaseous impurity (nucleation sites), forming a void. This effect can be seen everyday when drinking a carbonated beverage. The bubbles of carbon dioxide form at scratches in the glass where gaseous impurities, such as air, are harbored and act as nucleation sites for cavitation. The cavitational activity is directly proportional to the number density of particles present in the medium (Madanshetty and Apfel, 1991). The chemical effects of ultrasound are not observed when there are no dissolved gases in the system, when the sound intensity is not greater than the cavitation threshold of the system (Fitzgerald *et al.*, 1956), or when the reactant is not volatile enough to enter the cavitation bubble during its formation (Griffing, 1952).

The physical and chemical effects of ultrasound are a result of both stable and transient cavitational events, which are described in the following sections. Two competing theories exist to explain the chemical effects of ultrasound due to cavitation: the *hot-spot theory* and *the electrical theory*. The hot-spot theory postulates that when the bubbles cavitate, localized hot spots, reaching temperatures and pressures in excess of 5000 K and 500 atm are formed. On the other hand, the electrical theory postulates that an electrical charge is created on the surface of a cavitation bubble, forming enormous electrical field gradients across the bubble which are capable of bond breakage upon collapse (Margulis, 1985). The hot-spot theory is generally more accepted, although Margulis (1992 and 1994) reports many phenomena which

contradict this theory but are supported by the electrical theory. A Letter to the Editor published in 1996 completely discounted the electrical theory as a valid mechanism behind sonoluminence and sonochemistry (Lepoint-Mullie *et al.*).

2.3.1 Bubble dynamics

The chemical effects of ultrasound have been attributed to the collapse of both stable and transient cavitational events. The following sections provide a brief explanation of bubble dynamics and the modeling which has been published in the literature. For a comprehensive review of acoustic cavitation and bubble dynamics, refer to Neppiras (1980).

a. Stable cavitation

Stable cavitation bubbles are bubbles which are formed and oscillate around a mean radius in the sound field and exist for many acoustic cycles. For this to occur their growth rate during the rarefaction must be equivalent to their rate of contraction during the compression phase. This specifies that rectified diffusion, or the unequal transfer of mass into the bubble during the acoustic wave cycle, not occur. The wall motion of a stable bubble in an acoustic field is described by the relation

$$R\ddot{R} + \frac{3}{2}\dot{R}^2 = \frac{1}{\rho}\left[p_L(R) - p_\infty(t)\right] \tag{1}$$

where $p_L(R)$ is the liquid pressure just outside the bubble wall, given by

$$p_L(R) = p_T(R) - \frac{4\mu\dot{R}}{R} - \frac{2\sigma}{R} \tag{2}$$

where both Equations (1) and (2) are based on, but not limited to, the assumptions that the liquid phase is incompressible (ρ = constant) and viscous forces are neglected. The terms $\dot{R}$ and $\ddot{R}$ represent first and second order time derivatives of the bubble's radius, respectively. The pressure far from the bubble in an acoustic field with a pressure amplitude P_A and angular frequency ω is described by

$$p_\infty(t) = P_o - P_A \sin\omega t \tag{3}$$

where P_o is the hydrostatic (ambient) pressure. The pressure of the total mass content in the bubble at a given radius, $p_T(R)$, is the sum of both the permanent-gas pressure, $p_g(R)$, and vapor pressure, $p_v(R)$. When it is assumed that the bubble is filled with an ideal gas, contains no vapor, and behaves as an adiabatic system (PV^γ = constant), the Rayleigh-Plesset equation is obtained,

$$R\ddot{R} + \frac{3}{2}\dot{R}^2 = \frac{1}{\rho}\left[\left(P_o + \frac{2\sigma}{R_o}\right)\left(\frac{R_o}{R}\right)^{3\gamma} - \frac{2\sigma}{R} - \frac{4\eta\dot{R}}{R} - P_\infty\right] \tag{4}$$

where R_o is the bubble radius at equilibrium, γ is the specific heat ratio of the gas within the bubble and ρ, σ, and η are the density, surface tension and viscosity of the bulk fluid, respectively. Equation (4) is also valid for the isothermal case when γ is set equal to 1.

Bubbles with an equilibrium radius R_o in a liquid system, with a fixed temperature T and negligible viscous forces, will pulsate with a resonance frequency ω_r, as defined by

$$\omega_r^2 = \frac{1}{\rho R_o^2}\left[3\gamma\left(P_o + \frac{2\sigma}{R_o}\right) - \frac{2\sigma}{R_o}\right] \tag{5}$$

The eigenfrequency ω_r' takes into account damping of the linear oscillations due to viscous forces, as defined by

$$(\omega_r')^2 = (\omega_r)^2 - \left(\frac{2\mu}{\rho R_o^2}\right)^2 \qquad (6)$$

When the angular frequency of the ultrasound is equal to the resonant frequency of the bubble (i.e. when $\omega = \omega_r$), resonant cavitation occurs. Because many ultrasonic transducers are designed with a set frequency, operating under resonance conditions is easier to achieve by changing the system's parameters in order to alter the bubble's resonant frequency to match that of the transducer's. This can be done by varying the hydrostatic pressure (Cum *et al.*, 1988) and the system temperature (Cum *et al.*, 1990). Operating at resonant conditions has been found to increase the rate and yield of reactions, such as the oxidation of indane to indan-1-one in the presence of $KMnO_4$. The effect of varying the ultrasonic frequency in order to drive the bubble dynamics towards transient cavitation has also been investigated (Cum *et al.*, 1992).

b. Rectified diffusion

Rectified diffusion is the event where cavitation bubbles grow more during expansion than they shrink during contraction due to the unequal diffusion of gases and vapor from the bulk liquid phase into the bubble. A great deal of information on research and modeling of rectified diffusion is available in the literature (see, e.g., Crum, 1984 and 1980; Crum and Hansen, 1982) and will not be covered here.

c. Transient cavitation

A transient cavity is one which exists for only a few acoustic cycles. During its existence it grows to 2 or 3 times its initial size and, upon implosion, creates extreme temperatures and pressures within its cavity. The wall motion of a transient, gas- filled cavity is described by (Neppiras, 1980)

$$R\ddot{R} + \frac{3}{2}\dot{R}^2 = \frac{1}{\rho}\left[P\left(\frac{R_{max}}{R}\right)^{3\gamma} - P_m\right] \tag{7}$$

where R_{max} is the maximum radius the bubble obtains just before collapse, P is the gas pressure in the bubble at its maximum size, and P_m is the liquid pressure at transient collapse. Since the collapse of the bubble always occurs when the acoustic pressure is near its peak, P_m is similar in value to $(P_A + P_o)$ in an infinite fluid where the bubble density is very small, and can be approximated as P_o, the hydrostatic pressure, in an intense acoustic field where the bubble density is high. The ratio of the minimum bubble radius to the maximum radius is given by

$$\frac{R_{min}}{R_{max}} \approx \left[\frac{P}{P_m(\gamma - 1)}\right]^{\frac{1}{3(\gamma-1)}} \tag{8}$$

It is typically assumed that the bubble collapse is adiabatic, which allows the maximum temperature (T_{max}) and pressure (P_{max}) within the gas filled, transient bubble at the moment of collapse to be estimated using Equations (9) and (10), respectively. These relationships are

$$T_{max} = T_o\left[\frac{P_m(\gamma - 1)}{P}\right] \tag{9}$$

$$P_{max} = P\left[\frac{P_m(\gamma - 1)}{P}\right]^{\frac{\gamma}{\gamma-1}} \tag{10}$$

developed neglecting surface tension and viscosity of the fluid and assuming the cavity is filled with an ideal gas. If the cavity contains vapor as well as gas, the collapse will be cushioned, and the maximum pressure and temperature will decrease because some of the energy generated during collapse will go towards condensation of the vapor. The time for complete collapse τ_m is developed (Khoroshev, 1963) under the same assumptions, and is given by

$$\tau_m \approx 0.915\ R_{max}\left(\frac{\rho}{P_m}\right)^{\frac{1}{2}}\left(1+\frac{P}{P_m}\right) \tag{11}$$

d. Modeling

Models have been developed to explain the bubble dynamics and sonoluminescence for a single, stable cavitation bubble (Gaitan *et al.*, 1992). In addition, experimental results have been compared with simulations of the Keller-Miksis radial equation with a linear polytropic exponent approximation (Keller and Miksis, 1980), the Keller-Miksis radial equation which uses a more exact formulation for the internal pressure (Prosperetti *et al.*, 1986), and Flynn's formulation which includes thermal effects inside the bubble (Flynn, 1975).

Some authors have concluded that the cavitational effects of ultrasound are not due to a single cavitational event, but are due instead to events occurring within a cloud of bubbles (Atchley *et al.*, 1988). It has been found that bubble clouds scatter, focus, and channel the sound waves as they propagate through the medium (Leighton, 1995). Leighton remarked

that single-bubble theory should be reinterpreted, at least in modeling the local surroundings of the single bubble, to account for the bubble population and the effects of the bubbles on one another. This contradicts "classical" approaches, such as taken by Alippi (1992) who states that since the dynamics of bubbles in a sound field are non-linear, each event should be solved separately. Neppiras (1980) explains that when bubbles are in a cloud, the collapse is more violent because it initiates at the outermost layers of the cloud and then propagates inwards. This type of collapse occurs when the bubbles expand in phase (approximately) on the tension half-cycle.

2.3.2 Factors affecting cavitation

The ambient conditions of the reaction system can greatly influence the intensity of cavitation, which directly affects the reaction rate and/or yield. These conditions include the reaction temperature, hydrostatic pressure, irradiation frequency, acoustic power and ultrasonic intensity. In addition, the presence of dissolved gases, choice of solvent, sample preparation and choice of buffer can also have a significant effect on the cavitational intensity. Each of these factors is described in detail below.

a. Presence of dissolved gases

Dissolved gases act as nucleation sites for cavitation. As gases are removed from the reaction mixture, due to the implosion of the cavitation bubbles, further cavitation becomes more difficult. Bubbling gases through the mixture facilitates the production of cavitation bubbles; however, the selection of the gas is important. Because the collapse of the bubble

occurs in such a small amount of time (~ 3.5 μs as estimated by Prasad Naidu *et al.*, 1994), it can be assumed to occur adiabatically. Hence, as a general rule, a gas with a high specific heat ratio gives a greater cavitational effect than a gas with a low specific heat ratio. Monatomic gases, such as argon and helium, convert more energy upon cavitation than diatomic gases, such as nitrogen and oxygen, due to the larger ratio of specific heats. Gases which are extremely soluble in the reaction mixture result in a smaller cavitational effect because the bubbles formed may redissolve. The bubbles which do not dissolve often become so large (because of the easy penetration of gas into the bubble) that they float to the surface and explode. The thermal conductivity of the gas is also important because, although the collapse is modeled as adiabatic, there is a small amount of heat which is transferred to the bulk liquid mixture during collapse. As the thermal conductivity of the gas increases, the amount of heat loss due to thermal dissipation also increases.

The dependence of cavitational intensity on the characteristics of the dissolved gases has been studied by Entezari *et al.* (1997) who investigated the effect of ultrasound on the rate of carbon disulfide dissociation. They found that He gave the highest reaction rate and CO_2 gave the lowest, with the rate decreasing in the following order of gases present: He > H_2 > air > Ar > O_2 > CO_2. Since argon has a higher specific heat ratio that helium, they were puzzled with the observations. They concluded that the predominant factor in this system was the gas solubility, with helium possessing a higher solubility than argon.

When the formation of hydroxyl radicals plays an important role in the mechanism of the reaction, a finite amount of oxygen, in combination with a monotomic gas, may accelerate the rate over the use of a pure monotomic gas alone. The liberation of iodine from aqueous

potassium iodide was investigated under several different atmospheres consisting of various ratios of oxygen to argon (Hart and Henglein, 1985). The reaction was carried out in the presence of ammonium molybdate and hydrogen peroxide (H_2O_2), which catalyzes the oxidation of the iodide ion to iodine, and was found to have a maximum rate in the presence of 30% oxygen - 70% argon atmosphere. Similar results were found for the ultrasonic degradation of phenol in an aqueous solution (Berlan *et al.* 1994). Although the ratio of specific heats (γ) is higher for argon than for oxygen, it was determined that the concentration of oxygen facilitated the formation of hydroxyl radicals, which accelerated the reactions.

Bubble dynamics equations have been used to predict the amount of free radicals (in moles) generated during collapse in order to estimate the concentration of free radicals required for kinetic analysis (Prasad Naidu *et al.*, 1994). The authors started with the Rayleigh-Plesset equation (as given previously by Equation (4), which was altered slightly to account for the pressure of the vapor within the cavitational bubble. They assumed that the entire growth phase and the initial part of the collapse phase of the bubble was isothermal, thus setting $\alpha = 1$. They also assumed that the vapor in the cavity was equal to the saturation vapor pressure of the liquid (P_s), and used the boundary conditions

$$\text{when} \quad t = 0, \qquad R = R_o \qquad \text{and} \qquad \dot{R} = 0 \tag{12}$$

The collapse phase was assumed to become adiabatic once the pressure of the gas within the cavity became equal to the saturation vapor pressure of the liquid (i.e. $P_g = P_s$). The parameter R_2 was defined as the radius of the bubble at which the transition from isothermal to adiabatic collapse occurs. Using the same system as Hart and Henglein (1985) described in

the previous paragraph they sufficiently explained the experimental data, while accounting for the dissolved gases within their model (refer to the article for detailed information). However, the predictive ability of the model varied depending upon the type of dissolved gas. The model adequately explained the variation of experimental data obtained under an oxygen atmosphere, but deviated greatly from experiments conducted under a nitrogen atmosphere. One of the main reasons for this deviation may be because the authors assumed that the number of bubbles produced within the sonicated mixture was constant, regardless of gas content and KI concentration. As discussed previously, the number of bubbles produced would depend upon gas solubility. It would also depend upon KI concentration because KI has a much lower vapor pressure and higher surface tension than water, which would reduce the amount of bubbles formed. The model appears to have better predictive ability when the reaction is carried out in a nitrogen atmosphere at low KI concentration, but its predictive ability decreases as the concentration of KI in solution increases. In addition, the authors used stable bubble dynamics to predict transient cavitational behavior, which may also reduce the predictive ability of their model.

b. Ambient temperature

Contrary to chemical reactions in general, an increase in the ambient reaction temperature results in an overall decrease in the sonochemical effect. The decrease is a result of the following sequence of events: first, as the reaction temperature is raised, the equilibrium vapor pressure is also increased. This leads to easier bubble formation (due to the decrease of the cavitation threshold); however, the cavitation bubbles which are formed contain more

vapor. As discussed previously, vapor reduces the ultrasonic energy produced upon cavitation because it cushions the implosion, in addition to using enthalpy generated in the implosion for the purposes of condensation. In general, the largest sonochemical effects are observed at lower temperatures when a majority of the bubble contents is gas.

In certain reaction systems, an optimum reaction temperature may lead to more favorable results. In such systems, an increase in temperature will increase the kinetic reaction to a point at which the cushioning effect of the vapor in the bubble begins to dominate the system. When this occurs, the yield of the reaction begins to decrease upon further increase in ambient reaction temperature (see, e.g., Ibisi and Brown, 1967; Ley and Low, 1989). The yield may even reach a plateau with temperature, and then decrease when the temperature reaches a certain value or higher, as observed by Segal and Wang (1981) when investigating the degradation of thymine. In this case, the observed temperature effect was dominated by the reaction kinetics in and around the cavitating bubble. They argued that since thymine was relatively nonvolatile, the degradation reaction was occurring in the gas-liquid film between the cavitating bubble and the bulk liquid mixture (which will be discussed in greater detail in Section 2.7). As the reaction temperature increased, the rate of diffusion of thymine from the bulk liquid phase to the reaction zone was accelerated, thus increasing the yield. However, the increase in temperature was also simultaneously decreasing the intensity of cavitation, thus reducing the amount of free-radicals produced within the bubble. It was speculated that these free-radicals were required for the degradation reaction to occur, and that they diffuse from the vapor cavity to the gas-liquid film where reaction ensues. As the rates of the counterdiffusing reactants became comparable, a further increase in temperature had little or

no effect on the reaction (i.e., the yield plateaued as a function of temperature). However, as the temperature continued to be increased, the declining production of free-radicals began to have a negative effect on the reaction rate, and the yield decreased.

c. Ambient pressure

An increase in the ambient reaction pressure generally results in an overall increase in the sonochemical effect, as found by Moulton *et al.* (1987) when they were investigating the hydrogenation of soybean oil. The vapor pressure of the mixture was reduced while the cavitation threshold was increased with increasing system pressure. This increased the implosion, thus increasing the ultrasonic energy produced upon cavitation.

However, there is a limitation to this, as found by Moulton *et al.* (1983) when investigating the ultrasonic hydrogenation of soybean oil. When operating at an ambient pressure of 200 psig and greater, ultrasound had little effect on the catalyst activity. Yet, when the pressure was decreased to 115 psig, the effects of ultrasound were significantly increased. It appeared that operating at pressures of 200 psig and above increased the cavitation threshold in the system to a level at which the cavitation bubbles could no longer be produced, or were produced in such small quantities that they did not significantly affect the overall reaction. For any given system an optimum operating pressure will most likely exist (see, e.g., Berlan *et al.*, 1994).

As discussed in **Section 2.3.1.*a***, changing the hydrostatic pressure can alter the resonance frequency (Equation (6)) and equilibrium radius (Equation (4)) of the bubble, and drive the system towards a resonance conditions. This approach was taken by Cum *et al.* (1988) who

found that operating the system under resonance conditions increased the rate and yield of the reaction.

d. Choice of solvent

The natural cohesive forces of the solvent have a small affect on the formation and cavitation of microbubbles (Lorimer and Mason, 1987), with the greatest cavitational effects occurring in solvents with a higher viscosity. In addition, it is advisable to select a solvent with a low volatility because vapor within the bubble cushions the implosion, reducing the cavitational intensity. As found by several researchers (see, e.g., Fitzgerald *et al.*, 1956; Luche *et al.*, 1987b), cavitation is inhibited when the extremely volatile solvent diethyl ether, with vapor pressure of ~0.73 atm at 25 °C, is used as a solvent.

e. Sample preparation

The amount of time between sample preparation and sonication may affect the length of sonication time required before maximum cavitational intensity is achieved. When Henglein *et al.* (1992) sonicated their samples within 10 minutes after the solids were added to the solvent, 5 pulse numbers were required before maximum intensity was observed in the solution (they were using a 5-ms ultrasonic pulse train and measured intensity by the detection of luminescence signals). However, when the sample was left to sit for 9 days before the application of ultrasound, only 2 pulse numbers were required and the maximum intensity was higher than observed in the 10 minute sample. They speculated that this behavior could be

due to the behavior of the dissolved solids, which may have introduced dust particles into the mixture, acting as nucleation sites for cavitation.

f. Choice of buffer

If buffers are used which liberate CO_2 in the presence of ultrasound, such as sodium carbonate and calcium carbonate, the sonochemical effect will be decreased (Geier, 1989). The presence of CO_2 interferes with the delivery of the sound waves to the reaction medium.

g. Ultrasonic frequency

The frequency of the ultrasound has a significant effect on the cavitation process because it alters the critical size of the cavitation bubble. At very high frequencies, the cavitational effect is reduced because either (1) the rarefaction cycle of the sound wave produces a negative pressure insufficient to initiate cavitation or (2) the compression cycle occurs faster than the time required for the microbubble to collapse. In the past, typical sonochemical reactions were carried out at frequencies between 20 and 50 kHz. In some reactions, alteration of frequency has no apparent effect, such as the in the dissociation of carbon disulfide (Entezari *et al.*, 1997). However, in other reactions, such as oxidations, current research is finding that higher frequencies may lead to higher reaction rates. For example, the rate of sonochemical oxidation of iodide in the presence of air was 31 times greater when operating at a frequency of 900 kHz compared to operating at a frequency of 20 kHz (Entezai and Kruus, 1994). The huge increase in the rate of oxidation was not due to a larger power input, because the 900 kHz operating system had a power input of 25 W, while 20 kHz had a power input of 39 W.

With the knowledge of which frequency and reaction atmosphere resulted in the greatest cavitational intensity, the authors performed the same experiments under an atmosphere of argon and found that at 20 kHz the rate of oxidation was 1.14 times greater in the presence of argon than in the presence of air. This was expected as discussed in **Section 2.3.2.*a***. However, when operating at 900 kHz, the rate was 3.13 times greater in air. It seems likely, therefore, that although the intensity of cavitation was lower in the presence of air because of its lower polytropic ratio, the formation of hydroxyl radicals from the air-water mixture was increased due to the larger number of cavitational events at 900 kHz, thus increasing the rate of oxidation of iodide. These findings were reinforced in a subsequent studies (Petrier *et al.*, 1992b; Entezari *et al.*, 1996). However, Petrier *et al.* (1992b) also reasoned that since bubble lifetimes were shorter at higher frequencies (3×10^{-7} s at 514 kHz as compared to 3×10^{-5} s at 20 kHz), that the OH radicals have an opportunity to escape the cavitation bubble before undergoing any reaction. A similar hypothesis was been proposed by Mason *et al.* (1994) who speculated that the escape of the OH radicals to the bulk solution increases their availability for reaction.

The rate of sonochemical degradation of carbon tetrachloride was increased when using a frequency of 500 kHz, as compared to 20 kHz (Francony and Petrier, 1996). Each frequency level had a constant power dissipation of 30 W, and produced Cl^- and CO_2 as the primary products of degradation. However, these products were produced at a faster rate when operating at 500 kHz. When investigating a similar reaction, the degradation of trichloroethylene at 20 and 520 kHz, Drijvers *et al.* (1996) concluded that the reaction was "energetically more efficient" at 520 kHz. As a side note, the same authors also investigated

the effect of pH on the degradation kinetics and found that the rate constant increased as the buffer solution became more basic.

In conclusion, lower frequency ultrasound produces more violent cavitation, leading to higher localized temperatures and pressures at the cavitation site. However, higher frequencies may actually increase the number of free radicals in the system because, although cavitation is less violent, there are more cavitational events, thus more opportunities for free radicals to be produced (Crum, 1995). In addition, the shortened bubble lifetime may increase the amount of free-radicals which are able to escape from the cavitation site to the bulk mixture, where they facilitate the bulk reaction. It is contended that the optimum frequency is system specific and depends on whether intense temperatures and pressures are required, or if the rate of single electron transfer is more important.

h. Acoustic power

Many authors have found that as the power delivered to the reaction mixture increases, the rate of the reaction increases to a maximum and then decreases with a continued increase in power (see, e.g., Gutierrez and Henglein,1990). A possible explanation for the observed decrease at high powers is the formation of a dense cloud of cavitation bubbles near the probe tip which acts to block the energy transmitted from the probe to the fluid (see, e.g., Ratoarinoro *et al.*, 1995a; Contamine *et al.*, 1994).

The optimum power level is also dependent on the operating frequency (Whillock and Harvey, 1997b). When investigating the rate of corrosion of 304L stainless steel, the authors found that curve maxima were different (i.e. different power optimums) for different

ultrasonic frequencies. No maximum was observed when operating at 20 kHz, as was also found by Hagenson *et al.* (1994) when researching the synthesis of dibenzyl sulfide.

2.3.3 Sonoluminescence

Sonoluminescence is the emission of light associated with cavitation. It was discovered in 1935 by Frenzel and Schultz when they observed a faint luminenscence over a water bath when it was exposed to intense ultrasound. No general consensus has been reached as to what causes this light emission, although several hypotheses have been postulated (see, e.g., Lepoint-Mullie *et al.*, 1996). A review of sonoluminescense was done in 1984 by Walton and Reynolds which includes several of the theories in the literature attempting to explain the origin of sonoluminescence, although they believe that it is due primarily to the recombination of free-radicals generated within cavitation bubbles during collapse. However, Suslick *et al.* (1990) accepts an alternate theory that the light emission is caused by thermally created chemiluminescence. As is evident, more work is needed before a general consensus can be reached.

The experimental work performed in the area of sonoluminescence has resulted in several interesting observations. For instance, in an air-water system, it was found that sonoluminescence intensity is highest at lower temperatures and decreases exponentially with increasing system temperature, up to temperatures of 90 °C (363 K), where it becomes undetectable (Chendke and Fogler, 1985). The sonoluminescence intensity is dependent on the solvent, as it increases in the order of MeOH ~ EtOH < *n*-PrOH ~ *t*-BuOH < C_6H_6 (Sehgal *et al.*, 1977). It is also dependent on the dissolved gas in solution, as it decreases with

increasing thermal conductivity of dissolved rare gas in the order of Xe > Kr > Ar > Ne > He (Hickling, 1963). A theoretical study of sonoluminescence was published in 1993 by Kamath *et al.*

2.3.4 Estimation of ultrasonic parameters

The following sections and Table 2.2 provide a summary of pertinent ultrasonic parameters which have been estimated by different authors either through experimental research or model simulations. While the actual values of the parameters are system dependent, the values in the table are provided as estimates of orders of magnitude for modeling studies.

a. Ultrasonic velocities in pure fluids and mixtures

The ultrasonic velocity in pure fluids can be determined as a function of bulk temperature and carbon number using Equation (12)

$$v = a + \frac{c}{C} - \left(d + \frac{e}{C}\right)T \tag{13}$$

where the constants have been determined by Wang and Nur (1991) for *n*-alkanes and 1-alkenes, as given in Table 2.3 (units of v [=] m/s and T [=] °C). Values are also given in the reference for naphthenes as a function of temperature alone. As shown by Equation (12), the velocity increases linearly as the bulk temperature of the fluid decreases. In addition, the velocity increases as a function of carbon number, but the magnitude of the increase decreases with increasing carbon number.

Table 2.2. Estimates of parameters necessary for modeling of ultrasonic systems.

	Definition	Value	System conditions	Method of Determination	Dependent Upon	Reference
n	number of cavitation bubbles per unit time and liquid volume	2.6×10^{10} l/ℓ s	aqueous solvent ultrasonic bath freq: 20 kHz	model simulation	power input frequency vessel type position in vessel solvent dissolved gases	Prasad Naidu *et al.* (1994)
		4×10^5 l/ℓ s	organic solvent mixtures ultrasonic probe freq: 20 kHz	chemical dosimeter reaction kinetics	power input frequency solvent dissolved gases	Suslick and Hammerton (1986)
P_f	final pressure (maximum produced by collapsed bubble)	78 atm	aqueous solvent ultrasonic bath freq: 20 kHz	model simulation	bubble contents bulk liquid temp.	Prasad Naidu *et al.* (1994)
R_o	initial cavity size	2.0 μm	aqueous solvent ultrasonic bath freq: 20 kHz	model simulation	power input frequency	Prasad Naidu *et al.* (1994)
t_o	transient bubble collapse time	3.5 μs	aqueous solvent ultrasonic bath freq: 20 kHz	model simulation		Prasad Naidu *et al.* (1994)
T_f	final temperature (maximum produced by collapsed bubble)	2064 K	aqueous solvent ultrasonic bath freq: 20 kHz	model simulation	bubble contents bulk liquid temp.	Prasad Naidu *et al.* (1994)
v_{mj}	microjet velocity (jet perpendicular to solid surface)	100 m/s	water	microcinemagraphic sequences and flash microphotography		Suslick *et al.* (1990a)

Table 2.3. Values given for the constant terms in Equation (12).

Compound	a	c	d	e	reference
n-alkanes	1585.6	-2482.1	3.2594	7.4070	Wang and Nur (1991)
1-alkenes	1569.4	-2379.2	3.0804	8.8784	

The compressional velocity of ultrasound in a hydrocarbon mixture can be determined from the simple relationship (Wang and Nur, 1991)

$$v_{mixture} = \sum_{i=1}^{n} X_i v_i \tag{14}$$

where X_i and v_i are the volume fraction and pure component velocity of the i^{th} component in the mixture, respectively.

b. Acoustic power measurement

There are several methods available in the literature to determine the power dissipated (P_{diss}) in a reaction mixture. However, many authors have not reported the acoustic power dissipated in their reaction systems, making it difficult for future researchers to reproduce results or compare reaction conditions. One of the most common approaches used to determine the ultrasonic power dissipated in a reaction system is calorimetry, which assumes that all of the energy delivered to the system is dissipated as heat, as shown by

$$P_{diss} = \left(\frac{dT}{dt}\right)_{t=0} m_{solvent} C_{p,\ solvent} \tag{15}$$

where $m_{solvent}$ and $C_{p,\ solvent}$ are the mass and heat capacity of the solvent, respectively, and $(dT/dt)_{t=0}$ is the initial slope of the temperature rise of the reaction mixture versus time of

exposure to ultrasonic irradiation. The initial temperature rise of the system is independent of the initial bulk liquid temperature (below 40 °C), the height of the liquid in the vessel, and the horn height (see, e.g., Kimura *et al.*, 1996; Ratoarinoro *et al.*, 1995a).

When Hagenson and Doraiswamy (1997) used Equation (15) to estimate the power dissipated in their reaction system, they found it to be inadequate. It predicted that only 33% of the power delivered by the transducer was dissipated as heat, which would indicate that the other 67% of the power was lost in the transfer process, or by other means. It was concluded that Equation (15) needed to be modified to account for the heat absorbed by the reaction vessel as well as the solvent, as shown by

$$P_{diss} = \left(\frac{dT}{dt}\right)_{t=0} \left(m_{solvent} C_{p,\cdot solvent}\right) + \left(\frac{dT_v}{dt}\right)_{t=0} \left(A_{ws} x_w\right) \rho_{vessel} C_{p,\cdot vessel} \qquad (16)$$

where T_v is the temperature of the inner vessel wall (refer to article for figure), A_{ws} is the area of the wetted surface of the vessel, and x_w is the thickness of the inner wall. This provided a much more reasonable result. It was found that 57.5% of the power delivered by the probe was dissipated as heat, more closely agreeing with the manufacturer's information.

Other methods of determining the power dissipated in a reaction system are by using chemical dosimeters, such as the generation of HNO_3 from NO_3 in water (Koda *et al.*, 1996) and the Weissler reaction which measures the liberation of iodine from potassium iodide. A recent comparison of calorimetry and the Weissler reaction as measures of ultrasonic power (Kimura *et al.*, 1996) showed that the two methods give similar predictions.

The losses in a ultrasonic system occur several different ways. First, there is a loss of energy in the conversion of electrical energy to mechanical, or sound, energy. There are also losses by heat production, by the production of cavitation bubbles, and by sonoluminescence. There are losses from attenuation of energy through the fluid, also called viscous dissipation. In addition, anything added to the reactor, such as baffles, cooling coils, impellers, solid particles, and the walls of the vessel themselves, will cause losses due to reflection, absorption, and sound re-emission.

c. Ultrasonic intensity

The maximum ultrasonic intensity (I_{max}) is related to the pressure amplitude (P_A) by the following equation

$$I_{max} = \frac{P_A^2}{2\rho C} \tag{17}$$

where ρ is the density of the liquid medium and C is the velocity of sound in that medium. The intensity (I) will decrease as the distance from the transmitting source (d_T) increases, as shown by

$$I = I_{max}\, exp(-2\alpha d_T) \tag{18}$$

where α is the attenuation coefficient of the medium.

When using a probe system, the intensity (I_{diss}) of ultrasound at the surface of the ultrasonic device is equal to the power dissipated (P_{diss}) divided by the area of the probe tip (A_p), as shown by Equation (19), and is typically expressed in W/cm^2.

$$I_{diss} = P_{diss}/A_p \quad (19)$$

The acoustic intensity can also be quantitatively determined using a chemical dosimeter such the decomposition ratio of 5,10,15,20-tetrakis(4-sulfotophenyl) porphyrin (H_2TPPS^{4-}) (Nomura *et al.*, 1996).

2.4 Applications in Organic Synthesis

A significant amount of work has been published concerning the sonochemical effect on various systems in organic synthesis. Reviews of recent advances in organic synthesis were published by Bremner (1994) and Low (1992). Several books have chapters devoted to organic synthesis (see, e.g., Suslick, 1988; Ley and Low, 1989; Mason, 1990a,b; Price, 1992). Table 2.4 contains a representative list of organic reactions studied under the influence of ultrasound. These reactions (homogeneous and heterogeneous) are classified under the following heads:

A. Ultrasound initiates reaction

B. Ultrasound accelerates the rate of reaction

C. Ultrasound changes reaction pathway

D. Ultrasound has little or no effect on reaction

As is evident when reviewing the examples given in the table, reactions following an ionic mechanism are often unaffected, or only slightly affected, by ultrasound. In some cases ultrasound actually changes the pathway of the reaction by favoring free-radical mechanisms in reactions which follow either an ionic or free-radical pathway, depending on the reaction

parameters. Sonochemical activation of chemical reactions (i.e. the "true" sonochemical effects) occur if reactions requiring radicals or radical ion intermediates are key steps in the mechanism (see, e.g., Luche, 1992).

In addition to the reactions shown in Table 2.4, several other reactions have been investigated, such as: the esterification of several carboxylic acids (Khurana *et al.*, 1990), the chemical alteration of aqueous polycyclic aromatic hydrocarbons (Wheat and Tumeo, 1997), and the production of aldehydes from olefins in the presence of a water soluble rhodium-containing catalyst system (Cornils *et al.*, 1986). While the high temperatures created during cavitational implosions explain some of the bond cleavages observed as a result of sonication, the role of transient high pressure, electron exchange, and stereochemical effects must be investigated in greater detail (Luche, 1996). The importance of electron exchange was recently undertaken by Takizawa *et al.* (1996) using the hydroxylation of phenolic compounds.

Ultrasound has also been found to be very useful in the degradation of contaminants in water (Hoffmann *et al.*, 1996) such as chlorofluorocarbons CFC 11 and CFC 13 (Cheung and Kurup, 1994); HCFC-225ca, HCFC-225cb and HFC-134a (Hirai *et al.*, 1996); the pesticide parathion (Kotronarou *et al.*, 1992a); sodium hypochlorite (Mason *et al.*, 1996); pentachlorophenate (Petrier *et al.*, 1992a) and *p*-nitrophenol (Kotronarou *et al.*, 1991). Sonication also led to the complete destruction of aqueous solutions of chlorinated hydrocarbons such as methylene chloride, carbon tetrachloride, trichloroethylene, and α1,1,1-trichloroethane (Cheung *et al.*, 1991; Toy *et al.*, 1992 and 1990).

Table 2.4. Representative list of organic synthetic reactions studied under the influence of ultrasound.

Homogeneous Reactions:

TYPE	REACTION	TRADITIONAL CONDITIONS	ULTRASONIC CONDITIONS	REFERENCE
B	Diels-Alder cyclization reaction 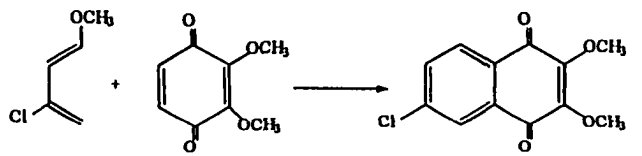 Solvent: toluene (benzene and methylene chloride are also investigated as solvents with different results) Other Diels-Alder cyclizations are reported	Stirring Conditions not specified Rxn time: 35.0 hrs Yield: 77.9%	Probe system Freq: 20 kHz Temp: 25 °C Rxn time: 3.5 hrs Yield: 97.3%	Javed *et al.* (1995)
D	Acid catalyzed ketalization of acetophenone 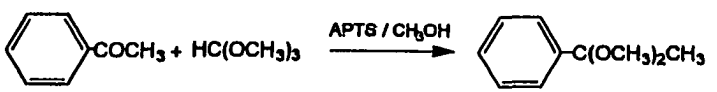 Follows an ionic mechanism	Stirring Temp: 12 °C Rxn time: 30 min Yield: 44% Rxn time: 3.5 hrs Yield: 94%	Bath system Temp: 12 °C Rxn time: 30 min Yield: 48% Rxn time: 3.5 hrs Yield: 94%	Einhorn *et al.* (1990)
B	Oxidation of indane to indan-1-one 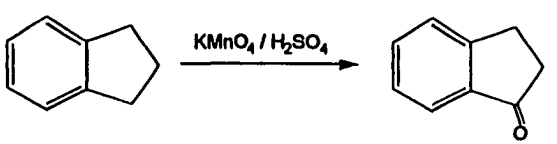	Stirring: 500 rpm Temp: 25 °C Press: 760 torr Rxn time: 3 hrs Yield ≤ 27% $k_{obs} = 5.12 \times 10^{-5}\ s^{-1}$	Probe system Freq: 21.5 kHz Power*: 90 W Temp: 25 °C Press: 760 torr Rxn time: 3 hrs Yield = 73% $k_{obs} = 2.96 \times 10^{-4}\ s^{-1}$	Cum *et al.* (1988)

Table 4, *continued.*

C	Kornblum-Russell alkylation of nitronate anions 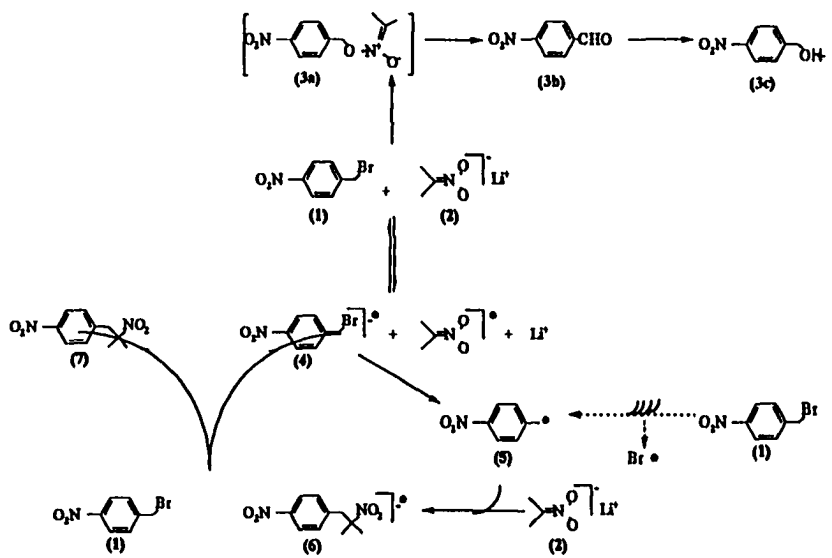 Ultrasound favored sequential electron transfer process over the polar (simultaneous bielectronic) mechanism Ratio of 7:3c reached a maximum with ultrasound power except in the case of standing waves, where the ratio continued to increase	Stirring Product: **3b**	Probe system Power: range of 0 - 35000 V^2 investigated Products: 7 and 3c in various ratios Effect of standing waves investigated and found to promote S_N1 pathway	Dickens and Luche (1991)
B	Solvolysis of 2-chloro-2-methylpropane 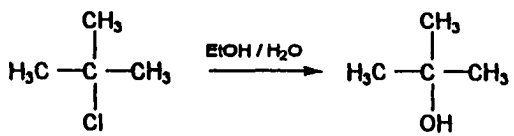 Solvent: 30% ethanol (v/v) aqueous solution	Temp: 0.5 °C Conversion: 85% k_{obs}: 2.43 x 10^{-4} s^{-1}	Bath system Freq: 80 kHz Power*: 100 W Temp: 0.5 °C Conversion: 85% k_{obs}: 4.30 x 10^{-4} s^{-1}	Lorimer and Mason (1980)

Table 4, *continued.*

B	Alkaline hydrolysis of nitrophenyl esters 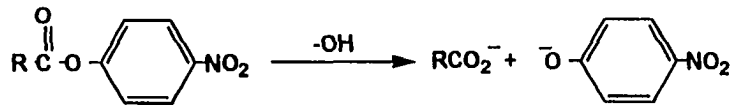 Compound 1: R = CH_3- 2: R = CH_3CH_2- 3: R = $(CH_3)_2CH$- 4: R = $(CH_3)_3C$- Solvent: 60:40 (v/v) mixture of pH 8.0 THAM buffer and acetonitrile	Stirring Conditions not given	Bath system Freq: 20 kHz Temp: 35 °C ~ 14.5% enhancement over stirring for all 4 compounds	Kristol *et al.* (1981)
			* Power rating quoted by the manufacturer	

Heterogeneous Reactions:

TYPE	REACTION	TRADITIONAL CONDITIONS	ULTRASONIC CONDITIONS	REFERENCE
B	Synthesis of 5,5-disubstituted hydantoins 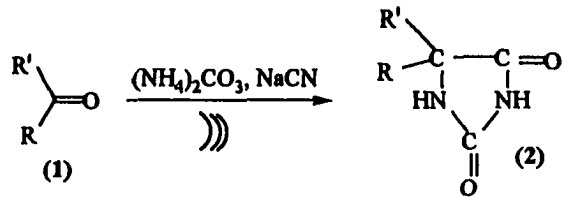 (1) (2) In one case, when R = *p*-ClC_6H_4COMe, conventional conditions did not yield the desired product (2), but the use of ultrasound led to an isolated yield of (2) of 96%	Stirring Several rxns studied (with different substrates): Rxn time: 4 - 26 hrs Temp: 58 - 70 °C Yield: 0 - 92%	Bath system Same set of reactions studied Rxn time: 3 - 4.5 hrs Temp: 45 - 50 °C Yield: 45 - 96%	Li *et al.* (1996)

Table 4, *continued.*

B	Epoxidation of long-chain unsaturated fatty esters 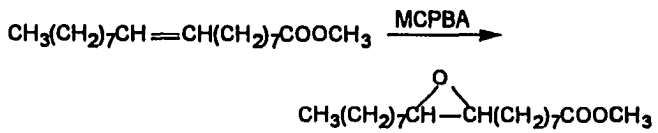 MCPBA = *m*-chloroperoxybenzoic acid Also experimented with reagent MMPP (magnesium mono-peroxyphthalate) in place of MCPBA Other examples of epoxidation reactions are given in article	Stirring Conditions not specified Rxn time: 2 hrs Yield: 48%	Probe system Freq: 20 kHz Temp: 20 °C Rxn time: 15 min Yield: 92%	Lie Ken Jie (1995)
B	Oxidation of arylalkanes 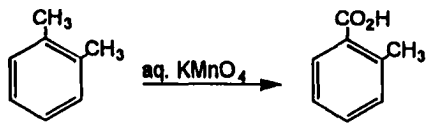 Solvent: water Other examples of oxidation reactions are given in article	Stirring: 150 rpm Temp: 30-35 °C Rxn time: 4 hrs Yield: 12%	Bath system Freq: 23 kHz Power*: 120 W Temp: 30-35 °C Rxn time: 4 hrs Yield: 80%	Soudagar and Samant (1995a)
B	Grignard reagent formation (several examples are given and different factors are varied and investigated)			Tuulmets *et al.* (1995)
B	Michael addition of nitroalkanes to monosubstituted α,β-unsaturated esters 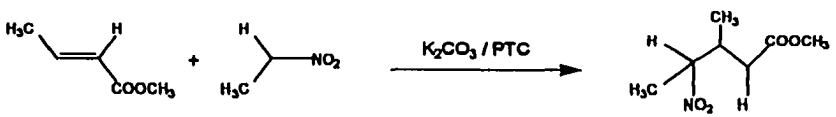 PTC: Aliquat® 336 Other examples of Michael addition reactions are given in article	Temp: 40 °C Rxn time: 2 days Yield: 85%	Bath system Freq: 60 kHz Power*: 80-160 W Temp: 25 °C Rxn time: 2 hrs Yield: 90%	Jouglet *et al.* (1991) Note: several other reactions are given in article

Table 4, *continued.*

B	Permanganate oxidation of 2-octanol 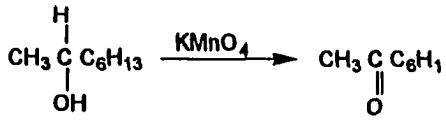 Solvent: hexane Other examples of reactions involving inorganic solids in organic solutions given in article	Stirring Temp: 50 °C Rxn time: 5 hrs Yield: 3%	Bath system Temp: 50 °C Rxn time: 5 hrs Yield: 93%	Ando and Kimura (1990)
B	*tert*-Butoxycarbonylation of amines from their salts 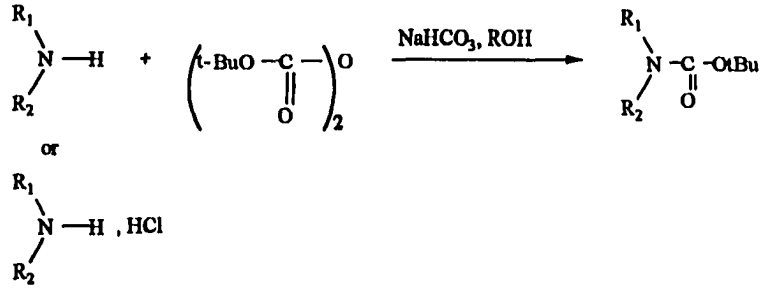 16 BOC preparations reported	Stirring Rxn time: >24 hrs	Bath system Rxn time: 1.5 - 6 hrs Yield: > 98% Solvent: Ethanol Also used methanol in some cases	Einhorn *et al.* (1991)
	Use of ultrasound in the preparation of biologically active compounds			Low (1995)
B	Synthesis of chalcones by Claisen-Schmidt condensation 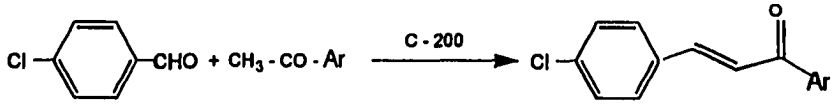 Solvent: ethanol (96%) Catalyst: activated barium hydroxide C-200	Stirring Temp: 25 °C Rxn time: 60 min Yield: 5% Catalyst wt: 1.0 g	Bath system Temp: 25 °C Rxn time: 10 min Yield: 76% Catalyst wt: 0.1 g	Fuentes *et al.* (1987b)

Table 4, *continued.*

B	The o-alkylation of 5-hydroxy chromones 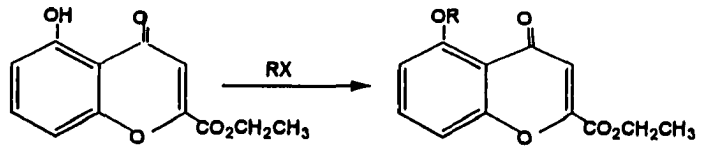 RX = benzyl bromide Solvent: N-methylpyrrolidinone (NMP) Other examples are given in article	Stirring Temp: 65 °C Rxn time: 105 min Yield: 48%	Probe system Temp: 65 °C Rxn time: 60 min Yield: 79%	Mason *et al.* (1990d)
B	Diels-Alder cycloaddition of *o*-quinone 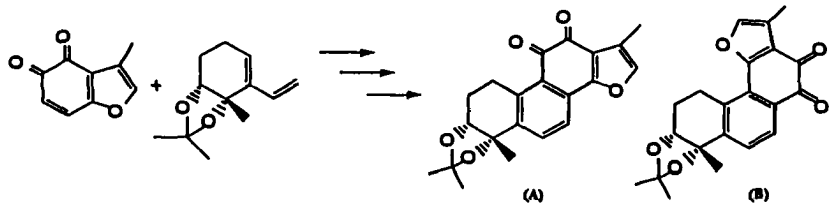 Ultrasound increased yield of cycloadducts and improved regioselectivity Other examples are given in article	Refluxing with benzene Yield of cycloadducts: 15% (**A**:**B**) = (1:1)	System not specified Yield of cycloadducts: 76% (**A**:**B**) = (5:1)	Lee and Snyder (1989)
B	Strecker synthesis of α-aminonitriles using an alumina support  Support: Al_2O_3 (improves the selectivity of $PhCH(CN)NH_2$) Solvent: acetonitrile Other examples of Strecker synthesis are given in article	Stirring Temp: 50 °C Rxn time: 24 hrs Yield: 64%	Bath system Freq: 45 kHz Power*: 100 W Temp: 50 °C Rxn time: 24 hrs Yield: 90%	Hanafusa *et al.* (1987), see also Menendez *et al.* (1986)

Table 4, *continued.*

B	Preparation of tricyclohexylborane by hydroboration 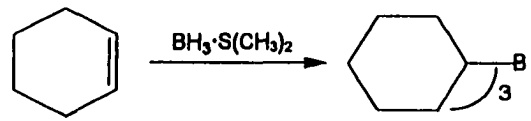 Solvent: tetrahydrofuran (THF)	Stirring Temp: 25 °C Rxn time: 24 hrs	Bath system Freq: 50 kHz Power*: 150 W Temp: 25 °C Rxn time: 1 hr	Lindley and Mason (1987b) Note: several other reactions are given in article
B	Ullmann coupling of 2-iodonitrobenzene 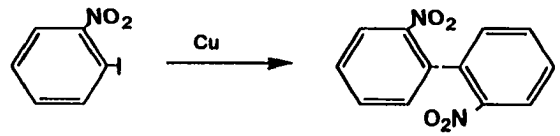 Mole ratio of Cu / substrate = 4 Copper powder presonicated for 15 minutes	Stirring Temp: 63 ± 1 °C Rxn time: 2 hrs Yield < 1.5%	Microtip probe system Freq: 20 kHz Power*: 135 W Temp: 63 ± 1 °C Rxn time: 2 hrs Yield: 70.4%	Lindley *et al.* (1987a)
B	Barbier reaction: retention of optical activity from S(+) 2-octyl halides 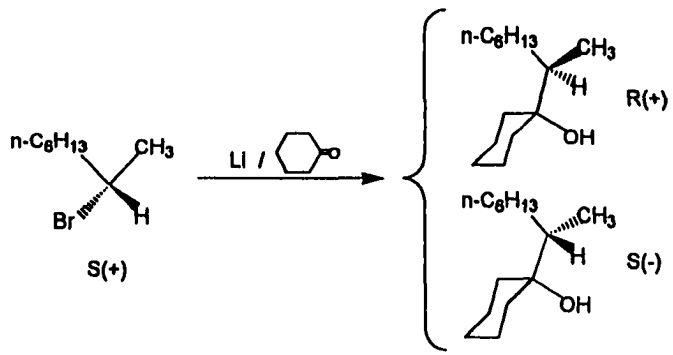 Solvent: tetrahydrofuran (THF) Other examples are given in the article with Cl or I as the halide	Stirring Temp: 0 °C Rxn time: 7 hrs Yield: 50% Configuration: R(+) %e.e: 6	Probe system Temp: 0 °C Rxn time: 30 min Yield: 59% Configuration: R(+) %e.e: 10	de Souza-Barboza *et al.* (1987), see also de Souza-Barboza *et al.* (1988)

Table 4, *continued.*

B	Selective reduction of α, β-unsaturated carbonyl compounds in the presence of Zn-$NiCl_2$ 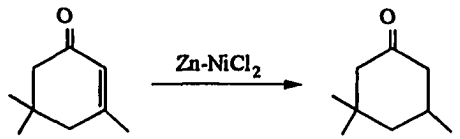 Solvent: Ethanol and water Nine other examples are given in the article	Stirring Rxn time: 48 hrs Conv: 62%	System conditions not specified Rxn time: 2.5 hrs Conv: 97%	Petrier and Luche (1987a)
B, D	Acyloin condensation and cyclization of carboxylic esters (15 examples given in article)			Fadel *et al.* (1990)
A	Reduction of methoxyaminosilane 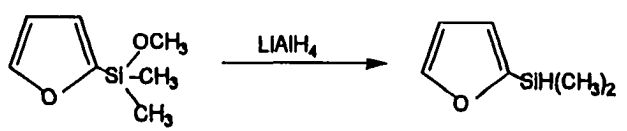 Solvent: pentane	Stirring No reaction	Bath system Temp: 35 °C Rxn time: 3 hrs Yield: 100%	Bremner (1986)
B	Synthesis of aldehydes from olefins and CO/H_2 using a water-soluble rhodium-containing catalyst	U.S. patented process		Cornils *et al.* (1986)
B	Platinum catalyzed hydrosilation of alkenes 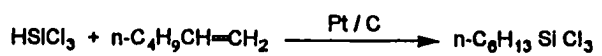 Other examples of hydrosilation reactions are reported	No reactions are given for direct comparison Wagner and Strother (1953) have performed these types of reactions at 45-115 psi and 100- 300 °C	Bath system Temp: ~ 30 °C Pressure: atmospheric Rxn time: 1 hr	Han and Boudjouk (1983)

Table 4, *continued.*

C	Change in pathway from the Friedel-Crafts reactions to nucleophilic substitution 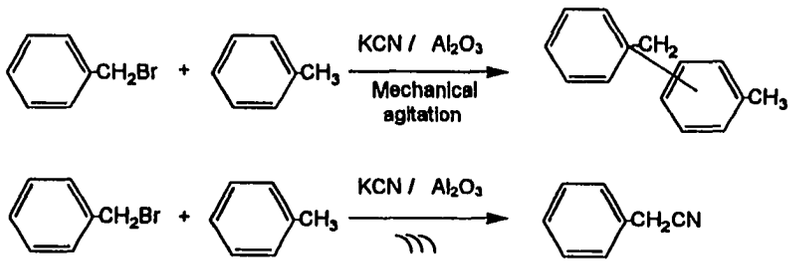	Stirring Temp: 50 °C Product: o- and p-benzyltoluene Yield: 75%	Bath system Freq: 45 kHz Power*: 200 W Product: benzyl cynanide Yield: 71%	Ando *et al.* (1984)
B	Reformatsky reaction 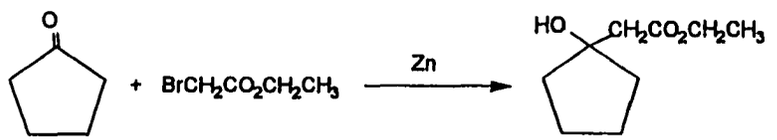 Various solvents and types of zinc powders were tested Other examples of Reformatsky reaction are given in article	Stirring Temp: 80 °C Rxn time: 12 hrs Yield: 50%	Bath system Freq: 50/60 Hz Power*: 150 W Temp: 25 - 30 °C Rxn time: 30 min Yield: 98%	Han and Boudjouk (1982), see also Boudjouk and Han (1984)
B	Aromatic carboxylic acid ester saponification Increased the yield or obtained similar yields to stirring in shorter reaction times	Reflux Rxn time: 90 min	Probe system Freq: 20 kHz Rxn time: 10 min	Moon *et al.* (1979), Moon (1987)
			* Power rating quoted by the manufacturer	

2.4.1 Homogeneous systems

a. Aqueous systems

The use of ultrasound in aqueous solutions leads to the sonolysis of the components of the solution, such as in the case of water where $H_2O \rightarrow OH^{\cdot} + H^{\cdot}$ (see, e.g., Henglein, 1987 and 1985). The free radicals in these solutions have been detected by spin trapping and ESR measurements (Riesz *et al.*, 1990; Krishna *et al.*, 1987; Mankino *et al.*, 1982 and 1983; Henglein and Kormann, 1985), a terephthalate dosimeter (see, e.g., Fang *et al.*, 1996), and a Fricke solution dosimeter (see, e.g., Jana and Chatterjee, 1995). In addition, the mechanism of radical formation has been investigated using isotopic techniques (see, e.g., Fisher *et al.*, 1986). Sonolysis of aqueous mixtures will be discussed in greater detail in **Section 2.7**.

b. Organic systems

As in the case of aqueous systems, the enhancing effects of ultrasound are not directly related to its thermal effects, but are instead a result of acceleration of the single electron transfer process. This step is required as an initial step in several reactions, such as cycloadditions involving carbodienes and heterodienes (Nebois *et al.*, 1996). In the cases where the reaction mechanism did not seem to require an SET step, ultrasound was found to have little or no effect on the reaction. It has also been found that adjusting the system to obtain standing waves has the favorable result of increasing a sequential electron transfer process and promoting it over a bielectronic mechanism (Dickens and Luche, 1991).

The degradation of CCl_4 was investigated in a variety of organic alcohols at two different frequencies, 20 kHz and 500 kHz (Petrier *et al.*, 1994). For each alcohol (methanol, butanol,

and 1,2-ethanediol) the rate constant for degradation was higher for 20 kHz than for 500 kHz. However, the magnitude of the difference was solvent dependent, with the largest difference with butanol and the smallest with 1,2-ethanediol. The reaction was also found to be faster in the presence of argon, as compared to the rate in the presence of oxygen.

2.4.2 Heterogeneous systems

a. Liquid-liquid systems

Ultrasound forms very fine emulsions in systems with two immiscible liquids, which is very beneficial when working with phase transfer catalyzed or biphasic systems (as will be discussed in Sections 2.6.1 and 2.6.2). When very fine emulsions are formed, the surface area available for reaction between the two phases is significantly increased, thus increasing the rate of the reaction. This aspect of ultrasound has also been used for coal, oil and water mixtures to increase the efficiency of combustion, as well as decrease the amount of pollutants produced during the combustion process (Dooher *et al.*, 1980).

b. Liquid-solid systems

The most pertinent effects of ultrasound on liquid-solid systems are mechanical, and are attributed to symmetric and asymmetric cavitation. When a bubble is able to collapse symmetrically, localized areas of high temperatures and pressures are generated in the fluid. In addition, shock waves are produced which have the potential of creating microscopic turbulence within interfacial films surrounding nearby solid particles, also referred to as microstreaming (Elder, 1959). This phenomena increases the transfer of mass across the film,

thus increasing the intrinsic mass transfer coefficient, as well as possibly thinning the film. Hagenson and Doraiswamy (1997) obtained evidence of a 2 fold increase in intrinsic mass transfer coefficient when modeling experimental data obtained for the synthesis of dibenzyl sulfide in the presence and absence ultrasound.

The shock waves produced by cavitation bubbles also increase the momentum of solid powders in solution, causing them to collide with such force that they fracture, leading to an overall decrease in the average particle size of inorganic solids. The particle size of inorganic solid KOH was reduced from its initial size of 240 μm to 15-20 μm within 5 minutes of sonication (Ratoarinoro *et al.*, 1992). Hagenson and Doraiswamy (1997) confirmed this trend when working with sodium sulfide (Na_2S). The particle size was reduced from an average initial size of 34 μm to 15 - 20 μm within 15 minutes, as shown in Figure 2.1. Figure 2.2 shows the histogram of the particle distribution, which is highly skewed to the right at lower sonication time, but becomes narrower as the exposure time is increased.

The effect of ultrasound on the particle size reduction of the inorganic particles TaS_2 and MoO_3 has also been investigated (Suslick *et al.*, 1987). The powders had an initial size distribution of 60 - 90 μm and, with sonication, were reduced to the size range of 5 to 10 μm. It may be possible to explain the minimum particle size 5 to 15 μm with the following rational: first, as the particle size decreases, the momentum of the particle generated by nearby shockwaves also decreases. At some point, i.e. some minimum particle size, the particles become too small to impact one another with the force required to cause particle fragmentation. The minimum size of particle obtained appears to depend upon the characteristics of the inorganic solid, the solvent, and the intensity of ultrasound in the system.

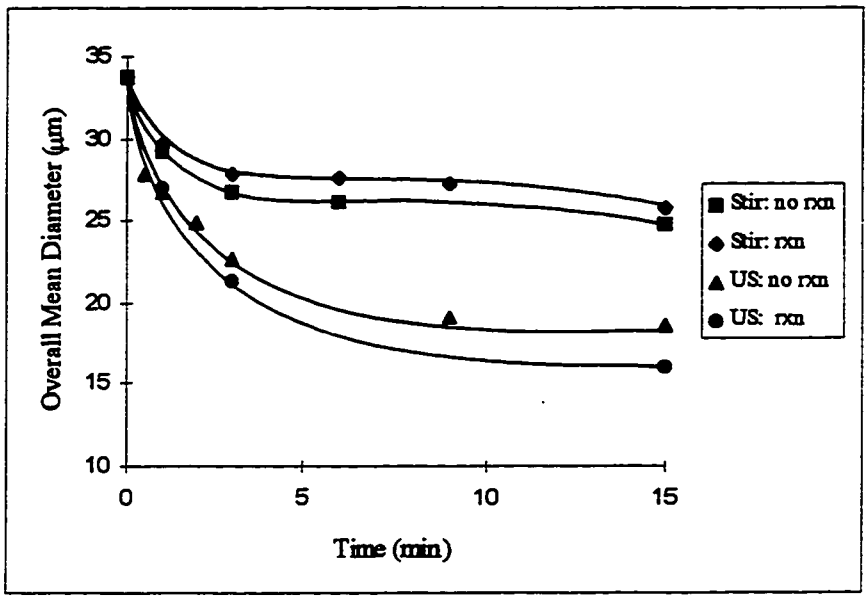

Figure 2.1. Particle degradation of Na_2S in the presence and absence of ultrasound with and without reaction (Hagenson and Doraiswamy, 1997).

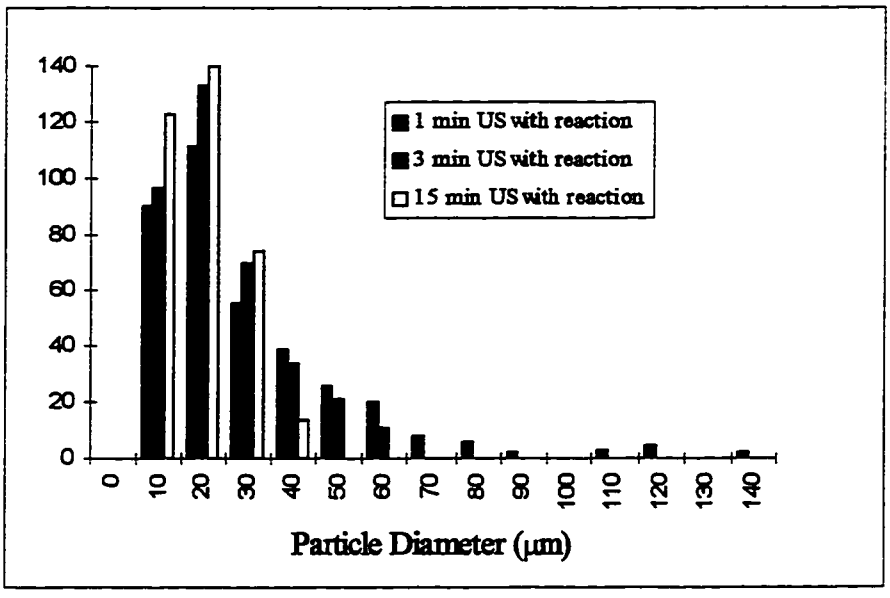

Figure 2.2. Histogram of average diameter data for samples of Na_2S in the presence of ultrasound (Hagenson and Doraiswamy, 1997).

When the bubble is collapsing near a solid surface which is several orders of magnitude larger than the cavitating bubble, i.e. a surface greater than 200 μm in diameter when operating at 20 kHz as estimated by Suslick *et al.* (1990), symmetric cavitation is hindered and collapse occurs asymmetrically (Neppiras, 1980). As the bubble collapses, microjets of solvent are formed perpendicular to the solid surface. These microjets lead to pitting and erosion of the surface, in addition to the well-known cleaning effects associated with ultrasound. This behavior leads to the enhancement of some heterogeneous reactions, such as the synthesis of silanes or organosilicon halides using magnesium hydride particles in a liquid medium. In this particular example, ultrasound facilitates the reaction by removing surface inhibiting halides from the magnesium particles, thus increasing their reactivity (Klein *et al.*, 1995).

Ultrasound can also be used to activate a solid. For example, zinc has been successfully activated for the promotion of the Simmons-Smith cyclopropanation of olefins (Repic and Vogt, 1982). Possible mechanisms behind the activation of different metal surfaces have been investigated in terms of the mechanical properties of the passivating surface layer and the passivated metal (Luche, 1994). There is a limit to the impurities ultrasound can remove, as found by Hagenson and Doraiswamy (1997). When investigating the solid phase reaction of benzyl chloride and sodium sulfide, ultrasound was not successful in removing the product layer, NaCl, from the surface of the unreacted solid, Na_2S. This product layer was responsible for limiting the rate of the reaction. Unfortunately, the amount of work done on the effect of ultrasound on inorganic impurities and surface layers is very small.

Metal powders

Metal powders behave differently from inorganic particles when exposed sonication. While inorganic particles are degraded in the presence of ultrasound, metallic particles decrease in size and then tend to agglomerate with prolonged sonication (see, e.g., Doktycz and Suslick, 1990). Using a scanning electron microscope, Doktycz and Suslick (1990) studied the agglomeration of several different metals which were ~ 10 μm in diameter. The only metal they tested which did not fuse was tungsten, with a melting point of 3410 °C. From this they concluded that the maximum collision temperature reached during sonication is less than 3410 °C. The surfaces of the particles also became very smooth over time (see, e.g., Suslick and Casadonte, 1987). From an independent experiment, they estimated the impact velocities of these small metal particles as 100 - 500 m/s. Suslick's hypothesis that the metallic particles were fusing as a result of collisions has been discredited by Margulis (1992), who contends that the particles would have to travel at speeds much higher than that of sound in liquids, which is ~ 1500 m/s.

Ultrasound has been found to successfully promote the reduction of metal ions in aqueous solutions of noble metals such as Ag, Pd, Au, Pt, and Rh in the presence of a stabilizer, producing stable, nanometer sized metal particles (Okitsu *et al.*, 1996). The atoms responsible for the reduction of the noble metals may be formed three ways: (1) by sonolysis of water, forming H·; (2) by hydrogen abstraction of RH molecules, forming R·; and (3) by pyrolysis of RH molecules during bubble collapse, forming H· or R·.

Extremely reactive metals such as lithium, magnesium, zinc and aluminum are commonly not used as catalysts because they are prone to deactivation due to the formation of coatings

on the metal surface in the presence of water or oxygen. Ultrasound has been shown to remove these coatings, making the metals viable candidates for catalysis. For example, ultrasound increases the catalytic activity of Ni powder by more than 10^5 (Suslick and Casadonte, 1987). This dramatic increase is attributed the reduction of the surface oxide layer covering the particles, as well as changes in surface morphology and the sweeping action of ultrasound. Several reactions carried out in the presence of lithium wire were also accelerated using ultrasound, such as the coupling of heteroaryl halides to form isomeric bipyridines (Osborne *et al.*, 1989) and the coupling of organic halides (Han and Boudjouk, 1981). In addition, ultrasound also activates transition-metal salts, enabling the reaction to be carried out at much milder conditions. For example, the traditional conditions used to synthesize the carbonyl anions, which are required to produce $V(CO)_6^-$, are 160 °C and 200 atm CO, plus the addition of the catalyst $Fe(CO)_5$. However, with exposure to ultrasound, the same yield of $V(CO)_6^-$ can be obtained at 10 °C and 4.4 atm of CO, without the use of the catalyst (Suslick and Johnson, 1984).

Solid catalysts

When the solid present in the medium acts as a catalyst, ultrasound can significantly influence the chemistry occurring within the system. The intensity of ultrasound can alter the stereoselectivity of a particular reaction, as observed in the case of the cyclization of the tetracyclic 19-iodotabersonine to the vindolinie epimers (Luche *et al.*, 1990b). It was determined that ultrasound affected the desorption of the radical anion from the metal surface. When the intensity of the ultrasound was low, as in the case of the ultrasonic bath system, the

desorption of the anion was slower and the stereoselectivity of the product was controlled by the absorption of the substrate. However, when the sound intensity was high, as in the case of the probe system, the desorption process was accelerated and the cyclization process occurred in the liquid phase, thus leading to lower stereoselectivity.

2.4.3 Effects on chemical bonding

In several reaction systems, ultrasound does not affect the crystalline structure of solids present in the system (see, e.g., Ando *et al.*, 1985; Hagenson and Doraiswamy, 1997), but it does affect the crystal formation of reaction products. In the presence of ultrasound an amorphous phase of palladium was synthesized by sonicating a mixture of palladium acetylactonate and toluene (Diodati *et al.*, 1997). The disordered phase of palladium had the same X-ray diffraction spectra as crystalline Pd, indicating that it was indeed a disordered phase of Pd and not a Pd-based compound such as PdH or PdO. The phase became increasingly disordered as the concentration of palladium acetylactonate in toluene increased. However, it appeared to be independent of acoustic power.

It has also been found that ultrasound affects the normal bonding of water contained within an ammonium alum crystal lattice (Homer *et al.*, 1995). Using NMR, it was detected that the water moves through the lattice when under the influence of sonication, and returns to its equilibrium sites when the ultrasound is removed. During sonication this mobility actually alters the normal melting point of the crystal, as was in the case of ammonium and potassium alums. It is speculated that ultrasound may affect other normal melting points of crystals which contain water within their crystalline lattice.

During investigations focused on the dispersion of metal powers in the presence of ultrasound, the ease of dispersion of the powder in a particular solvent was found to increase as the lattice energy of that metal decreased (Luche *et al.*, 1987b). For example, lithium could not be dispersed in toluene because the lattice energy of the metal was greater than the energy liberated by the cavitating solvent.

2.4.4 Modeling

Modeling the effects of ultrasound in a heterogeneous systems involves extremely complicated and intensive modeling efforts. Several authors have tackled segments of the modeling problem. The absorption of ultrasound in liquids containing clusters of molecules has been modeled by Lewis *et al.* (1991). The propagation of ultrasonic waves in suspensions and emulsions has been modeled by Ahuja (1973 and 1972) and Allegra *et al.* (1972), with the effect of particle shape and orientation considered by Ahuja and Hendee (1978), and the scattering effects of microparticles considered by Edwards and Jarzynski (1983). Greenwood *et al.* (1993) carried out modeling simulations which indicated that each particle in the slurry acts independently. Their experiments were conducted using a submersible transducer in the frequency range of 0.5 - 3.0 MHz. The effects of fluid viscosity, thermal properties of the system, concentration, density and elastic modulus differences between the solid and liquid were modeled by Harker and Temple (1988). Multicomponent, reacting liquid mixtures were modeled by Margulies and Schwarz (1985) using a hydroacoustic theory.

2.5 Other Applications

2.5.1 Organometallic chemistry

Table 2.5 lists a number of organometallic reactions that have been investigated under the influence of ultrasound. Please refer to the review by Luche *et al.* (1987b) and the books by Price (1992), Mason (1990a), Ley and Low (1989) and Suslick (1988) for more information on organometallic chemistry.

Table 2.5. Organometallic Reactions.

Reaction Type	Effect of ultrasound	Reference
Reduction of hexacyanoferrate (III) by thiosulfate ions mediated by $RuO_2 \cdot xH_2O$	Activation energy decreased from 20±1 kJ/mol to 18±1 kJ/mol with exposure to ultrasound	Mills *et al.* (1995)
Hydrostannation of several different substrates with Ph_3SnH	Rate enhancements of 100 to 600 times over traditional methods	Nakamura *et al.* (1989)
Synthesis of triorganylboranes	Increased yield and reduced reaction time	Brown and Racherla (1985)
Formation of iron-chromium catalyst (Fe_2O_3-Cr_2O_3)	Obtained catalyst of high quality	Romenskii *et al.* (1985)
Synthesis of π-allyltricarbonyliron complexes		Horton *et al.* (1984)
Effect on ligand substitution of metal carbonyls	Rates were first order in metal carbonyl concentration and were independent of ligand concentration	Suslick *et al.* (1983b); Suslick and Schubert (1983); Suslick *et al.* (1981)
Formation of lithium organometallic reagents	Greatly increased the rates and yields of reactions In some cases it even suppressed the formation of side reactions such as reductions and enolization	Luche and Damiano (1980)
Oxidation of aerated aqueous Fe^{2+} solutions in the presence of aliphatic alcohols	Oxidation increased in the order of MeOH<EtOH<*n*-PrOH<*n*-BuOH	Sehgal *et al.* (1980)

2.5.2 Polymerization

Reviews and books available in the literature concerning the use of ultrasound in polymerization processes include Price (1996), Urban and Salazar-Rojas (1988), Lorimer and Mason (1987), Mason (1990a,b) and Price (1992). In general, ultrasound accelerates the rates of polymerization and copolymerization, and in some cases, eliminates the need for an initiator. Ultrasound also accelerates emulsion polymerization, due to its ability to create fine emulsions (refer to **Section 2.4.2.*a***), and suspension polymerization (Hatate *et al.*, 1981), because of its prevention of agglomeration between monomer droplets with each other and with the reactor wall. The actual mechanism of polymerization in the presence of ultrasound is very complex because, in addition to combination of radicals with the primary polymer chain, existing molecules are fractured within the cavities and may combine with other molecules (see, e.g., Price *et al.*, 1990).

The copolymerization of sodium styrene sulphonate and vinyl pyrrolidone in an aqueous system was investigated at 3 different frequencies (20, 40 and 540 kHz) and at various acoustic intensities (Koda *et al.*, 1996). It was found that the rate of polymerization increased with intensity at 20 and 40 kHz, but was independent of intensity at 540 kHz. The highest conversions were obtained at 40 kHz, when the reaction rate was approximately twice as fast as the rate at 20 kHz. The kinetic model of Kruus and Patrabody (1985) was used to explain their experimental data.

Using a high power ultrasonic probe system, the polymerization of a pure vinyl monomer, methyl methacrylate, was carried out without the use of an initiator (Kruus and Patraboy, 1985). The rate of polymerization was proportional to the square root of intensity. A

polymer with an average molecular weight of 400,000 g/mol was obtained and a reaction mechanism was speculated which appeared to explain the experimental observations and produce rate constants of polymerization comparable to literature values.

The polymerization of poly(vinyl pyrrolidone) (PVP) was initiated from the sonication of vinyl pyrrolidone monomer at frequencies of 20 and 40 kHz, without the need for a catalyst (Koda *et al.*, 1995). However, polymerization did not occur at 540 kHz. It was also found that, at the lower frequencies, the yield of PVP increased linearly with sonication time, but was terminated immediately after irradiation was discontinued. Thus, sonication was required for the initiation and maintenance of the polymerization reaction.

When investigating the copolymer obtained from the reaction of acrylic acid and maleic anhydride, Lorimer and Mason (1995) found that ultrasound enhanced the chemical structure of the copolymer by changing the sequence length from 3 to 2, making the copolymer product 50% more efficient for the chelation of Ca^{2+} ions. In addition, they found that ultrasound was useful in increasing the conversion of reactants, while simultaneously degrading the polymer chain. This produced a polymer with a distribution of molecular weights which was narrower than obtained by traditional methods. They show that the degradation rate of the polymer can be determined as a function of sonication time (see also, Portenlanger and Heusinger, 1994) and power, and then used as a beneficial method to predict the mass % of the polymer chain.

2.5.3 Biotechnology

The use of ultrasound in the field of biotechnology has been investigated extensively (e.g. Sinisterra, 1992; Price, 1992; Suslick, 1988). Ley and Low (1989) have a chapter based on

enzyme-catalyzed reactions in the presence of ultrasound. Important findings in the field include the use of ultrasound to synthesize N-acetylamino acids from the amino acids and acetic anhydride without racemization (Veera Reedy and Ravindranath, 1992a). This reaction was later advantageously incorporated as a synthesis step in the production of α- , β- and cyclic spaglumic acids (Veera Reedy and Ravindranath, 1992b).

2.5.4 Medicinal uses

A number of publications and patents are available concerning the use of ultrasound for medicinal purposes. As discussed previously, ultrasound promotes the production of free-radicals in a given solvent. Similarly, continuous, 1 MHz, 1 W/cm^2 sonication enhanced the hydroxyl radical production of two anti-cancer drugs, adriamycin and mitomycin C (Tata *et al.*, 1996). It was speculated that the enhancement of these redox cycling drugs occurs according to Fenton's pathway. Exposure to ultrasound for 30 minutes did not alter the chemical structure of the drugs.

Ultrasound was also useful to a patented process in which pharmaceuticals were delivered to the body from performed porous polymeric microparticles (Supersaxo and Kou, 1995). These microparticles release low levels of a particular drug for prolonged periods of time, providing up to 30 days of controlled release. The release rate could be increased, by up to three orders of magnitude, upon exposure to ultrasound. In the absence of irradiation, the release rates returned to the presonicated levels. It was the authors hope that ultrasound could be used to deliver high doses of drugs, when needed, while continually maintaining the lower dosages in its absence.

2.6 Ultrasound in Conjunction with Other Enhancement Techniques

2.6.1 Phase transfer catalysis

Several authors have combined the use of ultrasound and phase transfer catalysts (PTC). These two enhancement techniques complement one another greatly when they are used for polyphase reactions because ultrasound has the ability to form fine emulsions between liquid-liquid phases, thereby increasing the interfacial area available for reaction. A PTC bridges the barrier between the aqueous and organic phases and facilitates the reaction between them. Hagenson *et al.* (1994) studied these combined enhancement techniques for the synthesis of dibenzyl sulfide from benzyl chloride and sodium sulfide. They found that after approximately 4 minutes of reaction, the conversion of benzyl chloride was enhanced by a factor of 1.5 in the presence of ultrasound alone, 5.9 in the presence 0.4% w/v of the PTC tetrabutylammonium bromide (TBAB), and 6.5% in the presence of both PTC and ultrasound, as shown in Figure 2.3. As is evident for this particular reaction, the use of ultrasound alone is not adequate to obtain a high yield of dibenzyl sulfide. The catalyst is required to assist with the ion exchange reaction between the sparingly soluble Na_2S and the organic liquid reactant benzyl chloride. However, ultrasound enhances the reaction even further through mechanical effects such as particle size degradation, which increases the surface area available for reaction, and the facilitation of mass transfer through the solid-liquid film (Hagenson and Doraiswamy, 1997).

The preparation of triazacyclo compounds in the presence of ultrasound and the PTC Bu_4NOH was investigated by Madison *et al.* (1994). After 5 hours of reaction time, the conversion of ethylene glycol ditosylate to 1,4,7-tritosyl-1,4,7-triazacyclononane

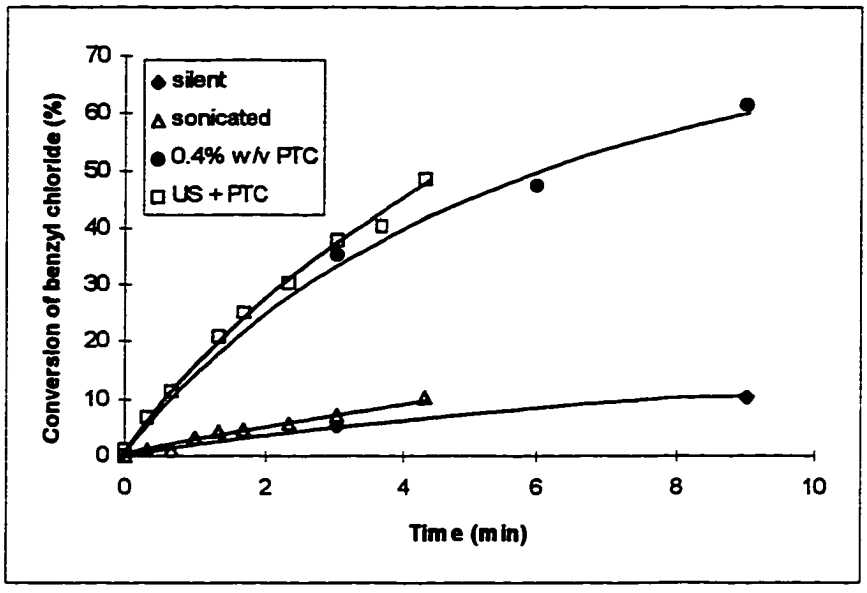

Figure 2.3. The use of PTC, ultrasound, and the combination on the conversion of benzyl chloride for the synthesis of dibenzyl sulfide (Hagenson *et al.*, 1994).

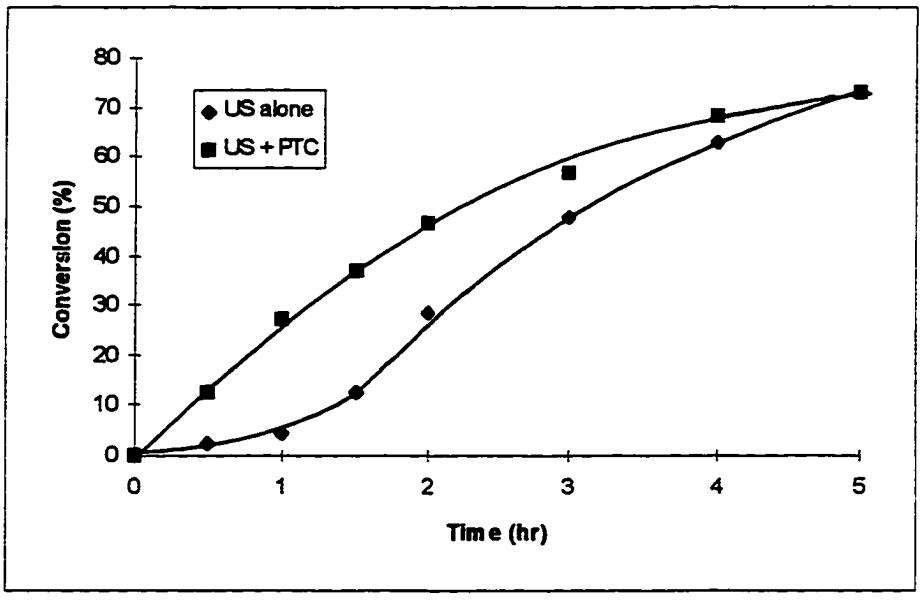

Figure 2.4. Use of ultrasound and the combination of PTC and ultrasound on the synthesis of Tos_3TACN (Mason *et al.*, 1994).

Table 2.6. Reactions which have investigated using PTC, ultrasound and/or combinations of the two enhancement techniques.

Reaction Type	Effect of ultrasound	Reference
Enhancement of the Cannizzaro reaction	Found benzyltriethylammonium chloride (TEBA) to be the most effective PTC	Polackova *et al.* (1996)
Hydrolysis of 2,4-dichlorophenyl benzoate	Enhanced the reaction over no catalyst, but the PTC cetyl trimethyl ammonium bromide was required for significant enhancement	Shirgaonkar and Pandit (1996)
Synthesis of dibenzyl sulfide	Ultrasound accelerated the reaction over stirring alone, but the PTC tetrabutyl ammonium bromide (TBAB) was required for substantial enhancement	Hagenson *et al.* (1994)
Preparation of triazacyclo compounds	After 5 hours both ultrasound and the PTC Bu_4NOH led similar yields	Mason *et al.* (1994)
β-Elimination reactions: Synthesis of cyclic ketene acetals	Greatly enhanced reaction when combined with PTC tetrabutyl ammonium bromide (TBAB) No additional solvent was required	Diez-Barra *et al.* (1992)
Dialkylation and cyclodialkylation of ethyl cyanoacetate	Increased reaction rate and yield	Lin *et al.* (1991)
o-Alkylation of 5-hydroxy chromone derivatives with alkyl bromides	Use of sonication with n-methyl pyrrolidionone at lower reaction times and temperatures or use of PTC (Aliquat 336) with no solvent gave comparable yields	Mason *et al.* (1990c)
Synthesis of RCN compounds from RBr and KCN supported on alumina	Ultrasound enhanced the reaction over either of the 2 PTCs used: 18-crown-6 and tetrabutyl ammonium chloride	Ando *et al.* (1984b)
Synthesis of silicon containing aziridines from dichlorocarbamates and vinyl- or allylsilanes with subsequent reduction and cyclization	The use of PTC or ultrasound resulted in comparable enhancements of ~ 1 order of magnitude over traditional methods	Lukevics *et al.* (1984)

(Tos_3TACN) increased from 6.1% with Bu_4NOH alone to 73% with both sonication and PTC. However, the authors did not draw attention to one important detail, which is apparent when graphing the experimental data provided in their article, and shown in Figure 2.4. When ultrasound is used in combination with PTC, the reaction rate is initially much greater than when ultrasound is used alone. However, with continued reaction time, the conversion in the case of ultrasound alone matches the conversion of US + PTC. Thus, when attempting to use a variety of enhancement techniques, preliminary rate data may give a good indication of whether or not several techniques are required. One technique alone may be sufficient and give comparable conversions without the costly separation processes required with the addition of a separate catalyst. Table 2.6 provides examples of other reactions which have been investigated combining the enhancement techniques of ultrasound and phase transfer catalysis.

2.6.2 Biphasing

Biphasing is the addition of an immiscible phase to the traditional reaction mixture in order to increase the yield of desired product by shifting the thermodynamic equilibrium in the direction of the reactants. The ability of ultrasound to create fine emulsions is, thus, very beneficial to biphasic systems. For example, it has been used successfully for the oxidation of secondary alcohols with sodium bromate in an aqueous-CCl_4 biphasic system mediated by ruthenium tetraoxide (Mills and Holland, 1995). For each of the four alcohols investigated, the reaction time was decreased from several hours to several minutes, and the yield of ketone in each case was 100% when ultrasound was used in conjunction with supplementary stirring.

The significant increase in reaction kinetics due to ultrasound was attributed primarily to the increased interfacial area available for reaction. The production of chloropropionamide in the biphasic system of water and 3-chloropropionitrile was also investigated in the presence of ultrasound (Farhat and Berchiesi, 1992). Ultrasound did not appear to affect the Cl-C bond.

2.6.3 Surfactants

The addition of surfactants to ultrasonic systems inhibits the production of H_2O_2, when compared to the sonolysis of nonsurfactant solutes (Alegria *et al.*, 1989). Three surfactants were examined: sodium dodecyl sulfate, dodecyltrimethylammonium bromide, and n-octyl-β-D-glucopyranoside (OGP). All three appeared to localize at the gas-liquid interface of the cavitation bubble.

2.6.4 Photolysis

The rate of decomposition of aqueous 1,1,1-trichloroethane was higher in the presence of both photolysis and sonolysis when compared to the use of either technique alone (Toy *et al.*, 1990). When both techniques were used simultaneously, the authors referred to the process as "photosonochemical".

It was also found that the rate of photolysis declorination of wastewater, which contained polychlorobiphenyls (PCB's), was greatly enhanced when ultrasound was used in conjunction with the photoactive material TiO_2, as compared to the use of TiO_2 alone (Mason, 1992a). The enhancement was attributed to the mechanical effects of ultrasound, such as particle degradation, surface cleaning, and increase mass transport.

2.7 Kinetic Analysis

2.7.1 Reaction zones

EPR and spin trapping studies of volatile and non-volatile solutes have provided evidence of three regions of sonochemical activity (i.e. three reaction zones) in sonicated systems (Riesz *et al.*, 1990). The three reaction zones, shown in Figure 2.5, are: Zone 1. The gaseous region of the cavitation bubble containing both permanent-gas and vaporized reaction mixture; Zone 2. The gas-liquid interface containing less-volatile reaction components and surfactant (if present in the reaction system); and Zone 3. The bulk liquid phase. The magnitude of reaction occurring in each zone depends on the ultrasonic conditions, such as the frequency, and on the characteristics of the reaction system, such as the volatility of the components involved. Within the gaseous region (Zone 1), volatile solutes and solvent are exposed to extreme temperatures and pressures upon cavitation, resulting in breakage of the molecules comparable to pyrolysis reactions following the Rice-Herzfeld mechanism (Misik

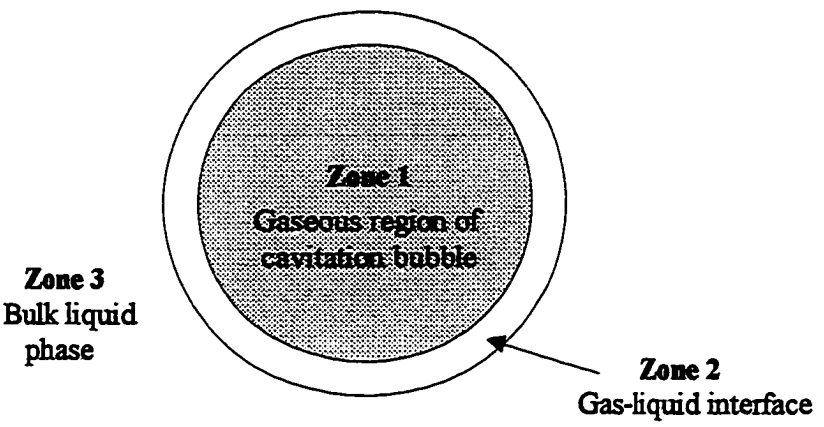

Figure 2.5. Three reaction zones of sonochemical reactions.

and Riesz, 1996a; Suslick *et al.*, 1983a). It was estimated that approximately 10% of the OH and H radicals generated in this region of the cavitation bubble escape to the bulk liquid (Zone 3) (Henglein, 1995). It was also found that superoxide anion radicals ($O_2^- \cdot$) were produced during the sonolysis of argon saturated aqueous solutions (Kondo *et al.*, 1996).

Estimates of the relative sizes of the reaction zones and the effective temperature in each zone have been made by Suslick and Hammerton (1986) and are described in the following section. Reactions with non-volatile solutes occur primarily in the interfacial region or in the bulk liquid phase (Sehgal *et al.*, 1982). As discussed in **Section 2.3.2.*b***, Segal and Wang (1981) speculated that the degradation of thymine, a compound of low volatility, occurs in the interfacial region. These findings were confirmed by Kondo *et al.* (1988) who found thymine radicals in both the bulk solution and interfacial region of the cavitation bubble. It was speculated that at low concentrations of non-volatile solute, the reactions which occur involve primarily secondary radical reaction, i.e. scavenging of H· and OH· radicals. While at high concentration of solute, pyrolysis of the solute occurs (Kondo *et al.*, 1989a). However, both mechanisms may be occurring simultaneously at all concentrations of solute (Misik and Riesz, 1996b). Other investigations of the sonolysis of aqueous solutions of nonvolatile solutes include: acetate (Gutierrez *et al.*, 1986); dipeptides, propionate and sugars (Kondo *et al.*, 1989a); nucleosides (Kondo *et al*, 1988b); nucleotides (Kondo et al, 1989a); and polymers (Henglein, 1988). The sonolysis of several organic liquids have also been studied, including: dimethylformamide, methylformamide, dimethylacetamide, toluene, *n*-alcohols, *n*-alkanes, cyclohexane, dioxane and tetrahydrofuran (Misik and Riesz, 1996b). The identified radicals were formed by either pyrolysis or H-abstraction. If the reactant was not volatile enough to

enter the liquid shell (Zone 2), the reaction was not chemically enhanced with the use of ultrasound (Ando *et al.*, 1996; Griffing, 1952).

In the bulk liquid phase (Zone 3), the reactions which occur involve radicals which escape the implosion. The kinetics are similar to that of radiation chemistry (Fuch and Heusinger, 1995; Kondo *et al.*, 1988a).

The sonolysis of water under atmospheres consisting of various ratios of argon and acetylene was investigated by Hart *et al.* (1990). They found several products, of which a great proportion consisted of two to eight carbon atoms. The products were similar to products observed in the pyrolysis or combustion of acetylene, with the interesting finding that the products with an even number of carbons were more plentiful than the products with an odd number of carbons. The authors concluded that the formation of products occurred in a single step, by a single cavitational event, and not in a series of steps or through reactive intermediates from surrounding cavitational events. They also developed a mechanism to account for the products observed. Other studies of the sonolysis of gaseous solutes in aqueous solutions include: ozone (Hart and Henglein, 1986a; Coate *et al.*, 1995); carbon dioxide (Henglein, 1985); and nitrous oxide (Hart and Henglein, 1986b).

Aqueous mixtures of carbon tetrachloride were degraded by ultrasound, forming CO_2 and Cl^- (Francony and Petrier, 1996). They detected trace amounts of $C > 4$ chains, but no chains longer that four carbons. Likewise, Drijvers *et al.* (1996) obtained C_2 and C_4 chains when they studied the degradation of trichloroethylene. They proposed that the reaction intermediates were formed during a single cavitational event because a free radical trap in the

bulk solution had no effect on the degradation rate. Aqueous mixtures of methanol produced primarily $CH_3\cdot$ and some $\cdot CH_2OH$ radicals (Riesz *et al.*, 1990).

2.7.2 Kinetic modeling

When studying the primary radical formation of n-alcohols, Misik and Riesz (1996a) found that the logarithm of the rate of radical formation, $k_{r.f.}$, decreased linearly with the vapor pressure of the alcohol. They speculated that the relationship could be described as

$$ln\,k_{r.f.} = ln A - \frac{E_a}{R_g T_o P_A (\gamma - 1)} P_v \qquad (19)$$

However, they did not validate the equation with experimental data. Suslick and Hammerton (1986) had earlier found the same linear relationship while studying ligand substitution of metal carbonyls. To investigate the relationship further, they performed experiments where they measured the rate constant as a function of reactant vapor pressure, while holding the total vapor pressure of the system constant. They achieved this by varying the reactant concentration and ambient reaction temperature, and using various solvent mixtures to hold the system vapor pressure constant. As a result, for two different reaction systems, they found that the observed rate constant increased linearly with reactant vapor pressure, and had a nonzero intercept. They concluded that the linear dependence indicated that the reaction was occurring within the vapor phase of the cavitational event (Zone 1 in Figure 2.5) and the nonzero intercept gave a quantitative value of the reaction occurring in the liquid phase, which they assumed to be the gas-liquid film surrounding the bubble (Zone 2) (see also Suslick, 1990). They used these findings to estimate the size of the bubble cavity relative to that of the

gas-liquid film surrounding the bubble and found it to be 2.0 x 10^4 : 1 before collapse. In addition, they estimated the effective temperatures to be ~ 5200 ± 650 K and ~ 1900 K for Zone 1 and Zone 2, respectively (see also Suslick *et al.*, 1986). The liquid reaction zone was estimated to extend ~ 200 nm from the bubble surface and had a lifetime of < 2 μs. This compares to another estimate for the cavitation region (not zone specific) as ~2000-4000 K made by Misik *et al.* (1995) through spin-trapping and knowledge of the kinetics of O-H bond pyrolysis. It seems likely that Zone 1 and Zone 2 become indistinguishable from one another during the collapse of the bubble, and immediately after collapse. This would result in a system is comparable to a point source at a very high temperature and pressure, with steep temperature and pressure gradients to the bulk liquid at ambient temperature and pressure, as shown in Figure 2.6.

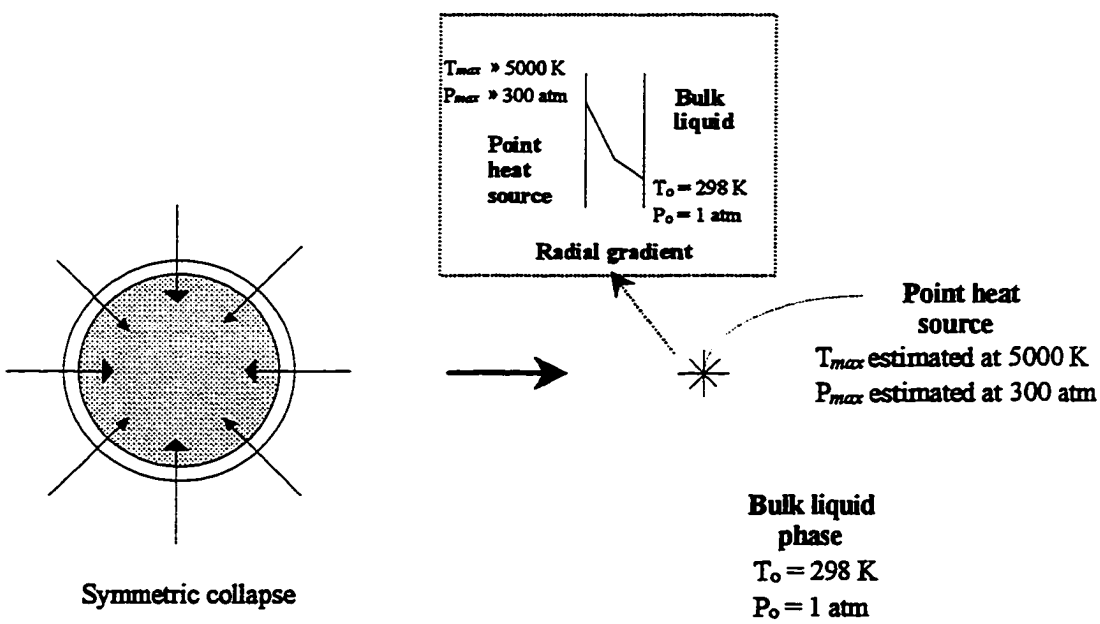

Figure 2.6. Symmetric collapse resulting in localized hot spot.

The kinetic approach discussed above, and shown by Equation (19), was expanded by Lorimer *et al.* (1991) who developed a kinetic model accounting for reaction both in the presence and absence of ultrasound. As a first step they defined three rate constants: k_{non} representing the rate constant in the absence of ultrasound, k_{US} representing the rate constant obtained in the presence of ultrasound, and k_{BUB} representing the rate constant associated with cavitational collapse. They also found that

$$k_{US} \neq k_{non} + k_{BUB} \tag{20}$$

or, in other words, the reaction rate constant in the presence of ultrasound cannot be accounted for by simply adding the rate constants in the absence of ultrasound and within the bubble region. The properties are not additive because the reaction within the cavitation region occurs at much higher temperatures and pressures than the reaction in the bulk liquid. In addition, although the reaction in the bulk is continuously occurring over time, the reaction in the bubble is only occurring for a fraction of the cycle time of the acoustic wave. Thus two more parameters must be defined: F_V for the fraction of reaction mixture volume occupied by bubbles and F_t for the cycle time (compression phase) during which the reaction occurs at the elevated temperatures of the cavitation region. Using this information, the following can be developed:

$$k_{US} = (1 - F_V)\, k_{non} + F_V\, k_{BUB} = k_{non} + F_V\, (k_{BUB} - k_{non}) \tag{21}$$

$$k_{BUB} = (1 - F_t)\, k_{non} + F_t\, k_{et} \tag{22}$$

where k_{et} is the rate constant of the reaction occurring at the elevated temperatures within the cavitation bubble. Substituting k_{BUB} from Equation (22) into (21) results in Equation (23)

$$k_{US} = k_{non} + F_t F_V (k_{et} - k_{non}) \tag{23}$$

which, upon rearrangement, gives

$$\left(\frac{k_{US}}{k_{non}} - 1\right) = F_t F_v \left(\frac{k_{et}}{k_{non}} - 1\right) \tag{24}$$

Since the reaction within the cavitation bubble occurs at temperatures estimated at over 1000 times the average bulk temperature, it is reasonable to assume that $k_{et} >> k_{non}$, (i.e. $k_{et}/k_{non} >> 1$). It is also reasonable to assume that the reaction occurring in the cavitation bubble follows Arrhenius behavior, shown by

$$k_{et} = A\, exp\left(\frac{E_a}{R_g T_{max}}\right) \tag{25}$$

where T_{max} is the maximum temperature reached in the transient cavitation bubble, which has been defined in Section 2.3.1.*c* as

$$T_{max} = T_o\left[\frac{P_m(\gamma - 1)}{P}\right] \tag{9}$$

Plugging (9) and (25) into (24), and rearranging, results in

$$ln\left(\frac{k_{US}}{k_{non}} - 1\right) = ln F_t F_V + \frac{E_a}{R_g T_o} - \frac{E_a}{R_g P_m(\gamma - 1)}\frac{P_V}{T_o} \tag{26}$$

where P_m is the acoustic pressure at the initiation of collapse, T_o is the ambient reaction temperature, and P_v is the vapor pressure of the reaction mixture.

Lorimer *et al.* (1991) found this method of analysis very promising when explaining kinetic data obtained from the solvolysis of 2-chloro-2-methyl propane in 30% (w/w) and 50% (w/w)

ethanol-water solutions. They also speculated that Equation (26) could be used to describe systems with non-aqueous solvents by making the modification that $k_{US} >> k_{non}$, (i.e. $k_{US}/k_{non} >> 1$).

Two factors that Lorimer *et al.* (1991) did not account for were that the activation energy and Arrhenius parameters might also be affected by ultrasound, (i.e. $E_{a,et} \neq E_{a,\,non}$ and $A_{et} \neq A_{non}$), which occurred in the reaction systems investigated by Tatsumoto and Fujii (1987), Mills *et al.* (1995) and Whillock and Harvey (1997a). The reason these parameters change is most likely due to the increased number of collisions of the chemical species reaction system, although more research is needed to explain these changes fully.

2.8 Mass Transfer Studies

2.8.1 Film transfer

Hagenson and Doraiswamy (1997) found that ultrasound significantly increased the intrinsic mass transfer coefficient and the effective diffusivity in a solid-liquid system. When investigating the synthesis of dibenzyl sulfide from sparingly soluble sodium sulfide and benzyl chloride in the solvent acetonitrile, they found that the reaction kinetics were adequately described using the sharp-interface model (SIM)

$$\frac{R_{Ao}}{3k_l}x_A + \frac{{R_{Ao}}^2}{6D_e}\left[1-3(1-x_A)^{2/3}+2(1-x_A)\right] + \frac{R_{Ao}}{k_s}\left[1-(1-x_A)^{1/3}\right] = \frac{\nu C_B M_A}{\rho_A}t \quad (27)$$

which is based on the conversion of the solid reactant A. The first term in Equation (27) accounts for the diffusional resistance of the liquid reactant through the solid-liquid interfacial

film, the second for the diffusional resistance of the liquid reactant through the product layer formed on the surface of the unreacted solid during the course of the reaction, and the third for the reaction occurring at the sharp interface between the product layer and unreacted solid. Because the reaction under investigation was only controlled by one of these resistances at any one time, Hagenson and Doraiswamy could extract the values of k_l, the intrinsic mass transfer coefficient, and D_e, the effective diffusivity, from the experimental data they obtained in the absence and presence of sonication. The results indicated that the intrinsic mass transfer coefficient and the effective diffusivity were increased 2 times and 3.3 times, respectively, in the presence of ultrasound as compared to stirring alone.

Ultrasound was found to enhance a Michael addition reaction over the use of very fast mechanical agitation (Ratoarinoro *et al.*, 1995). The rate of mass transfer was calculated using Equation (28), and the intrinsic mass transfer of hydroxide ions through the

$$r_{mt} = k_l a \frac{C_{Ao}}{V_l} \tag{28}$$

solid KOH-liquid toluene film was determined using the empirical power correlation given by Equation (29). The diffusivity of the ions through the solvent was estimated with the Wilke

$$k_l = \frac{D}{d_p}\left[2 + 0.4\left(\frac{e\, d_p^4 \rho^3}{\mu^3}\right)^{\frac{1}{4}}\left(\frac{\mu}{\rho D}\right)^{\frac{1}{3}}\right]F_c \tag{29}$$

and Chang (1955) correlation and was assumed to be the same for both mechanically agitated and sonicated reactions (the possibility of ultrasound increasing the diffusion of the ions through the solvent was not considered). When this correlation was used by Hagenson and

Doraiswamy (1997) to compare the empirical result with their experimentally obtained value, they found Equation (28) to grossly overestimate the value of the intrinsic mass transfer coefficient in the presence of ultrasound by over two orders of magnitude. The use this correlation as a predictive tool for k_l does not appear to be valid in the case of sonicated reactions. However, this was not critical to Ratoarinoro *et al.*'s conclusions concerning the enhancement of the Michael addition reaction, because they concluded that the reaction was kinetically controlled.

When investigating a diffusion limited reaction, Worsley and Mills (1996) found that ultrasound increased the rate of the reaction by a factor proportional to D/δ, where D is the diffusivity and δ is the diffusion layer thickness. It was concluded that ultrasound decreases the diffusion layer thickness. However, the effects on the diffusivity were not considered or investigated.

Using a 3-phase sparger reactor, the effects of ultrasound were investigated for a solid-liquid and a gas-liquid reaction (Jadav and Pangarkar, 1989). The authors concluded that ultrasound had a greater effect on the solid-liquid reaction, but that the enhancement in the mass transfer coefficient was not very significant. However, these authors used a correlation to determine the surface area of the particles in their system, and did not account for surface area changes over time, which can be quite significant (Hagenson and Doraiswamy, 1997).

Ultrasound has been shown to increase the mass transfer in a concurrent liquid-liquid extraction processes and in a two-phase, three component spray tower process. The effects of ultrasound on the liquid-liquid extraction process were studied using a horizontal settling column with the transducer directly attached to the column (Woodel and Vilbrandt, 1960).

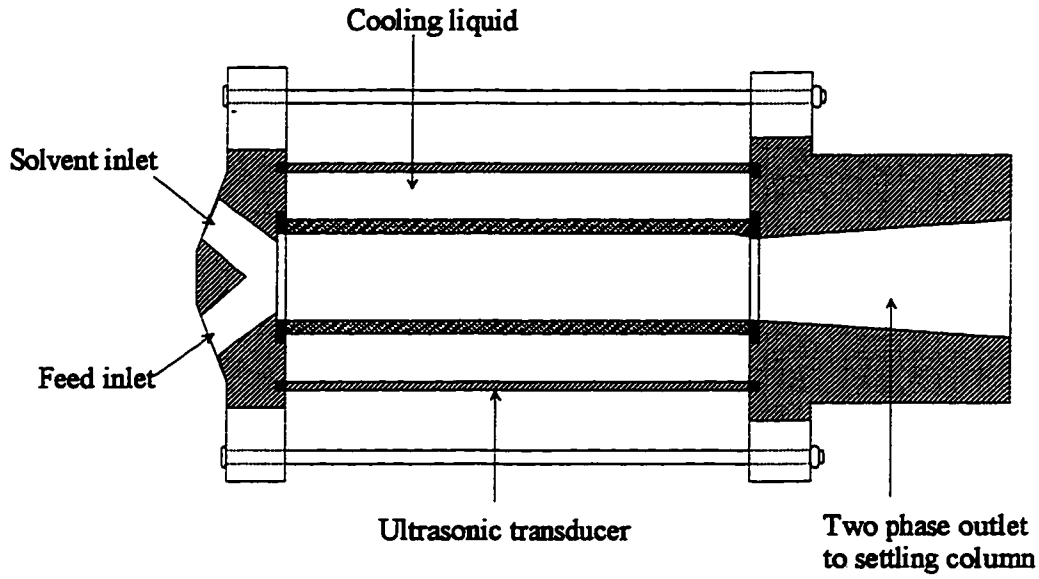

Figure 2.7. Ultrasonic horizontal settling column (Woodel and Vibrandt, 1960).

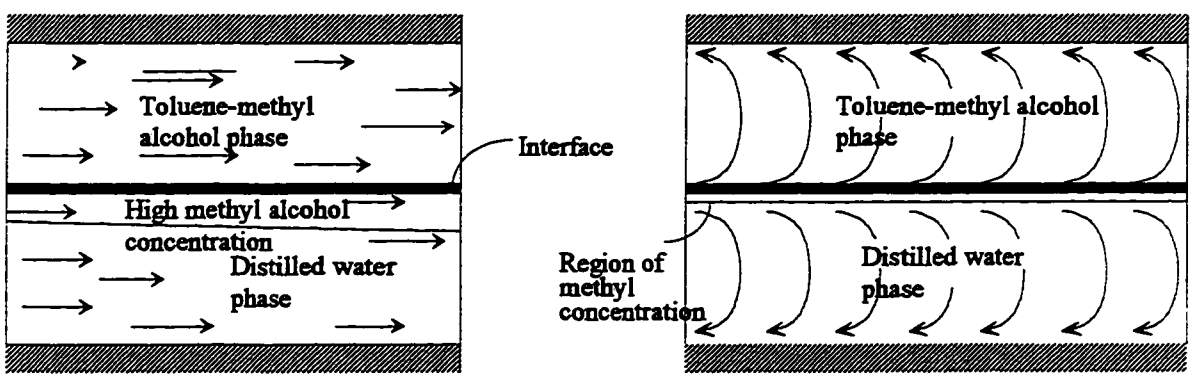

(a) Extraction with no ultrasound (b) Extraction upon exposure to ultrasound

Figure 2.8. Effect of ultrasound on the flow pattern within a horizontal settling column (Woodel and Vibrandt, 1960).

The liquid mixture was operated plug-flow as the liquids passed over the length of the transducer, as shown in Figure 2.7. The stage efficiency was found to increase as the residence time of the liquids increased, (i.e. for a power input of 50 Watts, the stage efficiency was increased from 19% with 5.9 seconds of contact time to 57% with 18 seconds of contact time). The beneficial effects of ultrasound were attributed to the different mixing patterns of the liquid phases (see Figure 2.8), the formation of eddies and circulation currents within a single phase, which reduced concentration gradients, and the removal of stagnant pockets of liquid at the interfacial boundary of the two phases.

2.8.2 Dissolution

Ultrasound has been found to increase the rate of dissolution of several different solid/liquid systems. For example, an exponential increase in the dissolution of renal calculi was observed in a chemolytic EDTA-citric acid solution in the presence of ultrasound (Geier, 1989). It was also found that the dissolution rate in the presence of ultrasound was dependent upon the system's pH and the citric acid concentration (when the pH was held constant).

Similarly, the rate of reactive dissolution of *p*-chloranil increased in the presence of ultrasound (Booth *et al.*, 1997). The diffusion layer thickness of the solid-liquid film decreased as the ultrasonic intensity increased and as the sample was moved closer to the tip of the horn. Using atomic force microscopy, it was found that ultrasound led to heavy pitting of the solid surface and suggested that transient ultrasonic cavitation plays an important role in the dissolution process.

When investigating the dissolution of sodium sulfide in acetonitrile, Hagenson and Doraiswamy (1998) found that not only did ultrasound increase the rate of dissolution of a sparingly solid solute in a solvent, but it induced supersaturation of the solid as well, as shown in Figure 2.9. The data points plotted in Figure 2.9 are average values of 3 - 6 replications, which had an overall pooled standard deviation (s_p) of 5.13, based on 101 data points. The concentration of sodium available in the bulk liquid solution reached a maximum of 1.4 times the equilibrium saturation concentration available using stirring alone. The supersaturation level appears to cycle, reaching minimum approximately every 20 minutes. This cyclization may be a result of random fluctuations in the average, or may be due to competing dissolution and precipitation processes.

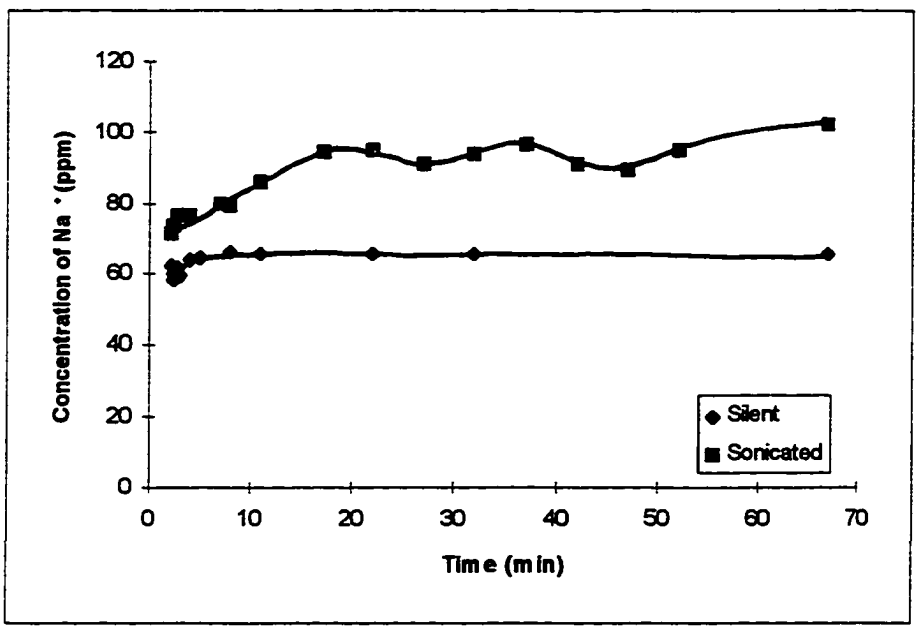

Figure 2.9. Supersaturation as a result of exposure to ultrasound (Hagenson and Doraiswamy, 1998).

The same type of experiment was performed for the dissolution of calcium citrate in water and similar results were obtained: the concentration of Ca^{+} available in the bulk liquid was 1.7 times greater in the presence of ultrasound than in the absence (Hagenson and Doraiswamy, 1998). These results are very exciting because, as shown by Equation (29), the rate of

$$-\frac{dC_A}{dt} = k_{sl}\, a\left(C_A^* - C_A\right) \tag{29}$$

mass transfer in the presence of ultrasound is increased because of three simultaneously occurring processes: an increase in the intrinsic mass-transfer coefficient for dissolution, an increase in the interfacial area, *and* an increase in the driving force for dissolution (refer to Figure 2.10). This phenomena has great potential in processes where the reaction occurs in the bulk liquid phase.

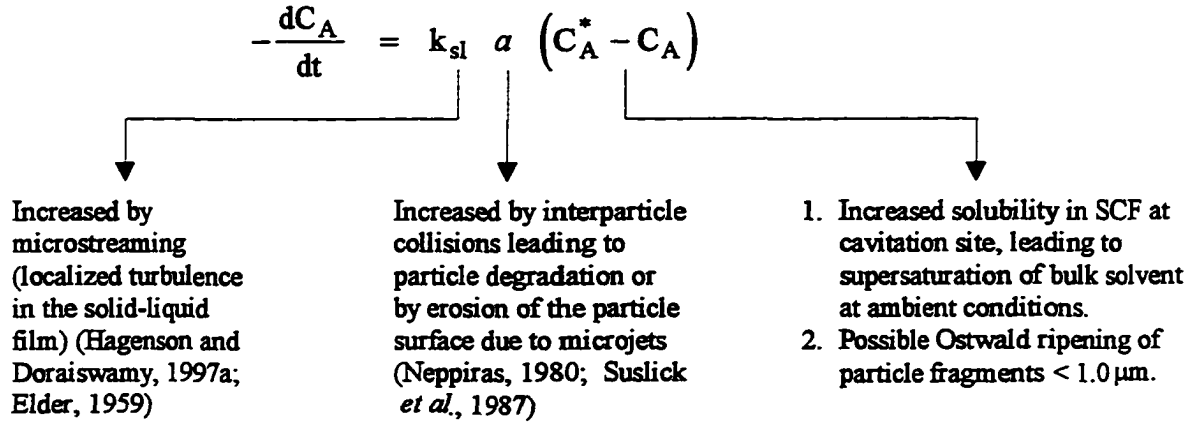

Figure 2.10. Ultrasonic enhancement of the rate of dissolution.

2.8.3 Permeability

The permeability of large molecular weight molecules through either polymeric or biological membranes was enhanced in the presence of ultrasound without permanent damage to the membrane material (Kost and Langer, 1988). However, the mechanism(s) of enhancement were not speculated. Some of the questions which should be addressed include: whether ultrasound was increasing the effective diffusivity of the molecules, if the membrane structure was altered in any way in the presence of ultrasound, or if any other type of mechanical effect could explain the increased permeability.

2.9 Methods of Producing Cavitation

Cavitation can be generated within a fluid using transducers, which are devices which convert one form of energy to another. Gas-driven transducers, such as dog whistles, use high velocity gas flow to generate ultrasound. Liquid-driven transducers, such as submarine propellers, force liquid across a vibrating plate or through an orifice, creating a cavitation zone. Electromechanical transducers, the most commonly used transducers in sonochemical research, convert electrical energy to sound energy.

When using gas or liquid driven transducers, cavitation is generated *in situ*, i.e. cavities are formed within the fluid by forcing the fluid through a physical object which generates shearing forces great enough to tear the fluid apart. Direct sonication occurs when a device which generates sound waves, such as a probe or horn, is place directly in a fluid system. Indirect sonication occurs when the sound waves propagate through some other medium before they come into contact with the vessel containing the reaction mixture, such is the case when using

an ultrasonic cleaning bath. As is evident by the nature of sonication, probe systems produce higher intensities in reaction mixtures as compared to ultrasonic cleaning baths. Cavitation generated *in situ* in liquids can reach intensities comparable to direct sonication, as found by Pandit and Joshi (1993) who hydrodynamically induced cavitation with a throttling valve to increase the hydrolysis of fatty oils. They compared the yields obtained using a hydrodynamic system to those using a probe system, and found them to generate similar reaction conditions and yields.

Cavitation can also be induced *in situ* using a focused electromagnetic acoustic transducer (EMAT) which produces a high-intensity lithotripter shock wave in the fluid concerned (Carnell, 1995). Once the shock wave is induced, cavitational bubbles are formed in the negative pressure region of the wave, causing rupturing of the fluid. Secondary cavitational transients, created by the collapse of the primary bubbles, may also occur.

2.9.1 Piezoelectric vs. magnetostrictive transducers

The two main types of electrochemical transducers used in industrial applications are piezoelectric and magnetostrictive. Piezoelectric transducers are constructed using a piezoelectric material, such as quartz, which expands and contracts in an alternating *electric* field, thus producing sound waves from the electric signal. Magnetostrictive transducers are constructed from materials, such as nickel alloys, which expand and contract in an alternating *magnetic* field. Each transducer has its own advantages and disadvantages, as outlined in Table 2.7 (Hunicke, 1990).

Table 2.7. Comparison of piezoelectric and magnetostrictive transducers (Hunicke, 1990).

Piezoelectric Transducers	Magnetostrictive Transducers
Relatively inexpensive	More expensive than piezoelectric for similar power ratings
Relatively small and light	Heavier and bulkier than piezoelectric
Damaged at temperatures > ~150 °C	With special precautions, can be operated at temperatures > 250 °C
Will age, i.e. have a reduced power output, considerably with continuous operation at high temperatures and/or over long periods of time	Will not degrade or fail over time by their very nature Some have been used successfully for over 20 years of commercial operation
May be damaged by large impact	Extremely resistant to mechanical damage, such as large impacts
Structure will be damaged if operated "dry"	No damage when operated "dry"

As is evident from the table, piezoelectric transducers are normally used with small volume processes and laboratory work. When large volumes and/or long, continuous reaction times are required, the more robust magnetostrictive transducer may be the preferred option .

2.10 Characterization of the Sound Field

Several methods exist to characterize the sound field of different acoustic reactors, including the chemiluminescence of luminol, the use of thermistor probes (Martin and Law, 1980), and the use of aluminum foil. The PPIMP, recently developed by Soudagar and Samant (1995), has the shape of a traditional ultrasonic probe and is fitted with a sandwich-type PZT piezoelectric crystal. It was designed with the intention of characterizing the sound field of ultrasonic cleaners, and was shown to be an effective characterization technique.

Using an electrochemical method (Trabelsi *et al.*, 1996) determined the active regions within their high frequency ultrasonic reactor using an electrode and monitoring the localized

current of the diffusion-controlled reduction of potassium ferricyanide. The regions with the highest current readings, leading to the highest Sherwood numbers, were taken as the most active regions in the reactor. The Sherwood number was determined using Equation (30)

$$Sh = \frac{k_d d_e}{D_{ox}} \tag{30}$$

where the mass-transfer coefficient is directly proportional to the reduction current, d_e is the electrode diameter, and $D_{ox} = 0.9 \times 10^{-9}$ m^2/s. Experiments using this technique of characterization gave conflicting results as compared to the active regions determined via calorimetry. Similar results were observed by Renaudin *et al.* (1994) when comparing two other methods of sound field characterization: chemiluminescence of luminol and a thermocouple probe. They found that the regions of highest acoustic intensity as determined with the thermocouple did not correspond to the regions giving the highest luminous intensity. The authors speculated that a phenomenon referred to as the "geyser" effect was occurring in the system (refer to the article for further explanation).

2.11 Ultrasonic System Types

2.11.1 Ultrasonic bath

Ultrasonic baths were originally manufactured for cleaning purposes. In general, the transducers are attached to the bottom of the cleaning baths, as shown in Figure 2.11a, although transducers can be submersed in a conventional tank to obtain similar effects (Figure 2.11b). Bath systems are the most widely used in the sonochemical research because they are

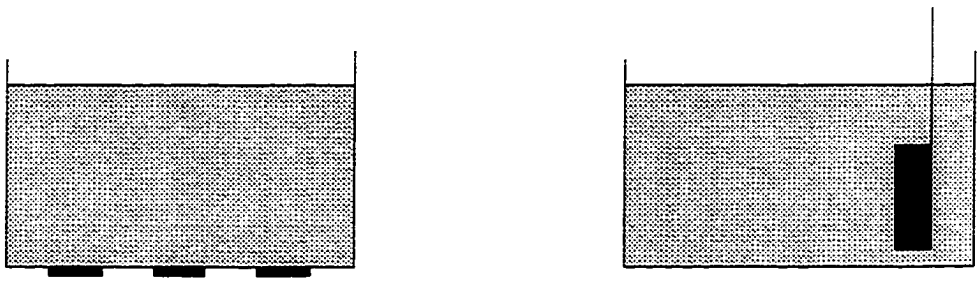

(a) Most common type of bath (b) Modification of existing tank

Figure 2.11. Ultrasonic bath systems with (a) mounted transducers and (b) submersed transducers.

readily available and relatively inexpensive. The reaction vessel is typically immersed in the coupling fluid contained in the bath (indirect sonication). However, the bath itself can be used as the reaction vessel, but would require additional mechanical agitation. In addition, the bath walls would be exposed the reaction mixture and/or the irradiation, making them susceptible to corrosion or erosion.

When indirect sonication is used, the ultrasonic power which reaches the reaction vessel is relatively low as compared to other ultrasonic systems, such as a probe. In addition, obtaining reproducible results may be difficult because the amount of power reaching the reaction mixture is highly dependent upon the placement in the bath, and varies from bath to bath. It also varies with time as the bath warms during operation (Lickiss and McGrath, 1996). Since each bath has very different characteristics, it is very important to determine the optimum conditions for each, and to place the reaction vessel in the same location for each experiment. In addition, it is important to use the same type of reaction vessel for each reaction because the shape of the bottom of the reaction vessel significantly influences the wave pattern, even

when placed in the same position in the bath (Mason *et al.*, 1994; Pugin, 1987; Weber and Chon, 1967).

Another disadvantage to using a bath system is that the coupling fluid surrounding the reaction vessel(s) will eventually increase in temperature, making the maintenance of isothermal conditions difficult. Cooling coils can be placed within the bath, but will affect the sound field and may reduce the amount of power reaching the vessel.

2.11.2 Probe (horn) systems

Probe systems, also called horn systems, are being used more frequently for sonochemical research in the laboratory. This may be because manufacturers are aware that this type of research is increasing and are providing equipment to meet the demand. In addition, probe systems are capable of delivering large amounts of power directly to the reaction mixture which can be regulated by varying the amplitude delivered the transducer. Disadvantages in using a probe system include erosion and pitting of the probe tip, which may contaminate the reaction solution, as found by Entezari *et al.* (1997) when investigating the dissociation of carbon disulfide. Several probes are available with removable tips, making replacement relatively inexpensive. Several different horn designs are available and are discussed in detail by Perkins (1990). His article also covers transducer construction, material considerations, methods of measuring input amplitude, and health and safety aspects.

Several authors have carried out experiments to determine the sound field characteristics in a probe system. It was found that a minimum liquid height must be maintained in the reaction vessel, below which the transducer does not function properly (Ratoarinoro *et al.*, 1995a).

They concluded that the probe should be immersed in at least 1 cm of fluid. Contamine *et al.* (1994) observed that when the power delivered to the system is low (i.e. 8 W); the distribution of ultrasonic intensity is characteristic of a standing wave in the axial direction. However, as the power delivered to the system is increased, the wave pattern dissipates and the intensity becomes higher near the probe tip and decreases axially. In the radial direction, they found that at low powers (i.e. 8 W) the intensity is slightly higher at the center of the reactor, but is comparable over the cross-section of the reactor. However, as the power delivered increases, the ultrasonic intensity increases at the center of the reactor and dissipates as one moves out in the radial direction. At an input power of 200 W, the active region in the radial direction is equal to that of the horn (the remaining radial direction had negligible activity).

Aluminum foil was used to characterize the sound field of a probe system, providing the data required to develop an empirical equation (Equation (31)) which can be used to estimate the order of magnitude of the pressure intensity (P_I), in atmospheres, as a function of distance (s), in meters, of the aluminum foil from the probe tip (Chivate and Pandit, 1995). The pressure

$$P_I = 9.82 \times 10^{-4} s^{-1.5} \tag{31}$$

intensities were found to be on the order of several thousands of atmospheres very near the probe tip, and to decrease exponentially with distance from the tip of the horn.

2.11.3 Planar transducers

This type of setup is typically made in the laboratory and it consists of a planar transducer (Figure 2.12) connected to a vessel which contains either the reaction mixture (a) or a coupling fluid (b) in which the reaction vessel is immersed. "Cup-horn" designs are very similar to planar transducer designs, with the exception that the horn is designed to allow for cooling capabilities, facilitating the maintenance of isothermal conditions (refer to Mason (1990c) for more details). Both planar transducer and cup-horn systems are capable of delivering higher powers than ultrasonic bath systems. However, they are both difficult to scale-up.

The active regions of a high frequency (500 kHz) planar transducer system, similar to Figure 2.12a, have been investigated by Renaudin *et al.* (1994). A thermocouple was used to probe the regions in the radial direction, based on the assumption that the measured

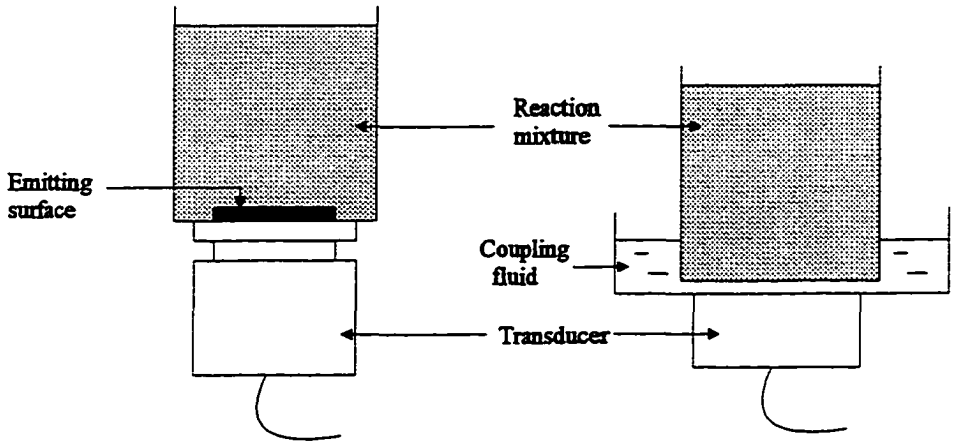

(a) Direct sonication (b) Indirect sonication

Figure 2.12. Planar transducer systems.

temperature was directly proportional to the cavitation intensity. The ultrasonic intensity was found to be higher at the center of the vessel, directly above the emitting surface, and to decrease in the radial direction. Similar behavior was observed when Contamine *et al.* (1994) investigated the value of the local mass transfer coefficient at different axial and radial positions in the reaction vessel. The axial variations in the local mass transfer coefficient were characteristic of a standing wave. Radially, the local mass transfer coefficient was the highest in the center of the reactor, above the emitting surface, and decreased as it moved out towards the edges. The value of the coefficient was also dependent upon the height of the liquid in the reaction vessel.

The concepts presented above are not new. This behavior was modeled by Aerstin *et al.* in 1967 and was experimentally verified with data obtained from the liberation of Cl from CCl_4. The equipment used is similar to the planar transducer system shown in Figure 2.12b. Starting from the basic principles describing the pressure variations of a propagating sound wave:

$$p_x = P_A \, exp^{-\alpha x} \, exp^{i(\omega t - kh)} \tag{32}$$

where p_x is the pressure amplitude at a distance x from the transducer, P_A is the pressure amplitude delivered by the transducer, α is the attenuation coefficient of the medium, ω is the angular frequency, k is the wave number ($= 2\pi/\lambda$), and h is the height of the liquid above the transducer. Simplifying assumptions were made specific to their system (for example, they used water as their medium, hence $\alpha \cong 0$), and the equation was solved for the pressure amplitude at $x = n\lambda/2$, resulting in

$$P_{\left(x=\frac{n\lambda}{2}\right)} = P_A \left| \frac{\left[(1-\sigma)^2(1-cos\,2kh)^2 + (1+\sigma)^2\, sin^2\, 2kh\right]^{1/2}}{1+\sigma^2+2\sigma\, cos\, 2kh} \right| \qquad (33)$$

where σ is the reflection coefficient at the solid-liquid interface (the contact area between the transducer and the reaction cell). Assuming 100% reflection ($\sigma = 1$), Equation (33) becomes undefined at values of h where

$$h = \frac{(2n+1)\lambda}{4}, \quad n = 0,1,2... \qquad (34)$$

This indicates the pressure amplitude is undefined at these points, thus maximum pressure intensity is achieved. When the liquid height in the cell is

$$h = \frac{(n+1)\lambda}{2}, \quad n = 0,1,2... \qquad (35)$$

the pressure amplitude given by Equation (33) is zero, thus the pressure intensity at these points is zero. As predicted with the model, a maximum in Cl_2 yield was observed when the liquid height above the transducer was equal to points given by Equation (34). No observable Cl_2 was produced when the liquid height was equal to Equation (35). Equation (33) also provided a good prediction of the yield of Cl_2 as a function of liquid height and input power to the horn.

2.11.4 Comparison of system types

A direct immersion horn, a titanium cylindrical crucible, a cup-horn (similar to the planar transducer shown in Figure 2.12) and a cleaning bath were compared using a Michael reaction, the addition of ethyl malonate to chalcone with solid KOH as a catalyst (Ratoarinoro

et al., 1992). The power transmitted to the reaction mixture per unit volume was kept constant in an attempt to make an accurate comparison of the different emitter types investigated. The yields obtained were 98% for the horn, 97% for the crucible, 91% for the cup-horn and 77 % for the bath. As discussed previously, the cleaning bath is the least efficient because a large amount of the power is dissipated in the liquid surrounding the reaction vessel.

2.12 Sonochemical Reactors with Electromechanical Transducers

Incorporating ultrasonic technology into current reactor design is becoming increasingly important in today's industries. Currently Germany's Clausthal Technical University, with the help of several companies including Hoechst, is operating a modular sonochemical reactor which produces up to 4 metric tons of Gringard reagent per year (Ondrey *et al.*, 1996). In France, the Electricite de France is funding the piloting of an ultrasonic electrolytic reactor to be used for the indirect oxidation of cyclohexanol to cyclohexone (Ondrey *et al.*, 1996). It is the hope of the present authors that this technology will be accepted and encouraged within the United States as a viable enhancement technique for several types of fine chemical processes.

2.12.1 Batch and/or continuous flow reactors

a. Mounted transducers

Berger's Sonochemical Reactor

The ultrasonic reactor design developed by Berger *et al.* (1996) contains 6-8 transducers built into the wall of a continuously stirred tank reactor, and 3-5 transducers also built into the bottom of the vessel, as shown in Figure 2.13. The reactor is equipped with an impeller for mechanical agitation, an external jacket for isothermal control, and reaction ports which allow

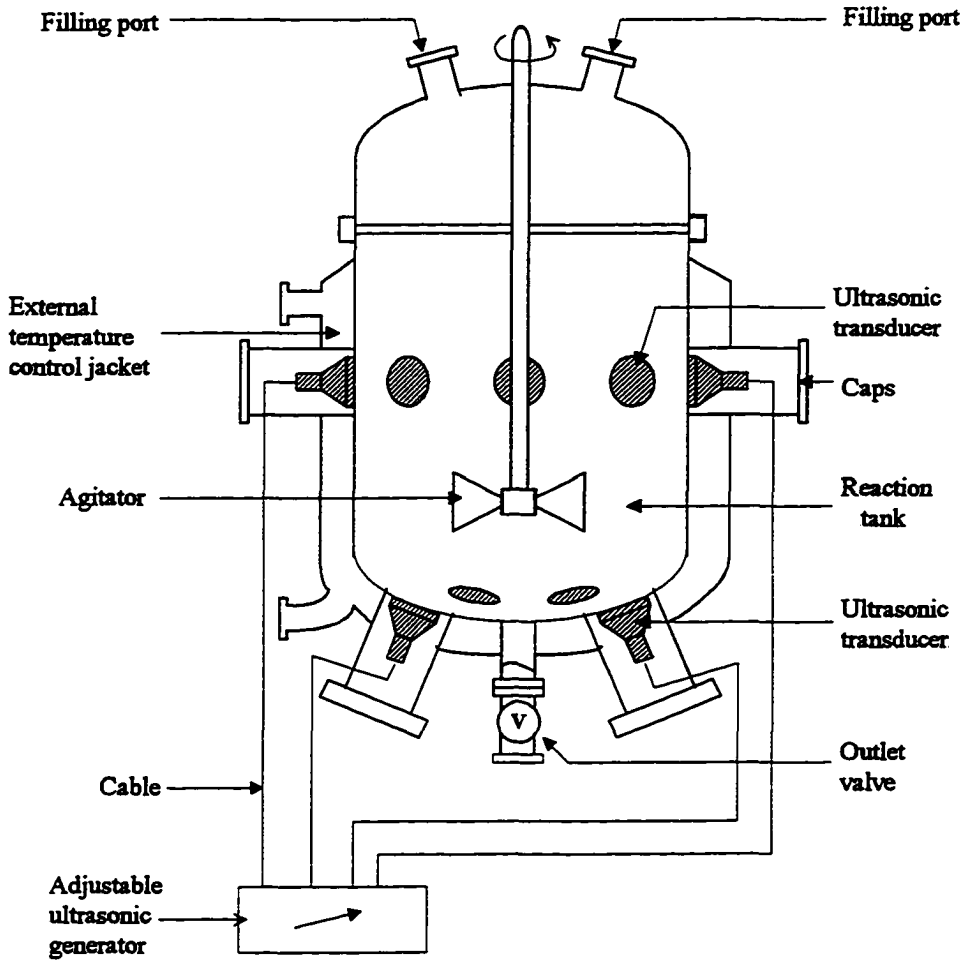

Figure 2.13. Sonochemical stirred tank reactor (Berger, 1996).

for operation in the batch, semi-batch, or continuous mode. The transducers may be operated independently of one another and are designed with caps protecting them from atmospheric disturbances. This reactor configuration was developed in hopes of remedying the problems of other types of sonichemical reactors, such as: the efficiency and reproducibility problems typically associated with ultrasonic baths and the small active cavitation region associated with ultrasonic probes which deliver power to a narrow band of liquid directly under the probe tip. This reactor also allows for sonication of a solid-liquid system, which is a problem with vibrating plate systems which only allow for liquid-liquid systems.

Hexagonal Bath System

This type of sonochemical reactor provides indirect sonication to the reaction vessel, as shown in Figure 2.14, and the design is similar to that of an ultrasonic bath. The outerhull of the reactor is hexagonal in shape, and is fitted with transducer mounted in the center of each

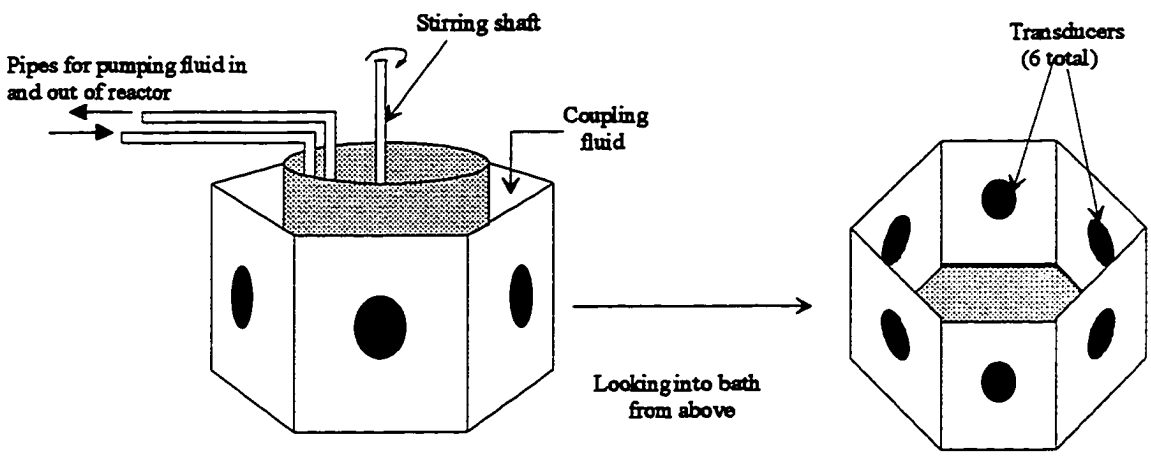

Figure 2.14. Hexagonal sonochemical reactor.

side. The hexagonal shape is used to facilitate the attachment of the transducers, as it is very difficult mount transducers on a rounded surface. Each transducers delivers 100 W of power which is focused towards the center of the bath. The reactor is simply a conventional type of mixed reactor which can be operated in the batch or continuous mode.

b. Unspecified systems

The Eastman Kodak Company has patented a process for producing aromatic carboxylic esters in the presence of ultrasound (Steinmetz and Matosky, 1993). While not many specifics are given, the reaction appears to be carried out in a continuous, pressurized reactor (although batch and semi-batch reactions are also reported) in the presence of ultrasound. The operating conditions for the ultrasound consist of a frequency in the range of 15 to 100 kHz and an acoustic intensity in the range of 1 to 20 kW/cm^2 (presumably delivered intensity).

2.12.2 Batch reactors with an external flow loop

a. Probe systems

Conventional batch reactors were modified by attaching an external flow loop which provides sonication to a small volume reaction mixture within the loop. This sonication can be provided using several methods, two of which are shown in Figure 2.15. This type of reactor has several advantages, one of the largest being that the sound fields created in small liquid volumes using probe(s) and mounted transducers have been well-characterized in the literature. In addition, the operator has control of the residence time of the mixture through

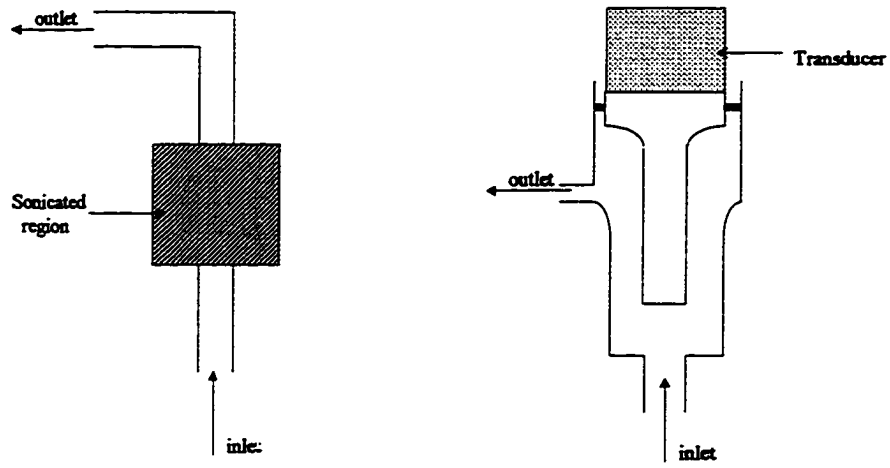

(a) Mounted transducer (b) Probe system

Figure 2.15. Flow loops used to sonicate external streams of batch and continuous flow reactors.

the active sonication region. The external flow loop is usually modular, facilitating maintenance of equipment.

One of the main disadvantages in using a reactor with an external flow loop is that the species activated in the sonicated region are short lived, and may not have the desired propensity for reaction once they reach the main reaction tank. However, if the species created in the sonicated zone is an intermediate required for a series reaction (i.e. if the reaction is $A \rightarrow B \rightarrow C$ and B is created in the presence of sonication) the overall reaction can be greatly enhanced using an external flow loop.

A process using a flow through cell with an ultrasonic amplifying horn, similar to the one shown in Figure 2.15b, was patented for the production of aluminum compounds of the form $Al_2(OH)_{6-a}X_a$ (where X is Cl^-, Br^-, F^-, I^-, SO_4^-, or NO_3^-) (Joshi and Parekh, 1993). The slurry consisted of 10 to 50 weight percent of alumina in an aqueous solution where additional

mechanical agitation was used (when necessary), in conjunction with the sonication. They reported using a typical frequency of 20 kHz, but did not give the intensities at which they were operating.

b. Mounted transducers

Harwell Sonochemical Reactor

The design for Harwell's sonochemical reactor (Anonymous, 1990) was a collaborative effort of nineteen different companies, including British Petroleum, Sandoz, Rhone-Poulenc and ABM Chemicals. As shown in Figure 2.16, it is a 20 liter batch reactor, fitted with an external flow loop which sonicates a small volume of the reaction mixture and returns it to the

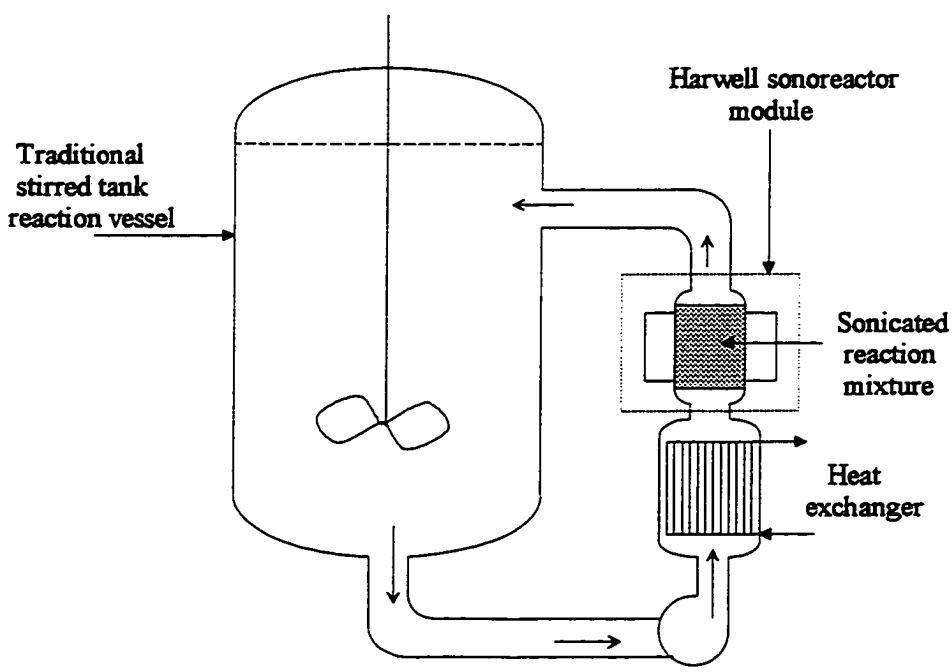

Figure 2.16. Harwell sonochemical reactor.

main vessel. The sonoreactor module contains three mounted transducers which are evenly spaced around the 13 cm diameter piping, which contains a buffer fluid (Mason and Berlan, 1992). The transducers are not brought directly into contact with the reactive stream to avoid corrosion and facilitate equipment maintenance.

2.12.3 Tubular reactors

Tubular sonochemical reactor designs exist which provide either direct or indirect sonication to the process stream. Several designs exist, some of which may be used to provide sonication to an external flow loop in a mixed reactor.

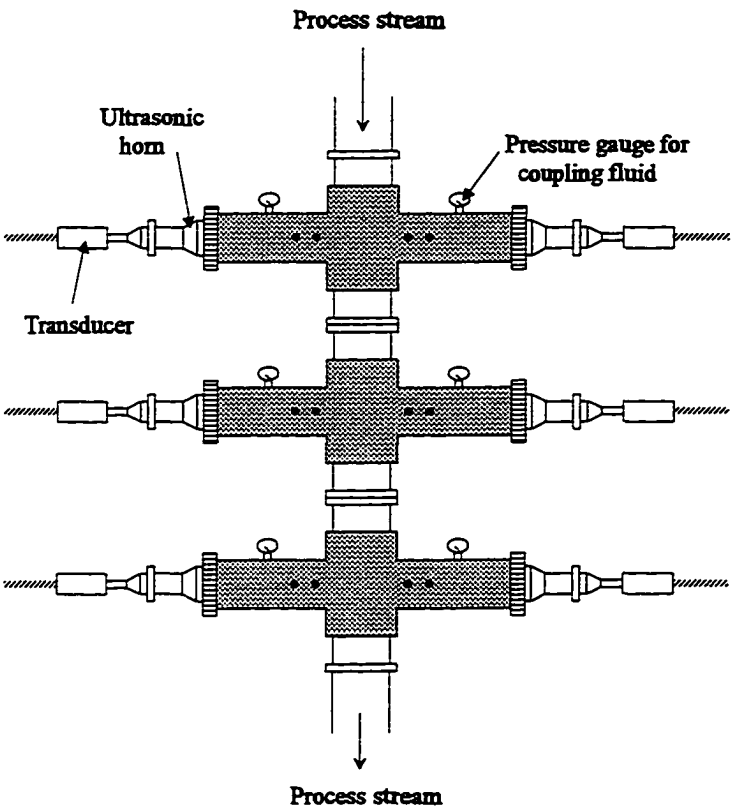

Figure 2.17. Branson sonochemical reactor (tubular configuration).

a. Probe systems

Branson sonochemical reactor

This sonochemical reactor, manufactured by Branson ultrasonics, consists of modular units which may be combined in series, as shown in Figure 2.17. Each unit consists of two ultrasonic horns in contact with a coupling fluid, which is used to reduce erosion and pitting of the probe tip. Using indirect sonication also prevents contamination of the process stream with fragments of the probe tip which may be incurred during the erosion process.

Ragaini's triphase catalyst reactor

Two types of ultrasonic reactors were patented by Ragaini (1992) which were designed specifically to enhance polyphase reactions. The first reactor (shown in Figure 2.18) has the ability to emulsify the inlet liquid streams before they come into contact with a triphase catalyst (i.e. a phase transfer catalyst bound on a polymeric support) contained in a fixed catalyst bed. The compartment has screens on either end to prevent the loss of the catalyst. Other options for this system include a gas inlet port, not shown, in which a gaseous reactant may be fed into the tank for mixing before contact with the catalyst. This type of reactor configuration greatly facilitates the reaction between the multiple phase reactants because the ultrasonic probe increases the interfacial area between the reactants before they come into contact with the catalyst bed. The author also states that it has great advantages over typical liquid-liquid-solid slurry reactors because the catalyst does not have to be separated from the reaction mixture at the end of each cycle, enabling an easier and more cost effective

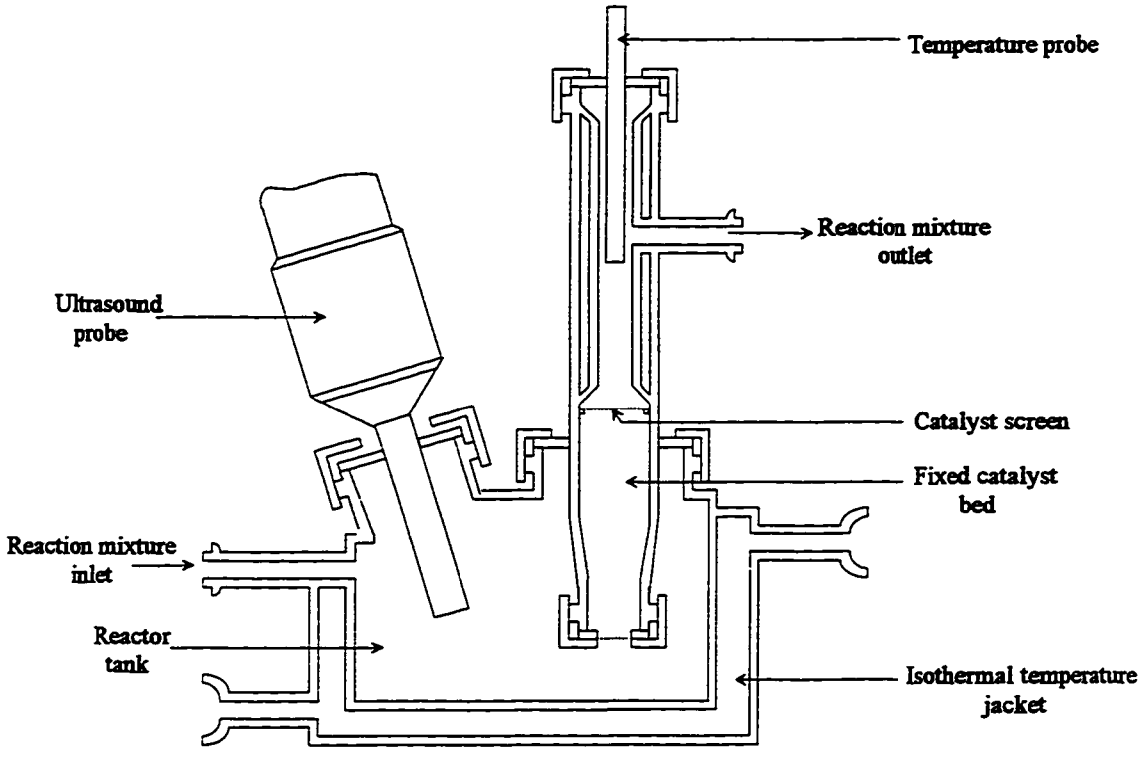

Figure 2.18. Ultrasonic reactor designed to emulsify immiscible liquid streams within the reaction chamber and then send the emulsified mixture through a fixed bed triphase catalyst chamber (Ragaini, 1992).

semicontinuous or continuous process. The second reactor developed by Ragaini (the cylinderical reactor with core cooling) is discussed in Section **2.12.3.*b.***

b. Mounted Transducers

Lewis Nearfield Acoustic Processor (NAP)

The Lewis Nearfield Acoustic Processor (NAP), also termed the Reverberatory Ultrasonic Mixing (RUM) System in some articles, is designed with transducers mounted, facing one another, on opposite sides of stainless steel plates (refer to Figure 2.19). The transducers

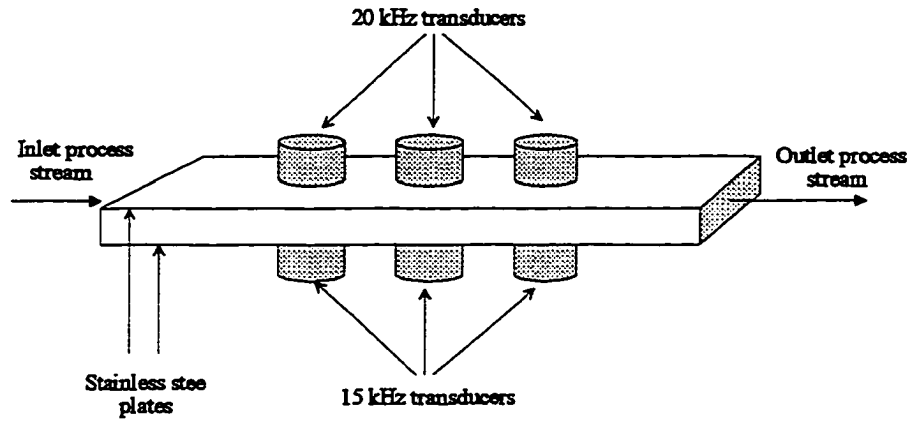

Figure 2.19. Lewis Nearfield Acoustic Processor (NAP).

operate at different frequencies, 15 kHz and 20 kHz, in order to generate an acoustic intensity within the process stream which is greater than the sum of the single plate intensities.

Cylindrical pipe reactor

This type of reactor provides indirect sonication to the process stream, and is designed with cooling capabilities to facilitate the maintenance of isothermal conditions (Figure 2.20).

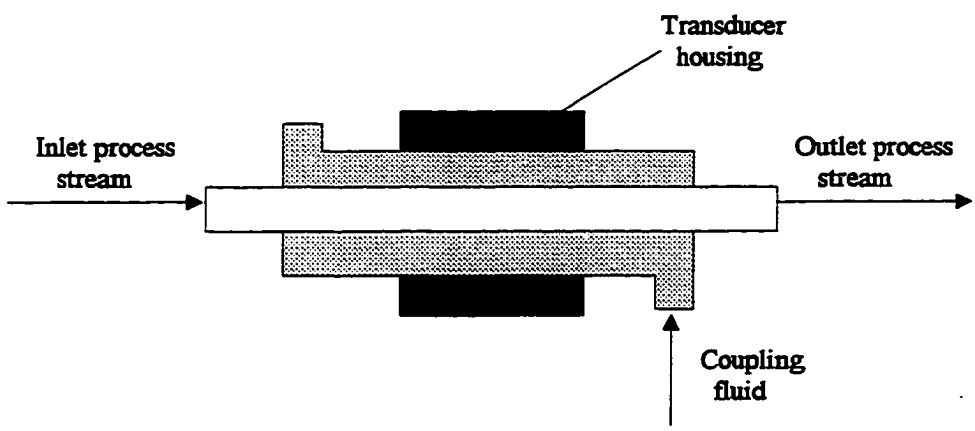

Figure 2.20. Cylindrical pipe reactor.

The length of the pipe is chosen so there will be a null point at the ends. Thus, it can be retrofitted to existing process pipework. One of the main problems with this type of design, however, is that it is very difficult to mount the transducers on the curved surface of the reactor. For this reason, the tube reactors in pentagonal and hexagonal shapes were designed.

Tube reactors

Tube reactors are designed in a variety of shapes, as shown in Figure 2.21, and can be retrofitted to existing process streams. Because it is difficult to mount transducers on round surfaces, flat edges of the pentagonal and hexagonal design facilitate mounting and enable direct bonding of the transducers. Each transducers should be mounted as to focus the acoustic energy towards the center of the reactor.

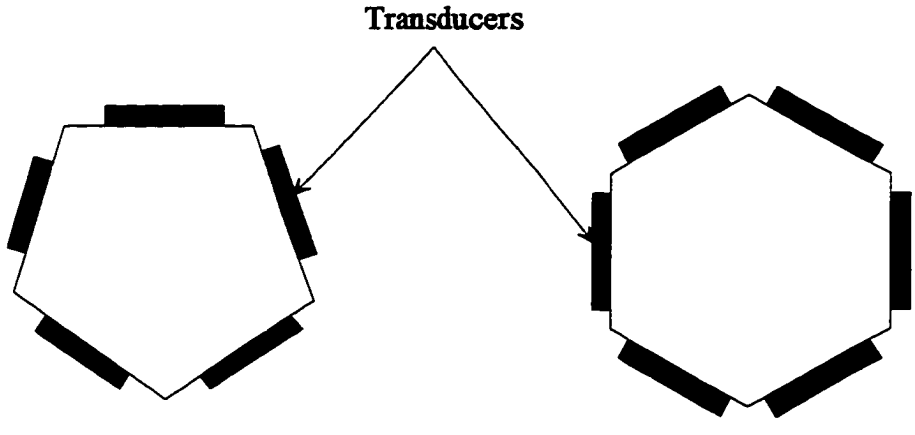

Figure 2.21. Cross sections of two types of tube reactors.

Martin Walter Push-Pull System

The Martin Walter push-pull system was developed in Straubenhardt, Germany, and is shown in Figure 2.22. The ends of the titanium bar are attached to opposing piezoelectric transducers. The length of the bar is equal to a multiple of the half-wavelengths of ultrasound produced. The two transducers are connected with electrical connections which run through the center of the bar. The transducers then operate in a push-pull mode, producing a "concertina" effect down its length. This type of system can be fitted into existing pipework and can be made to a considerable length, enabling the processing of large volumes.

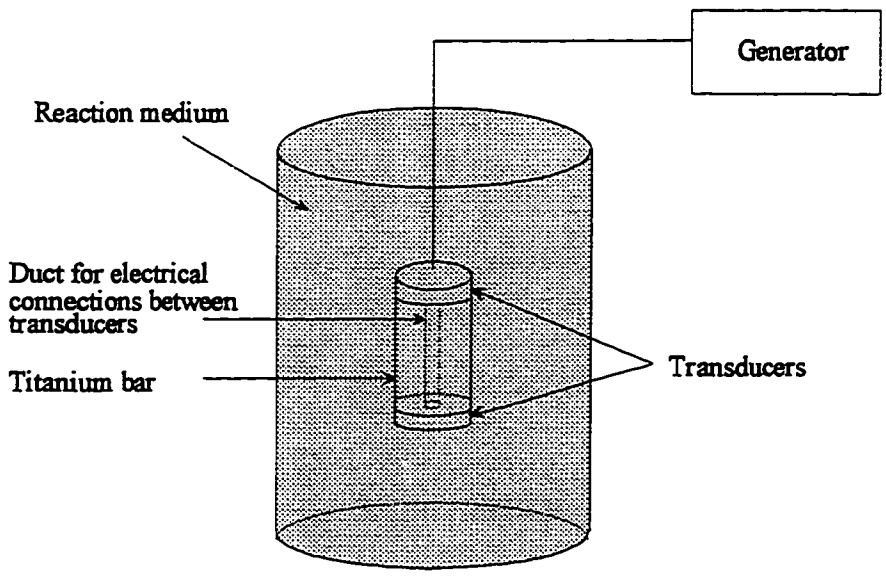

Figure 2.22. Martin Walter push-pull system.

Cylindrical reactor with core cooling

The cylinderical reactor with core cooling, shown in Figure 2.23, was the second reactor configuration proposed by Ragaini (1992). The transducers are mounted over the length of the catalyst bed in order to sonicate the immiscible reactant streams while they are in contact with the catalyst. The advantages of the first reactor configuration (shown in Figure 2.18) over this one are: 1. it may be less expensive because it consists of one ultrasonic probe, not multiple transducers, 2. the probe tip can be easily replaced if it becomes pitted, which is not the case when the transducers are part of the wall of the catalyst bed, and 3. the triphase catalyst is not exposed to ultrasound, which may otherwise lead to polymer degradation and reduce the life and effectiveness of the triphase catalyst.

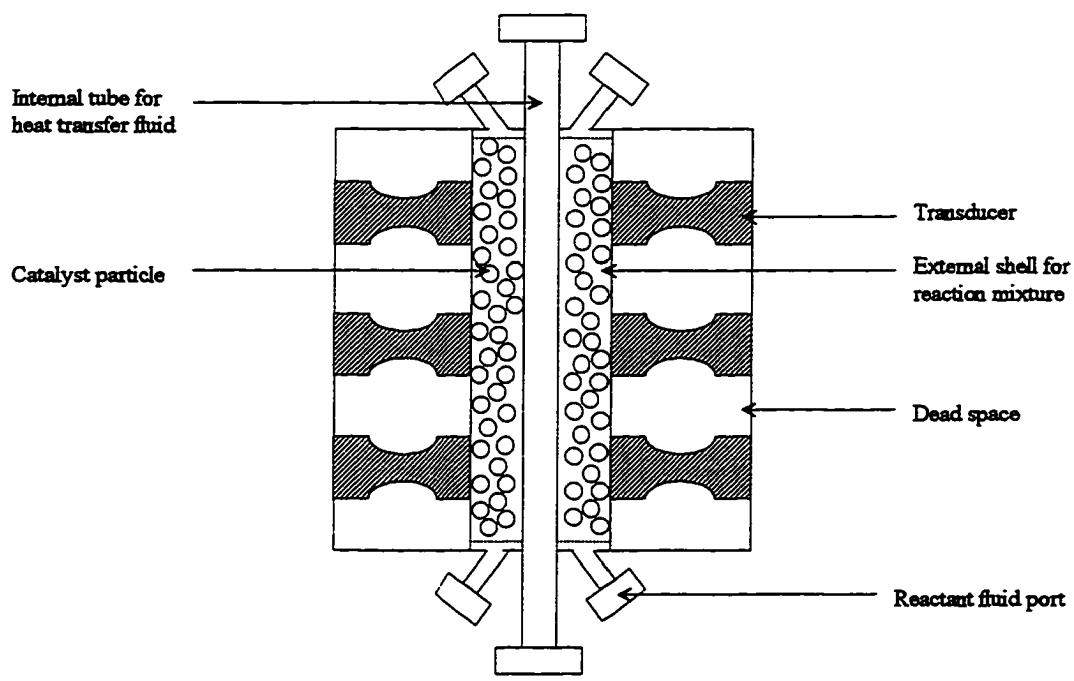

Figure 2.23. Shell and tube reactor configuration with transducers embedded in shell wall. The reaction mixture is contained on the shell side and the heat transfer fluid in contained in the tube (Ragaini, 1992).

Although this reactor was designed for use with triphase catalysts, any type of reaction system can be used. The internal tube provides core cooling to aid in maintaining isothermal conditions.

c. Miscellaneous

Sodeva sonotube

This ultrasonic system was designed by Sodeva, a company based in France. The radial collar is attached to a transducer and acts as a cylinderical resonator (refer to Figure 2.24). Using a length of 1.2 meters and an internal tube diameter of 42 mm, the unit can be operated at 2 kW with 80% efficiency (Mason, 1992a). The maximum ultrasonic power obtained is

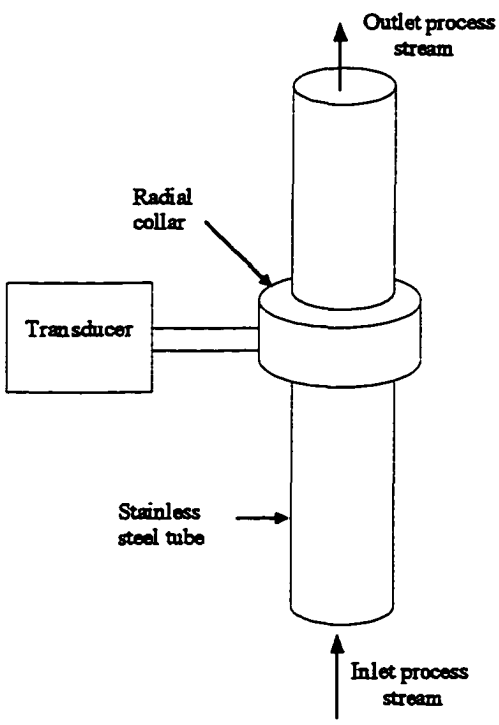

Figure 2.24. Sodeva sonotube.

located at half-wavelength distances along the process pipe. The ends of the pipe are null points, making it possible to retrofit the device to existing pipework.

2.13 Reactors Based on Alternative Methods of Generating Cavitation

2.13.1 Liquid whistle

As discussed in Section 2.9, cavitation can be formed in a fluid *in situ* by forcing the liquid across a vibrating blade, as shown in Figure 2.25. The frequency of the waves generated by the blade is dependent upon the flowrate of the fluid, which must be adjusted to a rate high enough to create cavitation in the fluid. Liquid whistles are very useful and inexpensive methods of producing fine emulsions in immiscible liquid streams, and have been used successfully in food technology (Mason *et al.*, 1996b). The apparatus may be installed on-line using an existing process stream, and is capable of processing large volumes. Solid-liquid

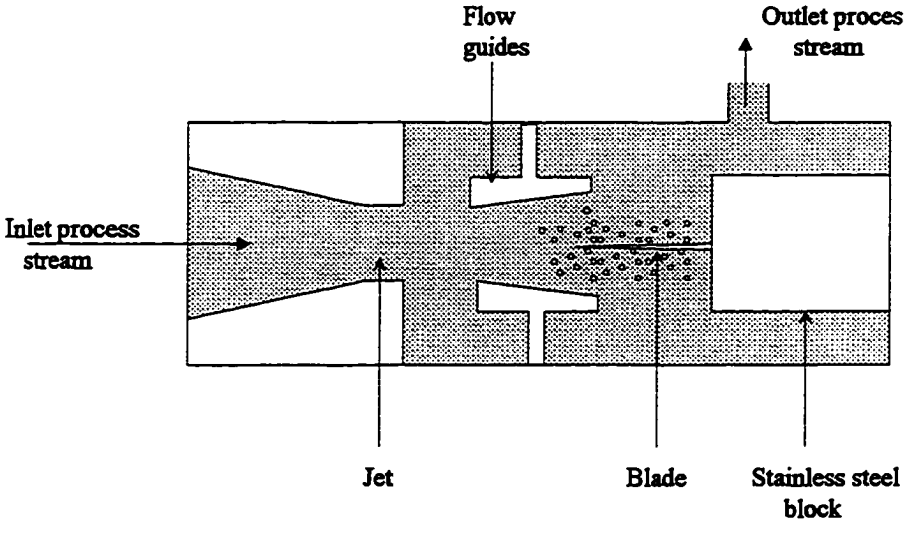

Figure 2.25. Liquid whistle.

systems can also be used, but the solid particles may cause rapid erosion of the blade. In addition, the intensity of cavitation may not be high enough for some applications (i.e. chemical reactions requiring high intensities to obtain desired effects).

2.13.2 Hydrodynamic cavitation reactor

Cavitation can also be generated *in situ* by forcing the fluid through an orifice, as shown in Figure 2.26, resulting in a pressure drop in the fluid. When the pressure falls below that of the vapor pressure of the fluid stream, cavitation sites are created. The magnitude of the pressure drop is dependent upon the flow rate of the fluid and the size of the orifice. When gases are dissolved in the fluid, cavitation may occur at pressures higher than the vapor pressure of the fluid (Pandit and Moholkar, 1996).

Workers who use hydrodynamic cavitation reactors typically refer to the dimensionless parameter termed the cavitation number, C_i, which is defined as

$$C_i = \frac{(P_2 - P_v)}{\frac{\rho \upsilon^2}{2}} \tag{36}$$

where P_2 is the pressure in the fluid after it passes through the orifice, P_v and ρ are the vapor pressure and density of the fluid, respectively, and υ is the velocity of the fluid at the orifice. The parameter C_i is independent of the liquid velocity in the pipe, but increases linearly with the ratio of orifice diameter to pipe diameter (Yan *et al.*, 1988). It has been shown that cavitation inception occurs when C_i is in the range of 1.5 - 2.5.

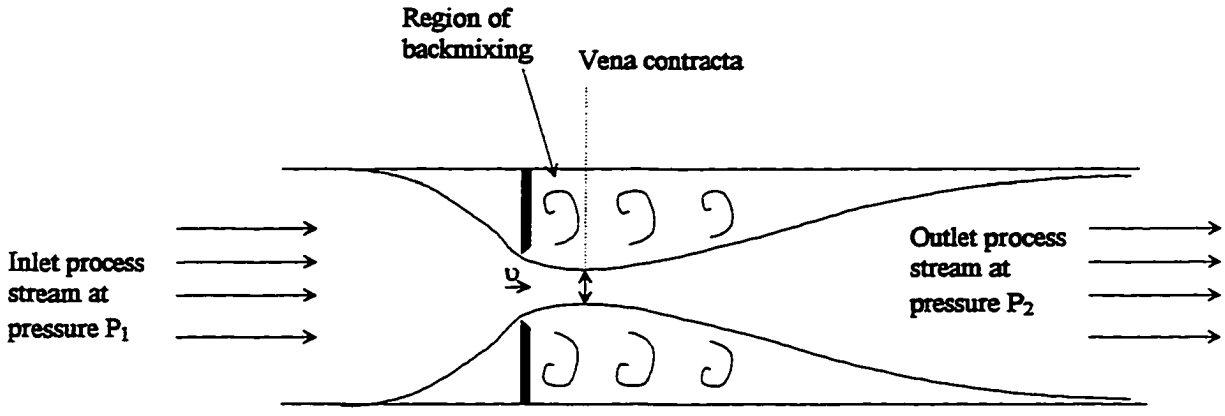

Figure 2.26. Flow through an orifice: hydrodynamically created cavitation.

2.14 Scale-up Considerations

When considering whether or not to scale-up a reaction which is accelerated with the use of ultrasound, there are several factors to consider. First, it is important to know what role ultrasound is playing in the enhancement. Are the effects truly chemical (i.e. is the enhancement due to the formation of free-radicals) or are they primarily physical? If they are physical, what effects are most important to the enhancement of the reaction? If particle degradation is the only critical role ultrasound is playing, a sonochemical reactor may not necessary. Rather the solids can be sonicated before they are placed within a conventional reactor. However, if the other physical effects of ultrasound are important, such as the enhanced rate of mass transfer and/or surface renewal, then sonication will be required over the course of the reaction.

In some cases, the use of ultrasound may generate a reaction intermediate which catalyzes the reaction, as in the case of the Diels-Alder cycloaddition between cyclopentadiene and methyl vinyl ketone (Reisse *et al.*, 1996). However, if this is the only role ultrasound is

playing, it may be more cost effective to physically add the necessary intermediate, instead of using ultrasound to generate it.

Once the conclusion is reached that ultrasound is required to obtain the desired reaction enhancement, factors which need to be considered before scale-up are the characteristics of the liquid reaction medium, such as the viscosity, vapor pressure and dissolved gas-type and concentration. As discussed in Section 2.3.2, the properties of the fluid and dissolved gases are extremely important to the type and amount of sonication required. In addition, the presence of solids, their nature, size and structure, will also affect the reactor selection. For example, when the reaction system is liquid-solid, a whistle reactor would not be a good selection because the blade would become quickly eroded by the presence of the solids.

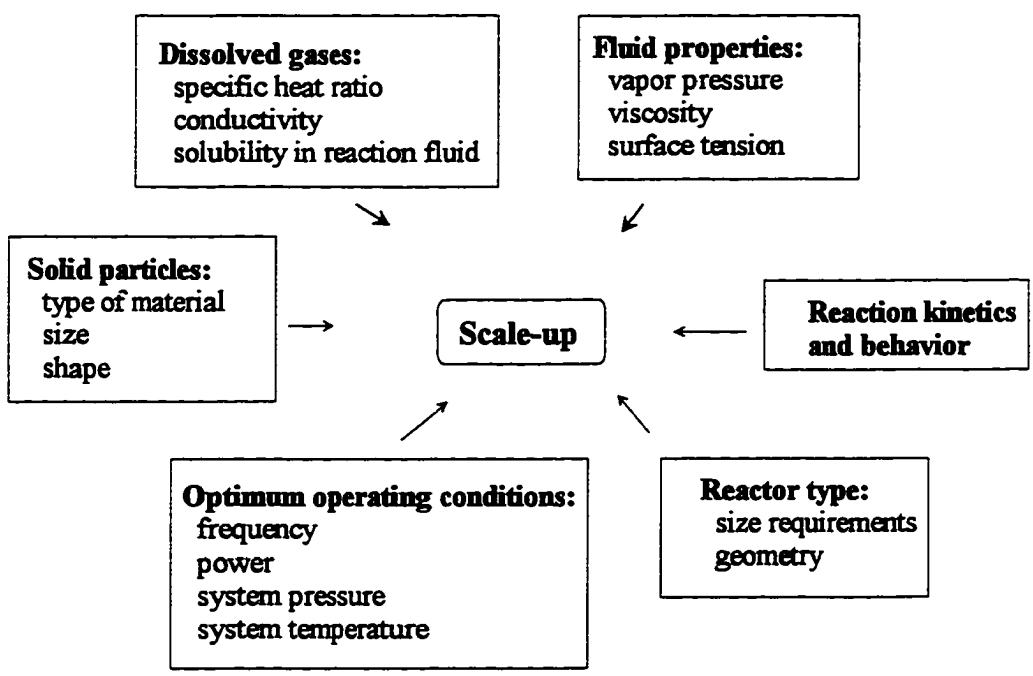

Figure 2.27. Scale-up considerations.

In addition to knowing the characteristics of the reaction mixture and the kinetics of the reaction, one must also have knowledge of the optimum system and ultrasonic conditions, such as the ambient reaction temperature, pressure, frequency and dissipated power, and how they interact with one another. Addition of equipment within a reactor (i.e. baffles, stirrers, and cooling coils) affect the distribution of ultrasonic energy because the waves reflect off of them. All scale-up considerations discussed thus far are summarized in Figure 2.27.

2.15 Conclusions

The advances in the field of ultrasound in the last twenty years have been plentiful, but there is still a lot of new frontier to be covered. Researchers have found that ultrasound chemically enhances reactions which depend upon a single electron transfer process as a key step. They have also found that ultrasound mechanically enhances reaction systems which follow an ionic mechanism. These enhancements are a result of increases in the intrinsic mass transfer coefficient, increases in surface area resulting from particle degradation, and, in some cases, increases in the driving force for dissolution.

Several other aspects of the effects of ultrasound on systems remains unclear. The manner by which free-radicals are produced within the cavitation bubble remains elusive, although several researchers have concluded that they are formed during the adiabatic implosion of the cavitation bubble. In addition, ultrasound has been found to enhance the effective diffusivity in a solid-liquid system, increase the intrinsic mass transfer coefficient, induce supersaturation, and increase the activation energy and frequency factor of various reaction systems. However, the actual mechanisms behind these enhancements have not been discerned. It will

take the combined work of scientists from all fields to resolve the role of ultrasound on reacting systems, and to make it a viable rate enhancement technique for commercial industrial processes.

2.16 Nomenclature

a	interfacial area of solid particles
A	Arrhenius parameter
A_p	area of probe tip
C	velocity of sound in the liquid medium
C_A^*	saturation concentration
C_A	concentration of solid reactant in solution
C_{Ao}	initial solid reactant concentration
C_B	concentration of liquid phase reactant
C_i	dimensionless cavitation number
$C_{p,\ solvent}$	heat capacity of the solvent
$C_{p,\ vessel}$	heat capacity of the reactor vessel
D	diffusivity of reactant through solvent
d_e	diameter of electrode
D_e	effective diffusivity
D_{ox}	diffusion constant

d_p	diameter of solid reactant
d_T	distance from transmitting source
e	power dissipated per unit mass of liquid
E_a	activation energy
F_c	shape factor
F_t	cycle time at which bubble phase reaction occurs
F_v	volume of reaction mixture occupied by bubbles
h	height of the liquid above the transducer
I	acoustic intensity
I_{diss}	intensity of ultrasound at the emitting surface
I_{max}	maximum acoustic intensity
k	wave number ($= 2\pi/\lambda$)
k_{BUB}	rate constant associated with bubble collapse
k_{sl}	solid-liquid mass transfer coefficient for dissolution
k_{et}	rate constant of reaction occuring within the bubble
k_l	intrinsic solid-liquid film transfer coefficient
k_{non}	rate constant in the absence of ultrasound
$k_{r.f.}$	rate constant of radical formation
k_s	rate constant of surface reaction

k_{US}	rate constant in the presence of ultrasound
$m_{solvent}$	mass of the solvent
M_A	molecular weight of solid reactant
P	pressure in the bubble at its maximum size
P_2	pressure in the fluid after it passes through the orifice
$p_\infty(t)$	pressure far from the bubble in an infinite liquid
P_A	pressure amplitude delivered by the transducer
P_{diss}	actual power dissipated in the reaction mixture
$p_g(R)$	pressure of permanent gas within bubble
P_I	pressure intensity
$p_L(R)$	liquid pressure just outside the bubble wall
P_m	liquid pressure at transient collapse
P_{max}	maximum pressure developed at moment of bubble collapse
P_o	hydrostatic pressure
P_s	saturation vapor pressure of the liquid
$p_T(R)$	pressure of total mass content within bubble
P_v	vapor pressure of the liquid
$p_v(R)$	pressure of vapor within bubble
p_x	pressure amplitude and distance x from the transducer

R	radius of bubble
$\dot{R}$	first derivative of bubble radius with respect to time
$\ddot{R}$	second derivative of bubble radius with respect to time
R_2	radius of cavitation bubble at which transition from isothermal to adiabatic collapse occurs
R_{Ao}	radius of solid reactant
R_g	universal gas constant
R_{max}	maximum bubble radius
R_{min}	minimum bubble radius
R_o	equilibrium bubble radius
r_{mt}	rate of mass transfer
s	distance of the aluminum foil from the probe tip
s_p	pooled standard deviation
t	time
T	temperature
T_o	ambient reaction temperature
T_{max}	maximum temperature developed at moment of bubble collapse
T_v	temperature of the inner vessel wall
v	wave velocity
V	volume of the liquid medium

x_A	conversion of solid reactant
X_i	volume fraction
x_w	thickness of the inner wall of the reactor vessel

Greek Letters

α	attenuation coefficient of the medium
δ	diffusion layer thickness
λ	wavelength
γ	polytropic ratio of specific heats of bubble mixture
μ	viscosity of the bulk liquid medium
ν	frequency ($= 2\pi/\omega$)
ν	stoichiometric coefficient in SIM model
ρ	density of the bulk liquid medium
ρ_A	density of solid reactant
ρ_{vessel}	density of the reactor vessel
σ	surface tension of the bulk liquid medium
σ_r	reflection coefficient at the liquid-solid interface
τ_m	time for complete transient collapse
ω	angular frequency
ω_r	resonance frequency

ω_r'	resonance eigenfrequency
υ	velocity of the fluid at the orifice

Acronyms and abbreviations

freq.	ultrasonic frequency
PTC	phase transfer catalyst
rxn	reaction
Sh	dimensionless Sherwood number
TBAB	tetrabutylammonium bromide
w/v	mass of solid per unit volume of organic phase (g/mL)

2.17 References

Aerstin, F.G.P., Timmerhaus, K.D. and Folger, H.S., "Effect of the Resonance Parameter on a Chemical Reaction Subjected to Ultrasonic Waves," *AIChE J.*, **1967**, 13(3), 453-456.

Ahuja, A. S. and Hendee, W. R., "Effects of Particle Shape and Orientation on Propagation of Sound in Suspensions," *J. Acoust. Soc. Am.*, **1978**, 63(4), 1074-1080.

Ahuja, A. S., "Wave Equation and Propagation Parameters for Sound Propagation in Suspensions," *J. Appl. Phys.*, **1973**, 44(11), 4863-4868.

Ahuja, A. S., "Formulation of Wave Equation for Calculating Velocity of Sound in Suspensions," *J. Acoust. Soc. Am.*, **1972**, 51(3), 916-919.

Alegria, A. E., Lion, Y. and Kondo, T., "Sonolysis of Aqueous Surfactant Solutions. Probing the Interfacial Region of Cavitation Bubbles by Spin Trapping," J. Phys. Chem., **1989**, 93(12), 4908-4913.

Allegra, J. R. and Hawley, S. A., "Attenuation of Sound in Suspensions and Emulsions: Theory and Experiments," *J. Acoust. Soc. Am.*, **1972**, 51(5), 1545-1564.

Alippi, A., Cataldo, F. and Galbato, A., "Ultrasound Cavitation in Sonochemistry: Decomposition of Carbon Tetrachloride in Aqueous Solutions of Potassium Iodide," *Ultrasonics*, **1992**, 30(3), 148-151.

Ando, T., Fujita, M., Kimura, T., Leveque, J.M., Luche, J.L. and Sohmiya, H., "Mechanism of Sonochemical Excitation in the Reactions of Lead Tetraacetate with Some Organic Substrates," *Ultrasonics Sonochemistry*, **1996**, 3, S223-S227.

Ando, T. and Kimura, T., "Reactivity and Selectivity in Organic Sonochemical Reactions Involving Inorganic Solids," *Ultrasonics*, **Sept. 1990**, 28, 326-332.

Ando, T., Ichihara, J. and Hanafusa, T., "Ultrasonic Acceleration of Solid-Liquid Two-Phase Organic Reactions," *Mem. Int. Sci. Ind. Res., Osaka Univ.*, **1985**, 42, 27-39.

Ando, T., Sumi, S., Kawate, T., Ichihara, J. and Terukiyp, H., "Sonochemical Switching of Reaction Pathways in Solid-Liquid Two-Phase Reactions," *J. Chem. Soc., Chem. Commun.*, **1984a**, 439-440.

Ando, T., Kawate, T., Ichihara, J. and Hanafuse, T., "Acceleration of Solid-Liquid Two-Phase Reaction by Means of Alumina-Water-Ultrasound. A substitute for a Phase Transfer Catalyst," *Chem. Lett.*, **1984b**, 725-728.

Anonymous, "Hartwell's Sonochemistry Reactor," *The Chemical Engineer*, **23 Aug. 1990**, 15.

Atchley, A. A., Frizzell, L. A., Apfel, R. E., et. al., "Thresholds for Cavitation Produced in Water by Pulsed Ultrasound," *Ultrasonics*, **Sept. 1988**, 26, 280-285.

Berger, H., Dragesser, N., Heumueller, R., Schaetzer, E., and Wagner, M., "Reactor for Carrying Out Chemical Reactions," U.S. Patent 5,484,573, dated January 16, 1996.

Berlan, J., Trabelsi, F., Delmas, H., Wilhelm, A.M. and Petrignani, J.F., "Oxidative Degradation of Phenol in Aqueous Media Using Ultrasound," *Ultrasonics Sonochemistry*, **1994**, 1(2), S97-S102.

Berlan, J. and Mason, T. J., "Sonochemistry: From Research Laboratories to Industrial Plants," *Ultrasonics*, **1992**, 30(4), 203-212.

Boldyrev, V.V., "Mechanochemistry and Sonochemistry," *Ultrasonics Sonochemistry*, **1995**, 2(2), S143-S145.

Booth, J., Compton, R.G., Hill, E., Marken, F. and Rebbitt, T.O., "A Novel Approach for the Quantitative Kinetic Study of Reactions at Solid/Liquid Interfaces in the Presence of Power Ultrasound," *Ultrasonics Sonochemistry*, **1997**, 4, 1-7.

Boudjouk, P.R. and Han, B.H., "Organic Sonochemistry Process," U.S. Patent 4,466,870 dated August 21, 1984.

Bremner, D.H., Mitchell, S.R. and Staines, H., "Investigation Into the Effect of Ultrasound on the Dimerization of Pivalic Acid Using Fenton's Reagent," *Ultrasonics Sonochemistry*, **1996**, 3, 47-52.

Bremner, D.H., "Recent Advances in Organic Synthesis Utilizing Ultrasound," *Ultrasonics Sonochemistry*, **1994**, 1(2), S119-S124.

Bremner, D.H., "Chemical Ultrasonics," *Chem. in Britian*, **1986**, July, 633-638.

Brohult, S., "Splitting of the Haemocyanin Molecule by Ultrasonic Waves," *Nature*, **1937**, 140(3549), 805.

Brown, H. C. and Racherla, U. S., "Ultrasonics in Organoborane Chemistry. Rapid Synthesis of Triorganylboranes via a Modified Organometallic Route," *Tetrahedron Letters*, **1985**, 26(36), 4311-4314.

Carnell, M.T., Fiadeiro, P.T. and Emmony, D.C., "Cavitation Phenomena Generated by a Lithotripter Shock Wave," *J. Acout. Soc. Am.*, **1995**, 97(1), 677-679.

Chendke, P. K. and Fogler, H. S, "Variation of Sonoluminescence Intensity of Water with Liquid Temperature," *J. Am. Chem. Soc.*, **1985**, 89, 1673-1677.

Cheung, H. M. and Kurup, S., "Sonochemical Destruction of CFC 11 and CFC 113 in Dilute Aqueous Solution," *Environ. Sci. Technol.*, **1994**, 28, 1619-1622.

Cheung, H.M., Bhatnagar, A., and Jansen, G., "Sonochemical Distruction of Chlorinated Hydrocarbons in Dilute Aqueous Solution," *Environ. Sci. Technol.*, **1991**, 25, 1510-1512.

Chivate, M.M. and Pandit, A.B., "Quantification of Cavitation Intensity in Fluid Bulk," *Ultrasonics Sonochemistry*, **1995**, 2(1), S19-S25.

Coate, R.B. and Towles, J.T., "Industrial Waste Water Treatment," U.S. Patent 5,466,367, dated Nov. 14, 1995.

Contamine, F., Faid, F., Wilhelm, A.M., Berlan, J. and Delmas, H., "Chemical Reactions Under Ultrasound: Discrimination of Chemical and Physical Effects," *Chem. Eng. Sci.*, **1994**, 49(24B), 5865-5873.

Cornils, B., Bahrmann, H., Lipps, W. and Konkol, W., "Process for the Production of Aldehydes," U.S. Patent 4,616,096, dated October 7, 1986.

Crum, L.A., "Comments on the Evolving Field of Sonochemistry by a Cavitation Physicist," *Ultrasonics Sonochemistry*, **1995**, 2(2), S147-S152.

Crum, L.A., "Rectified Diffusion," *Ultrasonics*, **1984**, Sept., 215-223.

Crum, L. A. and Hansen, G. M., "Generalized Equations for Rectified Diffusion," *J. Acoust. Soc. Am.*, **1982**, 72(5), 1586-1592.

Crum, L. A., "Measurements of the Growth of Air Bubbles by Rectified Diffusion," *J. Acoust. Soc. Am.*, **1980**, 68(1), 203-211.

Cum, G., Galli, G., Gallo, R., and Spadaro, A., "Role of Frequency in the Ultrasonic Activation of Chemical Reactions," *Ultrasonics*, **1992**, 30(4), 267-270.

Cum, G., Galli, G., Gallo, R. and Spadaro, A., "Temperature Effects in Ultrasonically Activated Chemical Reactions," *Il Nuovo Cimento*, **1990**, 12(10), 1423-1429.

Cum, G., Gallo, R. and Spadaro, A., "Effect of Static Pressure on the Ultrasonic Activation of Chemical Reactions. Selective Oxidation at Benzylic Carbon in the Liquid Phase," *J. Chem. Soc. Perkin Trans II*, **1988**, 375-383.

Davidson, R. S., Safdar, A., Spencer, J. D., and Robinson, B., "Applications of Ultrasound to Organic Chemistry," *Ultrasonics*, **Jan. 1987**, 25, 35-39.

de Souza-Barboza, J. C., Petrier, C. and Luche, J. L., "Ultrasound in Organic Synthesis. 13. Some Fundamental Aspects of the Sonochemical Barbier Reaction," *J. Org. Chem.*, **1988**, 53, 1212-1218.

de Souza-Barboza, J. C., Luche, J. L. and Petrier, C., "Ultrasound in Organic Synthesis 11. Retention of Optical Activity in Barbier Reactions from S(+) 2-Octyl Halides. Mechanistic Consequences," *Tetrahedron Letters*, **1987**, 28(18), 2013-2016.

Dickens, M. J. and Luche, J. L., "Further Evidence for the Effect of Ultrasonic Waves on Electron Transfer Processes - The Case of the Kornblum-Russell Reaction," *Tetrahedron Letters*, **1991**, 32(36), 4709-4712.

Diez-Barra, E., de la Hoz, A., et al., "Ultrasound and Phase Transfer Catalysis without Solvent in Elimination Reactions: Synthesis of Cyclic Ketene Acetals," *Synlett*, **November 1992**, 893-894.

Diodati, P., Giannini, G., Mirri, L., Petrillo, C. and Sacchetti, F., "Sonochemical Production of a Non-Crystalline Phase of Palladium," *Ultrasonics Sonochemistry*, **1997**, 4, 45-48.

Doktycz, S. J. and Suslick, K. S., "Interparticle Collisions Driven by Ultrasound," *Science*, 2 **March 1990**, 247, 1067-1069.

Dooher, J., Genberg, R., Moon, S., Gilmartin, B., Jakatt, S., Skura, J. and Wright, D., "Combustion Studies of Water/Oil Emulsion on a Commercial Boiler Using No. 2 Oil and Low and High Sulfur No. 6 Oil," *Fuel*, **1980**, 59(12), 883-891.

Drijvers, D., de Baets, R., de Visscher, A., and Van Langenhove, H., "Sonolysis of Trichloroethylene in Aqueous Solution: Volatile Organic Intermediates," *Ultrasonics Sonochemistry*, **1996**, 3, S83-S90.

Edwards, P. L. and Jarzynski, J., "Scattering of Focused Ultrasound by Spherical Microparticles," *J. Acoust. Soc. Am.*, **Sept. 1983**, 74(3), 1006-1012.

Einhorn, J., Einhorn, C. and Luche, J. L., "A Mild and Efficient Sonochemical *tert*-Butoxycarbonylation of Amines from Their Salts," *Synlett*, **Jan. 1991**, 37-38.

Einhorn, C., Einhorn, J., Dickens, M. J., and Luche, J. L., "Organic Sonochemistry - Some Illustrative Examples of a New Fundamental Approach," *Tetrahedron Letters*, **1990**, 31(29), 4129-4130.

Einhorn, C., Einhorn, J., Luche, J. L., "Sonochemistry: The Use of Ultrasonic Waves in Synthetic Organic Chemistry," *Synthesis*, **Nov. 1989**, 787-813.

Elder, S. A., "Cavitation Microstreaming," *J. Acoust. Soc. Am.*, **1959**, 31, 54-64.

Elder, S. A., Kolb, J. and W.L. Nyborg., "Small-Scale Acoustic Streaming Effects in Liquids," *J. Acoust. Soc. Am.*, **1954**, 26(5), 933.

Entezari, M.H., Kruus, P. and Otson, R., "The Effect of Frequency on Sonochemical Reactions III: Dissociation of Carbon Disulfide," *Ultrasonics Sonochemistry*, **1997**, 4, 49-54.

Entezari, M.H. and Kruus, P., "Effect of Frequency on Sonochemical Reactions II. Temperature and Intensity Effects," *Ultrasonics Sonochemistry*, **1996**, 3, 19-24.

Entezari, M.H. and Kruus, P., "Effect of Frequency on Sonochemical Reactions I: Oxidation of Iodide," *Ultrasonics Sonochemistry*, **1994**, 1(2), S75-S79.

Fadel, A., Canet, J. L. and Slalun, J., "Ultrasound Promoted Acyloin Condensation and Cyclization of Carboxylic Esters," *Letters*, **Feb.1990**, 89-91.

Fang, X., Mark, G. and von Sonntag, C., "OH Radical Formation by Ultrasound in Aqueous Solutions. Part 1: The Chemistry Underlying the Terephthalate Dosimeter," *Ultrasonics Sonochemistry*, **1996**, 3, 57-63.

Farhat, F. and Berchiesi, G., "Sonochemically Induced Reaction between Water and 3-Chloropropionitrile," *Synthetic Sommunications*, **1992**, 22(21), 3137-3140.

Fischer, C. H., Hart, E. J. and Henglein, A., "Ultrasonic Irradiation of Water in the Presence of ^{18,} $^{18}O2$: Isotope Exhange and Isotopic Distribution of H_2O_2," *J. Phys. Chem.*, **1986**, 90, 1954-1956.

Fitzgerald, M. E., Griffing, V. and Sullivan, J., "Chemical Effects of Ultrasonics - "Hot-Spot" Chemistry," *J. Chem. Phy.*, **1956**, 25(5), 926-933.

Flint, E.B. and Suslick, K.S., "The Temperature of Cavitation," *Science*, **1991**, 253, 1397-1399.

Flynn, H.G., "Cavitation Dynamics. I. A Mathematical Formulation," *J. Acoust. Soc. Am.*, **1975**, 57, 1379.

Flynn, H.G., Physical Acoustics, vol 1B, W.P. Mason, Ed., Academic Press, Inc., New York, 1964, Ch. 9.

Francony, A. and Petrier, C., "Sonochemical Degradation of Carbon Tetrachloride in Aqueous Solution at Two Frequencies: 20 kHz and 500 kHz," *Ultrasonics Sonochemistry*, **1996**, 3, S77-S82.

Frenzel, H. and Schultes, H., "Luminescenz im Ultraschallbeschickten Wasser," *Z. Phys. Chem.*, **1934**, Band 27(B), 421-424.

Fuchs, E. and Heusinger, H., "Sonolysis and Radiolysis of Glyceraldehyde in Deaerated Aqueous Solution," *Ultrasonics Sonochemistry*, **1995**, 2(2), S105-S109.

Fuentes, A., Marinas, J. M. and Sinisterra, J. V., "Catalyzed Synthesis of Chalcones Under Interfacial Solid-Liquid Conditions With Ultrasound," *Tetrahedron Letters*, **1987**, 28(39), 4541-4544.

Gaitan, D. F., Crum, L. A., Church, C. C. and Roy, R. A., "Sonoluminescence and Bubble Dynamics for a Single, Stable, Cavitation Bubble," *J. Acoust. Soc. Am.*, **1992**, 91(6), 3166-3183.

Geier, G.E., "Chemolytic EDTA-Citric Acid Composition for Dissolution of Calculi," U.S. Patent 4,845,125, dated July 4, 1989.

Gandhi, K.S. and Kumar, R., "Sonochemical Reaction Engineering," *Sadhana*, 1994, 19(6), 1055-1076.

Greenwood, M. S., Mai, J. and Good, M. S., "Attenuation Measurements of Ultrasound in a Kaolin-Water Slurry: A Linear Dependence Upon Frequency," *J. Acoust. Soc. Am.*, **1993**, 94(2), 908-916.

Griffing, V., "The Chemical Effects of Ultrasonics," *J. Chem. Phys.*, **June 1952**, 20(6), 939-942.

Gutierrez, M. and Henglein, A., "Chemical Action of Pulsed Ultrasound: Observation of an Unprecendented Intensity Effect," *J. Phys. Chem.*, **1990**, 94(9), 3625-3628.

Gutierrez, M., Henglein, A. and Fischer, Ch.-H., "Hot Spot Kinetics of the Sonolysis of Aqueous Acetate Solutions," *Int. J. Radiat. Biol.*, **1986**, 50, 313-321.

Hagenson L.C. and Doraiswamy, L.K., "Use of Ultrasound to Induce Supersaturation in a Solid-Liquid System," to be submitted for publication, **1998**.

Hagenson, L.C. and Doraiswamy, L.K., "Comparison of the Effects of Ultrasound and Mechanical Agitation on a Reacting Solid-Liquid System," *Chemical Eng. Sci.*, accepted for publication, **1997**.

Hagenson, L.C., Naik, S.D., and Doraiswamy, L.K., "Rate Enhancements in a Solid-Liquid Reaction Using PTC, Microphase, Ultrasound and Combinations Thereof," *Chem. Eng. Sci.*, **1994**, 49(24A), 4787-4800.

Han, B. H. and Boudjouk, P., "Organic Sonochemisty. Ultrasonic Acceleration of the Hydrosilation Reaction," *Organometallics*, **1983**, 2, 769-771.

Han, B. H. and Boudjouk, P., "Organic Sonochemistry. Sonic Acceleration of the Reformatsky Reaction," *J. Org. Chem.*, **1982**, 47, 5030-5032.

Han, B. H. and Boudjouk, P., "Organic Sonochemistry: Ultrasound Promoted Coupling of Organic Halides in the Presence of Lithium Wire," *Tetrahedron Letters*, **1981**, 22(9), 2757-2758.

Hanafusa, T., Ichihara, J. and Ashida, T., "Useful Synthesis of *α*-Aminonitriles by Means of Alumina and Ultrasound," *Chemistry Letters*, **1987**, 687-690.

Harker, A. H. and Temple, J. A. G., "Velocity and Attenuation of Ultrasound in Suspensions of Particles in Fluids," *J. Phys. D: Appl. Phys.*, **1988**, 21, 1576-1588.

Hart, E. J., Fischer, C. H., and Henglein, A., "Pyrolysis of Acetylene in Sonolytic Cavitation Bubbles in Aqueous Solution," *J. Phys. Chem.*, **1990**, (94), 284-290.

Hart, E. J. and Henglein, A., "Sonolysis of Ozone in Aqueous Solution," *J. Phys. Chem.*, **1986a**, 90, 3061-3062.

Hart, E. J. and Henglein, A., "Sonolytic Decomposition of Nitrous Oxide in Aqueous Solution," *J. Phys. Chem.*, **1986b**, 90, 5992-5995.

Hart, E. J. and Henglein, A., "Free Radical and Free Atom Reactions in the Sonolysis of Aqueous Iodide and Formate Solutions," *J. Phys. Chem.*, **1985**, 89, 4342-4347.

Harvey, E.N. , Barnes, D.K., McElroy, W.D. ,Whitely, A.H., Pease D.C. and Cooper K.W., *J. Cell Comp. Physiol.*, **1944**, 24, 1.

Hatate, Y., Ikeura, T., Shinonome, M., Kondo, K. and Nakashio, F., "Suspension Polymerization of Styrene Under Ultrasonic Irradiation," *J. Chem. Eng. Japan*, **1981**, 14(1), 38-43.

Henglein, A., "Chemical Effects of Continuous and Pulsed Ultrasound in Aqueous Solutions," *Ultrasonics Sonochemistry*, **1995**, 2(2), S115-S121.

Henglein, A., Herburger, D. and Gutierrez, M., "Sonochemistry: Some Factors That Determine the Ability of a Liquid to Cavitate in an Ultrasonic Field, " *J. Phys. Chem.*, **1992**, 96, 1126-1130.

Henglein, A. and Gutierrez, M., "Sonolysis of Polymers in Aqueous Solution. New Observations on Pyrolysis and Mechanical Degradation," *J. Phys. Chem.*, **1988**, 92, 3705-3707.

Henglein, A., "Sonochemistry: Historical Developments and Modern Aspects," *Ultrasonics*, **Jan. 1987**, 25, 6-16.

Henglein, A. and Kormann, C., "Scavenging of OH Radicals Produced in the Sonolysis of Water," *Int. J. Radiat. Biol.*, **1985**, 48(2), 251-258.

Henglein, A., "Sonolysis of Carbon Dioxide, Nitrous Oxide and Methane in Aqueous Solution, " *Z. Naturf.*, **1985**, 40b, 100-107.

Hickling, R., "Effects of Thermal Conduction in Sonoluminescence," *J. Acoust. Soc. Am.*, **1963**, 35, 967-974.

Hirai, K., Nagata, Y. and Maeda, Y., "Decomposition of Chlorofluorocarbons and Hydrofluorocarbons in Water by Ultrasonic Irradiation," *Ultrasonics Sonochemistry*, **1996**, 3, S205-S207..

Hoffmann, M.R., Hua, I., and Hochemer, R., "Application of Ultrasonic Irradiation for the Degradation of Chemical Contaminants in Water," *Ultrasonics Sonochemistry*, **1996**, 3, S163-S172.

Homer, J., Howard, M.J. and Gooda, S., "Effect of Ultrasound on Molecular Mobility in Certain Crystalline Compounds," *Ultrasonics Sonochemistry*, **1995**, 2(2), S71-S74.

Horton, A. M., Hollinshead, D. M. and Ley, S. V., "$Fe_2(CO)_9$ in Tetrahydrofuran or Under Sonochemical Conditions as Convenient Practical Routes to π-allyltricarbonyliron Lactone Complexes," *Tetrahedron*, **1984**, 40(10), 1737-1742.

Hunicke, R. L., "Industrial Applications of High Power Ultrasound for Chemical Reactions," *Ultrasonics*, **Sept. 1990**, 28, 291-294.

Ibisi, M. and Brown, B., "Variation of the Relative Intensity of Cavitation with Temperature," *J. Acoust. Soc. Am.*, **1967**, 41(3), 568-572.

Jadhav, S. V. and Pangarkar, V. G., "Gas-Liquid and Solid-Liquid Mass Transfer in Three-Phase Sparged Reactors With and Without Ultrasound," *J. Am. Oil Chem. Soc.*, **1989**, 66(3), 362-364.

Jana, A.K. and Chatterjee, S.N., "Estimation of Hydroxyl Free Radicals Produced by Ultrasound in Fricke Solution Used as a Chemical Dosimeter," *Ultrasonics Sonochemistry*, **1995**, 2(2), S87-S91.

Javed, T., Mason, T.J., Phull, S.S., Baker, N.R. and Robertson, A., "Influence of Ultrasound on the Diels-Alder Cyclization Reaction: Synthesis of Some Hydroquinone Derivatives and Lonapalene, and Anti-Psoriatic Agent," *Ultrasonics Sonochemistry*, **1995**, 2(1), S3-S4.

Joshi, V.K. and Parekh, J.C., "Methods for Preparing Basic Aluminum Compounds with Ultrasound," U.S. Patent 5,254,230, dated Oct. 19, 1993.

Jouglet, B., Blanco, L. and Rousseau, G., "New Method for the Reaction of Nitroalkanes with Unsaturated Esters," *Synlett*, **Dec. 1991**, 907-908.

Kamath, V., Prosperetti, A. and Egolfopoulos, F. N., "A Theoretical Study of Sonoluminescence," *J. Acoust. Soc. Am.*, **1993**, 94(1), 248-260.

Keller, J.B. and Miksis, M., "Bubble Oscillations of Large Amplitude," *J. Acoust. Soc. Am.*, **1980**, 68, 628.

Khoroshev, G.A., "Collapse of Vapor-Air Cavitation Bubbles," *Sov. Phys. -Acoustics*, **1963**, 9(3), 275-279.

Khurana, J. M., Sahoo, P. K. and Maikap, G. C, "Sonochemical Esterification of Carboxylic Acids in the Presence of Sulphuric Acid," *Synthetic Communications*, **1990**, 20(15), 2267-2271.

Kimura, T., Sakamoto, T., Leveque, J.M., Sohmiya, H., Fujita, M., Ikeda, S. and Ando, T., "Standardization of Ultrasonic Power for Sonochemical Reaction," *Ultrasonics Sonochemistry*, **1996**, 3, S157-S161.

Kirk-Othmer Encyclopedia of Chemical Technology, 3rd Ed., v23, John Wiley & Sons, N.Y., 1983, 462-490.

Klein, K.D., Knott, W., and Koerner, G., "Method for the Synthesis of Silanes or Organosilicon Hydrides by the Reduction of the Corresponding Silicon Halides or Organosilicon Halides," U.S. Patent 5,455,367, dated October 3, 1995.

Koda, S., Amano, T. and Nomura, H., "Copolymerization of Sodium Styrene Sulphonate and Vinylpyrrolidone Under Ultrasonic Irradiation," *Ultrasonics Sonochemistry*, **1996**, 3, S91-S95.

Koda, S., Suzuki, A. and Nomura, H., "Ultrasonic Polymerization of Poly(vinylpyrrolidone)," *Polymer Journal*, **1995**, 27(11), 1144-1146.

Kondo, T., Misik, V. and Riesz, P., "Sonochemistry of Cytochrome c. Evidence for Superoxide Formation by Ultrasound in Argon-Saturated Aqueous Solution," *Ultrasonics Sonochemistry*, **1996**, 3, S193-S199.

Kondo, T., Krishna, C. M. and Riesz, P., "Sonolysis of Concentrated Aqueous Solutions of Nonvolatile Solutes: Spin Trapping Evidence for Free Radicals Formed by Pyrolysis," *Radiat. Res.*, **1989a**, 118, 221-229.

Kondo, T., Krishna, C. M. and Riesz, P., "Pyrolysis Radicals Formed by Ultrasound in Aqueous Solutions of Nucleotides: A Spin-Trapping Study," *Int. J. Radiat. Biol.*, **1989b**, 57, 23-33

Kondo, T., Krishna, C. M. and Riesz, P., "Effect of Non-Volatile Scavengers of Hydroxyl Radicals on Thymine Radical Formation Induced by Gamma-Rays and Ultrasound," *Int. J. Radiat. Biol.*, **1988a**, 53(6), 891-899.

Kondo, T., Krishna, C. M. and Riesz, P., "Free Radical Generation by Ultrasound in Aqueous Solutions of Nucleic Acid Based and Nucleosides: An ESR and Spin-Trapping Study," *Int. J. Radiat. Biol.*, **1988b**, 53, 331-342.

Kost, J. and Langer, R.S., "Ultrasound Enhancement of Membrane Permeability," U.S. Patent 4,780,212, dated October 25, 1988.

Kotronarou, A., Mills, G. and Hoffmann, M. R., "Decomposition of Parathion in Aqueous Solution by Ultrasonic Irradiation," *Environ. Sci. Technol.*, **1992a**, 26, 1460-1462.

Kotronarou, A., Mills, G. and Hoffmann, M. R., "Oxidation of Hydrogen Sulfide in Aqueous Solution by Ultrasonic Irradiation," *Environ. Sci. Technol.*, **1992b**, 26, 2420-2428.

Kotronarou, A., Mills, G. and Hoffmann, M. R., "Ultrasonic Irradiation of *p*-Nitrophenol in Aqueous Solution," *J. Phys. Chem.*, **1991**, 95, 3630-3638.

Krishna, C., Lion, Y., and Kondo, T., "Thermal Decomposition of Methanol in the Sonolysis of Methanol-Water Mixtures. Spin-Trapping Evidence for Isotope Exchange Reactions," *J. Phys. Chem.*, **1987**, 91, 5847-5850.

Kristol, D. S., Klotz, H., and Parker, R. C., "The Effect of Ultrasound on the Alkaline Hydrolysis of Nitrophenyl Esters," *Tetrahedron Letters*, **1981**, 22, 907-908.

Kruus, P. and Patraboy, T.J., "Initiation of Polymerization with Ultrasound in Methyl Methacrylate," *J. Phys. Chem.*, **1985**, 89, 3379-3384.

Lee, J. and Snyder, J. K., "Ultrasound Promoted Diles-Alder Reactions: Synthesis of Tanshinone IIA, Nortanshinone, and (±)-Tanshindiol B," *J. Am. Chem. Soc.*, **1989**, 111, 1522-1524.

Leighton, T.G., "Bubble Population Phenomena in Acoustic Cavitation," *Ultrasonics Sonochemistry*, **1995**, 2(2), S123-S136.

Lepoint-Mullie, F., De Pauw, D. and Lepoint, T., "Analysis of the 'New Electrical Model' of Sonoluminescence," *Ultrasonics Sonochemistry*, **1996**, 3, 73-76.

Lewis, T. J., Barnes, C. and van der Slujis, M. J., "Simulated Ultrasound Adsorption in Liquids," *J. Acoust. Soc. Am.*, **1991**, 89(6), 2715-2724.

Ley, S.V. and Low, C.M.R., Ultrasound in Synthesis, Springer-Verlag, Berlin, 1989.

Li, J., Li, L., Li, T., Li, H. and Liu, J., "An Efficient and Convenient Procedure for the Synthesis of 5,5-Disubstituted Hydantoins Under Ultrasound," *Ultrasonics Sonochemistry*, **1996**, 3, S141-S143.

Lickiss, P.D. and McGrath, V.E., "Breaking the Sound Barrier," *Chem. in Britain*, **1996**, March, 47-50.

Lie Ken Jie, M.S.F. and Lam, C.K., "Ultrasound-Assisted Expoxidation Reaction of Long-Chain Unsaturated Fatty Esters," *Ultrasonics Sonochemistry*, **1995**, 2(1), S11-S14.

Lin, Q., Zhang, Y., Zhang, C., Song, W. and Qiu, Q., "The Application of Ultrasound to the Dialkylation and Cyclodialkylation of Ethyl Cyanoacetate Under Solid-Liquid Phase Transfer Conditions," *Chin. Chem. Lett.*, **1991**, 2(7), 517-20 (Eng.). see also *Chem. Abst.*, **1992**, 116, 193753t.

Lindley, J., Lorimer, J. P., and Mason, T. J., "Sonochemically Enhanced Ullmann Reactions," *Ultrasonics*, **Jan. 1987a**, 25, 45-48.

Lindley, J and Timothy, J. M., "Sonochemistry: Part 2 - Synthetic Applications," *Chem. Soc. Rev.*, **1987b**, 16, 275-311.

Lorimer, J.P. and Mason, T.J., "Some Recent Studies at Coventry University Sonochemistry Centre," *Ultrasonics Sonochemistry*, **1995**, 2(2), S79-S86.

Lorimer, J. P., Mason, T. J. and Fiddy, K., "Enhancement of Chemical Reactivity by Power Ultrasound: An Alternative Interpretation of the Hot Spot," *Ultrasonics*, **1991**, 29(4), 338-343.

Lorimer, J. P. and Timothy, J. M., "Sonochemistry: Part 1-The Physical Aspects," *Chem. Soc. Rev.*, **1987**, 16(1), 239-274.

Lorimer, J.P. and Mason, T.J., "Effect of Ultrasonic Irradiation on the Solvolysis of 2-Chloro-2-methylpropane in Aqueous Ethanol Mixtures," *J.C.S. Chem. Comm.*, **1980**, 1135-1136.

Low, C.M.R., "Ultrasound in Synthesis: Natural Products and Supersonic Reactions?," *Ultrasonics Sonochemistry*, **1995**, 2(2), S153-S163.

Luche, J.L., "Synthetically Useful Sonochemical Reactions in Solution," *Ultrasonics Sonochemistry*, **1996**, 3, S215-S221.

Luche, J.L., "Effect of Ultrasound on Heterogeneous Systems," *Ultrasonics Sonochemistry*, **1994**, 1(2), S111-S118.

Luche, J. L., "Developments of the New 'Experimental Theory' of Sonochemistry Initiated in Grenoble," *Ultrasonics*, **1992**, 30(3), 156-161.

Luche, J. L., Einhorn, C., Einhorn, J. and Sinisterra-Gago, J. V., "Organic Sonochemistry: A New Interpretation and Its Conseqences," *Tetrahedron Letters*, **1990a**, 31(29), 4125-4128.

Luche, J. L., Einhorn, C., Einhorn, J. *et al.*, "Ultrasonic Waves as Promoters of Radical Preocesses in Chemistry: the Case of Organometallic Reactions," *Ultrasonics*, **1990b**, 28(5), 316-321.

Luche, J. L., de Souza-Barboza, J. C. and Petrier, C., "Ultrasound in Organic Synthesis 11. Retention of Optical Activity in Barbier Reaction From S(+) 2-Octyl Halides. Mechanistic Consequences," *Tetrahedron Letters*, **1987a**, 28(18), 2031-2016.

Luche, J. L.and The Sonochemistry Group, "Organometallic Sonochemistry: Successes, Problems, and By-products," *Ultrasonics*, **Jan. 1987b**, 25, 40-44.

Luche, J. L. and Damiano, J. C., "Ultrasounds in Organic Synthesis. 1. Effect on the Formation of Lithium Organometalic Reagents," *J. Am. Chem. Soc.*, **1980**, 102, 7926-7927.

Lukevics, E., Dirnens, V. V., Goldberg, Y. S., et. al., "A Novel Synthesis of Silicon-Containing Aziridines," *J. Organometallic Chem.*, **1984**, 268, C29-C32.

Madanshetty, S. I. and Apfel, R. E., "Acoustic Microcavitation: Enhancement and Applications," *J. Acoust. Soc. Am.*, **Sept. 1991**, 90(3), 1508-1514.

Madigan, N. A., Hagan, R. S., Zhang, H. Coury, L.A., "Effects of Sonication on Electrode Surfaces and Metal Particles," *Ultrasonics Sonochemistry*, **1996**, 3, S239-S247.

Madison, S.A., Koek, J.H., Eshuis, J.J.W., and Potman, R.P., "Preparation of Organic Macrocyclic Compounds," U.S. Patent 5,326,861, dated July 5, 1994.

Makino, K., Mossoba, M. M. and Riesz, P., "Chemical Effects of Ultrasound on Aqueous Solutions. Formation of Hydroxyl Radicals and Hydrogen Atoms," *J. Phys. Chem.*, **1983**, *87*, 1369-1377.

Makino, K., Mossoba, M. M. and Riesz, P., "Chemical Effects of Ultrasound on Aqueous Solutions. Evidence for ·OH and ·H by Spin Trapping," *J. Am. Chem. Soc.*, **1982**, 104, 3537-3539.

Margulis, M.A., "Fundamental Problems of Sonochemistry and Cavitation," *Ultrasonics Sonochemistry*, **1994**, 1(2), S87-S90.

Margulis, M. A., "Fundamental Aspects of Sonochemistry," *Ultrasonics*, **1992**, 30(3), 152-155.

Margulis, M. A., "Sonoluminescence and Sonochemical Reactions in Cavitation Fields. A Review," *Ultrasonics*, **1985**, 23, 157-169.

Margulies, T. S. and Schwarz, W. H., "Sound Wave Propagation in Fluids with Coupled Chemical Reactions," *J. Acoust. Soc. Am.*, **1985**, 78(2), 605-615.

Martin, C.J. and Law, A.N.R., "The Use of Thermistor Probes to Measure Energy Distribution in Ultrasound Fields," Ultrasonics, 1980, May, 127-133.

Mason, T.J., Newman, A., Lorimer, J.P., Lindley, J. and Hutt, K., "Ultrasonically Assisted Catalytic Decomposition of Aqueous Sodium Hypochlorite," *Ultrasonics Sonochemistry*, **1996a**, 3, 53-55.

Mason, T.J., Paniwnyk, L. and Lorimer, J.P., "The Uses of Ultrasound in Food Technology," *Ultrasonics Sonochemistry*, **1996b**, 3, S253-S260.

Mason, T.J., Lorimer, J.P., Bates, D.M. and Zhao, Y., "Dosimetry in Sonochemistry: The Use of Aqueous Terephthalate Ion as a Flourescence Monitor," *Ultrasonics Sonochemistry*, **1994**, 1(2), S91-S95.

Mason, T.J., "Sonochemistry: Current Trends and Future Prospects," contained within Current Tends in Sonochemistry, ed. by G.J. Price, Royal Society of Chemistry, Cambridge, 1992a.

Mason, T. J., "Industrial Sonochemistry: Potential and Practicality," *Ultrasonics*, **1992b**, 30(3), 192-196.

Mason, T.J. and Berlan, J., "Ultrasound in Industrial Processes: The Problems of Scale-up," contained within Current Tends in Sonochemistry, ed. by G.J. Price, Royal Society of Chemistry, Cambridge, 1992, 148-157.

Mason, T. J., Lorimer, J. P. and Bates, D. M., "Quantifying Sonochemistry: Casting Some Light on a 'Black Art'," *Ultrasonics*, **1992**, 30(1), 40-42.

Mason, T. J., Practical Sonochemistry: User's Guide to Applications in Chemistry and Chemical Engineering, Ellis Horwook Limited, England, 1991.

Mason, T. J., Chemistry With Ultrasound: Critical Reports on Applied Chemistry Volume 28, Elsevier Applied Science, New York, 1990a.

Mason, T. J., Sonochemistry: The Uses of Ultrasound in Chemistry, Royal Society of Chemistry, Cambridge, 1990b.

Mason, T.J., "A Survey of Commercially Available Sources of Ultrasound Suitable for Sonochemistry," contained within Sonochemistry: The Uses of Ultrasound in Chemistry, ed. by T.J. Mason, Royal Society of Chemistry, Cambridge, 1990c, 64.

Mason, T. J., Lorimer, J.P., Paniwnyk, L., Harris, A.R., Wright, P.W., Bram, G., Loupy, A., Ferradou, G., and Sansoulet, J.., "The *o*-Alkylation of 5-Hydroxy Chromones. A Comparison of Two Non-Classical Techniques. PTC in the Absence of Solvent and Sonochemical Activation in Polar Aprotic Solvents," *Synth. Commu.*, **1990c**, 20(22), 3411-3420.

Mason, T. J., Lorimer, J. P. and Walton, D. J., "Sonoelectrochemistry," *Ultrasonics*, **1990d**, 28(5), 333-337.

Mason, T. J. and Lorimer, J. P., "An Introduction to Sonochemistry," *Endeavour, New Series*, **1989**, 13(3), 123-128.

Mason, T. J., "Use of Ultrasound in Chemical Synthesis," *Ultrasonics*, **Sept. 1986**, 24, 245-253.

Mason, T. J., Lorimer, J. P and Mistry, B. P., "The Effect of Ultrasound on the Solvolysis of 2-Chloro-2-Methylpropane in Aqueous Ethanol," *Tetrahedron*, **1985**, 41(22), 5201-5204.

Menendez, J.C., Trigo, G.G., and Sollhuber, M.M., "The Application of Ultrasound to the Strecker Synthesis on 9,10-Dimethoxy-1,3,4,6,7,11b-hexahydrobenzo[a]quinolizin-2-one," *Tetrahedron Letters*, **1986**, 27(28), 3285-3288.

Miethchen, R., "Selected Applications of Sonochemistry in Organic Chemistry," *Ultrasonics*, **1992**, 30(3), 173-179.

Mills, A. and Holland, C., "Effect of Ultrasound on the Kinetics of Oxidation of Octan-2-ol and Other Secondary Alcohols with Sodium Bromate, Mediated by Ruthenium Tetraoxide in a Biphasic System," *Ultrasonics Sonochemistry*, **1995**, 2(1), S33-S38.

Mills, A., Li, X. and Meadows, G., "Effect of Ultrasound on the Kinetics of Reduction of Hexacyanoferrate(III) by Thiosulfate Ions Mediated by Ruthenium Dioxide Hydrate," *Ultrasonics Sonochemistry*, **1995**, 2(1), S39-S41.

Misik, V. and Riesz, P., "EPR Study of Free Radicals Induced by Ultrasound in Organic Liquids II. Probing the Temperatures of Cavitation Regions," *Ultrasonics Sonochemistry*, **1996a**, 3, 25-37.

Misik, V. and Riesz, P., "Recent Applications of EPR and Spin Trapping to Sonochemical Studies of Organic Liquids and Aqueous Solutions," *Ultrasonics Sonochemistry*, **1996b**, 3, S173-S186.

Misik, V., Miyoshi, N. and Riesz, P., "EPR Spin-Trapping Study of the Sonolysis of H_2O/D_2O Mixtures: Probing Temperatures of Cavitation Regions," *J. Phys. Chem.*, **1995**, 99, 3605-3611.

Moon, S., "Sound Chemistry," *Chemtech*, **July 1987**, 434-437.

Moon, S., Duchin, L and Cooney, J. V., "Application of Ultrasound to Organic Reactions: Ultrasonic Catalysis on Hydrolysis of Carboxylic Acid Esters," *Tetrahedron Letters*, **1979**, 41, 3917-3920.

Moulton, K. J., Koritala, S., and Warner, K., "Continuous Ultrasonic Hydrogenation of Soybean Oil. II. Operating Conditions and Oil Quality," *JAOCS*, **1987**, 64(4), 542-547.

Moulton, K. J., Koritala, S. and Frankel, E. N., "Ultrasonic Hydrogenation of Soybean Oil," *JAOCS*, **1983**, 60(7), 1257-1258.

Nakamura, E., Machii, D. and Inubushi, T., "Homogeneous Sonochemistry in Radical Chain Reactions. Sonochemical Hydrostannation and Tin Hydride Reduction," *J.Am. Chem. Soc.*, **1989**, 111, 6849-6850.

Naude C.F. and Ellis A.T., "On the Mechanism of Cavitation Damage by Non-Hemispherical Cavities in Contact with a Solid Boundary," *Trans. ASME J. Basic Eng*, **1961**, 83, 648-656.

Nebois, P., Bouaziz, Z., Fillion, H., Moeini, L., Aurell Piquer, M.J., Luche, J.L., Riera, A., Moyano, A. and Pericas, M.A., "The Diels-Alder Cycloaddition, an Intriguing Problem in Organic Sonochemistry," *Ultrasonics Sonochemistry*, **1996**, 3, 7-13.

Neppiras, E.A., "Acoustic Cavitation," *Phys. Rep.*, **1980**, 61(3), 159-251.

Noltingk B.E. and Neppiras, E.A., "Cavitation produced by ultrasonics," *Proc. Phys. Soc.*, **1950**, 63B, 674-685.

Nomura, H., Koda, S., Yasuda, K. and Kojima, Y., "Quantification of Ultrasonic Intensity Based on the Decomposition Reaction of Porphyrin," *Ultrasonics Sonochemistry*, **1996**, 3, S153-S156.

Okitsu, K., Mizukoshi, Y., Bandow, H., Maeda, Y., Yamamoto, T. and Nagata, Y., "Formation of Noble Metal Particles by Ultrasonic Irradiation," *Ultrasonics Sonochemistry*, **1996**, 3, S249-S251.

Ondrey, G., Kim, I. and Parkinson, G., "Reactors for the 21st Century," *Chem. Eng.*, **1996**, June, 39-45.

Osborne, A. G., Glass, K. J. and Staley, M. L., "Ultrasound Promoted Coupling of Heteroaryl Halides in the Presence of Lithium Wire. Novel Formation of Isomeric Bipyridines in a Wurtz-Type Reaction," *Tetrahedron Letters*, **1989**, 30(27), 3567-3568.

Pandit, A.B. and Moholkar, V.S., "Harness Cavitation to Improve Processing," *Chem. Eng. Progress*, **1996**, July, 57-68.

Pandit, A. B. and Joshi, J. B., "Hydrolysis of Fatty Oils: Effect of Cavitation," *Chemical Engineering Science*, **1993**, 48(19), 3440-3442.

Perkins, J.P., "Power Ultrasound," contained within Sonochemistry: The Uses of Ultrasound in Chemistry, ed. by T.J. Mason, Royal Society of Chemistry, Cambridge, 1990, 47-59.

Petrier, C., Reyman, D., and Luche, J.L., "β-Carboline as a Probe for the Sonolysis of Alcohols and Chloromethanes," *Ultrasonics Sonochemistry*, **1994**, 1(2), S103-S105.

Petrier, C., Micolle, M., and Merlin, G., "Characteristics of Pentachlorophenate Degradation in Aqueous Solution by Means of Ultrasound," *Environ. Sci. Technol.*, **1992a**, 26, 1639-1642.

Petrier, C., Jeunet, A., and Luche, J.L., "Unexpected Frequency Effects on the Rate of Oxidative Processes Induced by Ultrasound," *J. Am. Chem. Soc*, **1992b**, 114(8), 3148-3150.

Petrier, C. and Luche, J. L., "Ultrasonically Improved Reductive Properties of an Aqueous Zn-$NiCl_2$ System - 1. Selective Reduction of α,β - Unsaturated Carbonyl Compounds," *Tetrahedron Letters*, **1987a**, 28(21), 2347-2350.

Petrier, C. and Luche, J. L., "Ultrasonically Improved Reductive Properties of an Aqueous Zn-$NiCl_2$ System - 2. Regioselectivity in the Reduction of (-)-Carvone," *Tetrahedron Letters*, **1987b**, 28(21), 2351-2352.

Polackova, V., Tomova, V., Elecko, P. and Toma, S., "Ultrasound-Promoted Cannizzaro Reaction Under Phase Transfer Conditions," *Ultrasonics Sonochemistry*, **1996**, 3, 15-17.

Portenlanger, G. and Heusinger, H., "Polymer Formation from Aqueous Solutions of α-D-glucose by Ultrasound and γ-rays," *Ultrasonics Sonochemistry*, **1994**, 1(2), S125-S129.

Prasad Naidu, D. V., Rajan, R., Kumar, R., Gandhi, K. S., Arakeri, V. H. and Chandrasekaran, S., "Modeling of a Batch Sonochemical Reactor," *Chemical Engineering Science*, **1994**, 49(6), 877-888.

Price, G.J., "Ultrasonically Enhanced Polymer Synthesis," *Ultrasonics Sonochemistry*, **1996**, 3, S229-S238.

Price, G.J., Current Tends in Sonochemistry, Royal Society of Chemistry, Cambridge, 1992.

Price, G.J., Daw, M.R., Newcombe, N.J. and Smith, P.F., "Polymerization and Copolymerization Using High Intensity Ultrasound," *British Polymer Journal*, **1990**, 23, 63-66.

Prosperetti, A., Crum, L.A., and Commander, K.W., "Nonlinear Bubble Dynamics," *J. Acoust. Soc. Am.*, **1986**, 83, 502.

Pugin, B., "Qualitative Characterization of Ultrasound Reactors for Heterogeneous Sonochemistry," *Ultrasonics*, **Jan. 1987**, 25, 49-55.

Ragaini, V., "Method for Conducting Chemical Reactions in Polyphase Systems," U.S. Patent 5,108,654, dated April 28, 1992.

Rayleigh, Lord (Strutt, John William), "On the Pressure Developed in a Liquid During the Collapse of a Spherical Cavity," *Philos. Mag. Ser 6*, **1917**, 34(200), 94-98.

Ratoarinoro, N., Contamine, F., Wilhelm, A. M., Berlan, J. and Delmas, H., "Power Measurement in Sonochemistry," *Ultrasonics Sonochemistry*, **1995a**, 2(1), S43-S47.

Ratoarinoro, N., Contamine, F., Wilhelm, A. M., Berlan, J. and Delmas, H., "Activation of a Solid-Liquid Chemical Reaction by Ultrasound," *Chemical Engineering Science*, **1995b**, 50(3), 554-558.

Ratoarinoro, N., Wilhelm, A. M., Berlan, J. and Delmas, H., "Effects of Ultrasound Emitter Type and Power on a Heterogeneous Reaction," *Chem. Eng. Journal*, **1992**, 50, 27-31.

Reisse, J., Caulier, T., Deckerkheer, C., Fabre, O., Vandercammen, J., Delplancke, J.L. and Winand, R., "Quantitative Sonochemistry," *Ultrasonics Sonochemistry*, **1996**, 3, S147-S151.

Renaudin, V., Gondrexon, N., Boldo, P., Petrier, C., Bernis, A. and Gonthier, Y., "Method for Determining the Chemically Active Zones in a High-Frequency Ultrasonic Reactor," *Ultrasonics Sonochemistry*, **1994**, 1(2), S81-S85.

Repic, O., Lee, P. G. and Giger, U., "Large Scale Cyclopropanation," *Organic Preparations and Procedures Int.*, **1984**, 16(1), 25-30.

Repic, O. and Vogt, S., "Ultrasound in Organic Synthesis: Cyclopropanation of Olefins with Zinc-Diiodomethane," *Tetrahedron Letters*, **1982**, 23(27), 2729-2732.

Richards, W.T. and Loomis, A.L., "The Chemical Effects of High Frequency Sound Waves I. A Preliminary Study," *J. Am. Chem. Soc.*, **1927**, 49, 3086-3100.

Riesz, P., Kondo, T. and Krishna, C., "Sonochemistry of Volatile and Non-Volatile Solutes in Aqueous Solutions: E.P.R. and Spin Trapping Studies," *Ultrasonics*, **Sept. 1990**, 28, 295-303.

Romenskii, A.V., Popik, I.V., Loboiko, A.Y., and Atroshchenko, V.I., *Khim. Tekhnol. (Kiev)*, **1985**, 1, 21-23 (Russian); *Chem. Abst.* 120614z, **1985**, 102, 467.

Schmid, G. and Rommel, O., "Zerreißen von Makromolekülen mit Ultraschall," *Z. Phys. Chem*, **1939**, Band 185(A), 97-139.

Schultz R. and Henglein A., *Z Naturforsch*, **1953**, 8b, 160.

Sehgal, C., Yu, T. J., Sutherland, R. G. and Verrall, R. E., "Use of 2,2-Diphenyl-1-picrylhdrazyl to Investigate the Chemical Behavior of Free Radicals Induced by Ultrasonic Cavitation," *J. Phys. Chem.*, **1982**, 86, 2982-2986.

Sehgal, C. M. and Wang, S. Y., "Threshold Intensities and Kinetics of Sonoreaction of Thymine in Aqueous Solutions at Low Ultrasonic Intensities," *J. Am. Chem. Soc.*, **1981**, 103, 6606-6611.

Seghal, C., Sutherland, R. G. and Verrall, R. E., "Cavitation Induced Oxidation of Aerated Aqueous Fe^{2+} Solutions in the Presence of Aliphatic Alcohols," *J. Phys. Chem.*, **1980**, 84, 2920-2922.

Sehgal, C., Steer, R. P., Sutherland, R. G. and Verrall, R. E., "Sonoluminescence of Aqueous Solutions," *J. Phys. Chem.*, **1977**, 81(26), 2618-2620.

Shirgaonkar, I.Z. and Pandit, A.B., "Sonochemical Effects in a Supplementary Role," *Ultrasonics Sonochemistry*, **1996**, 3, S135-S139.

Sinisterra, J. V., "Application of Ultrasound to Biotechnology: an Overview," *Ultrasonics*, **1992**, 30(3), 180-185.

Soudagar, S.R. and Samant, S.D., "Investigation of Ultrasound Catalyzed Oxidation of Arylalkanes Using Aqueous Potassium Permanganate," *Ultrasonics Sonochemistry*, **1995a**, 2(1), S15-S18.

Soudagar, S.R. and Samant, S.D., "Semiquantitative Characterization of Ultrasonic Cleaner Using a Novel Piezoelectric Pressure Intensity Measurement Probe," *Ultrasonics Sonochemistry*, **1995b**, 2(1), S49-S53.

Steinmetz, G.R. and Matosky, A.J., "Process for the Preparation of Aromatic Carboxylic Acid Esters," U.S. Patent 5,233,075, dated Aug. 3, 1993.

Supersaxo, A. and Kou, J.H., "Controlled Delivery of Pharmaceuticals from Preformed Porous Polymeric Microparticles," U.S. Patent 5,470,582, dated Nov. 28, 1995.

Suslick, K.S. and Kemper, K.A., in: Bubble Dynamics and Interface Phenomena, Ed. by J.R. Blake, Khiwer Academic Publishers, Dordrecht, Netherlands, 1994.

Suslick, K. S., "Sonochemistry," *Science*, **23 March 1990**, 247, 1439-1445.

Suslick, K. S. and Doktycz, S.J., "Sounding Out New Chemistry," *New Scientist*, **1990**, 125, 50-53.

Suslick, K. S., Doktycz, S. J. and Flint, E. B., "On the Origin of Sonoluminescence and Sonochemistry," *Ultrasonics*, **1990**, 28(4), 280-290.

Suslick, K. S., "The Chemical Effects of Ultrasound," *Scientific American*, **Feb. 1989**, 80-86.

Suslick, K. S., Ultrasound : Its Chemcial, Physical and Biological Effects, VCH Publishers, New York, 1988.

Suslick, K. S. and Casadonte, D. J., "Heterogeneous Sonocatalysis with Nickel Powder," *J. Am. Chem. Soc.*, **1987**, 109, 3459-3461.

Suslick, K. S., Casadonte, D. J., Green, M. L. H. and Thompson, M. E., "Effects of High Intensity Ultrasound on Inorganic Solids, " *Ultrasonics*, **Jan. 1987**, 25, 56-59.

Suslick, K. S., "Organometallic Sonochemistry," *Adv. Organometallic Chem.*, **1986**, 25, 73-119.

Suslick, K. S. and Hammerton, D. A., "The Site of Sonochemical Reactions," *IEEE Transaction on Ultrasonics, Ferroelectrics and Frequency Control*, **1986**, UFFC-33(2), 143-147.

Suslick, K. S., Hammerton, D. A. and Raymond, E. C., "The Sonochemical Hot Spot," *J. Am. Chem. Soc.*, **1986**, 108, 5641-5642.

Suslick, K. S. and Johnson, R. E., "Sonochemical Activation of Transition Metals," *J. Am. Chem. Soc.*, **1984**, 106, 6856-6858.

Suslick, K. S., Gawienowski, J. J., Schubert, P. F., and Wang, H. H., "Sonochemistry in Non-aqueous Liquids," *Ultrasonics*, **1984**, 22, 33-36.

Suslick, K. S. and Schubert, P. F., "Sonochemistry of $Mn_2(CO)_{10}$ and $Re_2(CO)_{10}$," *J. Am. Chem. Soc.*, **1983**, 105, 6042-6044.

Suslick, K. S., Gawlenowski, J. J., Schubert, P. F. and Wang, H. H., "Alkane Sonochemistry," *J. Phys. Chem.*, **1983a**, 87, 2299-2301.

Suslick, K. S., Goodale, J. W., Schubert, P. F. and Wang, H. H., "Sonochemistry and Sonocatalysis of Metal Carbonyls," *J. Am. Chem. Soc.*, **1983b**, 105, 5781-5785.

Suslick, K. S., Schubert, P. F. and Goodale, J. W., "Sonochemistry and Sonocatalysis of Iron Carbonyls," *J. Am. Chem. Soc.*, **1981**, 103, 7342-7344.

Takizawa, Y., Akama, M., Yoshihara, N., Nojima, O., Arai, K. and Okouchi, S., "Hydroxylation of Phenolic Compounds Under the Condition of Ultrasound in Aqueous Solution," *Ultrasonics Sonochemistry*, **1996**, 3, S201-S204..

Tata, D.B., Biglow, J., Wu, J., Tritton, T.R. and Dunn, F., "Ultrasound-Enhanced Hydroxyl Radical Production From Two Clinically Employed Anticancer Drugs: Adriamycin and Mitomycin C.," *Ultrasonics Sonochemistry*, **1996**, 3, 39-45.

Tatsumoto, N. and Fujii, S., "The Chemical Dissolution of Calcium Salt Crystal by Irradiating the Ultrasound: The Effect of Stirring the Solution," *J. Acoust. Soc. Jpn.*, **1987**, E 8(5), 191-195.

Thornycroft, J.I. and Barnaby, S.W., "Torpedo-Boat Destroyers," *Minutes of the Proceedings of the Inst. C.E.*, **1895**, 122(4), 51-69.

Toy, M.S., Stringham, R.S. and Passell, T.O., "Sonolysis Transformation of 1,1,1-Trichloroethane in Water and Its Process Analyses," Pollution Prevention in Industrial Processes (ACS Symposium Series 508), Ch. 23, Ed. by Breen, J.J. and Dellarco, M.J., Am. Chem. Soc., Washington D.C., 1992.

Toy, M.S., Carter, M.K. and Passell, T.O., "Photosonochemical Decomposition of Aqueous 1,1,1-Trichloroethane," *Environ. Tech.*, **1990**, 11(9), 837-842.

Trabelsi, F., Ait-Iyazidi, H., Berlan, J., Fabre, P. -L., Delmas, H. and Wilhelm, A.M., "Electrochemical Determination of the Active Zones in a High-Frequency Ultrasonic Reactor," *Ultrasonics Sonochemistry*, **1996**, 3, S125-S130.

Tuulmets, A., Kaubi, K. and Heinoja, K, "Influence of Sonication on Grignard Reagent Formation," *Ultrasonics Sonochemistry*, **1995**, 2(2), S75-S78.

Umemura, S., Kawabata, K., Sasaki, K., Yumita, N., Umemura, K. and Nishigaki, N., "Recent Advances in Sonodynamic Approach to Cancer Therapy," *Ultrasonics Sonochemistry*, **1996**, 3, S187-S191.

Urban, M. W. and Salazar-Rojas, E.M., "Ultrasonic PTC Modification of Poly(vinylidene fluoride) Surfaces and Their Characterization," *Macromolecules*, **1988**, 21, 372-378.

Uzgiris, E.E., Opsahl, L.R., Vosburgh, K.G., Anthony, T.R., and Cline, H.E., "Targeted Thermal Release of Drug-Polymer Conjugates," U.S. Patent 5,490,840, dated Feb. 13, 1996.

Veera Reddy, A. and Ravindranath, B., "Acetylation Under Ultrasonic Conditions: Convenient Preparation of n-Acetylamino Acids," *Synthetic Communications*, **1992a**, 22(2), 257-264.

Veera Reddy, A. and Ravindranath, B., "Synthesis of *a*-, *b*- and Cyclic Spaglumic Acids," *Int. J. Peptide Protein Res.*, **1992b**, 40, 472-476.

Walton, A. J. and Reynolds, G. T., "Sonoluminescence,"*Advances in Physics*, **1984**, 33(6), 595-660.

Wang, J.X. and Zhao, K., "Synthesis of *cis* and *trans*-2,6-Diphenyl-1,4-Diselenafulvenes from Phenylacetylene with Selenium and Base Under PTC-Ultrasound Conditions," *Synthetic Comm.*, **1996**, 26(8), 1617-1622.

Wang, Z. and Nur, A. "Ultrasonic Velocities in Pure Hydrocarbons and Mixtures," *J. Acoust. Soc. Am.*, **1991**, 89(6), 2725-2730.

Weber, M. E. and Chon, W. Y., "Distribution of Ultrasonic Cavitation Intensities in a Liquid System," *Can. J. Chem. Eng.*, **1967**, 45, 238-240.

Weiss, J., *Nature*, **1944**, 153, 748.

Weissler, A., "Sonochemistry: The Production of Chemical Changes with Sound Waves," *J. Acoust. Soc. Am.*, **1953**, 25(4), 651-657.

Weissler, A., Cooper, H. and Snyder, S., "The Chemical Effects of Ultrasonic Irradiation: Reaction Between Carbon Tetrachloride and Water," *J. Acoust. Soc. Am.*, **1948**, 20(4), 589.

Wheat, P.E. and Tumeo, M.A., "Ultrasound Induced Aqueous Polycyclic Aromatic Hydrocarbon Reactivity," *Ultrasonics Sonochemistry*, **1997**, 4, 55-59.

Whillock, G.O.H. and Harvey, B.F., "Ultrasonically Enhanced Corrosion of 304L Stainless Steel I: The Effect of Temperature and Hydrostatic Pressure," *Ultrasonics Sonochemistry*, **1997a**, 4, 23-31.

Whillock, G.O.H. and Harvey, B.F., "Ultrasonically Enhanced Corrosion of 304L Stainless Steel II: The Effect of Frequency, Acoustic Power and Horn to Specimen Distance," *Ultrasonics Sonochemistry*, **1997b**, 4, 33-38.

Wilke, C.R. and Chang, P., "Correlation of Diffusion Coefficients in Dilute Solutions," *AIChE J.*, **1955**, 1(2), 264-270.

Witekowa, S. and Farbotko, W., "Dispersion Effect of Ultrasonic Waves. II. Ultrasonic Waves Effect on the Catalytic Activity of Calcium Carbonate," *Soc. Sci. Lodz. Acta. Chim.* (Eng.), **1974**, 18, 99-103; *Chem. Abst.*, **1975**, 82.7935k.

Wood, R.W. and Loomis, A.L., "The Physical and Biological Effects of High Frequency Sound Waves of Great Intensity," *Philos. Mag. Ser. 7*, **1927**, 4(22), 417-436.

Woodle, H.A. and Vilbrandt, F.C., "Mechanisms by Which Ultrasonic Energy Affects Rates in Liquid-Liquid Extraction," *AIChE J.*, **1960**, 6(2), 296-298.

Worsley, D. and Mills, A., "The Effects of Power Ultrasound on the Oxidation of Water by Ce^{IV} Ions Mediated by Thermally Activated Ruthenium Dioxide Hydrate," *Ultrasonics Sonochemistry*, **1996**, 3, S119-S123.

Yan, Y., Thorpe, R.B., and Pandit, A.B., "Cavitation Noise and Its Suppression by Air in Orifice Flow," in Proceedings of International Symposium on Flow Induced Vibrations and Noise, AIChE, Chicago, **1988**, 25-40.

Zapior, B. and Lomnicka, A., "Use of Ultrasonic Waves for the Modification of the Nickel (II) Oxide Catalyst," *Zesz. Nauk. Uniw. Jagiellon., Pr. Chem.* (Pol.), **1975**, 20, 109-117; *Chem. Abst.*, **1976**, 85. 25765w.

CHAPTER 3.
RATE ENHANCEMENTS IN A SOLID-LIQUID REACTION USING PTC, MICROPHASES, ULTRASOUND AND COMBINATIONS THEREOF

A paper published in *Chemical Engineering Science*[1].

Leigh C. Hagenson, Sanjeev D. Naik and L. K. Doraiswamy

Abstract

A phase transfer catalyst (PTC) provides an elegant and efficient way of effecting reaction between components present in two immiscible phases: liquid-liquid and liquid-solid. Such reactions can also be initiated or enhanced by other strategies, such as use of a microphase or ultrasound. Results are reported in this paper on rates and rate enhancements in a model solid-liquid reaction (synthesis of benzyl sulfide from benzyl chloride and sodium sulfide in a suitable organic solvent) in the presence of PTC, microphase and ultrasound. The study is then extended to include the effects of combinations of these strategies. A preliminary kinetic analysis of the results is also attempted.

For the system studied it is found that the accelerating effect of PTC is the most profound, while that of microphase or ultrasound is only marginal when they are used individually. On the other hand, the effects of microphase and ultrasound acquire far greater significance in the presence of PTC.

---

[1] Reprinted from Chemical Engineering Science, 49(24A), L. C. Hagenson, S. D. Naik and L. K. Doraiswamy, Rate Enhancements in a Solid-Liquid Reaction Using PTC, Microphases, Ultrasound and Combinations Thereof, 4787-4800, Copyright 1994, with kind permission from Elsevier Science Ltd., The Boulevard, Langford Lane, Kidlington 0X5 1GB, UK

3.1 Introduction

The problem of bringing together a water soluble nucleophilic reagent and a hydrophobic reagent can be solved without the modification of reaction pathways, or use of expensive dipolar aprotic solvents like dimethylformamide (DMF), by using a phase transfer catalyst (PTC). A PTC ion-pairs with the reactive anion of the nucleophile and, due to its lipophilic nature, extracts it into the organic phase where reaction occurs (see, e.g., Dehmlow and Dehmlow, 1993). The nucleophile can be in an immiscible liquid (aqueous) phase [liquid-liquid PTC (LLPTC)] or in a solid phase [solid-liquid PTC (SLPTC)], as shown in Figure 3.1.

In some cases SLPTC has certain advantages over LLPTC; for example, it prevents the undesirable effects of the water of solvation migrating with the ion-pair into the organic medium. However, SLPTC often suffers from slower reaction rates, possibly because the dissolution of the sparingly soluble solid limits the kinetics of the reaction. When this is the case, the use of a microphase (MP) may enhance reaction by facilitating the transport of the reactants across interfacial boundaries. A microphase can consist of particles, droplets or bubbles that are smaller than the diffusion length (~60-100 microns) of the solute. It is usually on the order of 1-10 microns. Particles larger than the film thickness do not enhance reaction rates. The use of a microphase in enhancing the rates of gas adsorption, liquid extraction and solid dissolution has been reviewed by Mehra (1990). The microphase physically 'lifts' the reactive anion, or in some cases adsorbs it from the diffusion film, and transports it into the organic bulk where reaction ensues (Janakiraman and Sharma, 1985). By virtue of its ability

to enter the diffusion film surrounding a liquid or a solid phase, a microphase can lead to steeper concentration gradients and enhanced transport (Figure 3.2).

Thus it is anticipated that the use of a microphase in an SLPTC system will further enhance the reaction over that with PTC alone (Figure 3.3). The microphase introduces a 'double ferrying action' which aids the phase transfer catalyst in its role of transferring the reactive species from one phase, solid or aqueous, to the organic phase.

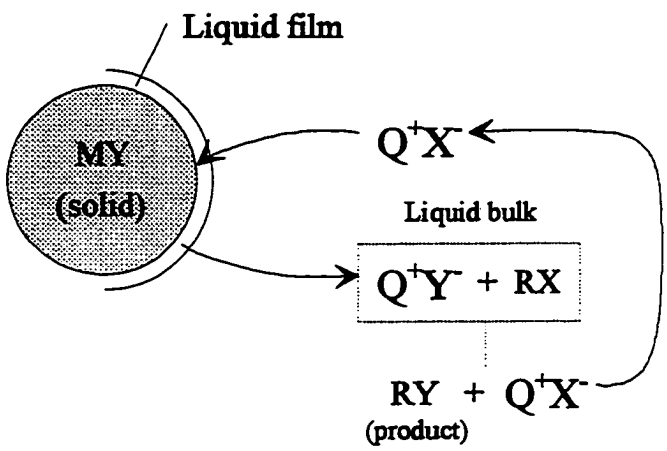

Figure 3.1 Visual representation of PTC action.

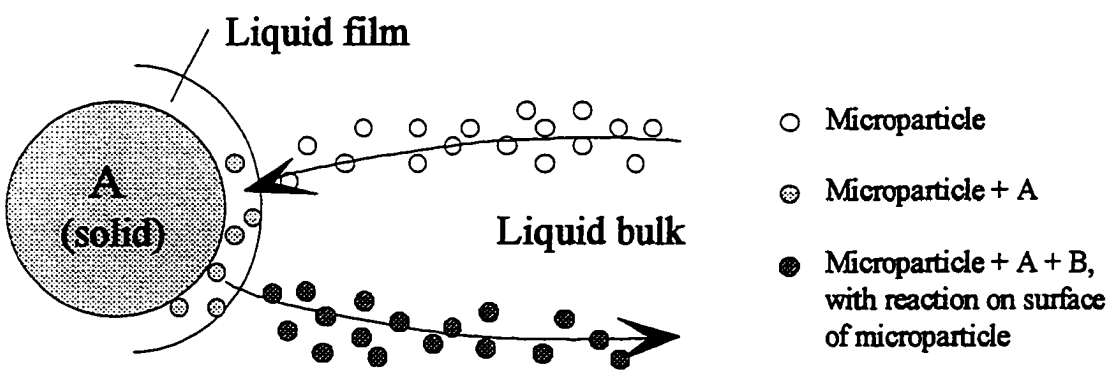

Figure 3.2 Solid-liquid reaction facilitated by microphase action.

Ultrasound has also been shown to assist in initiating reactions and enhancing reaction rates in systems catalyzed by PTC (see, e.g., Diez-Barra *et al.*, 1992). The chemical effects of ultrasound have been attributed to the implosive collapse of cavitation bubbles which are formed during the rarefaction period of sound waves. These bubbles are initiated at localized sites in the liquid mixture which contain minute quantities of dissolved gases. The mixture of gases and vaporized reaction mixture which is trapped within a microbubble is exposed to extreme temperatures and pressures upon implosion and the molecules are fractured, forming highly reactive species with a great propensity for reaction with the surrounding molecules. This type of ultrasonic action is termed *sonochemistry*. The dynamics of cavitation bubbles have been described at considerable length and will not be discussed here (see, e.g., Cum *et al.*, 1992; Suslick, 1988).

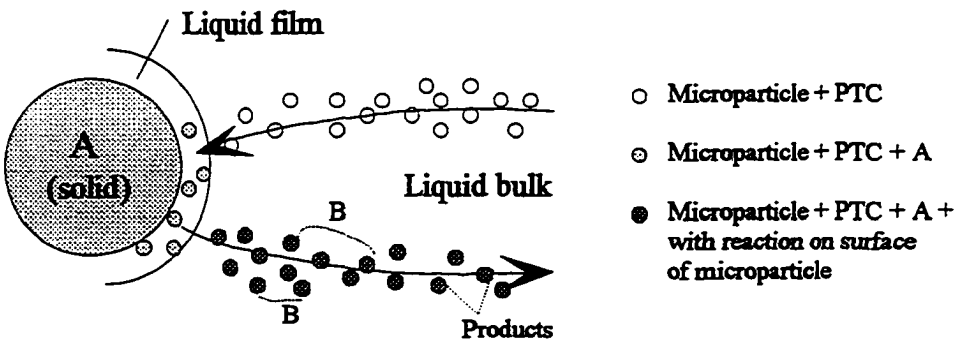

Figure 3.3 Enhancement of solid-liquid reaction with the combined action of a phase transfer catalyst and microphase.

Ultrasound can also affect immiscible reaction mixtures mechanically by forming a very fine emulsion, which considerably increases the interfacial contact area between the two phases. When one of the phases is a solid, ultrasonic irradiation has several additional enhancing effects. One of the most influential and well-known is its ability to clean and

remove unreactive coatings from surfaces of solid particles, thus facilitating reaction. This is especially useful when the solid also acts as a catalyst (see, e.g., Suslick and Johnson, 1984; Ando and Kimura, 1990). These cleaning effects have been largely attributed to microstreaming and asymmetric acoustic cavitation. The former, microstreaming (or acoustic streaming), is the microscopic turbulence and/or thinning of the solid-liquid film layer created by shock waves which have propagated from nearby symmetric cavitations in the liquid bulk. Microstreaming greatly increases the mass transfer of the reactive anions to and from the solid surface. The latter, asymmetric acoustic cavitation, occurs when the microbubbles implode near the surface of the solid particle. This phenomenon has been described in detail by Suslick (1990). Since there is not enough room near a solid for spherically-symmetric cavitation to occur, microjets of solvent are formed which bombard the solid surface and result in pitting and erosion. This exposes unreacted surfaces of the solid, in addition to increasing the surface area available for reaction.

The conditions under which the reaction is carried out can greatly influence the effect of ultrasound on the rate or yield. These parameters include (but are not limited to) the reaction temperature, solvent, and irradiation intensity.

3.1.1 Objective

Research is in progress in this laboratory on the individual and combined effects of PTC, microphase, and ultrasound on the rates of organic reactions. The present paper reports the experimental results obtained on a model solid-liquid reaction (synthesis of benzyl sulfide from

benzyl chloride and sodium sulfide in a suitable organic solvent). Specifically, the following aspects have been studied:

1) The effect of phase transfer catalyst.
2) The effect of microphase.
3) The effect of ultrasonic irradiation.
4) The combined effect of PTC and microphase.
5) The combined effect of PTC and ultrasound.
6) The combined effect of PTC, microphase and ultrasound.

A preliminary kinetic analysis of the experimental data is attempted. A detailed modeling study will be reported in a subsequent communication.

3.1.2 Previous work on sulfide synthesis

Landini and Rolla (1974) were among the first to report the synthesis of symmetrical sulfides using a phase transfer catalyst. Kim and Noh (1974) synthesized bis-(*p*-nitrophenyl) sulfide by heating *p*-nitrochlorobenzene with aqueous sodium sulfide with Aliquat 336 (tricaprylmethylammonium chloride) as PTC. Other reports of sulfide synthesis using PTC include those of Tozzi and Cassandrini (1975), Evans (1984) using molten aryl halides, Kutil *et al.* (1982, 1985) using an anionic surfactant, and Kutil *et al.* (1985) using an anionic surfactant and NaOH. All the above papers report the use of a PTC in a liquid-liquid system for sulfide synthesis. Pradhan and Sharma (1990) report the synthesis of dibenzyl sulfide from benzyl chloride in toluene and solid sodium sulfide using a variety of PTCs. Tetrabutylammonium bromide (TBAB) was found to be the best catalyst in their study.

3.2 Mechanism of PTC Action

The mechanism of a typical phase transfer catalyzed reaction is expected to resemble an S_N2 displacement reaction scheme. The general reaction

$$RX_{org} + MY_{aq} \xrightarrow{PTC} RY_{org} + MX_{aq}$$

follows the catalytic cycle:

$$RX + [Q^+Y^-] \longrightarrow RY + [Q^+X^-] \quad \text{organic phase}$$

interface

$$M^+X^- + [Q^+Y^-] \longleftrightarrow M^+Y^- + [Q^+X^-] \quad \text{aqueous phase}$$

The cation of the PTC (Q^+) extracts the anion Y^- from the aqueous phase and pulls it into the organic phase. Since Y^- is virtually unsolvated and unable to pair with the surrounding alkyl groups, it reacts rapidly with the substrate RX. The new salt, Q^+X^-, returns to the aqueous phase where X^- reacts with the metal cation M^+. This cycle repeats itself until equilibrium is attained or the reaction is complete.

The reaction investigated is

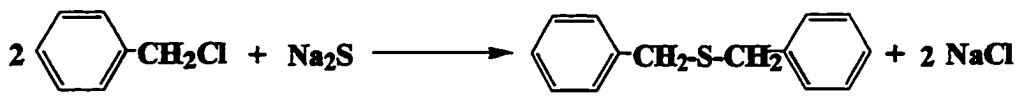

Benzyl Chloride (organic liquid)	Sodium Sulfide (solid)	Benzyl Sulfide (organic liquid)	Sodium Chloride (solid)

with TBAB as PTC and acetonitrile as solvent. The mechanism of this reaction is slightly more complicated than that depicted by the general PTC model because the anions of the

quaternary ammonium salt (bromide) and those of the organic substrate (chloride) are not the same. Also, two quaternary salt cations are needed to ion-pair with each reactive sulfide anion. Therefore, the proposed mechanism involves two interfacial ion-exchange steps (1 and 3) and the main reaction step (2) in the organic phase:

$$Na_2S_{(s)} + 2Q^+Br^-_{org} \longleftrightarrow 2NaBr_{(s)} + Q^+\text{-}S^{2-}\text{-}Q^+_{org} \quad \text{---(1)}$$

$$Q^+\text{-}S^{2-}\text{-}Q^+_{org} + 2C_6H_5CH_2Cl_{org} \longleftrightarrow C_6H_5CH_2\text{-}S\text{-}CH_2C_6H_{5\,org} + 2Q^+Cl^-_{org} \quad \text{---(2)}$$

$$Na_2S_{(s)} + 2Q^+Cl^-_{org} \longrightarrow 2NaCl_{(s)} + Q^+\text{-}S^{2-}\text{-}Q^+_{org} \quad \text{---(3)}$$

The reaction is initiated by bromide exchange (1) at the solid surface between the quaternary salt cation (Q^+) and Na^+, following which the quaternary ammonium cation carries the sulfide ion into the organic bulk where (2) ensues. Reaction (2) generates Q^+Cl^-, which can also ion-pair with the sulfide anion at the solid surface (3). Reaction (2) is then repeated, regenerating Q^+Cl^-. The catalytic cycle involving Q^+Cl^- continues, with the possibility of (1) occurring simultaneously with (3), depending on the relative rates of (1) and (3). With time, there is a possibility that the sequence of steps will change in terms of the relative importance of (1) and (3) in the catalytic cycle.

3.3 Experimental Apparatus and Procedures

A typical reaction mixture consisted of 1.22 $x10^{-3}$ gmol/ml benzyl chloride (99% purity), 10% w/v sodium sulfide (60% purity) and 0.4% w/v PTC (Zeeland Chemicals, Inc.). TBAB was used exclusively as the phase transfer catalyst, and acetonitrile (HPLC grade) as the solvent in all studies except where otherwise stated. The PTC reactions were

conducted using a mechanically agitated stainless steel reactor operated in the batch mode. Isothermal conditions were maintained to within ± 1.0 °C using a constant temperature water cooling bath equipped with a cooling coil.

The sodium sulfide was purchased in technical grade flakes, crushed and sieved. Average particle sizes are indicated when discussing the experimental results. Two microphases were tested: silica gel (15 - 35 μm) and fumed silica (0.014 μm). In all experiments, a microphase loading of 1.0% w/v was used.

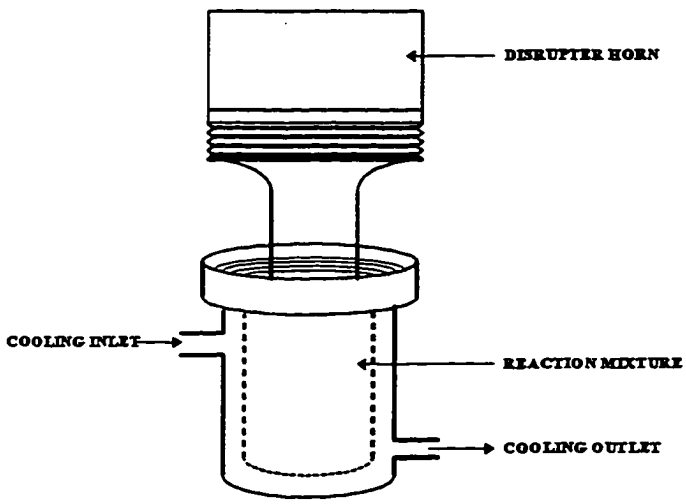

Figure 3.4 Experimental apparatus for sonochemical research.

Ultrasound reactions were conducted using Sonicator® XL2020 (Misonix, Inc.), which supplies a constant frequency of 20 kHz to the 1/2 in (1.27 cm) standard titanium horn. The reaction mixture was contained in a sealed stainless steel sonication vessel. Although high intensity ultrasound leads to large ambient temperature increases in the reaction mixture (a 0.1 °C increase per unit time ultrasonic irradiation was observed in the absence of external cooling), isothermal conditions were maintained to within ± 0.5 °C using an external cooling

jacket as shown schematically in Figure 3.4. The reaction vessel also contained a port (not shown in the figure) through which a thermocouple was inserted directly into the reaction mixture for temperature observation. The amplitude and power output could be varied to a maximum of 120 μm and 475 W, respectively. Results were highly reproducible with 5 replicates giving an average standard deviation of only 0.5% conversion of benzyl chloride.

The organic phase was analyzed for benzyl chloride and benzyl sulfide using a Hewlett Packard 5730A gas chromatograph fitted with a 1/8 in (0.318 cm) x 6.56 ft (2.0 m) stainless steel packed column. The packing consisted of 10% SP2250 (liquid phase) and Carbopack (solid support) with a mesh size of 100/120. The oven was programmed to operate at an initial temperature of 150 °C (held for 2 minutes) which was increased at a rate of 32 °C/min to a final temperature of 300 °C.

3.4 Results and Discussion

3.4.1 Reaction with PTC alone

a. Parametric study

Two of the most important parameters affecting a phase transfer catalyzed reaction are catalyst concentration and temperature. To study the effects of these parameters, experiments were carried out at three different catalyst concentrations (0.2, 0.4 and 0.8% w/v) and three ambient reaction temperatures (25, 30 and 35 °C). Sodium sulfide particle size was kept constant at <170 μm. As a basis for comparison, the reaction was also conducted in the absence of PTC (referred to as the base reaction).

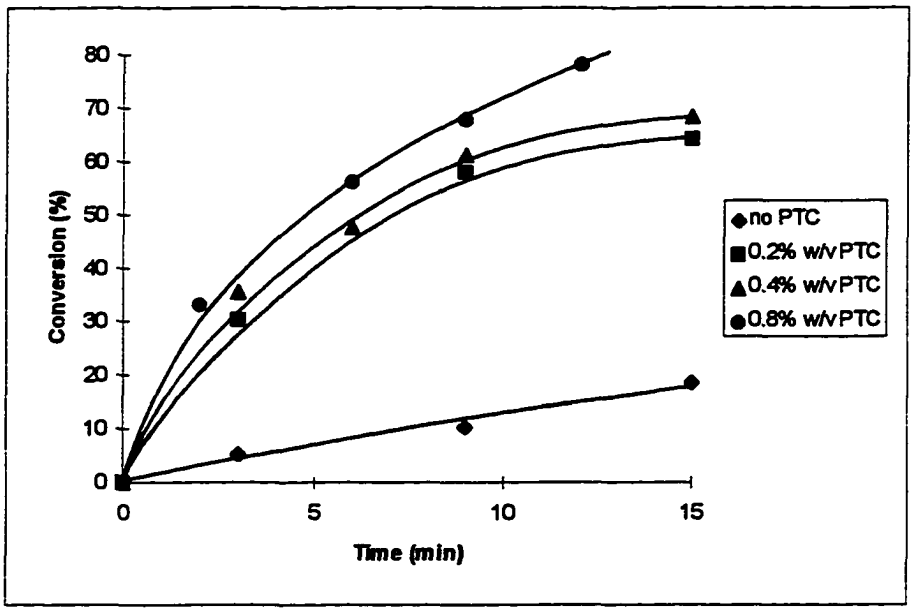

Figure 3.5 Effect of PTC concentration on conversion.
(Na_2S <170 μm, agitation = 1740 rpm, PTC = TBAB, temp = 25 °C)

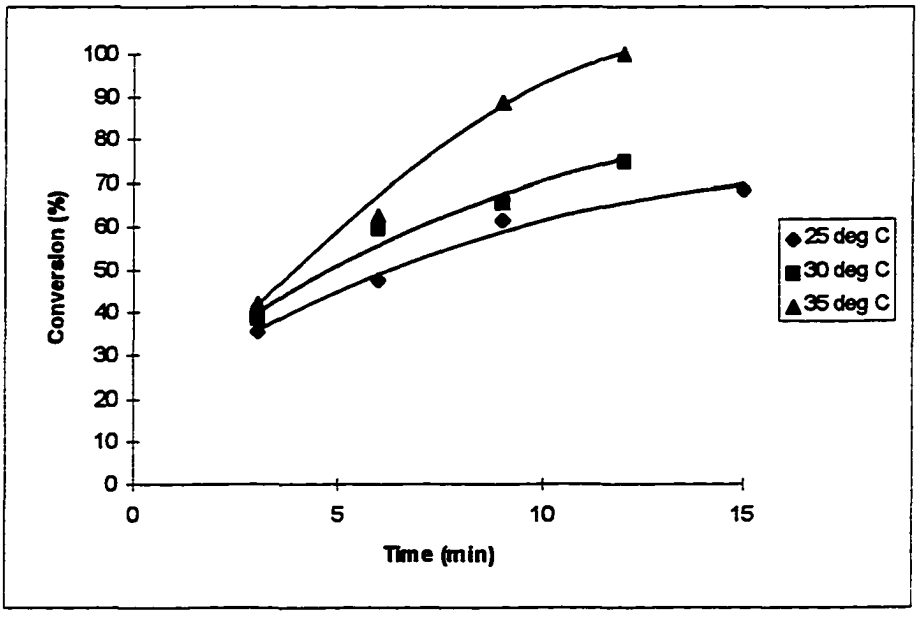

Figure 3.6 Effect of ambient reaction temperature on conversion.
(Na_2S <170 μm, agitation speed = 1740 rpm, PTC = 0.4% w/v TBAB)

The results at 25 °C on the effect of PTC concentration are summarized in Figure 3.5, which also shows data obtained for the case of no PTC. It is observed that even in the absence of PTC a conversion of about 20% occurs in 15 minutes of reaction time. This is probably because of a small but finite solubility of sodium sulfide in the organic phase. The addition of PTC leads to a substantial enhancement in reaction rate. For example, at a reaction time of 10 minutes, the conversion obtained with a PTC concentration of 0.4% w/v is around 58%, and around 70% when using 0.8% w/v. There is a small conversion of approximately 10% in its absence.

Similar studies were conducted at 30 and 35 °C, keeping the PTC concentration constant at 0.4% w/v, as shown in Figure 3.6. As expected, an increase in temperature leads to an increase in conversion. However, when comparing Figure 3.5 to Figure 3.6, it appears that the effect of PTC concentration is perhaps more dominant than that of reaction temperature.

b. Kinetic analysis

Although there is considerable literature on the mechanistic details of LLPTC reactions, little is understood about SLPTC. Melville and Goddard (1990) report two possible models for SLPTC, depending upon whether or not the solid has some finite solubility in the organic solvent. These models may be briefly described as:

Model I: If the solid (MY_s) is sparingly soluble in the organic solvent, the PTC can ion-pair with the dissolved species MY_{org} (Figure 3.7a).

Model II: If the solid is completely insoluble in the organic solvent, then the PTC ion-pairs at, or close to, the solid surface (Figure 3.7b).

However, Model I does not seem to represent true PTC action because the reactive anion Y^- is already in the organic phase where reaction occurs. Thus there is no *a priori* requirement for PTC (whose sole purpose is to ion-pair with the reactive anion from one phase and ferry it to the other phase where reaction proceeds). In addition, although there is a finite solubility of Na_2S in acetonitrile in the system under investigation, the reaction observed in the absence of PTC is small (if not negligible) when compared to that when a small amount of PTC is present. Model I alone cannot be used to explain this large enhancement. However, a scheme similar to Model II may be postulated to explain this reaction (Figure 3.7c). Here the dissolved species reacts to a small extent (independent of PTC action), while simultaneously PTC ferries the anions from the solid surface into the organic phase. This scheme accounts for the reaction occurring due to the finite solubility of the nucleophile as well as by PTC action. For instance, at 0.4% w/v PTC (25 °C), the approximate enhancements due to PTC action before and after accounting for reaction due to dissolved sodium sulfide are 24-fold and 18-fold, respectively. Similarly, for the same PTC concentration at 30 °C, the enhancements are 9-fold and 7-fold, respectively.

Since the reaction due to dissolved sulfide is small, it has been neglected and Model II has been chosen as the mechanism of the reaction in this preliminary kinetic study. Therefore, the kinetics of the reaction depend solely on benzyl chloride concentration (C_{BzCl}) and the concentration of $Q^+\text{-}S^{2-}\text{-}Q^+$. Since $Q^+\text{-}S^{2-}\text{-}Q^+$ concentration is indirectly dependent on the concentration of the catalyst (C_{PTC}), the kinetic model can be written as:

$$-r_{BzCl} = k\,(C_{BzCl})^n (C_{PTC})^m \qquad (1)$$

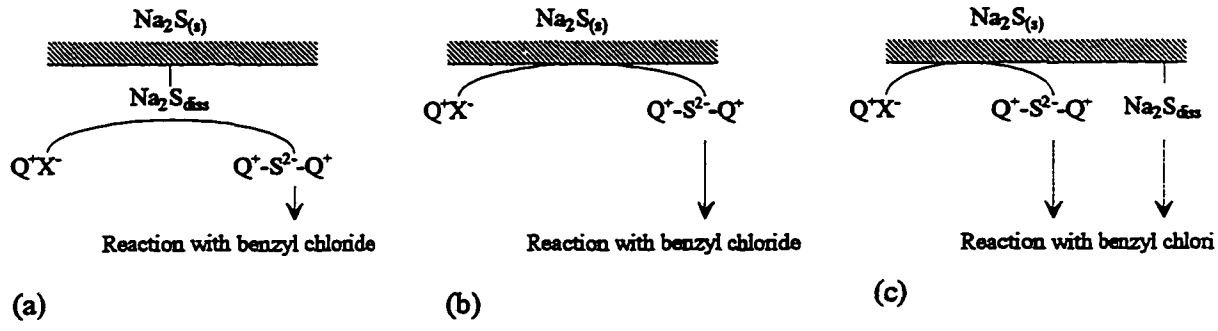

Figure 3.7 Models used to explain PTC action.

There has been some ambiguity in reports so far about the order of reaction with respect to the organic substrate with changing PTC concentration. While some (see, e.g., Starks and Owens, 1973; Yadav and Sharma, 1981) report a first order dependence on the organic substrate, independent of PTC concentration, others (see, e.g., Ramsden *et al.*, 1989) report that the order of reaction changes with PTC concentration. In this system, it was observed that the order fluctuated around 1.0. Taking into account the statistical error involved, it is concluded that the order can be taken to be unity, irrespective of the PTC concentration. Equation (1) can now be written as:

$$-r_{BzCl} = k_1(C_{BzCl})^n \qquad (2)$$

where the pseudo first order constant k_1 is some complex function of the initial PTC concentration.

Combining the data for different catalyst concentrations at 25 °C, the original rate equation (1) can be determined. This gives

$$-r_{BzCl} = k\,(C_{BzCl})^{0.97}(C_{PTC})^{0.43} \qquad (3)$$

or, in a more acceptable form

$$-r_{BzCl} = 0.00281\,(C_{BzCl})^{1.0}(C_{PTC})^{0.5} \quad (4)$$

For a given PTC concentration of 1.26×10^{-5} gmol/ml, fitting the pseudo first order rate equation (1) to the data obtained at 25, 30 and 35 °C yields some very unexpected and unusual results. The preliminary kinetic analysis indicates that the order with respect to benzyl chloride decreases with increasing temperature from 0.97 to 0.85 to 0.35, respectively. The observed trends are very interesting, especially since a change in reaction order with changing ambient reaction temperature has not yet been reported in PTC studies. It suggests that there is a shift in reaction from kinetic control at lower temperatures toward mass transfer control at higher temperatures. For complete kinetic control, the order with respect to the organic substrate is unity (as has been observed in this and many other PTC systems). When the reaction is completely controlled by mass transfer, the rate is zero order with respect to the organic substrate (benzyl chloride) and depends solely on the rate of transport of the sulfide ion from the solid surface to the organic bulk. With increasing temperature, the rate of intrinsic kinetics increases rapidly (exponentially) and becomes very fast compared to the rate of mass transfer. Thus, at higher temperatures, the reaction shifts toward mass transfer control.

3.4.2 Reactions under the influence of microphases

The first step in studying the effect of microphase on a PTC system is to choose a suitable microphase. The following results indicate that this choice is critical. While a literature search on microphase action has only revealed enhancements due to microphases in heterogeneous systems, it has been found in the present study that microphases may lead to

suppression of reactions as well. However, the right microphase, when used together with PTC, can lead to an enhancement in reaction rate, even for the case where the effect of microphase alone is not significant.

a. Silica gel as a microphase

The use of silica gel (15 - 35 μm) as microphase suppresses the action of the PTC (Figure 3.8). A possible cause of this retardation is the adsorption or absorption of PTC on the silica gel, accompanied by swelling or agglomeration of the gel particles in acetonitrile. When the silica gel particles swell, they become larger than the diffusion length of the solute and microphase action is no longer possible. This also prevents any PTC that may be

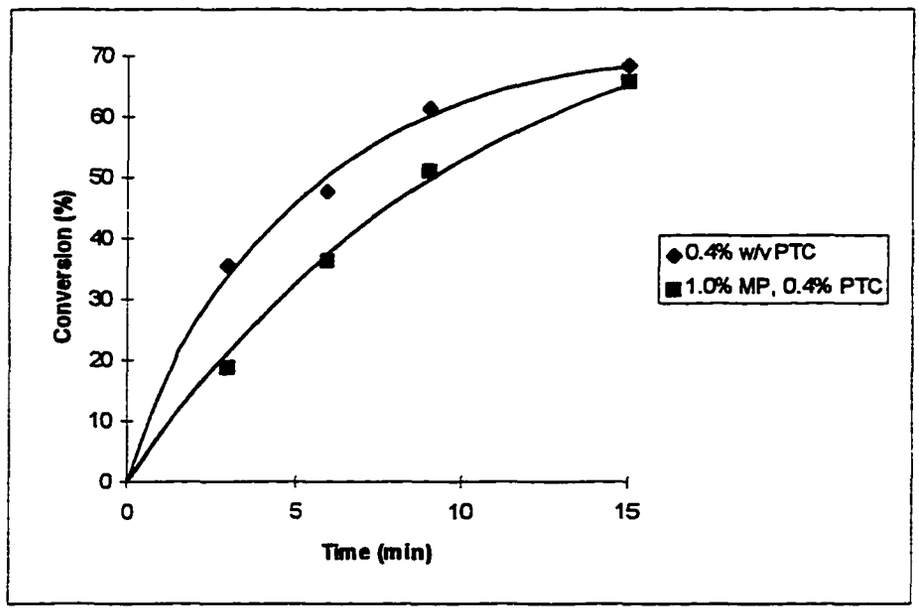

Figure 3.8 Effects of the nature of the microphase.
(Na_2S <170 μm, PTC = TBAB, MP = silica gel, temp = 25 °C)

adsorbed/absorbed on the microphase from reaching the solid surface. Thus it is unable to transfer the reactive species into the organic phase. However, it is important to note that mere adsorption/absorption of PTC on a microphase is not expected to suppress PTC action unless the microparticles are larger than the film thickness surrounding the immiscible reactant.

b. Fumed silica as a microphase

Fumed silica (0.014 μm) was then used as the microphase. Without PTC, the conversions obtained when using this microphase were not significantly different from those obtained in the base reaction (i.e. in the absence of both PTC and microphase). However, even under conditions of high agitation speeds (1740 rpm) and small Na_2S particle sizes (< 170 μm), the

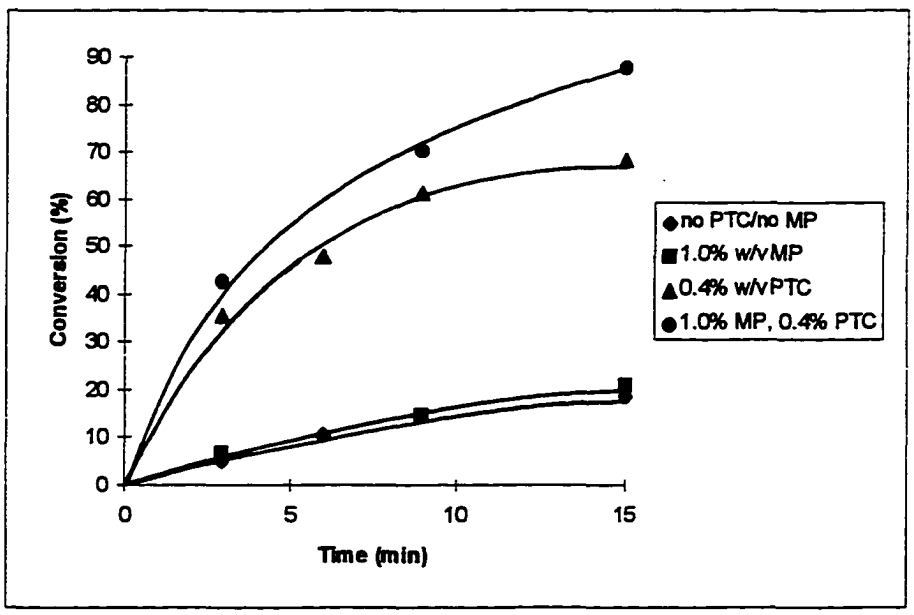

Figure 3.9 Effect of combinations of microphase (MP) and PTC action.
(Na_2S <170 μm, PTC = TBAB, MP = fumed silica, temp = 25 °C)

effect of microphase (microphase loading = 1.0 % w/v) on PTC action was found to be significant (Figure 3.9). The rate of reaction with the combined effects of PTC and microphase is about 1.24 times that with PTC alone. This is a significant increase, especially since the reaction was carried out under conditions of limited microphase action (as discussed in the next section).

c. Effect of Na_2S particle size

The results presented up to this point have been for very small sodium sulfide particles where mass transfer effects are expected to be small. These reaction conditions are less conducive to effective microphase action. Larger sized sodium sulfide particles will ensure a greater role of mass transfer in the reaction process and possibly greater microphase action. Hence several runs were conducted using sodium sulfide particles of a mean size of 565 μm to test this hypothesis. In reactions where PTC alone was used, the conversions obtained with a larger particle size of Na_2S were much lower than those obtained with smaller particles (Figure 3.10). The results also indicate, as expected, that the contribution of the microphase to reaction enhancement is greater with larger particles than with smaller Na_2S particles. After a 40 minute reaction time, the following conversions were obtained:

No PTC or microphase	7.0 %
Only PTC	25.7 %
Only microphase	31.4 %
Both PTC and microphase	35.4 %

Thus while a microphase alone has little or no affect on reaction when smaller Na_2S particles are used, the effect is greater than that with PTC alone for the larger particles. Also the combined effect of PTC and microphase is greater than their individual effects. Table 3.1 summarizes the enhancement factors attributed to PTC and/or microphase action when Na_2S particles of average size 565 μm are used. The microphase used in all cases was fumed silica.

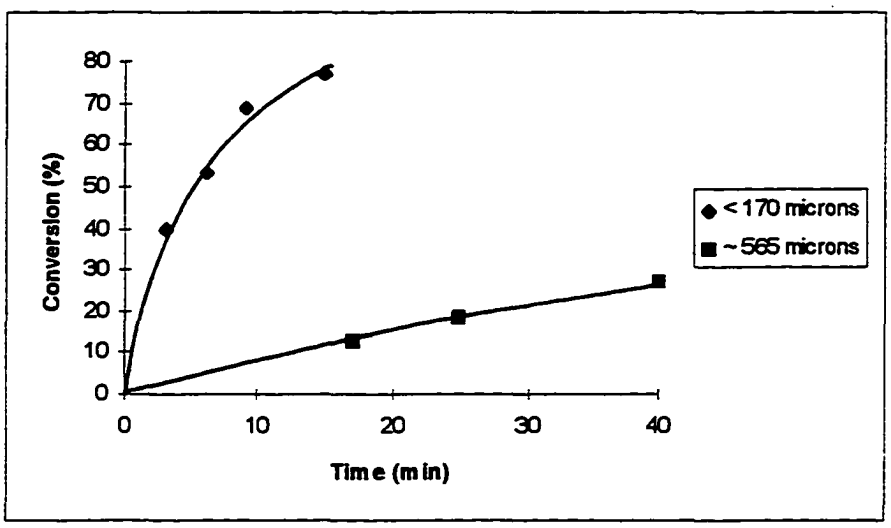

Figure 3.10 Effect of Na_2S particle size on PTC action.
(agitation = 1740 rpm, PTC = 0.4% w/v TBAB, temp = 25 °C)

Thus the addition of a microphase enhances the reaction rate by a factor of 4.46 compared to the base reaction (in the absence of PTC and microphase), while the addition of PTC alone induces a slightly lower enhancement (3.65). The combined ferrying action of microphase and PTC together is clearly greater than each of the individual effects and a five-fold increase in rate is observed.

Table 3.1 Rate enhancements attributed to effects of PTC and/or microphases.

Conditions	Enhancement A	Enhancement B
No PTC or microphase	1.0	--
Only PTC	3.65	1.0
Only microphase	4.46	1.32
Both PTC and microphase	5.02	1.38

Enhancement A = reaction rate/reaction rate with no PTC or microphase
Enhancement B = reaction rate/reaction rate with PTC only

As anticipated, the microphase is more useful under reaction conditions where transport of the sulfide ions from the solid surface across the diffusion film surrounding the particles into the organic phase affects the rate of reaction. It is under these conditions that the role of microphases is more crucial in a PTC system. These findings also indicate that microphase can, in some cases, be an effective substitute for PTC (which is often difficult to recover from the organic phase).

3.4.3 Reactions under the influence of ultrasound

a. Effect of acoustic intensity

The intensity of the sound waves must be great enough to overcome the cavitation threshold, the negative pressure required to form the microbubbles. This is required to initiate the chemical effects of ultrasound. Once cavitation is produced, Mason (1990) reports that the rate of reaction increases with increasing intensity to an optimum level, and then decreases with further increase in intensity. He attributes these findings to (1) the reaction mixture becoming overcrowded with microbubbles which limits the ability of the waves to penetrate into the liquid and/or (2) the microbubbles formed growing too large (or joining with surrounding bubbles) before implosive cavitation can occur.

The model reaction is also seen to be dependent upon acoustic intensity (Figure 3.11), though a decrease in rate is not observed. This may either be due to the limits on the intensity level which can be achieved with the ultrasonic equipment in use or to the ultrasound not producing any sonochemical effects. The acoustic intensity entering the reaction mixture is determined by first measuring the ultrasonic power delivered to the horn during sonication. This power is dependent upon the mixture in the reaction vessel and is monitored by a microprocessor controller (available with Sonicator® XL2020). Dividing the power by the area of the horn, gives the intensity delivered to the reaction mixture in W/cm^2 (assuming all available power is dissipated into the reaction system from the probe tip). Since the maximum conversion in reaction mixtures containing 0.4% w/v PTC is achieved at an intensity of 150 W/cm^2, this intensity was used for all subsequent sonochemical reactions.

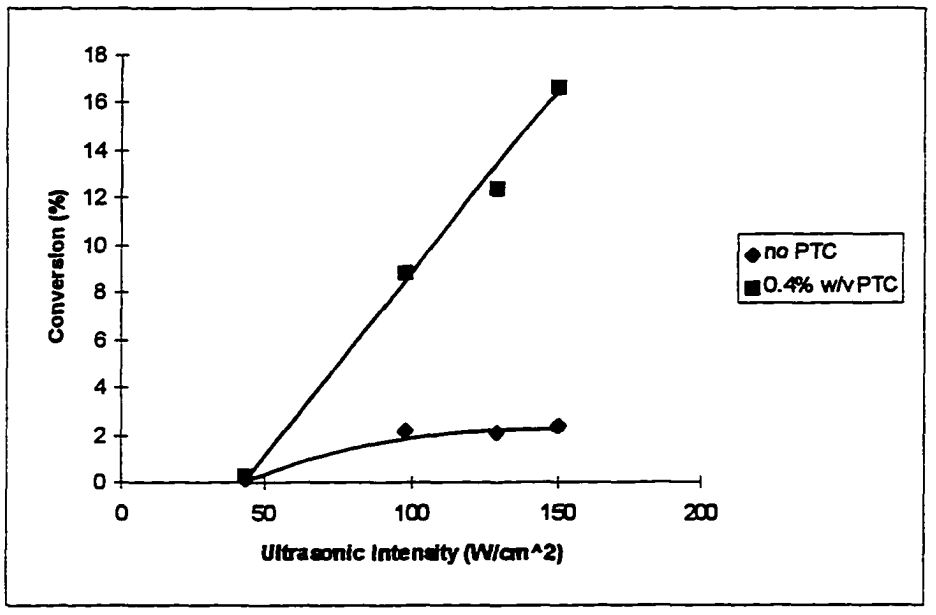

Figure 3.11 Effect of acoustic intensity on the conversion of benzyl chloride.
(Na_2S particle size <170 μm, no mechanical agitation, PTC = TBAB, temp = 25 °C, reaction time = 60 seconds)

b. Effect of catalyst concentration

The conversion of benzyl chloride is expected to increase with catalyst concentration, as was observed in the absence of ultrasonic irradiation. This is indeed the case (Figure 3.12). Although it appears that the determination of a kinetic model should be fairly simple, it is not. While attempting to find a rate equation by using the same mathematical method as use in the case of PTC alone, the reaction order of benzyl chloride was found to be around 8 or higher. This is not reasonable. A possible explanation for this is the variable surface area of Na_2S available for reaction as a result of ultrasound action. As is well documented, ultrasound waves are known to cause a reduction in the size of solid particles present in the system. Therefore, it is expected that the surface area of Na_2S available for reaction is continuously increasing. In the absence of precise data on the solubility of Na_2S in the organic phase, no quantitative analysis is attempted in the present study.

It is also interesting to compare the individual effects of PTC, microphase and ultrasound on the conversion of benzyl chloride with that of the base reaction. From the results presented in Figure 3.13, it appears that the effects due to ultrasound are mechanical (i.e. efficient agitation and particle size reduction), and not chemical. This speculation may be substantiated with the following observations: first, the effect due to ultrasound alone is small and approximately equal to, or slightly greater than, the effect due to microphase alone. Next, PTC is required in this system for a significant amount of reaction to occur. In addition, the enhancements due to PTC are very large and chemical. Therefore, since the increase in conversion when using ultrasound alone is approximately equal to the that of microphase alone, and in no way compares with the increase obtained when using PTC alone, it is

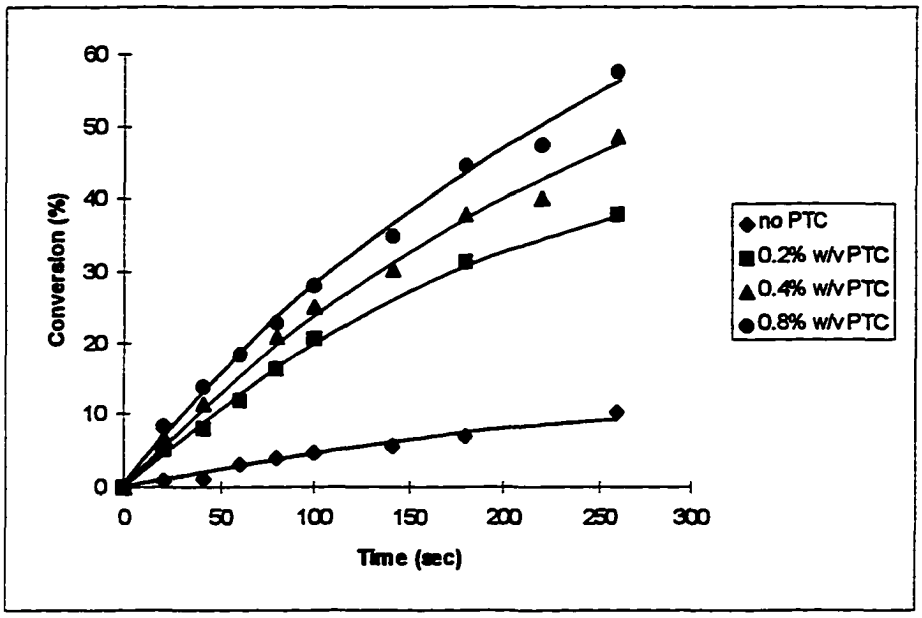

Figure 3.12 Effect of catalyst concentration for reaction with ultrasound.
(Na_2S particle size <170 μm, no mechanical agitation, PTC = TBAB, temp = 25 °C, ultrasonic intensity = 150 W/cm^2)

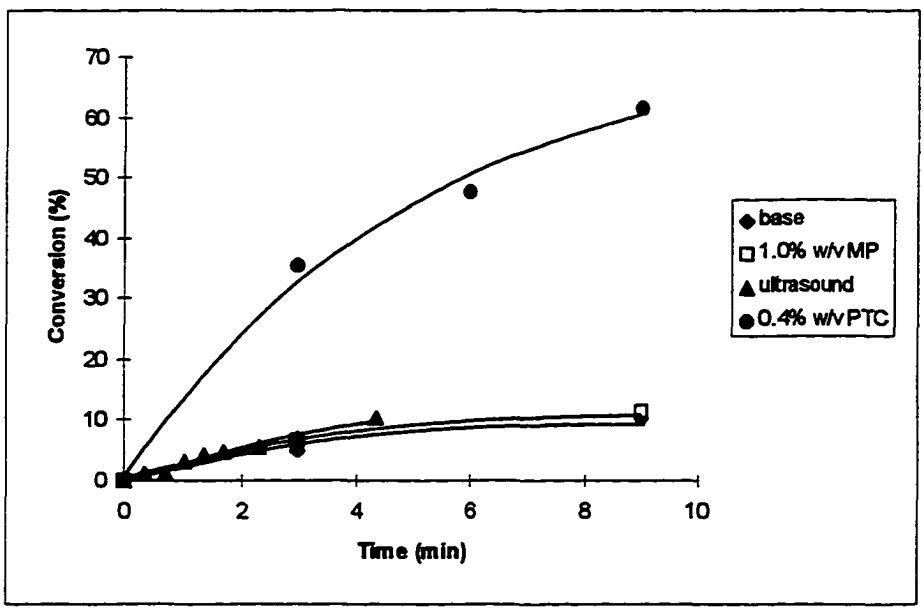

Figure 3.13 Comparison of the individual effect on the base reaction.
(Na_2S particle size <170 μm, no mechanical agitation, PTC = TBAB, MP = fumed silica, temp = 25 °C, ultrasonic intensity = 150 W/cm^2)

concluded that the effects of ultrasound on this reaction system are mechanical effects. Since the synthesis of benzyl sulfide follows an ionic mechanism, these results are not very surprising. Several others (see, e.g., Einhorn *et al.*, 1990; Luche, 1992) have also discovered that ultrasound does not produce any significant chemical effects in reactions following ionic pathways. Some (see, e.g., Luche, 1990) have also determined that ultrasound instigates free-radical mechanisms in reactions which can follow either an ionic or free-radical pathway (depending on reaction parameters).

c. Effect of reaction temperature

It is believed that an increase in the ambient reaction temperature results in an overall decrease in the sonochemical effect primarily because of the increase in the amount of vapor in the system (Suslick, 1988; Mason, 1990, among others). When the vapor pressure of the mixture is increased, it becomes easier to form cavitation bubbles; however, these bubbles contain more vapor than at lower reaction temperatures. The vapor cushions the implosion of the microbubble, reducing the ultrasonic energy produced upon cavitation and thus the chemical effects of ultrasound. Increasing reaction temperature also decreases the viscosity of the system. The significance of which is discussed in the next section.

The results obtained on the present system at three reaction temperatures (25, 30 and 35 °C), as presented in Figure 3.14, do not uphold this trend. It may be clearly seen that the behavior is similar to that of any normal reaction, i.e. the conversion increases with increasing temperature. The reason for this may be directly related to the conclusion reached earlier, that

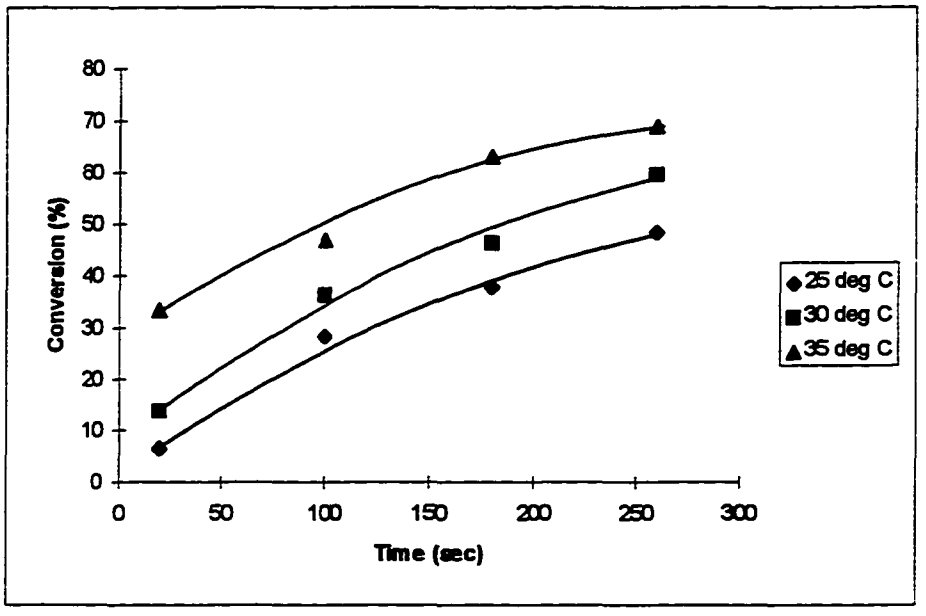

Figure 3.14 Effect of ambient temperature on reaction with ultrasound.
(Na_2S particle size <170 μm, no mechanical agitation, PTC = 0.4% w/v TBAB, ultrasonic intensity = 150 W/cm^2)

ultrasound has no chemical effects on this system. Therefore, an increase in ambient reaction temperature leads to the conventional increase in conversion.

d. Effect of solvent

When selecting a solvent there are many parameters which must be taken into consideration. When using a phase transfer catalyst, it is important to find a solvent which dissolves the catalyst completely. Some chemical distributors, such as Fluka, include solubility tables of phase transfer reagents in their annual catalogs. When using ultrasound, the viscosity and vapor pressure of the solvent have a significant effect upon the sonochemical event. The viscosity, which is related to the natural cohesive forces of the fluid, is directly proportional to the cavitational threshold. Increasing the viscosity increases the sonochemical

effect because, although the bubbles are more difficult to initiate, the collapse is more violent. However, there is a point where the viscous forces are so strong that cavitation can no longer be initiated, after which the sonochemical effect is greatly reduced.

An experimental comparison is made between two different solvents, acetonitrile (which has been used in all previous experiments) and *n*-butyl alcohol. The alcohol has a vapor pressure 0.087 times lower and viscosity 8 times greater than that of acetonitrile at a temperature of 25 °C. In addition, solubility tables report that Na_2S is slightly soluble in alcohols. Therefore, using *n*-butyl alcohol as solvent is expected to lead to higher conversions than acetonitrile. Figure 3.15 shows that this is indeed the case. The increase in conversion when using *n*-butyl alcohol is most likely due to the increased solubility of Na_2S in that solvent instead of the increased cavitational effect since, as stated previously, it appears that ultrasound has little or no chemical effect on this system.

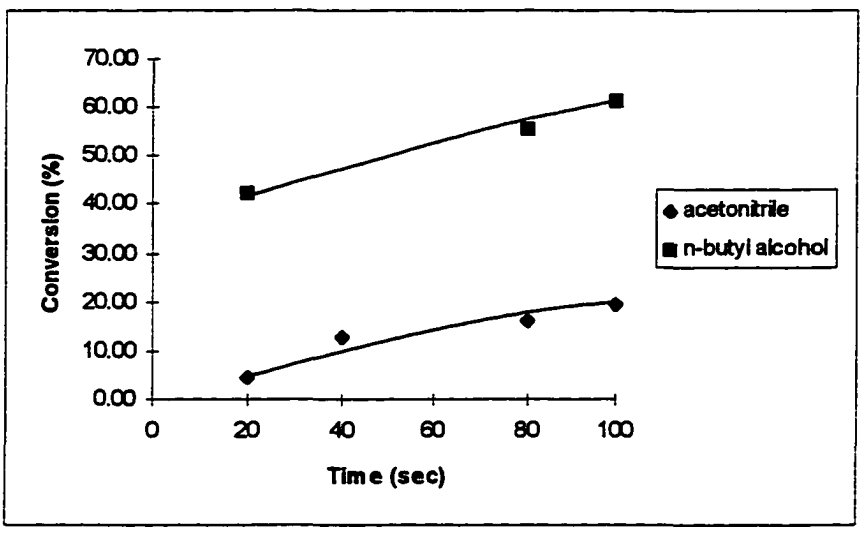

Figure 3.15 Effect of solvent choice on reaction with ultrasound and PTC.
(Na_2S particle size <170 μm, no mechanical agitation, PTC = TBAB, temp = 25 °C, ultrasonic intensity = 150 W/cm^2)

e. Combined effect of PTC, microphase and ultrasonic irradiation

The addition of microphase to the system under the influence of PTC and ultrasound results in an even greater increase of conversion (Figure 3.16). This is expected to be related to the combined effects of increased surface area of Na_2S available for reaction due to ultrasound and facilitated mass transfer due to both ultrasound and microphase. A more detailed explanation will be given in the following section.

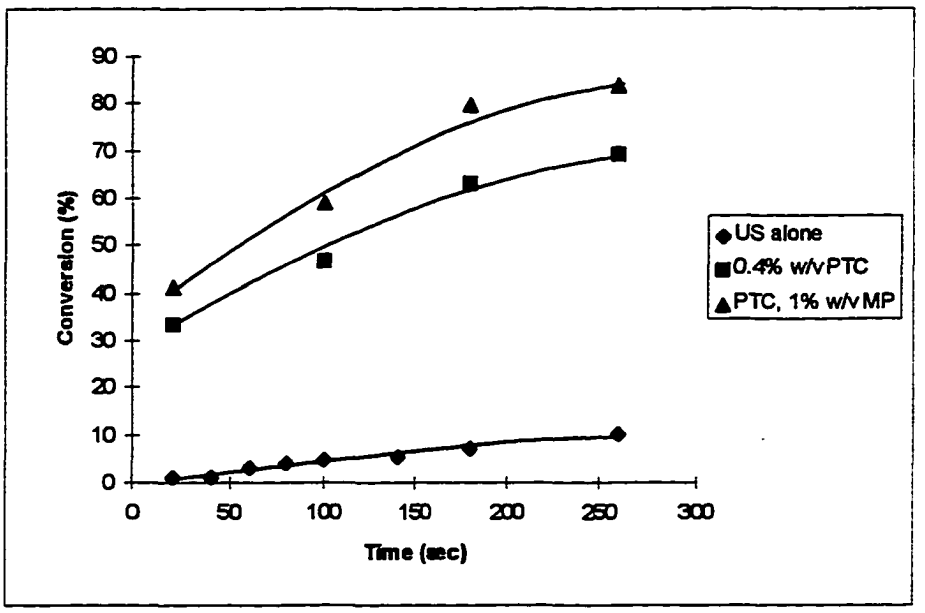

Figure 3.16 Combined effect of PTC and microphase in a sonochemical system.
(Na_2S particle size <170 μm, no mechanical agitation, PTC = TBAB, MP = fumed silica, temp = 25 °C, ultrasonic intensity = 150 W/cm^2)

3.4.7 Summary of individual and combined effects of PTC, microphase and ultrasound

In order to compare the strategies which have been used and to fully understand their effects on the synthesis of benzyl sulfide from benzyl chloride and sodium sulfide, the individual and combined effects of PTC, microphase and ultrasound have been summarized in

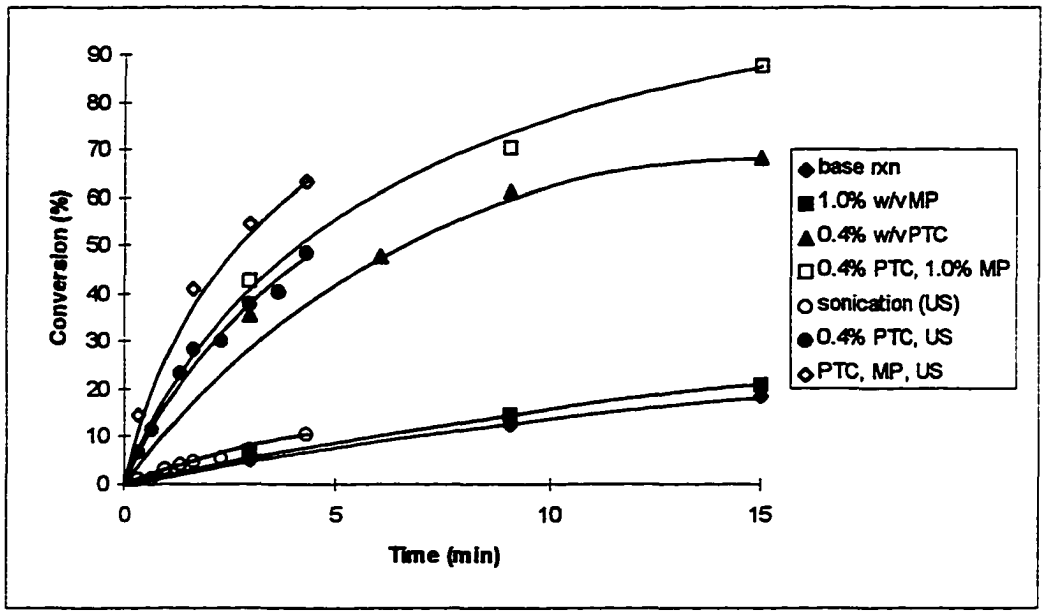

Figure 3.17 Individual and combined effects of PTC, microphase and ultrasound.
(Na_2S particle size <170 μm, no mechanical agitation, PTC = TBAB, MP = fumed silica, temp = 25 °C, ultrasonic intensity = 150 W/cm^2)

Figure 3.17. It is clear from this figure that the presence of PTC is necessary for a significant amount of reaction to occur. Therefore, other methods of rate enhancement investigated are only effective when used in conjunction with PTC.

Other conclusions which are speculated are not as obvious. Considering first the base reaction, it is noted that molecular diffusion and solubility of Na_2S in acetonitrile are not affected by ultrasound or microphase; hence, their individual affects on the reaction are likely to be minimal, as indeed observed in Figure 3.17. Facilitation of mass transfer from the diffusion film into the organic bulk by the microphase has little effect on the rate, possibly due to the negligible role of mass transfer in the reaction at 25 °C. Also, very little dissolved Na_2S is present in the film to be ferried into the organic phase, and the microphase does not have any specific affinity for the inorganic solid salt.

The minor increase in conversion due to ultrasound alone is most likely a result of the increased surface area available for the base reaction, facilitated mass transfer and efficient agitation of the reaction mixture.

The large enhancement due to PTC alone implies that the catalytic cycle which ferries the sulfide anions into the organic phase is required for significant reaction to occur. The amount of reaction is slightly increased with the addition of ultrasound because, again, it produces an increased surface area for reaction as a direct result of the reduction of Na_2S particle size and increases the mass transfer of the reactive anions through the phenomena of microstreaming.

It is speculated that the addition of PTC and microphase gives even higher conversions because PTC probably adheres to the surface of the microphase and is convectively transported into the diffusion film by it. This hypothesis is based on the assumption that the convective flow of microphase particles through the diffusion film is faster than the diffusion of PTC molecules.

The effect of PTC and microphase is further enhanced with ultrasonic irradiation because of the increased mass transfer, efficiency of agitation and Na_2S surface area available for reaction.

3.5 Conclusions

The present research was undertaken to study the individual and combined effects of a phase transfer catalyst (PTC), microphase (MP) and ultrasound (US) in enhancing the rate of a solid-liquid reaction. Using the reaction of benzyl chloride (liquid) with sodium sulfide (solid) as a model system, the following conclusions were reached: (1) all three techniques

give enhancements in the rate, but the effect of PTC is the most profound; (2) while in the cases of MP and US enhancement occurs due to an increase in mass transfer, a definite chemical effect is involved in the case of PTC; (3) the role of MP is not necessarily one of enhancement, for certain microphases (i.e. silica gel) can retard the reaction; (4) the reaction order can decrease perceptibly with increase in temperature, indicating no dependence on the substrate concentration and hence zero order; (5) the effects of PTC, MP and US appear to be more than just additive, and when all three are used together a considerable enhancement can be obtained (about 150%). The results of a detailed modeling study will be reported in a future communication.

3.6 Nomenclature

Symbols

C_{BzCl}	concentrations of benzyl chloride (mol/mL)
C_{PTC}	concentrations of PTC (mol/mL)
I	ultrasonic intensity (W/cm^2)
k	rate constant ($mL^{0.5}\ mol^{-0.5}\ s^{-1}$)
$-r_{BzCl}$	rate of disappearance of benzyl chloride ($mol\ mL^{-1}\ s^{-1}$)
T	temperature (°C)
t	reaction time (s)

Acronyms and abbreviations

LLPTC	liquid-liquid phase transfer catalysis
MP	microphase
PTC	phase transfer catalysis
SLPTC	solid-liquid phase transfer catalysis
TBAB	tetrabutylammonium bromide
w/v	mass of solid per unit volume of organic phase (g/mL)

Chemical species

Q^+	the cation of PTC

3.7 References

Ando, T. and Kimura, T., 1990, Reactivity and Selectivity in Organic Sonochemical Reactions Involving Inorganic Solids, *Ultrasonics*, **28(5)**, 326-332.

Cum, G., Galli, G., Gallo, R. and Spadaro, A., 1992, Role of Frequency in the Ultrasonic Activation of Chemical Reactions, *Ultrasonics*, **30(4)**, 267-270.

Dehmlow, E. V. and Dehmlow, S. S., 1993, *Phase Transfer Catalysis, Monographs in Chemistry*, 3rd Edition, pp. 6-10, VCH Publishers, New York.

Diez-Barra, E., de la Hoz, A., Diaz-Ortiz, A. and Prieto, P., 1992, Ultrasound and Phase Transfer Catalysis without Solvent in Elimination Reactions: Synthesis of Cyclic Ketene Acetals, *Synlett*, **November**, 893-894.

Einhorn, C., Einhorn, J., Dickens, M. J. and Luche, J. L., 1990, Organic Sonochemistry - Some Illustrative Examples of a New Fundamental Approach. *Tetrahedron Letters*, **31**, 4129-4130.

Evans, T. L., 1984, Phase Transfer Catalyzed Melt Synthesis of Diaryl Sulfides, *Synth. Commun.*, **14(5)**, 435-443.

Janakiraman, B. and Sharma, M. M., 1985, Solid-Liquid and Liquid-Liquid Slow and Fast Reactions: Enhancements by Fine Carbon Particles, *Chem. Engng. Sci.*, **40(2)**, 235-247.

Kim, I. K. and Noh, J. S., 1974, Novel Synthesis of bis-(p-nitrophenyl) sulfide, *Taehan Hwahak Hoechi*,**18(6)**, 421-422 [1975, *Chem. Abstr.*, **82**, 124967h].

Kutil, B., Cuda, J. and Kempny, L., 1982, Isolation of Dibenzyl Sulfide or Dibenzyl Disulfide, *Czech. CS*, 187958 [1982, *Chem. Abstr.*, **97**, 72064z].

Kutil, B., Cuda, J., Simandl, J. and Lorenc, J., 1985, Dibenzyl Sulfide or Dibenzyl Disulfide, *Czech. CS*, 220023 [1986, *Chem. Abstr.*, **105**, 172042t].

Landini, D. and Rolla, F., 1974, A Convenient Synthesis of Primary and Secondary Dialkyl and Aryl Sulfides in the Presence of Phase Transfer Catalysts, *Synthesis*, 565-566.

Luche, J. L., 1992, Developments of the New 'Experimental Theory' of Sonochemistry Initiated in Grenoble, *Ultrasonics*, **30(3)**, 156-167.

Luche, J. L., Einhorn, C., Einhorn, J., de Souza Barboza, J. C., Petrier, C., Dupuy, C., Delair, P., Allavena, C. and Tuschl, T., 1990, Ultrasonic Waves as Promoters of Radical Processes in Chemistry: the Case of Organometallic Reactions, *Ultrasonics*, **28(5)**, 316-321.

Mason, T. J., 1990, *Chemistry with Ultrasound*, pp. 44-45, Elsevier Science Publishing, New York.

Mehra, A., 1990, *Handbook of Heat and Mass Transfer Volume 4, Advances in Reactor Design and Combustion Science*, pp. 735, Ed. by N. Cheremisinoff, Gulf Publishing, Houston.

Melville, J. B. and Goddard, J. D., 1990, *Handbook of Heat and Mass Transfer*, pp. 345, Ed. by N. Cheremisinoff, Gulf Publishing, Houston.

Pradhan, N. C. and Sharma, M. M., 1990, Kinetics of the Reactions of Benzyl Chloride/ *p*-Chlorobenzyl Chloride with Solid Sodium Sulfide: Phase Transfer Catalysis and Role of the Omega Phase, *Ind. Engng. Chem. Research*, **29**, 1103-1108.

Ramsden, J. H., Drago, R. S. and Riley, R., 1989, A Kinetic Study of Sulfide Oxidation by Sodium Hypochlorite Using Phase Transfer Catalysis, *J. Amer. Chem. Soc.*, 111, 3958-3961.

Starks, C. M. and Owens, R. M., 1973, Phase Transfer Catalysis II. Kinetic Details of Cyanide Displacement on 1-Halooctanes, *J. Amer. Chem. Soc.*, **95**, 3613.

Suslick, K. S., 1990, Sonochemistry, *Science*, **247**, 1439-1445.

Suslick, K. S., 1988, *Ultrasound : Its Chemical, Physical and Biological Effects*, pp. 48-61, VCH Publishers, New York.

Suslick, K. S. and Johnson, R. E., 1984, Sonochemical Activation of Transition Metals, *J. Amer. Chem. Soc.*, **106**, 6856-6858.

Tozzi, A. and Cassandrini, P., 1975, Catalysts for Organic Sulfide Manufacture, *Ger. Offen.*, 2513805, [1976, *Chem. Abstr.*, **84**, 4476s].

Yadav, G. D. and Sharma, M. M., 1981, Kinetics of Reactions of Benzyl Chloride with Sodium Acetate/Benzoate: Phase Transfer Catalysis in Solid/Liquid Systems, *Ind. Engng. Chem. Process. Des. Dev.*, **20**, 385.

CHAPTER 4.
COMPARISON OF THE EFFECTS OF ULTRASOUND AND MECHANICAL AGITATION ON A REACTING SOLID-LIQUID SYSTEM

A paper accepted for publication in *Chemical Engineering Science*.

Leigh C. Hagenson and L. K. Doraiswamy

Abstract

Ultrasound has been shown to have desirable effects on both homogeneous and heterogeneous reactions, such as increasing the conversion, enhancing the selectivity, and improving the yield. Enhancements due to ultrasound may be attributed to its chemical or mechanical effects, or to both simultaneously. The chemical effects of ultrasound are due to the implosion of microbubbles, generating free-radicals with a great propensity for reaction. Mechanical effects are caused by shock waves formed during symmetric cavitation, or by microjets formed during asymmetric cavitation. Research emphasis in this area has largely been restricted to the chemical effects of ultrasound and physical descriptions of cavitation. The present study is among a very few to attempt a chemical engineering analysis of the problem. More specifically, it seeks to discern the mechanisms behind the mechanical effects by selecting a model solid-liquid noncatalytic reacting system in which the chemical effects of ultrasound are negligible. Using several investigative techniques, the expected effects of ultrasound are observed, such as the degradation of the solid reactant, leading to increased surface area. More importantly, some novel findings of the effects of ultrasound on mass transfer parameters are reported. Results clearly show that ultrasound enhances the intrinsic mass transfer coefficient as well as the effective diffusivity of the organic reactant through the

ionic lattice of the product layer. Discerning the effects of ultrasound on mass transfer parameters, as done in this paper, is an important step towards understanding the effects of ultrasound and determining its applications for the chemical industry.

4.1 Introduction

4.1.1 General

Ultrasound has been used successfully to enhance the rates of mass transfer and reaction in several homogeneous (see, e.g., Berlan *et al.*, 1994; Cum *et al.*, 1988) and heterogeneous (see, e.g., Lie Ken Jie, 1995; Luche, 1994) systems. The true chemical effects of ultrasound are attributed to the implosive collapse of microbubbles which are formed during the rarefaction, or negative pressure period, of sound waves. The molecules of the vaporized reaction mixture within the bubbles are fractured, forming highly reactive free radicals. The mechanism leading to the formation of these free radicals is in dispute, with two competing theories to explain the phenomenon: the *hot-spot theory* (Noltingk and Neppiras, 1950) and the *electrical theory* (Margulis, 1985). Arguments for and against these theories are discussed elsewhere (see, e.g., Broeckaert *et al.*, 1992; Suslick *et al.*, 1990).

The implosive collapse of microbubbles, typically referred to as cavitation, results in a variety of mechanical effects as well. When solid particles are in the vicinity of the cavitation bubble, the implosion may occur symmetrically or asymmetrically, depending on the proximity of the solids. Symmetric cavitations create shock waves which propagate to the surrounding solids causing microscopic turbulence and/or thinning of the solid-liquid film. This

phenomenon is called *microstreaming* and is thought to be responsible for increasing the rate of mass transfer of reactants and/or products through the film. When solid particles are in close proximity to the bubble, it is unable to collapse symmetrically. This is known as *asymmetric cavitation* and is responsible for the formation of microjets of solvent which bombard the solid surface, leading to pitting and erosion. Ultrasound can enhance the rates of mass transfer and reaction through these mechanical effects alone, even if it does not influence the reaction chemically, i.e. have a "sonochemical" effect.

The majority of articles published thus far in the field of sonochemistry are qualitative accounts of the effects of ultrasound on the initiation, enhancement, and kinetics of chemical reactions. Several types of reactions in organic synthesis have been investigated, including: Diels-Alder cyclizations (see, e.g., Javed *et al.*, 1995), oxidations (see, e.g., Entezai and Kruus, 1994; Soudagar and Samant, 1995), Kornblum-Russell alkylations (see, e.g., Dickens and Luche, 1991), Michael additions (see, e.g., Jouglet *et al.*, 1991), Claisen-Schmidt condensations (see, e.g., Fuentes *et al.*, 1987), Strecker syntheses (see, e.g., Hanafusa *et al.*, 1987), and Barbier reactions (see, e.g., de Souza-Barboza *et al.*, 1987). The effect of ultrasound on other chemical systems, such as organometallic and biological, have been compiled by Suslick (1988), Mason (1990a and 1990b) and Sinisterra (1992).

Unfortunately, contributions based on a chemical engineering approach to the analysis of sonochemical reactions have been surprisingly few. A sonochemical reactor design analysis was developed by Prasad Naidu *et al.* (1994), which attempts to explain the effect of dissolved gases in a liquid reaction mixture using a model system: the liberation of iodine from an aqueous potassium iodide solution. Their modeling efforts were a result of the

experimental observations made earlier that the rate of iodine liberation was dependent on the atmosphere under which the sonochemical reaction was conducted (Hart and Henglein, 1985).

When the effects of ultrasound were compared those of vigorous mechanical agitation, ultrasound was found to give a higher chemical yield, even though the two methods had similar power consumption (Ratoarinoro *et al.*, 1995). The authors used an empirical power correlation given by

$$k_l = \frac{D}{d_p}\left[2 + 0.4\left(\frac{e\, d_p^4 \rho_l^3}{\mu_l^3}\right)^{\frac{1}{4}}\left(\frac{\mu_l}{\rho_l D}\right)^{\frac{1}{3}}\right]F_c \qquad (1)$$

to predict the intrinsic mass transfer coefficient in the presence of ultrasound. When this correlation was used by the present authors to estimate an experimentally determined intrinsic mass transfer coefficient, it overestimated the experimental value by over two orders of magnitude. Thus the validity of this particular correlation for the determination of mass transfer coefficients in the presence of ultrasound is in question. However, this was not critical to the findings of Ratoarinoro *et al.* because the mass-transfer step was not the rate limiting factor in the reaction under investigation.

The effects of ultrasound on the intrinsic mass transfer coefficient of a diffusion limited reaction, the reduction of ferri- ferrocyanide, were investigated using an electrochemical method (Contamine *et al.*, 1994). The current intensity was measured during the course of the reaction at different axial and radial positions in the reactor, enabling the localized intrinsic mass transfer coefficient of the ions to the solid surface to be determined. For a batch reactor with a probe configuration, the localized values of the mass transfer coefficient, measured in

the axial direction, were characteristic of a standing wave when the power delivered to the system was low (i.e. 8 W). However, as the power delivered to the system was increased, the wave pattern dissipated and mass transfer became higher near the probe tip and decreased as the axial direction from the probe tip increased. In the radial direction, it was found that at low powers (i.e. 8 W), mass transfer was slightly higher at the center of the reactor, but was comparable over the cross-section of the reactor. However, as the power delivered increased, mass transfer increased at the center of the reactor and dissipated in the radial direction towards the reactor walls. At an input power of 200 W, the active region in the radial direction was equal to the diameter of the horn (the remaining radial direction had negligible activity).

In summary, the literature review provided answers to some of the questions concerning the design and scale-up of reactors. First, it was shown that ultrasound enhances the chemical yield over mechanical agitation alone, even when the mechanical agitation uses approximately the same power consumption. Second, it appears that use of existing correlations, based on experiments using mechanical agitation, to predict intrinsic mass transfer coefficients in the presence of ultrasound may not be sufficient. More work is necessary to discern the mechanical effects of ultrasound on solid-liquid system parameters, such as intrinsic mass transfer coefficients and diffusivities, before correlations can be developed to predict these effects.

4.1.2 Kinetic modeling approach

The system under investigation in this work is the reaction between a noncatalytic sparingly soluble solid and an organic liquid. The common approach to this type of reaction is to assume that the reaction takes place either in the solid-liquid film, in the liquid bulk, or in both simultaneously (see, e.g., Doraiswamy and Sharma, 1984; Levenspiel, 1972), and is presented as the "Common approach" in Figure 4.1. However, when the solid is sparingly soluble, the most rigorous approach would be to allow for reaction both in the solid and liquid phases. This possibility has been considered by Phadtare and Doraiswamy (1965), and is presented as the "Rigorous approach" in the flowchart shown in the figure. Determining the rate limiting step, or steps, by initially accounting for all reaction possibilities may lead to a new understanding of the reaction pathway that could have been otherwise overlooked.

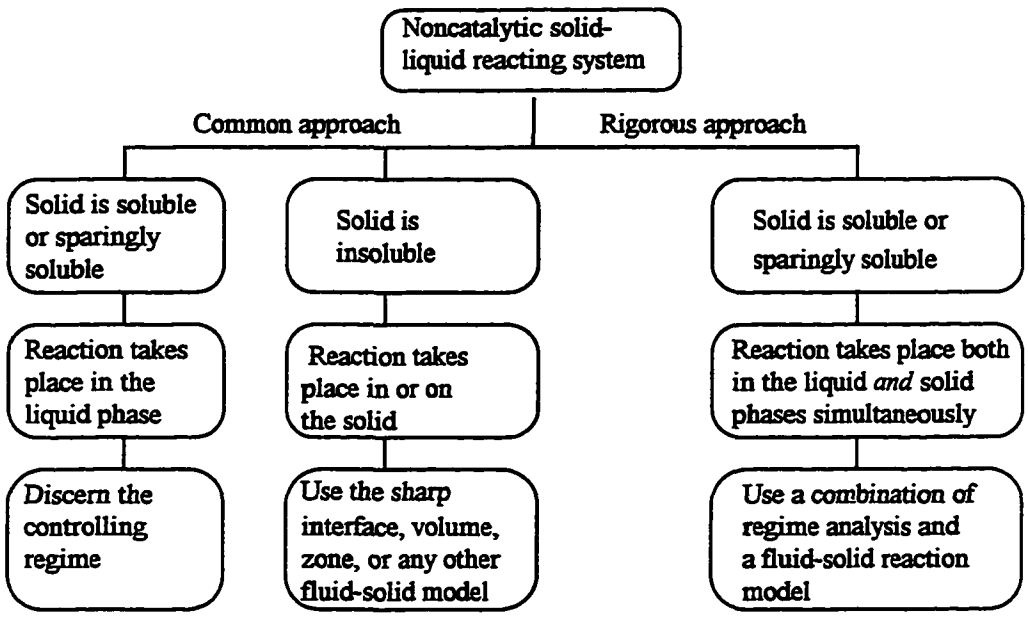

Figure 4.1 Flowchart of modeling approaches when using noncatalytic solid/liquid reaction systems.

4.1.3 Objectives

This paper is a continuation of research published earlier (Hagenson *et al.*, 1994) which investigated the relative effects of a phase transfer catalyst (unsupported tetrabutylammonium bromide), microphase, and ultrasound on a model reaction. The present research focuses on the effects of ultrasound alone using the same model reaction: synthesis of dibenzyl sulfide from benzyl chloride and solid sodium sulfide.

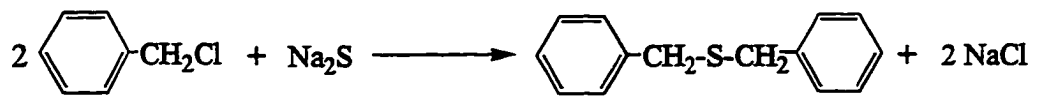

Benzyl Chloride (organic liquid)	Sodium Sulfide (solid)	Benzyl Sulfide (organic liquid)	Sodium Chlorid (solid)

The objective of the present investigation is to study the reaction from many different angles, including tracking the changes in the morphology of the surface using a scanning electron microscope, following the effects on the particle size using an image analyzer, determining the effect on the surface area using the B.E.T. method on an absorption isotherm apparatus, and determining the kinetics by measuring the concentrations of reactant and product with a gas chromatograph. Through the use of such tangible information, coupled with a study of the reaction kinetics, the effects of ultrasound on this solid-liquid system are sought to be more rigorously explored.

4.2 Experimental Apparatus, Procedure and Tools

A typical reaction mixture consisted of 1.085×10^{-3} mol/ml benzyl chloride (99% purity) and 10% w/v high purity sodium sulfide (purchased as anhydrous) in acetonitrile as solvent.

The "silent" reactions (reactions conducted in the absence of ultrasound) were carried out in an enclosed stainless steel reaction vessel operated in the batch mode. The reaction mixture was mechanically agitated using an impeller. The temperature was maintained to within ± 1.0 °C by jacket cooling and was monitored using a thermocouple inserted directly into the mixture.

The sodium sulfide was purchased from Aldrich as chunks, crushed, and sieved to provide the same average particle size for all batches. The lot of sodium sulfide significantly affected the reaction rate and will be discussed later. The purities of the lots used were reported by Aldrich as 102.0% for lot #14025MF and 102.5% for lot #11927MN. These numbers represent the sulfide concentration in the compound as determined by titration with sodium thiosulfate. Impurities in the product were not reported in the certificate of analysis.

Since replications could not be made of all experimental values reported in this paper due to a limited supply of sodium sulfide in each lot, the primary purpose of using lot #11927MN was for error estimation. Reported values for the rate parameters obtained using lot #11927MN had an average standard deviation of 4% based on 6 different reaction curves. The experimental data were also combined and the residuals were scrutinized for each of the reaction models investigated in this paper.

Ultrasound reactions were conducted using Sonicator XL2020 (Misonix, Inc.), which supplied a constant frequency of 20 kHz to the 1/2 inch titanium horn. The power and intensity of ultrasound were experimentally determined, and are reported in Section 4.3.1. The horn was fitted to the same stainless steel reaction vessel as used for the silent reactions (see Figure 4.2) in order to preserve similarity of reactor geometries for comparison of

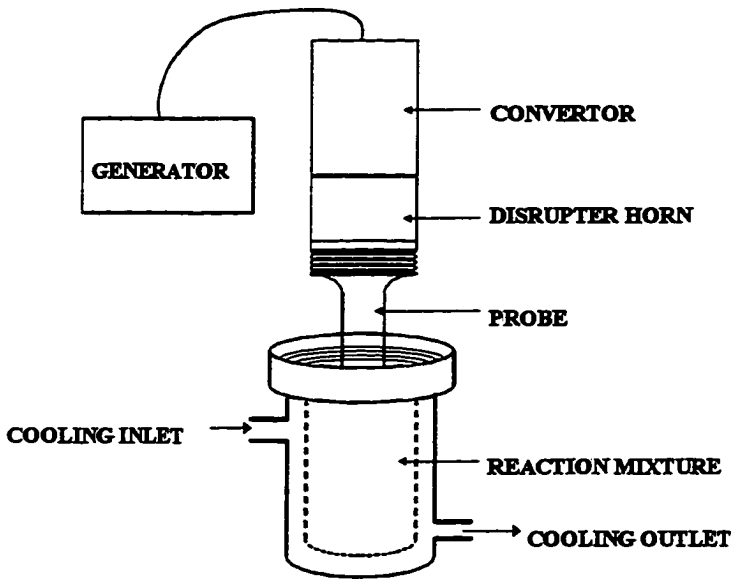

Figure 4.2 Experimental apparatus used for sonochemical research.

experimental data. Isothermal conditions were maintained to within ± 0.5 °C. No additional mechanical agitation was used.

The particle size of the sodium sulfide was determined using an image analyzer with a component system purchased from Fryer Co. Measurements were made at a magnification of 5x and were obtained from batches of over 400 particles.

The morphology of the solid surface of the sodium sulfide was examined using a Hitachi Variable Pressure Scanning Electron Microscope (SEM). Most of the samples required 6 to 10 kV of signal for a clear picture.

To determine the surface area of the sodium sulfide, an adsorption isotherm was measured using an ASAP2010 (Adsorption, Surface Area and Porosity System) and then fitted using the B.E.T. equation. The samples were degassed at room temperature for 12 hours. The temperature could not be increased because the sodium sulfide degradated at higher

temperatures. This also introduced the problem of an inability to remove excess water which was absorbed by the anhydrous sodium sulfide, possibly affecting the surface area results. The adsorption isotherm was taken at -77 °K under nitrogen. Argon was not used because the sample sizes were large and measurements were consistent using nitrogen.

The composition of the organic phase was determined using a Perkin Elmer Autosystem Gas Chromatograph with a 1/8 in x 6.56 ft (0.318 cm x 2.0 m) stainless steel packed column. The packing consisted of 10% SP2250 (liquid phase) on Supelcoport (solid support) with a mesh size of 100/120. The oven was programmed with a initial temperature of 150 °C, held for 2 minutes, and then increased at a rate of 32 °C/min to a final temperature of 300 °C. The peaks were well-defined and had good separation with retention times of 2.76 and 7.66 min for benzyl chloride and dibenzyl sulfide, respectively.

4.3 Results and Discussion

4.3.1 Power measurement

A common problem in the sonochemical literature is that the power delivered to the system (as quoted by the manufacturer) is mentioned, but the actual power dissipated (P_{diss}) in the reaction mixture is rarely reported. One of the most common methods of measuring P_{diss}, introduced by Lorimer *et al.* (1991), is to use the equation

$$P_{diss} = \left(\frac{dT}{dt}\right)_{t=0} mC_p \qquad (2)$$

where m and C_p are the mass and heat capacity of the solvent, respectively, and $(dT/dt)_{t=0}$ is the initial slope of the temperature of the reaction mixture versus the time it is exposed to

ultrasonic irradiation. This equation is based on the use of calorimetry and assumes that all of the power entering the reaction mixture is dissipated as heat.

Before performing experiments to determine the ultrasonic power dissipated in the reaction system under investigation, the reactor jacket was emptied and the stainless steel reaction vessel was well insulated to prevent any heat losses to the surroundings. Temperature readings were recorded at 5 second intervals. Because Equation (2) takes only the heat capacity of the solvent into consideration, and because the system under investigation is heterogeneous, the experiment was repeated 8 times: 4 times with 40 ml of solvent (acetonitrile) and 4.0 grams of sodium sulfide (simulating a typical reaction mixture), and 4 times with 42 ml of solvent. The additional 2 ml of solvent was introduced to account for the volume change upon removing the solids from the system. The recorded temperatures were plotted against time for each of the 8 reactions, as shown in Figure 4.3.

Experimental data obtained from the eight different experiments indicated that the addition of the solids to the system had no significant effect on the initial temperature rise of the system, thus all of the experimental data were combined. The values used for the parameters given in Equation (2) are: $m = 8.06 \times 10^{-4}$ kmol acetonitrile, $C_p(T = 22\ ^\circ K) = 9.12 \times 10^4$ J/kmol °K, and $\left(\frac{dT}{dt}\right)_{t=0} = 0.7472\ ^\circ K/s$. The power actually dissipated by the reaction mixture was 54.9 W, whereas the power delivered (as measured from the generator output)

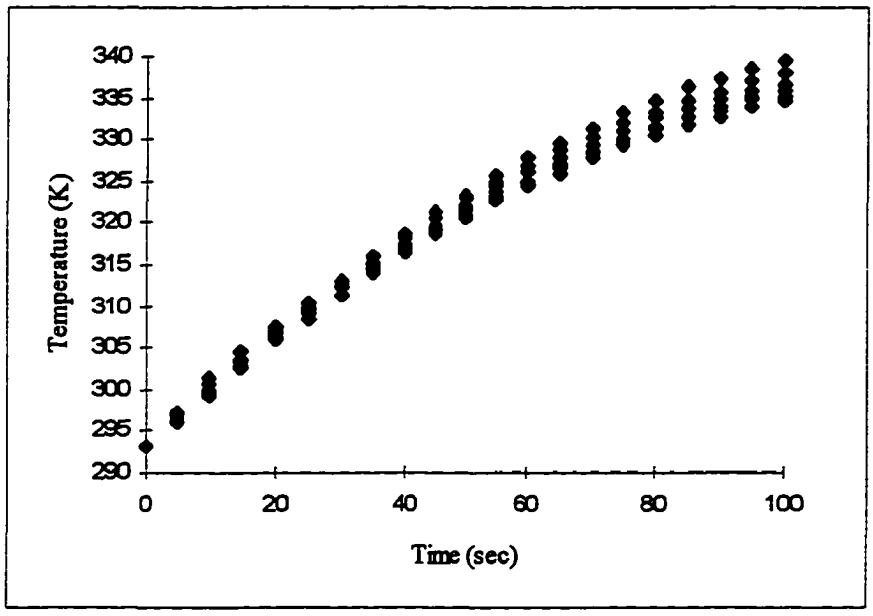

Figure 4.3 Determination of power dissipated by the reaction system: power delivered = 166 W.

was 166 W. This indicates that approximately 67% of the power quoted by the manufacturer as being delivered to the horn was lost during the transfer process to the mixture. The manufacturer of the equipment used in this experiment (Misonix, Inc.) had no direct explanation as to why the losses were so large. They quoted only a 10 to 30% loss in the transfer process from the generator to the probe tip (refer to Figure 4.2), depending upon the age and tuning parameters of the instrument. Although the losses will not be explained in detail here, a large portion result from the conversion of electrical energy over the piezoelectric crystal and mechanical losses from the propagation of waves through the horn.

When Equation 2 is altered to account for the heat absorbed by the reaction vessel, as given by Equation 3,

$$P_{diss} = \left(\frac{dT}{dt}\right)_{t=0} \left(m_{solvent} C_{p,\cdot solvent}\right) + \left(\frac{dT_v}{dt}\right)_{t=0} \left(A_{ws}\, x_w\right) \rho_{vessel} C_{p,\,vessel} \qquad (3)$$

the result is much more reasonable. The second term in Equation (3) accounts for the temperature rise in the inner wall of the vessel, separating the reaction mixture from the stagnant air layer in the jacket. Using the values $A_{ws} = 1.34 \times 10^{-2}$ m^2, $x_w = 2.4 \times 10^{-3}$ m, $\rho_{vessel} = 7820$ kg/m^3 and $C_{p,\,vessel} = 477$ J/kg °K for the stainless steel reaction vessel, and the experimentally determined value $\left(\frac{dT_v}{dt}\right)_{t=0} = 0.3374$ °K/s for the initial temperature rise of the wall, it was found that 95.4 W were dissipated. Thus 42.5% of the power delivered was lost in the transfer process. This is still lower than one would expect given the manufacturer's information. However, it is more reasonable than predicted using Equation (2)[1]. Equation (3) is an adequate approximation because the reaction mixture is well-mixed and the jacket is filled with stagnant air, providing a good insulator between the outer jacket wall and the reaction fluid.

When using a probe system, the intensity (I_{diss}) of ultrasound in the reaction mixture is equal to the power dissipated (P_{diss}) divided by the area of the probe tip (A) and is typically expressed in W/cm^2, as given in Equation (4).

$$I_{diss} = P_{diss}/A \qquad (4)$$

[1] Since knowledge of the method used to calculate the power dissipated is critical, it is suggested that authors report the power delivered as quoted by the manufacturer, the method used to determine the power dissipated, and the experimental value determined using that method. This will make it easier for future researchers to compare and contrast their results with published values.

Since the probe tip has an area of 1.27 cm^2, the intensity is 75 W/cm^2. (As a side note, the power setting and horn configuration used in these studies result in an input amplitude of 108 microns.)

4.3.2 Particle size analysis

One of the first steps in the study of the effect of ultrasound on this system was to analyze the particle size of the solid reactant over time under the experimental conditions studied. Samples of sodium sulfide were taken from each of the batches and the size distribution, based on the average diameter of over 400 particles from each batch, was found using image analysis. The overall mean diameter of each distribution is shown in Figure 4.4 as a function of time and experimental conditions.

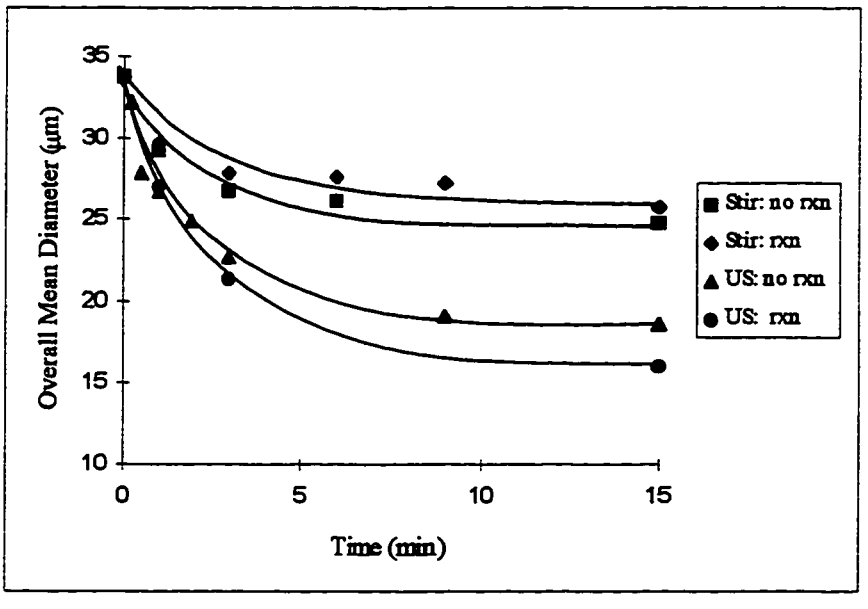

Figure 4.4 The mean particle size of sodium sulfide as a function of time for the different experimental conditions studied.

As expected, the mean particle size decreased at a faster rate when using ultrasound as compared to mechanical agitation. There is a slight difference in the mean diameter of particles in the presence and absence of reaction, with particles in the presence of reaction being slightly smaller than their unreacted counterparts. However, reaction has not greatly affected the overall trend in particle size for each of the cases studied.

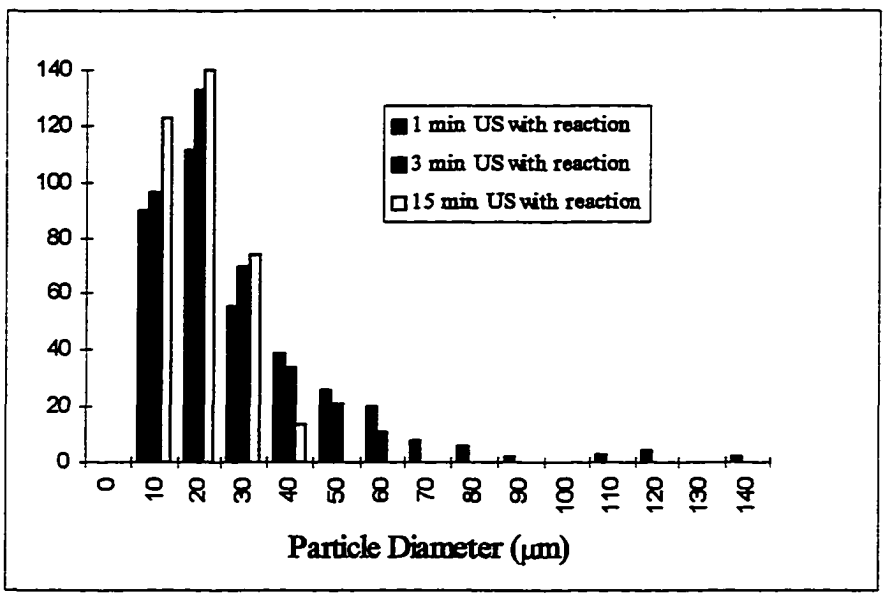

Figure 4.5 Histogram of diameter data for samples under the influence of ultrasound.

The distributions of particles for three sonicated reactions are shown in Figure 4.5. Each distribution has some degree of skewness to the right, but the skewness becomes less prevalent with continued exposure to sonication. This indicates that the larger particles (particles greater than ~ 40 μm) are broken down to particles in the size range 5 - 40 μm within 15 minutes of continuous exposure to ultrasound, with the mean size of ~16 μm. These observed effects of ultrasound on Na_2S are supported, in part, by the studies of

Ratoarinoro *et al.* (1992). Using a cup-horn, they found similar effects when continuously sonicating another inorganic solid, KOH. The KOH particles were reduced from their initial size of 240 μm to a size ranging from 15 to 20 μm within 5 minutes of sonication. The time required to reach a minimum particle size range is dependent upon the properties of the solid and the sonochemical equipment used.

4.3.3 Kinetic studies

Several authors have investigated the synthesis of dibenzyl sulfide in the presence of a phase transfer catalyst (PTC), including Landini and Rolla (1974) and Tozzi and Cassandrini (1975) who used tributylhexadecylphosphonium bromide (TBHDPB) and dilauryldimethylammonium chloride, respectively. Pradhan and Sharma (1990) report the synthesis of dibenzyl sulfide using a hydrated form of sodium sulfide ($Na_2S{\cdot}5H_2O$). They concluded that, in the presence tetrabutylammonium bromide (TBAB), the controlling mechanism of the reaction is simultaneous diffusion and reaction in the solid-liquid film, also known as Regime 3. In our previous publication (Hagenson *et al.*, 1994), conversion of the liquid reactant benzyl chloride was reported to increase from 10% to ~80% in the presence of the PTC tetrabutylammonium bromide (TBAB) for a reaction time of 15 minutes and a temperature of 25 °C. However, the kinetics of this reaction in the absence of a phase transfer catalyst have not been explored in any of the previous publications, and are the intention of the present kinetic analysis.

Kinetic studies were planned to account for liquid and solid phase reactions, but the actual kinetic analysis of the data was broken into two parts: analysis of the liquid phase reaction,

described in Section 4.3.3.a, and analysis of the solid phase reaction, described in Section 4.3.3.b. This modeling approach is in keeping with the "Rigorous approach" strategy shown in Figure 4.1 in Section 4.1.2.

a. Liquid phase reaction

Since the majority of reactions involving a sparingly soluble solid and a liquid occur either in the solid-liquid film, the liquid bulk, or in both simultaneously (see Figure 4.1, Section 4.1.2), the first step in modeling the liquid phase reaction was to use a power law model (Equation 5) to describe the reaction kinetics, where A and B represent sodium sulfide and benzyl chloride, respectively. Because the concentration of Na_2S available for reaction at any given time is

$$-r_B = kC_A^n C_B^m \qquad (5)$$

unknown, and cannot be determined, the method of initial rates was used to determine the reaction orders for A and B. Solids were placed in the reactor and allowed to dissolve for a certain length of time, corresponding to the initial concentration of A desired, where the dissolution rate of Na_2S was predetermined using atomic emission spectroscopy. When the desired initial concentration of A was attained, a specified amount of B was injected into the reactor vessel. This method of experimentation provided the experimental data necessary to use the method of initial rates to determine the reaction orders. A power law model was again used, and it was linearized, as shown in Equation 6, in order to obtain the initial estimates of k, n, and m required for nonlinear regression analysis, where ε is the random error term. However, when

$$ln(-r_{AO}) = ln\ k + n\ ln\ C_{AO} + m\ ln\ C_{BO} + \varepsilon \qquad (6)$$

this model was used, the residuals contained well defined curvature, indicating that the linear model did not adequately explain the variation in the data. In addition, poor R^2 values were obtained (i.e. ~0.5) and the relative p-values of both parameters were greater than 0.1 (p-values have a range from 0 to 1, where a low p-value supports the significance of the parameter). As expected, the p-values were reduced when one of the associated variables was eliminated from the model equation, but the curvature in the residual plots remained, indicating a significant lack of fit. From these modeling results, it was concluded that the power law model was inadequate to describe the experimental data.

The next step was to speculate on the mechanism of the reaction in order to obtain a mechanistic model which could be used to explain the experimental data. Several chemists were consulted, and a variety of reaction mechanisms were investigated, some of which are shown in Table 4.1. In addition, anhydrous hydrochloric acid was added to the reaction mixture in order to detect any sodium complexes which would not be detected by gas chromatography (g.c.). The addition of HCl would displace the sodium ion, forming an organic compound, i.e. benzyl mercaptan, which would be detectable by g.c. However, no compounds were detected, with the exception of benzyl chloride and dibenzyl sulfide (the reactant and desired product). In addition, the same problems were encountered when modeling the experimental data: the residual analysis of nearly all of the attempted models exhibited a significant degree of curvature and gave poor values of R^2. Thus again it was concluded that the derived models were inadequate in describing the kinetic data.

Table 4.1 Liquid phase reaction model discrimination.

Mechanism	Model Equation	Reasons for Rejection
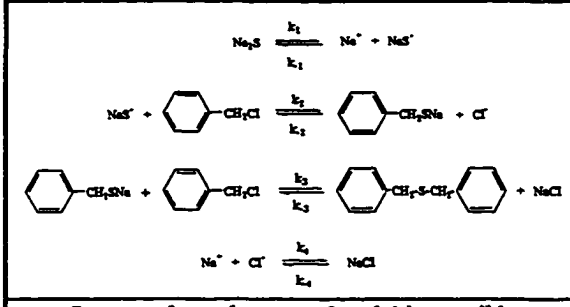	$-\frac{1}{r_{Na_2S}} = k_a \frac{C_{Na^+}}{C_{Na_2S}C_{\varphi Cl}} + k_b \frac{1}{C_{Na_2S}}$ where $k_a = \frac{k_{-1}}{k_1 k_2}$ $k_b = \frac{1}{k_1}$	1. Constant term β_o should be close to 0, but is predicted as >>0. 2. Prediction for k_b is negative. 3. Experimental 1/r vs. fitted is nonlinear.
Same as above, but steps 2 and 4 irreversible	Same as above	Same as above
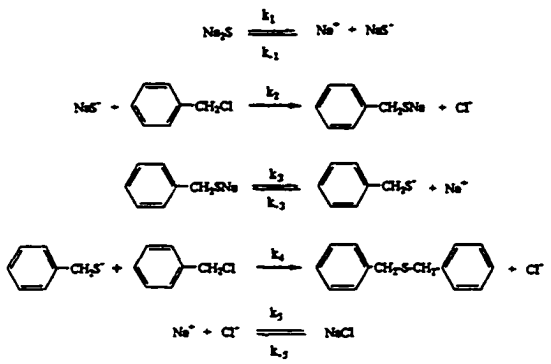	$-\frac{1}{r_{Na_2S}} = k_a \frac{1}{C_{\varphi Cl}} + k_b \frac{1}{C_{Na_2S}}$ where $k_a = \frac{k_{-1}}{2k_1 k_2}$ $k_b = \frac{1}{k_1}$	1. Constant term β_o should be close to 0, but is predicted as >>0. 2. Prediction for k_b is negative. 3. Experimental 1/r vs. fitted is nonlinear. 4. Curvature in residual plots.

The presence of a liquid phase reaction was also investigated experimentally. Sodium sulfide was agitated in the solvent until it was saturated, and then the excess sodium sulfide was filtered out of solution. Benzyl chloride was then added to the saturated solution, agitated for 15 minutes, and analyzed for products. However, sodium sulfide is so sparingly soluble (~1.43 x 10^{-6} mol Na_2S/ml solution at saturation) in solvent acetonitrile that the amount of benzyl sulfide produced was negligible, and well within the experimental variability of the gas chromatograph.

At this point in the kinetic analysis, it appeared that the liquid phase reaction was negligible. This conclusion was supported by both the experimental and modeling studies. Thus attention was focused on the solid-phase reaction.

b. Solid phase reaction

Since the solid reactant, sodium sulfide, is nonporous and the reaction is irreversible, as determined by thermodynamic calculations based on the Gibbs free energy of reaction, the sharp interface model (SIM) was used to describe the reaction occurring in or on the solid surface. This proved successful both in the presence and absence of sonication, and is described below.

The SIM model has been described in detail by Mazet (1992), Doraiswamy and Sharma (1984), and Levenspiel (1972), and is based on the following assumptions: 1. the reacting solid is nonporous, 2. isothermal conditions are maintained, 3. the counterdiffusion of reactants and products is equimolal, 4. the size of the solid particle is constant, 5. pseudo-steady-state diffusion through the product layer is valid, and 6. the reaction is irreversible and first order with respect to the liquid reactant. The validity of assumption 4 is questionable, because the particle size changes over time, as shown in Figure 4.4. However, after 3 minutes of reaction, the change in particle size is small. Thus the radius of the particle used in the modeling was the radius after 3 minutes of agitation (i.e. 26 μm) or sonication (i.e. 20 μm). The overall SIM model (for a spherical pellet) is given by the well-known relation

$$\frac{R_o}{3k_l}x_A+\frac{R_o^{\,2}}{6D_e}\left[1-3(1-x_A)^{2/3}+2(1-x_A)\right]+\frac{R_o}{k_s}\left[1-(1-x_A)^{1/3}\right]=\frac{\nu C_B M_A}{\rho_A}t \qquad (7)$$

where x_A is the conversion of the solid reactant. The first term in Equation (7) accounts for diffusion of the liquid reactant through the solid-liquid film, the second accounts for diffusion of the same reactant through the product layer surrounding the unreacted core of the solid,

and the third accounts for the reaction on the surface of the unreacted core. These terms can limit the progress of the reaction individually, simultaneously, or in combination with one another. After analyzing the experimental data, it became clear that, for this particular system, only one term limits the course of the reaction at any time, but the limiting step depends on the extent of conversion of the solid. The final results of the kinetic analysis are discussed in the following sections.

c. Silent reactions

The conversion of benzyl chloride to dibenzyl sulfide for the silent reactions is shown in Figure 4.6 for four different temperatures. No side products were detected on the gas chromatograph when the organic phase was analyzed. In addition, anhydrous hydrochloric acid was added to the samples to protonate any sodium complexes and then analyzed for side products where none were found. Thus it was assumed that the reaction only produced the products dibenzyl sulfide and sodium chloride. The negative value for the Gibbs free energy of reaction indicated that the reaction was irreversible.

The SIM model of the experimental data for the silent reactions, when using sodium sulfide lot # 14025MF, indicates that the reaction is limited by diffusion of benzyl chloride through the product layer. The product layer on the surface of the unreacted core of the sodium sulfide is most likely sodium chloride which crystallizes as the reaction progresses. The experimental data in Figure 4.6 are described by Equation 8. Because the terms R_o, C_B, M_A, and ρ_A are known, and the relationship between x_A and t was obtained experimentally, the

$$\frac{R_o^2}{6D_e}\left[1-3(1-x_A)^{2/3}+2(1-x_A)\right]=\frac{C_B M_A}{2\rho_A}t \qquad (8)$$

value of the effective diffusivity was extracted from Equation (8), and is shown in Figure 4.7 as a function of absolute temperature.

It is difficult at this time to determine the type of diffusion occurring in this system because the temperature range is narrow. It is apparent, however, that the values of the effective diffusivities are very low, with an order of magnitude of 10^{-11} cm^2/sec. Typical diffusivity data given for gases in solids are on the order of 10^{-5} cm^2/sec, for liquids in solids are 10^{-7} cm^2/sec, and for solids in solids are $< 10^{-10}$ cm^2/sec. Thus the limiting diffusional step could either be Knudsen diffusion in very small pores or solid state diffusion.

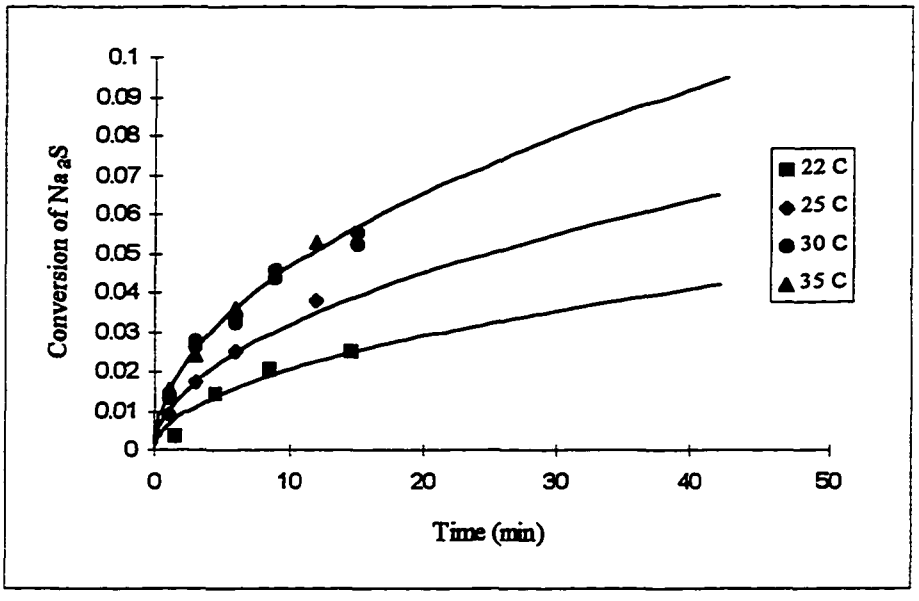

Figure 4.6 Effect of temperature on the silent reaction: Na_2S lot #14025MF.

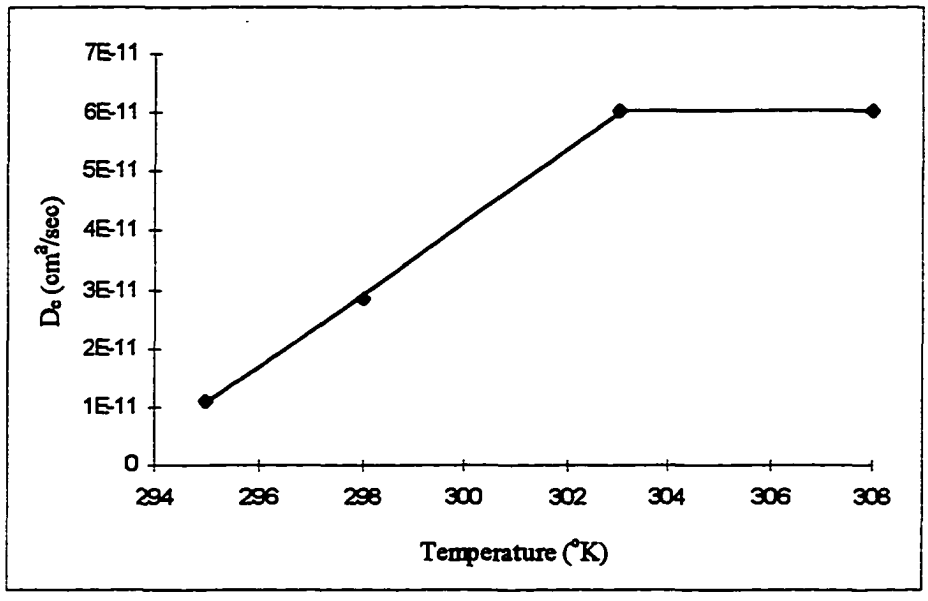

Figure 4.7 Increase of effective diffusivity with absolute temperature for silent reactions.

d. Sonochemical reactions

The addition of ultrasound to the model reaction leads to a significant increase in the conversion of benzyl chloride to sodium sulfide, as shown in Figure 4.8. Another interesting feature of this figure is the discontinuity in the curve for ultrasound at approximately 5 minutes. Looking at the data collected for ultrasound at different temperatures (see Figure 4.9), it is apparent that the transition occurs at approximately the same time for all of the reaction curves. At lower times the rate limiting step is the transfer of benzyl chloride through the solid-liquid film (as shown by Equation 9), while at higher times the reaction is controlled by the effective diffusion of benzyl chloride through the product layer (shown previously in Equation 8). Referring back to Figure 4.8 showing the

$$\frac{R_o}{3k_l} x_A = \frac{C_B M_A}{2\rho_A} t \qquad (9)$$

enhancement of the model reaction with ultrasound, it appears that the same transition from film transfer limited diffusion to ash layer limited diffusion may be occurring. However, there is not enough experimental data in this region to substantiate the film transfer model. An additional amount of experimental data would have been gathered, but there was a limited amount of sodium sulfide lot #14025MF. The lot of sodium sulfide used significantly affected the results, as will be discussed in Section 4.3.5.

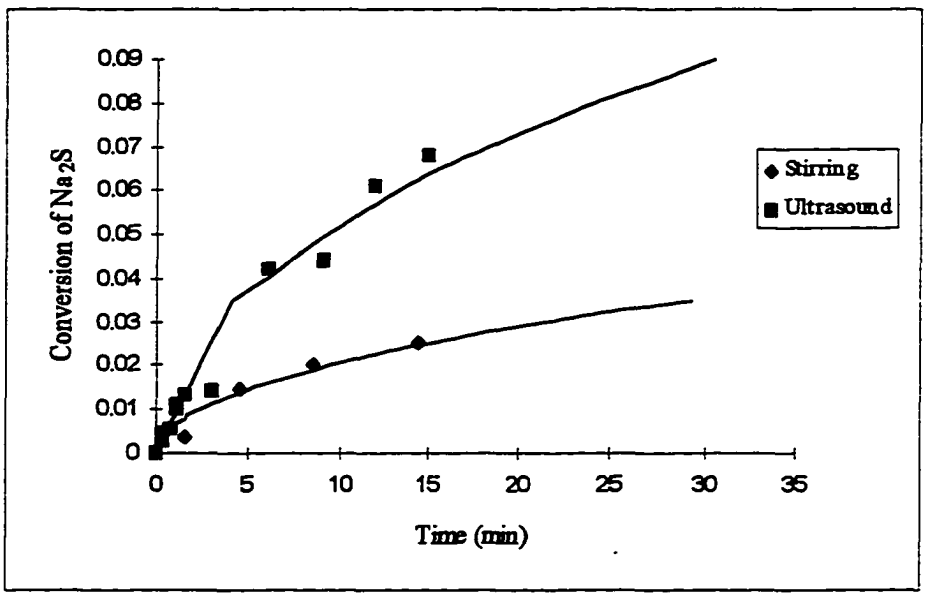

Figure 4.8 Enhancement of the model reaction with the addition of ultrasound.

As in the case of the mechanically agitated reactions, the values of k_l and D_e in the presence of sonication can be extracted from the experimentally determined relationship between x_A and t. The intrinsic liquid-phase mass transfer coefficient, k_l, increases linearly with temperature (see Figure 4.10) until 30 °C, when it becomes constant. The effective

diffusivity increases with temperature until 30 °C where it plateaus, as shown in Figure 4.11. It cannot be determined at this time whether the relationship is linear as in the case of stirring, or curvilinear. This may be due to such factors as cavitation, exposure to extreme temperature and pressure, and/or other localized conditions caused by sonication. It also may be likely that the effect of temperature on the effective diffusivity of the elementary steps involved in the overall reaction are different, and what is observed is the resultant of these effects. It is obvious that ultrasound significantly increases the effective diffusivity of benzyl chloride through the product layer. And, as in the case of the silent reactions, the values of the effective diffusivity are on the order of magnitude of 10^{-11} cm^2/sec, which indicates Knudsen diffusion through very small pores or solid state diffusion. The effect of ultrasound on the effective diffusivity poses an interesting problem for future research.

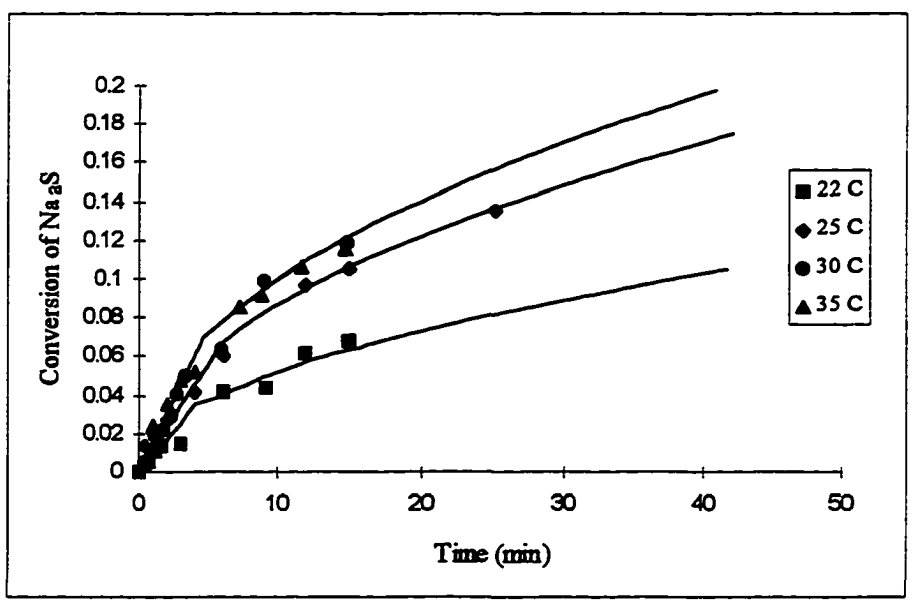

Figure 4.9 Effect of temperature on the sonochemical reaction.

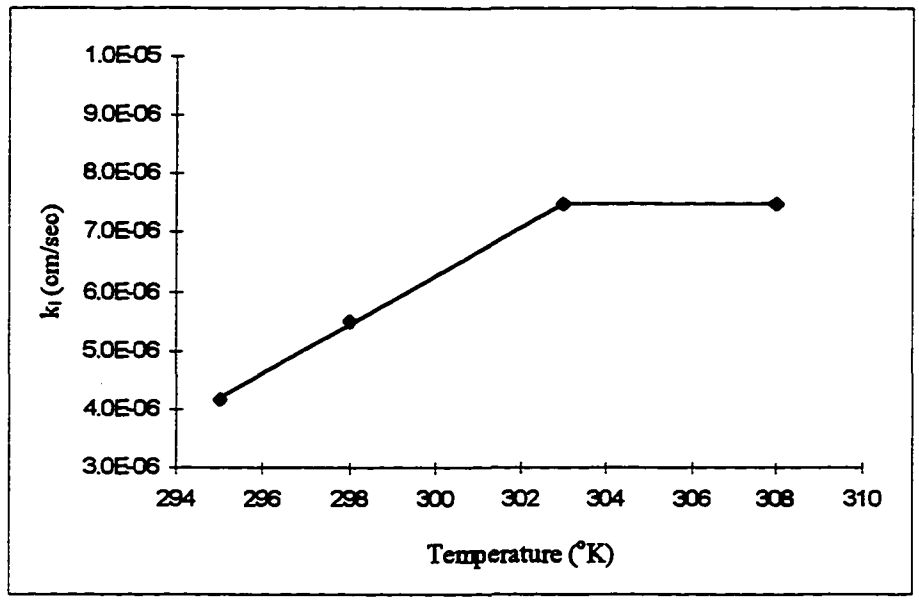

Figure 4.10 Effect of temperature on the intrinsic mass transfer coefficient (k_l) for ultrasound.

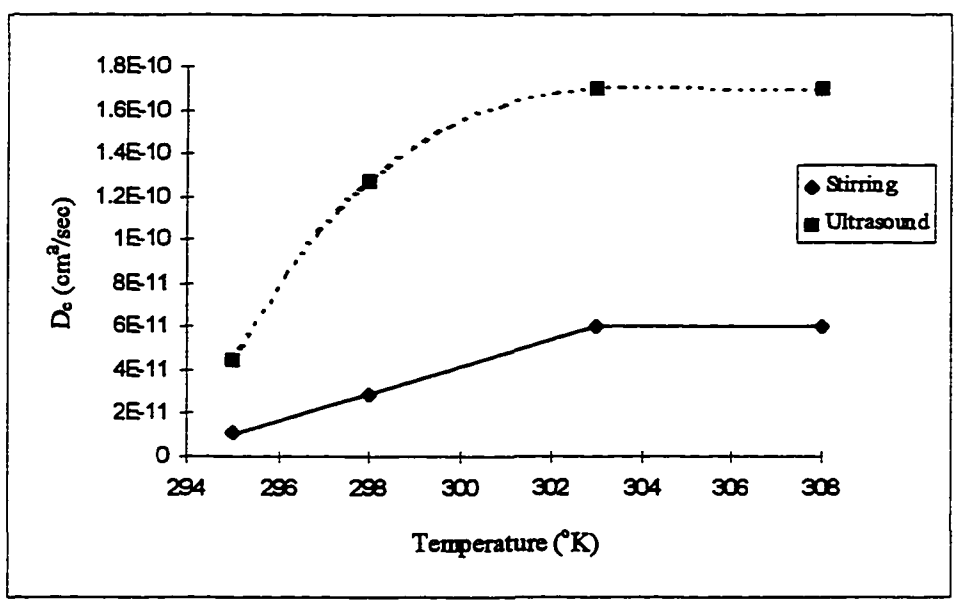

Figure 4.11 Effect of temperature on the effective diffusivity (D_e) when using ultrasound.

4.3.4 Effect on surface area

After the solid particles were filtered and dried, they were analyzed on an ASAP 2010, using the B.E.T. method, to determine their surface area. The results shown in Figure 4.12 uphold those from the kinetic analysis, i.e. the surface area of the solids increases when reaction occurs within the system, clearly indicating the presence of a product layer (NaCl), which is more porous than its unreacted counterpart (Na_2S). In addition, although the salt layer is more porous, the surface area measurement of 2.5 m^2/g indicates that the pores are not very large. Another factor apparent from the figure is that the particles exposed to ultrasound had a higher surface area than those subject to stirring. This result can also be intuitively guessed since ultrasound leads to particle degradation, thereby increasing the interfacial area available for solid-liquid contact.

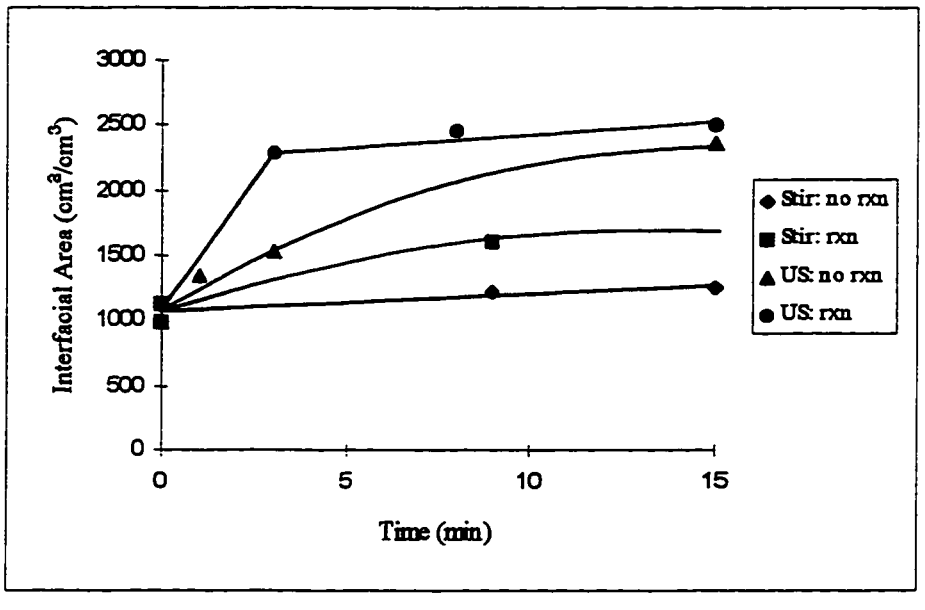

Figure 4.12 Effect of mechanical agitation and ultrasound, in the presence and absence of reaction, on the interfacial area.

4.3.5 Effect of sodium sulfide purity

Unfortunately, the lot from which anhydrous sodium sulfide was used as a reactant had a large effect on the overall conversion of benzyl chloride. Because previous publications concerning this reaction did not report this, it was an unexpected and undesired factor in conducting the overall research. Figure 4.13 shows the difference in conversion of benzyl chloride obtained when using two different lots of anhydrous sodium sulfide. For both stirring and sonicated reactions, lot #11927 led to a higher conversion of Na_2S, thus a higher rate of reaction. However, this effect is much more pronounced in the presence of ultrasound. When modeling the data, it was found that both the effective diffusivity and the intrinsic mass transfer coefficients are higher for lot #11927MN than for lot #14025MF. The experimentally determined values are summarized in Table 4.2.

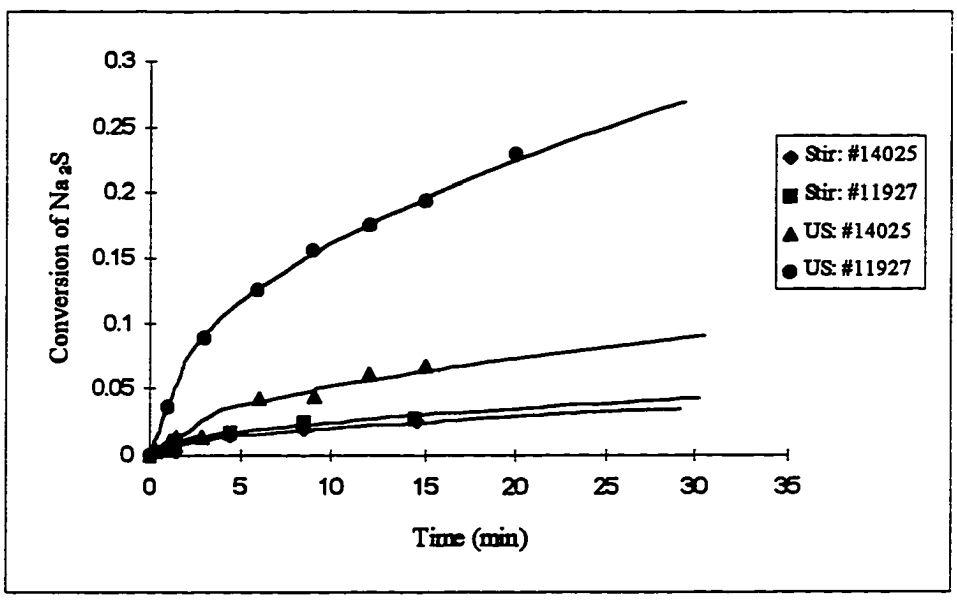

Figure 4.13 Conversion of benzyl chloride to dibenzyl sulfide for different lots of anhydrous sodium sulfide: temperature = 22 °C.

Table 4.2 Effect of sodium sulfide lot on the rate parameters k_l and D_e.

T = 22 °C	Stirring lot #14025MF	Stirring lot #11927MN	Ultrasound lot #14025MF	Ultrasound lot #11927MN
k_l (cm/sec)	-----	1.4×10^{-5} ($\pm 0.12 \times 10^{-5}$)*	4.2×10^{-6}	2.7×10^{-5} ($\pm 0.07 \times 10^{-5}$)*
D_e (cm^2/sec)	1.1×10^{-11}	1.4×10^{-10} ($\pm 0.07 \times 10^{-10}$)*	4.5×10^{-11}	4.6×10^{-10} ($\pm 0.04 \times 10^{-10}$)*

*standard deviation is based on 6 replicated reaction curves

The intrinsic mass transfer coefficient in the case of stirring, lot #14025MF, could not be experimentally determined for reasons previously discussed. The standard deviations for all values were calculated for reactions using lot #11927MN, but replicates were not made of complete rate curves for lot #14025MF because the manufacturer had a limited supply. In addition, a complete statistical analysis was performed on all of the solid-phase reaction models which supported the data shown in Table 4.2.

Alterations in rate parameters caused by changing the lot of solid reactant are most likely due to impurities within the crystal during its production, even though both lots were purchased from Aldrich Chemical and were of similar purity. X-ray diffraction was used to analyze both lots, but no differences between them could be observed. Both the identification of the impurity (or impurities) and its (their) role in altering the rate parameters of this model reaction are unknown at this time.

4.3.6 Morphology of the solid surface

A scanning electron microscope was used to look at the effect of both mechanical agitation and ultrasound on the morphology of the surface of the sodium sulfide particles. For comparison, images were first taken of samples obtained directly from the sieve, i.e. which had not been exposed to either ultrasound or stirring. As shown in Figures 4.14 a and b, the solids appeared to be nonporous and had a block-like structure.

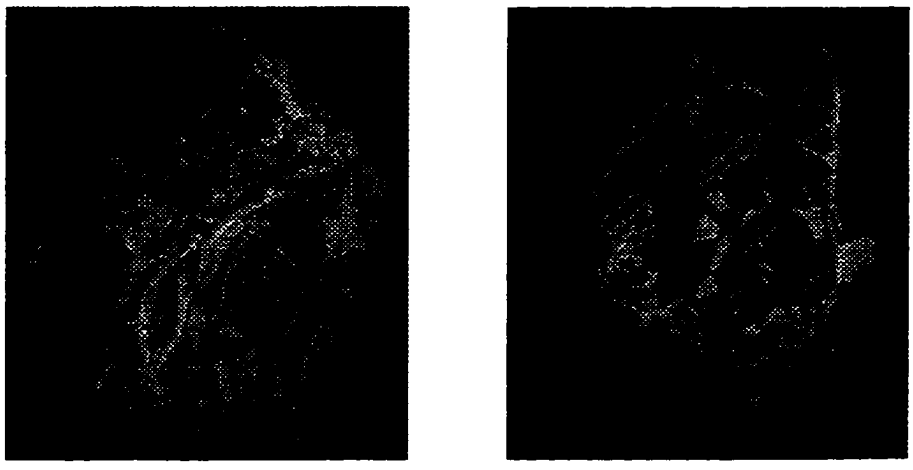

(a) (b)

Figure 4.14 SEM images of fresh (unaltered) particles of anhydrous sodium sulfide.

After the particles were exposed to 15 minutes of stirring (Figure 4.15a) or ultrasound (Figure 4.15b) in acetonitrile the structure of the particles changed dramatically. The somewhat flat and smooth surface of the fresh sample became very rough and grainy. In addition, the block-like structure had been eliminated. However, when comparing the morphology of the mechanically agitated particles to those exposed to sonication, no significant distinguishing features were apparent.

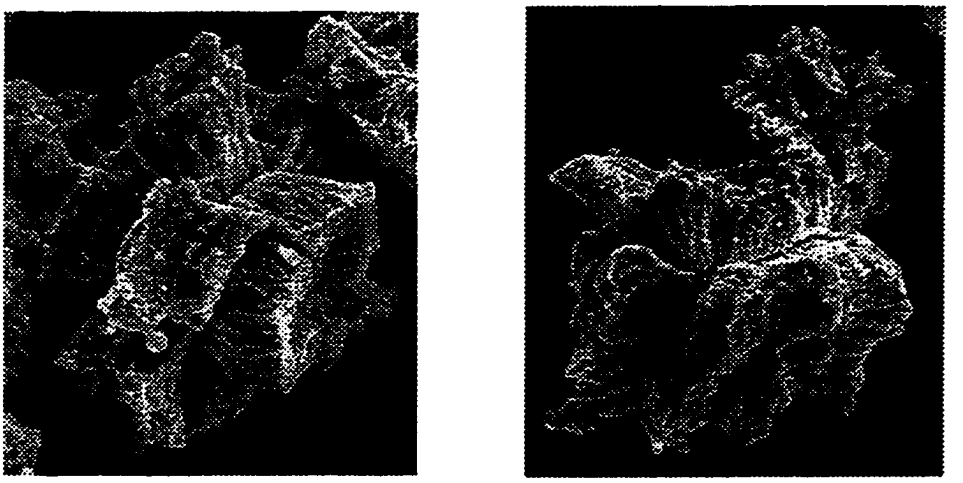

(a) (b)

Figure 4.15 Appearance of solid sodium sulfide particles after exposure to 15 minutes of mechanical agitation (a) or ultrasound (b).

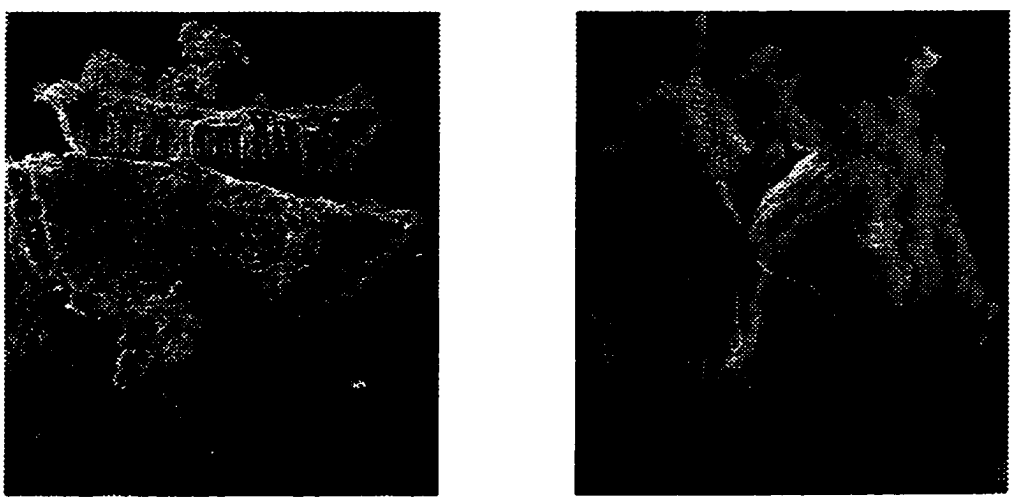

(a) (b)

Figure 4.16 Appearance of solid sodium sulfide particles in the presence of reaction and mechanical agitation (a) or ultrasound (b).

Images taken after 15 minutes of reaction in the presence of stirring (Figure 4.16a) or ultrasound (Figure 4.16b) are very dissimilar. Particles subject to simultaneous reaction and stirring were very rough and grainy, as they were in the absence of reaction (Figure 4.15a). However, the particles in the presence of reaction and sonication (Figure 4.16b) appeared to be smoother.

The shape of the particles as shown in these figures may lead to questions concerning the use of the spherical form of the sharp-interface model. However, when the particles are irregularly shaped, as in this case, the spherical form of the SIM model should provide parameter estimates with higher accuracy.

4.4 Conclusions

Several findings are reported in this paper concerning a solid-liquid reaction and how it is affected by exposure to ultrasonic irradiation. The most important of these are that ultrasound increases

1. the intrinsic mass transfer coefficient of the liquid reactant through the interfacial film by a factor of ~2, and
2. the effective diffusivity of the liquid reactant through the product layer surrounding the unreacted core by a factor 3.3 (4.1 for lot #14025).

Other investigative methods such as particle size analysis and surface area determination support the modeling results.

It is difficult to discern why the intrinsic effective diffusivity is enhanced more for one lot than the other, but impurities affecting the formation of the product layer may be the most logical explanation. Further work in this area is clearly necessary.

4.5 Nomenclature

A	probe tip area
A_{ws}	area of wetted surface of reaction vessel
C_A	concentration of solid reactant
C_{AO}	initial concentration of solid reactant
C_B	concentration of liquid reactant
C_{BO}	initial concentration of liquid reactant
C_p	heat capacity of solvent
$C_{p,\ vessel}$	heat capacity of reaction vessel (stainless steel)
D	diffusivity of reactant through solvent
D_e	effective diffusivity of liquid reactant through solid product layer
d_p	diameter of solid reactant
e	power dissipated per unit mass of liquid
F_c	shape factor
I	intensity of ultrasound
k_l	intrinsic solid-liquid film transfer coefficient

k_s	rate constant of surface reaction
m	mass of solvent
M_A	molecular weight of solid reactant
n	stoichiometric coefficient
P_{diss}	power dissipated in reaction system
R	regression coefficient
R_o	radius of solid reactant particle
$-r_{AO}$	initial rate of disappearance of solid reactant
$-r_B$	rate of disappearance of liquid reactant
t	time
T	temperature
T_v	temperature of the reactor vessel
x_A	fractional conversion of solid reactant
x_w	thickness of the inner wall of the reaction vessel

Greek letters

μ_l	viscosity of bulk liquid
ρ_A	density of solid reactant
ρ_l	density of bulk liquid
ρ_{vessel}	density of reaction vessel (stainless steel)

4.6 References

Berlan, J., Trabelsi, F., Delmas, H., Wilhelm, A.M. and Petrignani, J.F., 1994, Oxidative Degradation of Phenol in Aqueous Media Using Ultrasound. *Ultrasonics Sonochemistry* **1(2)**, S97-S102.

Broeckaert, L., Caulier, T., Fabre, O., Maerschalk, C., Reisse, J., Vandercammen, J., Yang, D.H., Lepoint, Th. and Mullie, F., 1992, Quantitative Homogeneous Sonochemistry: Scope and Limitations. *Current Trends in Sonochemistry*, pp. 8-25. Ed. by G.J. Price, Royal Society of Chemistry, Cambridge.

Contamine, F., Faid, F., Wilhelm, A.M., Berlan, J. and Delmas, H., 1994, Chemical Reactions Under Ultrasound: Discrimination of Chemical and Physical Effects. *Chem. Engng Sci.* **49(24B)**, 5865-5873.

Cum, G., Gallo, R. and Spadaro, A., 1988, Effect of Static Pressure on the Ultrasonic Activation of Chemical Reactions. Selective Oxidation at Benzylic Carbon in the Liquid Phase. *J. Chem. Soc. Perkin Trans II* 375-383.

de Souza-Barboza, J. C., Luche, J. L. and Petrier, C., 1987, Ultrasound in Organic Synthesis 11. Retention of Optical Activity in Barbier Reactions from S(+) 2-Octyl Halides. Mechanistic Consequences. *Tetrahedron Letters* **28(18)**, 2013-2016.

Dickens, M. J. and Luche, J. L., 1991, Further Evidence for the Effect of Ultrasonic Waves on Electron Transfer Processes - The Case of the Kornblum-Russell Reaction. *Tetrahedron Letters* **32(36)**, 4709-4712.

Doriaswamy, L.K. and Sharma, M.M., 1984, *Heterogeneous Reactions: Analysis, Examples, and Reactor Design, Vol. 2: Fluid-Fluid-Solid Reactions*, pp. 449-479. John Wiley and Sons, New York.

Entezari, M.H. and Kruus, P., 1994, Effect of Frequency on Sonochemical Reactions I: Oxidation of Iodide. *Ultrasonics Sonochemistry*, **1(2)**, S75-S79.

Fuentes, A., Marinas, J. M. and Sinisterra, J. V., 1987, Catalyzed Synthesis of Chalcones Under Interfacial Solid-Liquid Conditions With Ultrasound. *Tetrahedron Letters* **28(39)**, 4541-4544.

Hagenson, L.C., Naik, S.D. and Doraiswamy, L.K., 1994, Rate Enhancements in a Solid-Liquid Reaction Using PTC, Microphase, Ultrasound and Combinations Thereof. *Chem. Engng. Sci.* **49(24A)**, 4787-4800.

Hanafusa, T., Ichihara, J. and Ashida, T., 1987, Useful Synthesis of *a*-Aminonitriles by Means of Alumina and Ultrasound. *Chem. Letters*, 687-690.

Hart, E. J. and Henglein, A., 1985, Free Radical and Free Atom Reactions in the Sonolysis of Aqueous Iodide and Formate Solutions. *J. Phys. Chem.* **89**, 4342-4347.

Javed, T., Mason, T.J., Phull, S.S., Baker, N.R. and Robertson, A., 1995, Influence of Ultrasound on the Diels-Alder Cyclization Reaction: Synthesis of Some Hydroquinone Derivatives and Lonapalene, and Anti-Psoriatic Agent. *Ultrasonics Sonochemistry* **2(1)**, S3-S4.

Jouglet, B., Blanco, L. and Rousseau, G., 1991, New Method for the Reaction of Nitroalkanes with Unsaturated Esters. *Synlett* **Dec.**, 907-908.

Landini, D. and Rolla, F.A., 1974, Convenient Synthesis of Primary and Secondary Dialkyl and Aryl Sulfides in the Presence of Phase-Transfer Catalysts. *Synthesis*, 565.

Levenspiel, O., 1972, *Chemical Reaction Engineering*, 2nd Ed., pp. 357-377. John Wiley and Sons, NY.

Lie Ken Jie, M.S.F. and Lam, C.K., 1995, Ultrasound-Assisted Epoxidation Reaction of Long-Chain Unsaturated Fatty Esters. *Ultrasonics Sonochemistry* **2(1)**, S11-S14.

Lorimer, J. P., Mason, T. J. and Fiddy, K., 1991, Enhancement of Chemical Reactivity by Power Ultrasound: An Alternative Interpretation of the Hot Spot. *Ultrasonics* **29(4)**, 338-343.

Luche, J.L., 1994, Effect of Ultrasound on Heterogeneous Systems. *Ultrasonics Sonochemistry* **1(2)**, S111-S118.

Margulis, M. A., 1985, Sonoluminescence and Sonochemical Reactions in Cavitation Fields. A Review. *Ultrasonics* **July**, 157-169.

Mason, T. J., 1990a , *Chemistry With Ultrasound*. Elsevier Applied Science.

Mason, T. J., 1990b, *Sonochemistry*. Royal Society of Chemistry, Cambridge.

Mazet, N., 1992, Modeling of Gas-Solid Reactions. 1. Nonporous Solids. *International. Chem. Engng.* **32(2)**, 271-284.

Noltingk B.E. and Neppiras, E.A., 1950, Cavitation produced by ultrasonics. *Proc. Phys. Soc.* **63B**, 674-685.

Phadtare, P.G. and Doraiswamy, L.K., 1965, Mass Transfer Model for Kolbe-Schmitt Carbonation of 2-naphthol. *Ind. Eng. Chem. Process Design and Dev.* **4**, 274.

Pradhan, N. C. and Sharma, M. M., 1990, Kinetics of Reactions of Benzyl Chloride/p-Chlorobenzyl Chloride with Sodium Sulfide: Phase-Transfer Catalysis and the Role of the Omega Phase. *Ind. Eng. Chem. Res.* **29**, 1103-1108.

Prasad Naidu, D. V., Rajan, R., Kumar, R., Gandhi, K. S., Arakeri, V. H. and Chandrasekaran, S., 1994, Modeling of a Batch Sonochemical Reactor. *Chem. Engng Sci.* **49(6)**, 877-888.

Ratoarinoro, N., Contamine, F., Wilhelm, A. M., Berlan, J. and Delmas, H., 1995, Activation of a Solid-Liquid Chemical Reaction by Ultrasound. *Chem. Engng Sci.* **50(3)**, 554-558.

Ratoarinoro, N., Wilhelm, A. M., Berlan, J. and Delmas, H., 1992, Effects of Ultrasound Emitter Type and Power on a Heterogeneous Reaction. *Chem. Eng. J.* **50**, 27-31.

Sinisterra, J. V., 1992, Application of Ultrasound to Biotechnology: an Overview. *Ultrasonics* **30(3)**, 180-185.

Soudagar, S.R. and Samant, S.D., 1995, Investigation of Ultrasound Catalyzed Oxidation of Arylalkanes Using Aqueous Potassium Permanganate. *Ultrasonics Sonochemistry* **2(1)**, S15-S18.

Suslick, K. S., Doktycz, S. J. and Flint, E. B., 1990, On the Origin of Sonoluminescence and Sonochemistry. *Ultrasonics* **28(4)**, 280-290.

Suslick, K. S., 1988, *Ultrasound : Its Chemical, Physical and Biological Effects*, VCH Publishers, New York.

Tozzi, A. and Cassandrini, P., 1975, Catalysts for Organic Sulfide Manufacture. *Ger. Offen.* 2513805; 1976, *Chem. Abstr.* **84**, 4476.

CHAPTER 5.
USE OF ULTRASOUND TO INDUCE SUPERSATURATION IN A SOLID-LIQUID SYSTEM

A paper prepared for submission to *Chemical Engineering Science*

Leigh C. Hagenson and L. K. Doraiswamy

Abstract

Ultrasound has been found to induce the supersaturation of a sparingly soluble solid in a liquid system. Two different types of solid-liquid systems were investigated: sodium sulfide in acetonitrile and calcium citrate in water, with the former being investigated in more detail. In the presence of ultrasound, the concentrations of these solutes in their respective solvents were increased at least 1.4 times the equilibrium saturation concentrations. Possible mechanisms leading to this enhancement are discussed.

5.1 Introduction

It is well known that the rate of dissolution of a solute A in a solvent depends upon the intrinsic mass transfer coefficient k_{sl}, the interfacial area a and the driving force (C_A^*-C_A), as shown by Equation (1). Although several methods exist to enhance the rate of mass

$$-\frac{dC_A}{dt} = k_{sl}\, a\left(C_A^* - C_A\right) \tag{1}$$

transfer by increasing k_{sl} and a, there is no technique capable of increasing the driving force, until now. The use of ultrasound has been found to increase the ***driving force*** for mass

transfer, with the added benefit of simultaneously increasing the both the intrinsic mass transfer coefficient (k_{sl}) and the interfacial area (a). This paper intends to: 1. present experimental evidence that high-power ultrasound induces supersaturation in a model solid-liquid system; 2. postulate the mechanism by which this supersaturation is achieved; and 3. examine if this phenomenon is unique to the model system investigated.

5.2 Theory

When an ultrasonic wave propagates through a liquid medium, cavitation bubbles are formed during the rarefaction, or negative pressure period, of the sound wave. The maximum temperature (T_{max}) and pressure (P_{max}) attained during an adiabatic bubble collapse for a gas filled, transient bubble can be estimated using Equations (2) and (3), respectively

$$T_{max} = T_o\left[\frac{P_m(\gamma - 1)}{P}\right] \tag{2}$$

$$P_{max} = P\left[\frac{P_m(\gamma - 1)}{P}\right]^{\frac{\gamma}{\gamma - 1}} \tag{3}$$

(Neppiras, 1980). These relationships were developed neglecting surface tension and viscosity of the fluid, and assuming ideality of the gas. If the cavity contains vapor as well as gas, the collapse will be cushioned and the maximum pressure and temperature will be reduced because some of the energy will be used to condense the vapor.

When a cavitational bubble implodes, a localized hot spot is formed along with extremely large temperature and pressure gradients, as shown in Figure 5.1. The solvent within the

temperature and pressure gradient will, with some range, exist as a supercritical fluid (SCF) (Hoffmann *et al.*, 1996). In the absence of ultrasound, it has been shown that solid particles which are typically insoluble or only slightly soluble in a solvent at ambient conditions may have very high solubilities in the same solvent when it is in a supercritical state (see, e.g., Tester and Modell, 1997; Mullin, 1993).

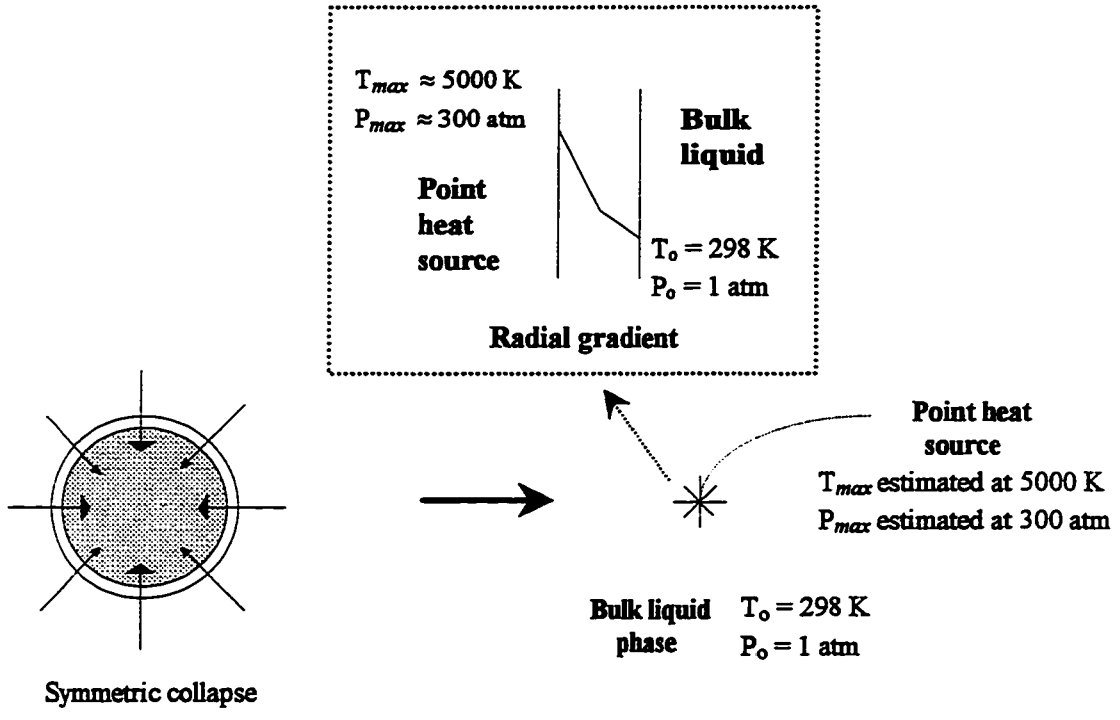

Figure 5.1 Symmetric collapse resulting in localized hot spot.

When solid particles are present in the fluid system, the cavitational event may occur symmetrically or asymmetrically, depending upon the proximity and size of the solids. Small solid particles (< ~200 μm in diameter) do not perturb the symmetry of the collapse, and collapse occurs as in Figure 5.1. In addition to the formation of a point heat source,

symmetric cavitation is responsible for the formation of large shock waves which produce a variety of physical events, such as microstreaming and particle acceleration. Microstreaming is the localized turbulence of the solid-liquid film which accelerates the rate of mass transfer through the film by increasing the intrinsic mass transfer coefficient. Shock waves also cause nearby particles to move away from the cavitational event in a radial direction with great speed. These particles collide with surrounding particles with such force that particle degradation occurs and, in the case of metallic particles, fusion and localized melting may result.

When a bubble cavitates near a solid which is several orders of magnitude larger than the bubble (i.e. particles > ~200 μm in diameter), the cavitation is retarded and the bubble implodes asymmetrically, forming a microjet of solvent perpendicular to the solid surface, which causes surface erosion and is responsible for the cleaning effects of ultrasound.

5.3 Experimental Apparatus, Procedure and Tools

The model heterogeneous system under investigation is the dissolution of 10% w/v high purity sodium sulfide (purchased as anhydrous) in acetonitrile. The "silent" reactions, reactions in the absence of ultrasound) were carried out in an enclosed stainless steel reaction vessel operated in the batch mode. The reaction mixture was mechanically agitated using an impeller and the temperature was maintained to within ± 1.0 °C by jacket cooling and measured using a thermocouple inserted directly into the mixture.

Ultrasound reactions were conducted using Sonicator XL2020 (Misonix, Inc.), which supplied a constant frequency of 20 kHz to the 1/2 in titanium horn. The power of ultrasound dissipated by the reaction system was 95.4 W as determined experimentally using calorimetry (Hagenson and Doraiswamy, 1997a). The power entering the system as quoted by the manufacturer was 166 W; thus 42.5% of the power delivered was lost in the transfer process. The horn was fitted to the same stainless steel reaction vessel as used for the silent reactions (see Figure 5.2) in order to preserve similarity of reactor geometries for comparison of experimental data. The dissolution experiments were carried out in the batch mode in a random order. Isothermal conditions were maintained to within ± 0.5 °C.

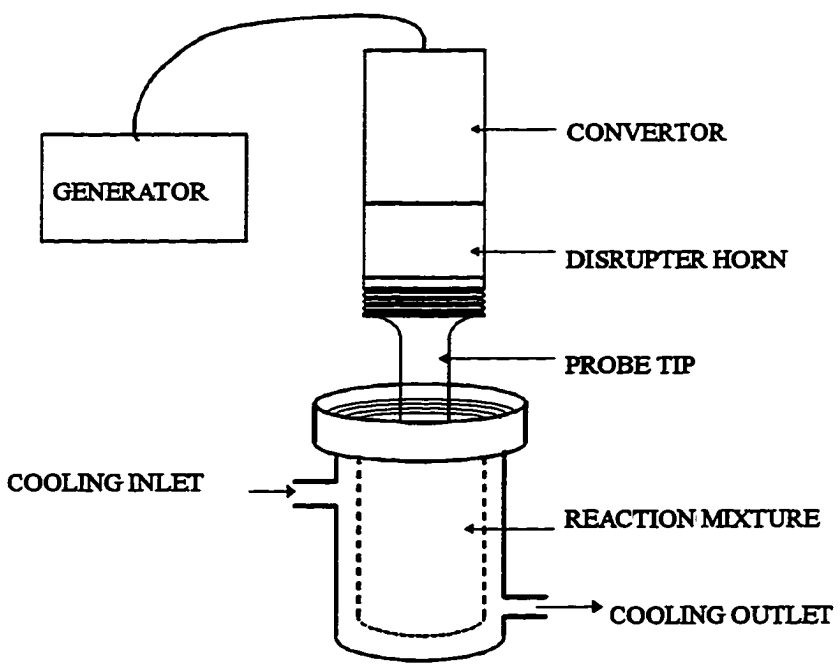

Figure 5.2 Experimental apparatus used for sonochemical research.

The sodium sulfide was purchased from Aldrich as anhydrous chunks. It was crushed, and sieved to provide the same average particle size (~ 34 μm) for all batches. Although measures were taken to preserve the anhydrous nature of the solid, water was unavoidably absorbed during the experimental process. Several batches of sodium sulfide were analyzed using X-ray diffraction, and were found to be comprised of $Na_2S \cdot 5H_2O$. The fully hydrated form is $Na_2S \cdot 9H_2O$.

A Smith-Hieftje Atomic Absorption Spectrophotometer with a wavelength of 589 nm and a bandwidth of 0.5 was used to measure the concentration (ppm) of Na^+ in acetonitrile. Standards and samples were analyzed using a 50:50 water/acetonitrile matrix.

5.4 Results

Results of the dissolution studies of sodium sulfide in acetonitrile are shown in Figure 5.3. The data points shown in the graph are mean values of 2 to 8 independent measurements obtained from randomized, batch experiments. Since the variances of the silent and sonicated reactions were found to be equal through hypothesis testing, they could be pooled giving $S_p^2 = 26.32$ based on 101 data points. Thus, the standard deviation of each mean ($\bar{x}$) given in Figure 5.3 is 5.13 ppm Na^+.

As is apparent in the figure, ultrasound greatly increases the rate of dissolution of Na^+ in solvent acetonitrile over that of stirring alone. At this point, two observations can be made; first, ultrasound increases the amount of Na^+ in solution, past the equilibrium saturation level of 65.1 ppm obtained after 5 minutes of stirring alone, to 92.4 ppm at 17 minutes of

sonication. This is 1.4 times the saturation concentration C_A^*. Second, although the concentration of Na^+ in solution begins to decrease between 17 and 27 minutes of sonication, it increases to the same concentration level at 37 minutes as was observed at 17 minutes. This behavior continues in a cyclic manner for 67 minutes of continuous sonication.

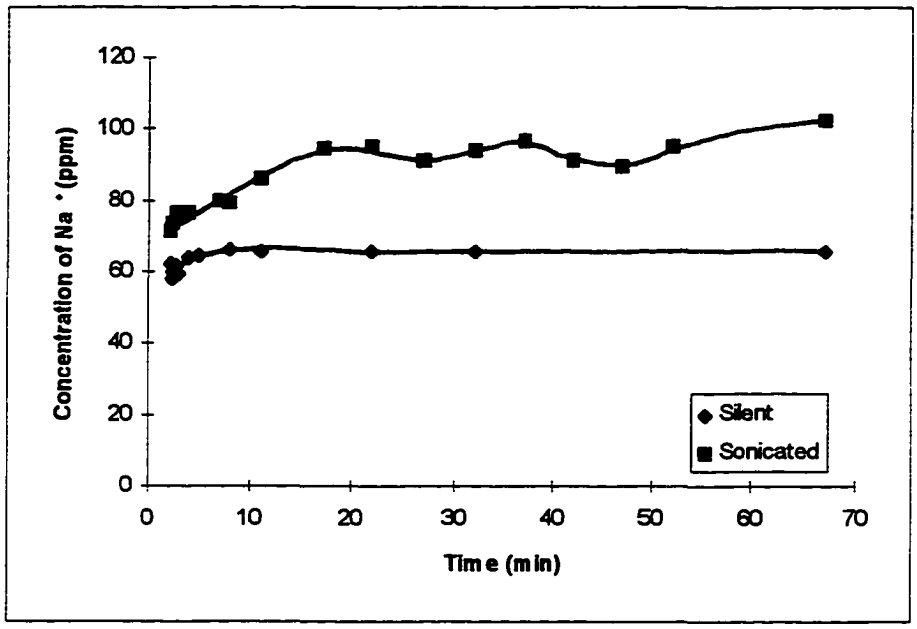

Figure 5.3 Supersaturation as a result of exposure to ultrasound.

In addition to analyzing the concentration of Na^+ in the bulk solution, experiments were also conducted on the filtered solvent. After each of the batch dissolution studies were performed, the heterogeneous system was filtered and the clear filtrate was left to sit in a clean sample vial. After 1 1/2 hours, precipitation of the sodium sulfide was observed. The crystals obtained from the filtrate are shown in Figure 5.4 for **a.** 8 minute and **b.** 17 minute sonicated samples. The crystals within each batch are approximately the same length and width. The lengths of the crystals obtained from the 8 minute sonication sample were normally distributed

with a mean of 18.6 μm (with a 95% confidence interval of $18.13 < \mu < 19.03$) and an average width of 5.5 μm. The lengths for the 17 minute sample were also normally distributed, with a skew to the left, with a mean of 23.3 μm (with a 95% confidence interval of $22.48 < \mu < 24.16$) and an average width of 5.8 μm. This type of crystal formation is indicative of primary, homogeneous nucleation.

To ensure that the sodium sulfide was not altered during dissolution and exposure to ultrasound, X-ray diffraction studies were carried out on the solid before dissolution and after 17, 47 and 67 minutes of dissolution and exposure to ultrasound. Each sample was found to contain $Na_2S \cdot 5H_2O$. No other complexes of sodium were present.

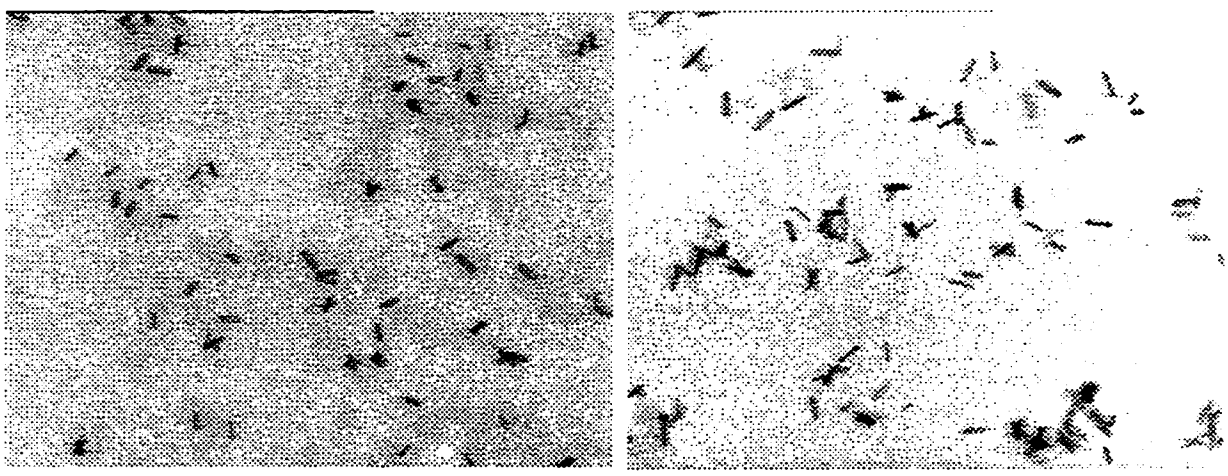

a. 8 minutes of sonication **b. 17 minutes of sonication**

Figure 5.4 Crystal formation in filtrate of supersaturated solutions (dissolution temperature = 22 °C).

5.5 Discussion

Several simultaneous events are occurring in a system exposed to high power ultrasound which may lead to the enhancement of the dissolution rate of a sparingly soluble solute (A) in a solvent. These events are summarized in Figure 5.5, and are explained in more detail in the following paragraphs. References are given to direct the reader to more information concerning the various enhancements.

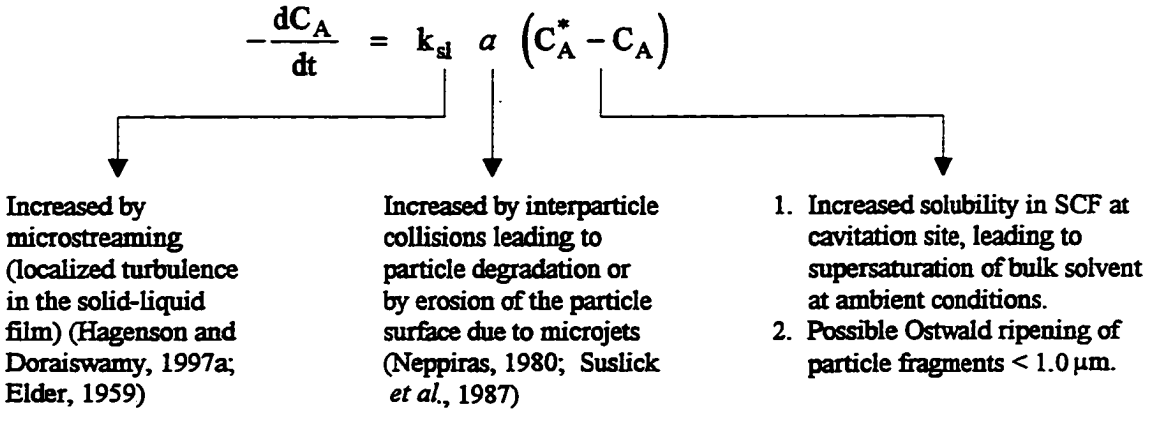

Figure 5.5 Ultrasonic enhancement of dissolution.

5.5.1 Formation of supercritical fluid

The solubility of a non-volatile solute in a solvent can be altered dramatically when the temperature and pressure of the system are slightly above the critical point of the solvent. In the metastable region at temperatures and pressures above the critical point, the solvent is neither a distinct liquid or a distinct gas, and is referred to as a supercritical fluid (SFC). The solubility of a solute in the presence of this fluid may be significantly greater than at ambient conditions. The cyclic behavior of the concentration of Na^+ in solution as a function of

sonication time, exhibited in Figure 5.3, may be due to random fluctuations in the average, or may be a result of counteracting mechanisms of dissolution and precipitation. It is important at this point to reiterate that the dissolution studies were carried out in a batch reactor in a randomized order.

If one knows the total amount of solute dissolved (ppm) as a function of temperature both below and above the critical point of the solvent, the concentration of the solute (A) can be determined for each cavitational event, as shown by

$$C_{A,\,\text{per bubble}}(t) = \int_{T_o}^{T_c} f_m \text{ solubitity} + \int_{T_c}^{UCL} f_n \text{ solubility} \tag{4}$$

Then knowing the number of cavitational events (N) per unit time of sonication, the total concentration of solute obtained as a result of sonication ($C_{A,\,BUB}$) can be determined, as shown by Equation (5). The number of cavitational events has been estimated by Prasad

$$C_{A,\,BUB}(t) = \sum_{i=1}^{N} C_{A,\,\text{per bubble}} \tag{5}$$

Naidu (1994) by measuring the liberation of iodine. Using an ultrasonic bath with a frequency of 25 kHz and an input power of 250 W, they estimated that 2.64×10^{10} bubbles were collapsing per unit volume (l) per unit time (s) in an aqueous solution. For the purposes of this paper, this number serves only as a very rough estimate because of the differences in system configuration (probe with different operating parameters) and solvent/solute mixture. For more information as to why this is only a rough approximation, refer to Hagenson and Doraiswamy (1997b).

Next, assuming that the concentration of solute dissolved as a result of bubble collapse is independent of the concentration dissolved as a result of agitation of the solvent, and assuming that all of the solute dissolved remains solubilized (i.e., there is no precipitation of solute depleting the concentration in the solvent), then the total concentration of solute dissolved per unit time for the sonicated system is given by

$$C_{A,US}(t) = C_A(t) + C_{A,BUB}(t) \tag{6}$$

However, as discussed previously, precipitation of the solute may be occurring, and the processes of dissolution and precipitation may be occurring simultaneously. As is apparent, a large amount of information is required before this approach to determining the enhanced solubility as a result of cavitation can be verified or expanded.

5.5.2 Gibbs-Thompson relationship

In addition to enhanced solubility of a solute as a result of cavitation formation, another mechanism may be acting simultaneously which is indirectly caused by the cavitational event. In 1900, Ostwald applied the relationship of particle size and solubility, originally developed by Thompson in 1878, to solid-liquid systems. He found that very small particles (<1.0 μm) will continue to dissolve even after equilibrium saturation of the solvent has been attained. The increased solubility is due to the pressure difference between the bulk fluid and the curved interface of the small solid particle. This relationship is termed "Gibbs-Thompson", "Ostwald-Freundlich" or "Gibbs-Kelvin", and is given by

$$ln\left[\frac{C_A(r)}{C_A^*}\right] = \frac{2M\gamma}{\nu RT_o\rho r} \quad (7)$$

where $C_A(r)$ is the solubility of the small particles of size r, C_A^* is the equilibrium solubility of the substance, M and ρ are the molecular weight and density of the solute, γ is the interfacial tension of the crystal in contact with its own solution, R is the gas-constant, T is the temperature of the system and ν is the number of ions in a formula unit of solute.

If Gibbs-Thompson relationship is used to explain the all of the observed enhancement in solubility of Na_2S in acetonitrile, then Equation (7) can be used to predict the radius of the particles required to obtain such an enhancement. Using $C_A(r)/ C_A^* = 1.4$, the radius of particles required are approximately 8.77×10^{-10} m or 8.77 Å (angstroms). The unit crystal size of Na_2S is 6.53 Å. It is feasible that, upon exposure to ultrasound, extremely small pieces of Na_2S are broken off of the parent crystal. Particle fragmentation occurs as a result of the formation of shock waves from cavitation. In addition, the surface of the particles may be bombarded by microjets of solvent formed during asymmetric cavitation, leading to erosion of the particles. Both of these mechanical effects of ultrasound may produce particles in solution which are smaller that 1.0 μm and are capable of dissolving past the point of equilibrium saturation. However, minimum radii of particles produced by such processes are not known at this time.

5.5.3 Supersaturation of an aqueous system

The supersaturaton of Na_2S in acetonitrile in the presence of ultrasound is not a unique phenomena. The dissolution of calcium citrate in water was investigated in order to determine if it was possible to induce supersaturation in an aqueous system as well as the organic system previously studied. The magnitude of supersaturation achieved with ultrasound is slightly higher than that of the organic system (i.e. $C_A/C_A^* = 1.7$ and 1.4 for the aqueous and organic systems, respectively), as shown in Figure 5.6. The trend is also slightly different. The dotted line is representative of the saturation concentration of Ca^{2+} in the absence of ultrasound.

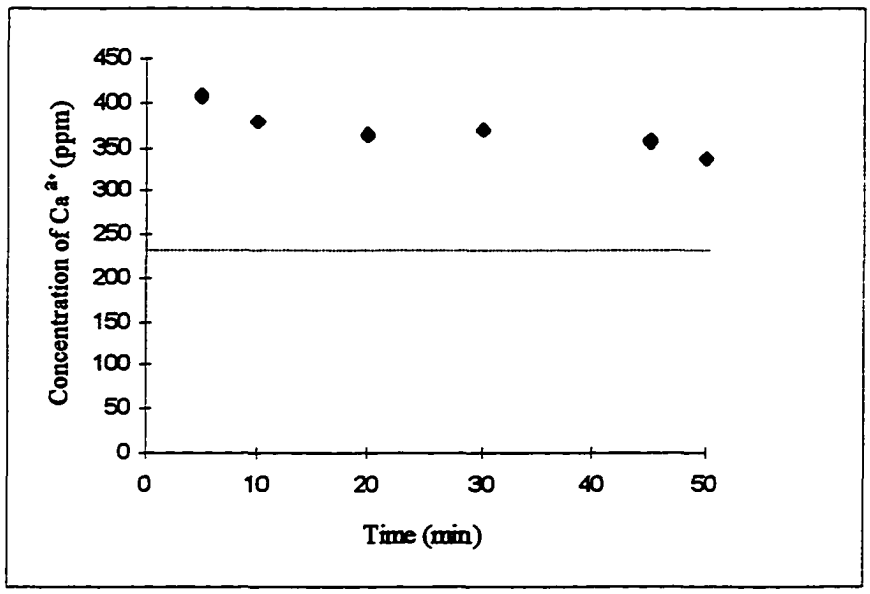

Figure 5.6 Dissolution of calcium citrate in water.

5.6 Conclusions

Ultrasound significantly enhances the solubility of an inorganic solid in a model organic and aqueous system. The solubilities of two model systems, calcium citrate in water and of sodium sulfide in acetonitrile, were increased 1.4 times or more than the equilibrium saturation concentration obtained with mechanical agitation. The concentration of solute may have been increased in the presence of ultrasound because of the well-known formation of cavitation bubbles in the bulk liquid mixture during the rarefaction period of the sound wave. When these bubbles implode, localized hot-spots are formed which contain solvent in a supercritical state. The solid, which is typically insoluble or sparingly soluble in the solvent at ambient conditions, is highly soluble in the solvent when it exists as a supercritical fluid (SCF). Thus, although the solubility of the solute is significantly greater in the regions containing SCF, the "memory" of this increased solubility is maintained even after the hot-spot dissipates into the bulk fluid at ambient temperature and pressure. The solubility may have also been increased due to the pressure difference between the bulk fluid and the curved interface of the small solid particle.

The applications of using ultrasound to enhance the solubility of a sparingly soluble solid are numerous. It would be very beneficial if a chemical reaction occurred in the liquid phase and was limited by the quantity of solid reactant available in solution. It could also be used to increase the quantity of toxins in solution to increase the rate of bioremediation.

5.7 Nomenclature

Symbols

a	interfacial area
C_A	concentration of solid
$C_{A,BUB}$	concentration of A in solution as a result of cavitation
C_A^*	equilibrium saturation concentration of solid A in solvent B
k_{sl}	intrinsic mass transfer coefficient
M	molecular weight of the solute
N	number of cavitational events per unit time
r	radius of the solute particles
R	gas constant
T_c	critical temperature of the solvent
T_o	ambient temperature of the solvent

Greek letters

γ	surface tension between the solute and the solvent
ν	number of ions in a formula unit of the solute
ρ	density of the solute

Acronyms

SFC	supercritical fluid
UCL	upper critical limit of the solvent

5.8 References

Hagenson, L.C. and Doraiswamy, L.K., "Comparison of the Effects of Ultrasound and Mechanical Agitation on a Reacting Solid-Liquid System," **1997a**, accepted for publication in *Chemical Engineering Science*.

Hagenson, L.C. and Doraiswamy, L.K., "Sonochemistry: Science and Engineering," **1997b**, to be submitted for publication.

Hoffmann, M.R., Hua, I., and Hochemer, R., "Application of Ultrasonic Irradiation for the Degradation of Chemical Contaminants in Water," *Ultrasonics Sonochemistry*, **1996**, 3, S163-S172.

Mullin, J.W., Crystallization, 3rd Edition, Butterworth-Heinemann, Boston, 1993.

Neppiras, E.A., "Acoustic Cavitation," *Phys. Rep.*, **1980**, 61(3), 159-251.

Prasad Naidu, D.V., Rajan, R., Kumar, R., Gandhi, K.S., Arakeri, V.H. and Chandrasekaran, S., "Modeling of a Batch Sonochemical Reactor," *Chemical Engineering Science*, **1994**, 49(6), 877-888.

Tester, J.W. and Modell, M., Thermodynamics and Its Applications, 3rd Edition, Prentice Hall, New Jersey, 1997.

CHAPTER 6.
GENERAL CONCLUSIONS

The primary objectives of this research were to discern the mechanical and chemical effects of ultrasound on a model solid-liquid system. Research in this field was necessary because the effects of ultrasound on the parameters concerning chemical engineering design and scale-up, such as the intrinsic mass transfer coefficient and the effective diffusivity, were uncertain. To investigate such effects of ultrasound, a model solid-liquid reaction was selected and used throughout the research program. The reaction, the synthesis of dibenzyl chloride from benzyl chloride and solid sodium sulfide, was affected exclusively by the mechanical effects of ultrasound because it follows an ionic mechanism.

Before detailed modeling of the kinetics of the reaction could be undertaken, it was necessary to discern where the reaction was occurring. Typically, when a reaction involves a sparingly soluble solid reactant and a liquid phase reactant, the reaction is assumed to take place in the liquid phase. However, a non-traditional approach was used in this research which assumed that the reaction could take place in both the liquid and solid phases simultaneously. After an exhaustive investigation, it was concluded that the reaction occurred on the solid surface and that the liquid phase reaction was negligible. It was also found that the experimental data were adequately explained using the sharp-interface model. At low times, the reaction was limited by the diffusion of benzyl chloride through the solid-liquid film, while at higher reaction times, the effective diffusion of benzyl chloride through product layer became the rate controlling step. Using this model, information about the effects of

ultrasound on mass transfer parameters was obtained. It was concluded that ultrasound increases:

1. the intrinsic mass transfer coefficient of the liquid reactant through the interfacial film by a factor of ~2, and
2. the effective diffusivity of the liquid reactant through the product layer surrounding the unreacted core by a factor 3.3 (4.1 for lot #14025).

Other investigative methods such as particle size analysis and surface area determination supported the modeling results.

During the course of the research, another effect of ultrasound was found which was previously unreported. Ultrasound enhanced the solubility of a sparingly soluble solid by a factor of 1.4 over the equilibrium saturation concentration obtained with stirring alone. The concentration of Na^+ in solution as a function of sonication time was cyclic in nature, possibly due to random fluctuation in the average or to competing dissolution and precipitation processes. The concentration of solute was increased in the presence of ultrasound most likely because of the formation of localized areas of cavitation containing solvent in a supercritical state. A typically insoluble solid becomes highly soluble, in several cases, when the solvent exists as a supercritical fluid (SCF). Thus, the solubility of the solute is significantly greater in the regions containing SCF and the "memory" of this increased solubility is maintained, even after the hot spot dissipates into the bulk fluid at ambient temperature and pressure.